MNFC

Micro/Nanofabrication Center

Research Report 2022

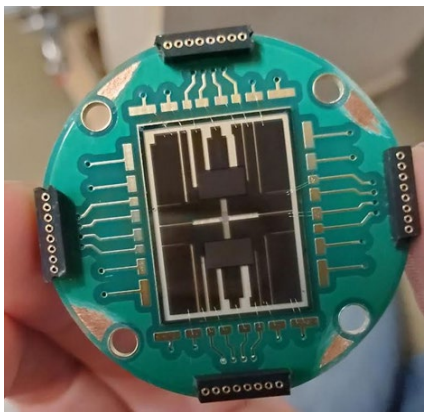

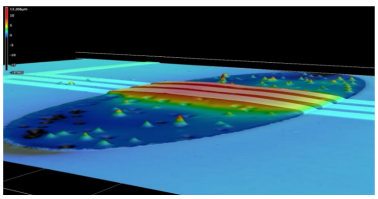

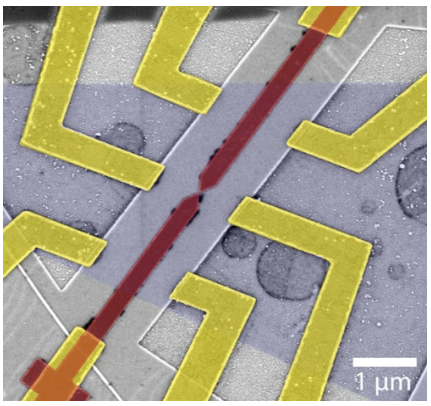

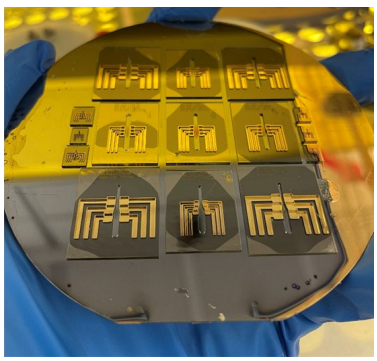

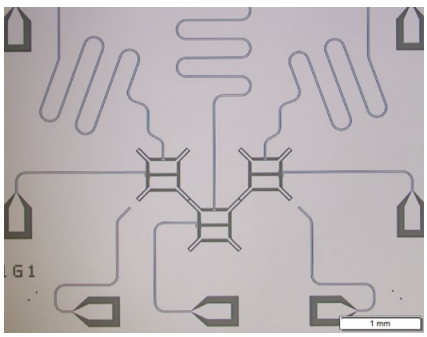

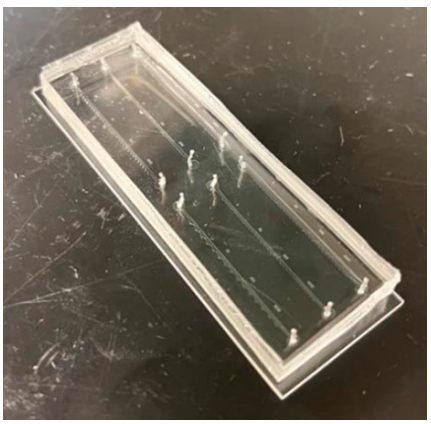

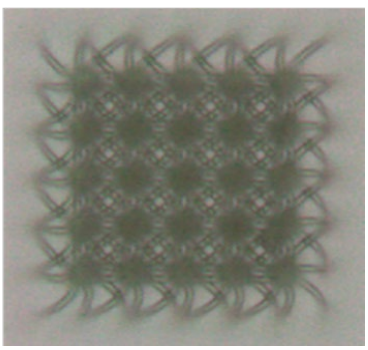

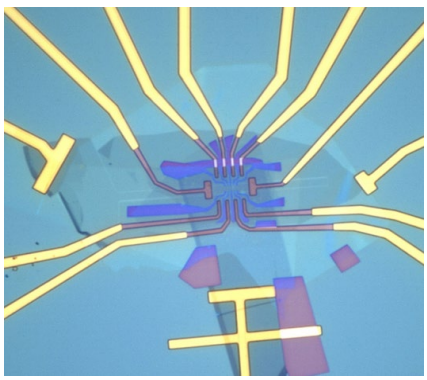

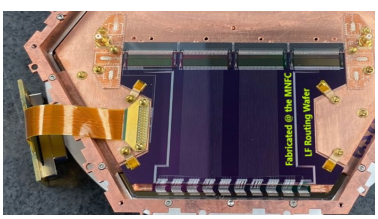

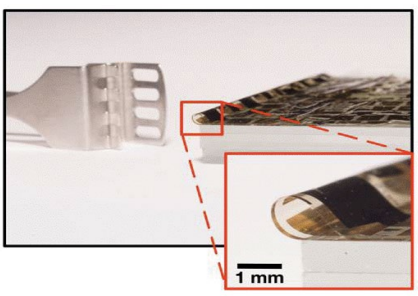

INTRODUCTION

The Micro/Nanofabrication Center (MNFC) at Princeton University, is a state of the art, professionally staffed, shared research facility that in 2022 served 167 labmembers, including researchers from 8 different Princeton University departments (33 research groups), 12 external academic users (the University of Maryland, the University of Pennsylvania, and the University of Tennessee), and 21 industrial collaborators from 10 companies (see *MNFC Usage in 2022* below).

MNFC consists of class 100-10,000 cleanroom space with capabilities in the areas of lithography (laser, contact, e-beam), wet processing, deposition (ALD, CVD, PVD), etching, 3D printing. MNFC also has stand-alone Packaging Laboratory housing a full range of services including dicing, scribing/cleaving, wire bonding (wedge, ball), flip-chip bonding, and lapping/polishing techniques (see paragraph *MNFC Major Equipment*).

All MNFC labmembers are properly trained for working in a controlled environment during in-person cleanroom orientation course. MNFC staff also performs one-on-one short courses to familiarize labmembers with how to prepare samples, and operate equipment. In 2022, the MNFC supported the Research Experiences for Undergraduates (REU) program (spring course lead by Dr. James S. Smith), and ECE 308 Electronic and Photonic Devices course for undergraduate students (by Prof. Antoine Kahn).

Year 2022 brought several milestones to our facility:

- We performed corrective work associated with the abatement system to support new equipment.
- We installed, and developed processes for two new PlasmaTherm etchers, APEX III-V, and Versaline systems, state of the art tools for reactive ion etching of the III-V semiconductors and silicon, respectively.
- We have extended Soft Materials Processing capabilities by being able to produce 3D polymer structures with feature sizes from submicron to the millimeter scale using new, state of the art two-photon polymerization 3D printer: Nanoscribe PP GT2.

This report outlines the research utilized in the MNFC in 2022 in quantum materials, electronics, energy generation and storage, sensing and spectroscopy, microfluids, MEMS, photonic metamaterials, and more. The information was provided by researchers themselves.

We thank all the MNFC labmembers who shared their data with us, and all your continued support. Please enjoy reading about the great diversity in research areas contained in these pages.

MNFC Team:

- **Dr. Zuzanna Lewicka**, Interim Director, New Labmember Onboarding, PECVD & ALD Process Engineering
- **Joseph Palmer**, Operations Manager, PVD Process Engineering
- **Roman Akhmechet**, Photolithography, Plasma Etch, and Soft Systems
- **Dr. Magdalena Moczala-Dusanowska**, Nanolithography and Metrology
- **Brien Ely**, Equipment Engineering
- **Paul Cole**, Infrastructure and Materials Specialist
- **Bert Harrop**, Packaging Lab Manager, Backend and Package Engineering
- **Daniel McNesby**, IT Support

CONTENTS

MNFC USAGE in 2022

Data presented below has been collected through NEMO (MNFC software for managing reservations, tool utilization, billing, etc) between 1/1/2022 – 12/31/2022.

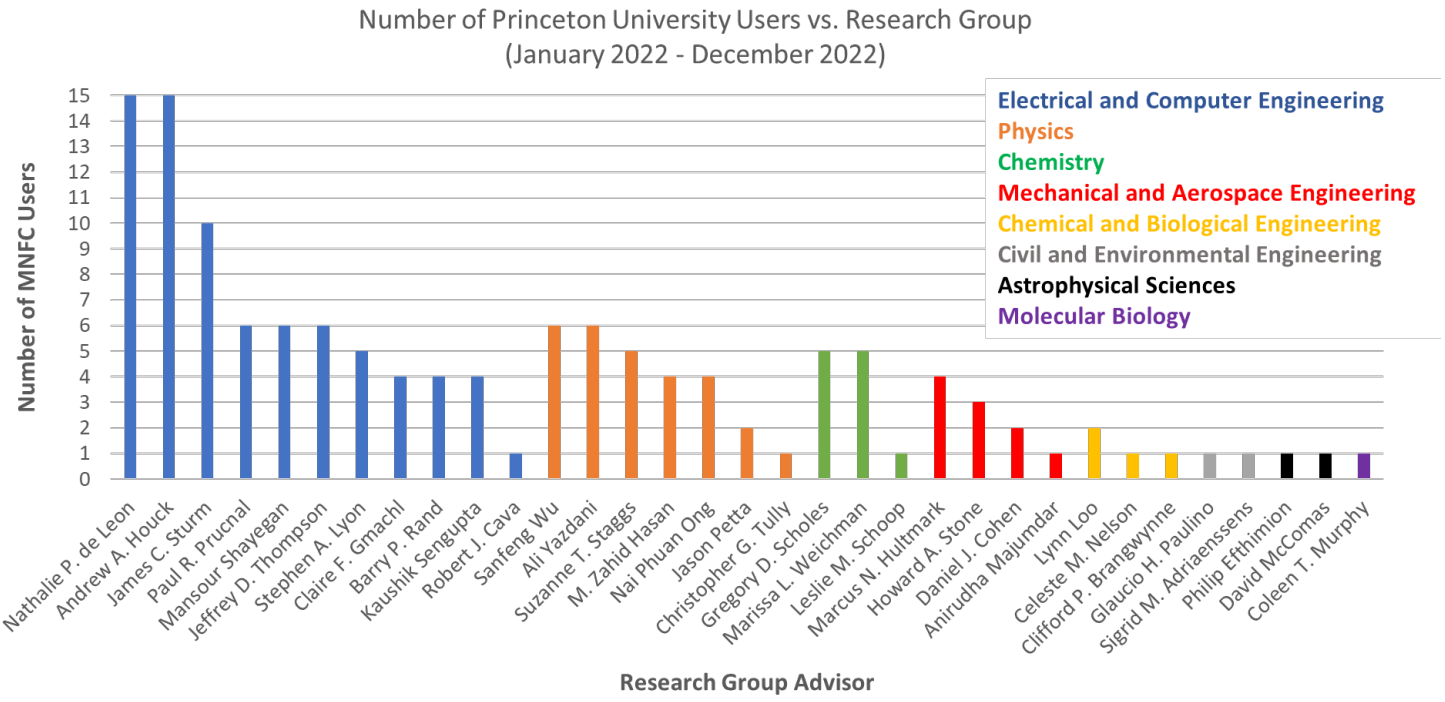

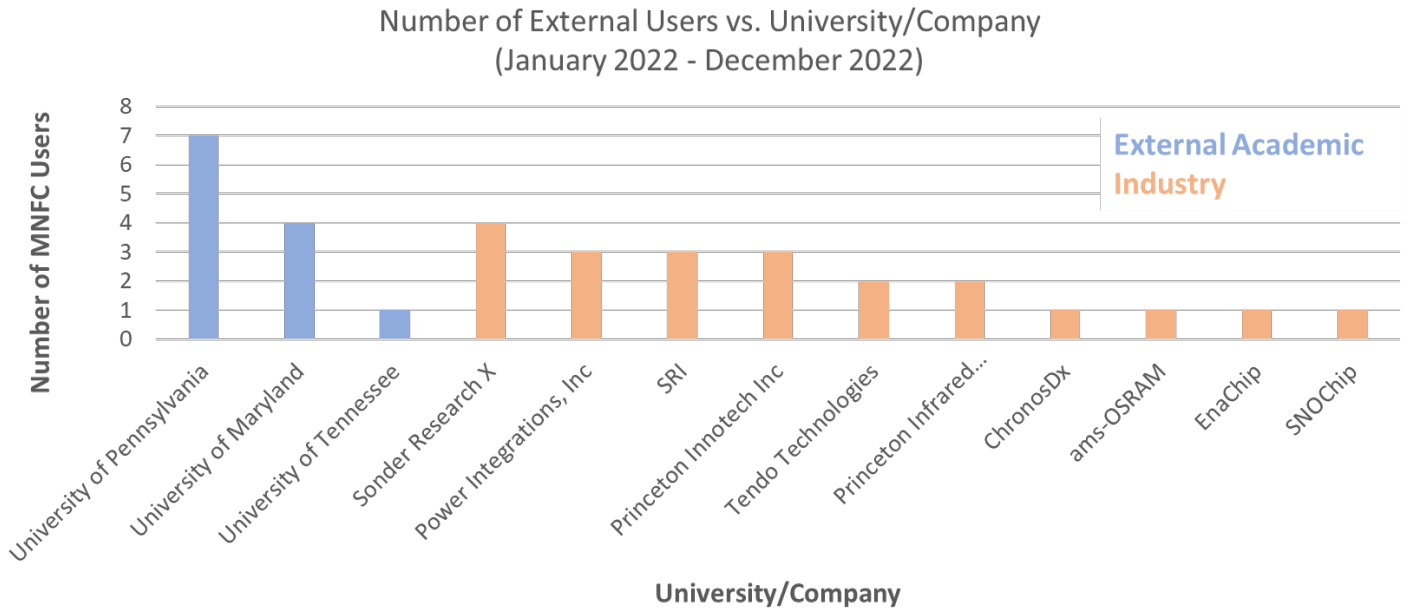

MNFC MAJOR EQUIPMENT

DEPOSITION - PVD

- Angstrom metal sputter with a load lock
- Angstrom metal sputter with no load lock for fast and easy swapping of targets; with an argon ion gun for substrate pre-cleaning
- Angstrom dielectric sputter
- Angstrom dual chamber e-beam evaporator with six pockets, the upper chamber is a load lock for increased pumping speed
- Angstrom Nexdep single-chamber e-beam evaporator with six pockets
- Angstrom Covap thermal evaporator
- Edwards E306A thermal evaporator primarily for Indium evaporation

NANO & MICRO LITHOGRAPHY

- Raith EBPG 5150 high speed and high-resolution e-beam lithography writer, 100kV
- Raith E-Line e-beam writer, 5-30kV
- Heidelberg DWL66+ with grayscale and backside alignment, 900 nm and 2 µm
- Nanonex Nanoimprinter
- Suss MA6, MJB4 mask aligners
- Yield Engineering Systems oven for dehydration, HMDS priming, image reversal

PLASMA ETCH

- PlasmaTherm Versaline Si precision etch: CF_4, CHF_3, C_4F_8, SF6, O_2, Ar (is being installed)
- PlasmaTherm III-V etcher for vertical, smooth sidewalls: Cl_2, BCl_3, $SiCl_4$, CHF_3, SF6, O_2, Ar, N_2 (is being installed)
- PlasmaTherm APEX SLR metal etcher: Cl_2, BCl_3, Ar, O_2, SF6, and CHF_3
- PlasmaTherm APEX SLR diamond etcher: Cl_2, O_2, H_2, N_2, and Ar
- SAMCO 200iPB RIE (III-V and compound semiconductor); Cl_2, BCl_3, $SiCl_4$, Ar, and O_2
- SAMCO 800iPB Deep RIE (Si) using Bosch; SF6, C_4F_8, O_2, CF_4, and Ar
- TePla M4L isotropic asher; O_2, Ar, and CF_4
- PlasmaPro 80 RIE; SF6, CF_4, CHF_3, O_2, Ar, and N_2 use: Si, SiO_2, SiNx, SiC, Al, Al_2O_3
- PlasmaTherm 720 SLR RIE shallow etching of Si, SiO_2, SiNx, some metals, and III/V's: Cl_2, BCl_3, H_2, Ar, O_2, SF6, CF_4

ALD, CVD & THERMAL PROCESSES

- Savannah ALD thermal Al_2O_3
- Oxford PlasmaPro 100 PECVD SiO_2, SiNx, α-Si
- CVD Equipment atmospheric furnace system for oxidation and annealing
- SSI Solaris 150 Rapid Thermal Processing systems

SURFACE CHEMISTRY AND WET PROCESSING

- RCA processing hood
- Semi-Tool Spin Rinse Dryers
- Plasma surface activation
- UV / ozone cleaning
- Critical point dryer
- Automatic developer stations
- Polos chrome etch processor

CHARACTERIZATION & METROLOGY

- Hitachi S-4700 SEM
- KLA Tencor P-15 profilometer, Gaertner ellipsometer
- Filmetrics F40UV reflectometer
- Keyence confocal microscope
- Keyence VHX6000 digital microscope

SOFT MATERIALS & MICROFLUIDICS

- Photonic Professional GT2 high resolution 3D printer
- Form Labs Form2 SLA 3D printers
- Heidelberg microPG101 (direct laser patterning of SU-8, 2µm and 5µm)
- PDMS processing tools: centrifugal mixer, degassing oven, curing oven, spin coater, punch press, plasma cleaner
- SCS Parylene coater
- KLA Tencor D-120 profilometer

PACKAGING

- ADT Dicing Saw (taping, UV curing tools)
- Loomis LSD-100 Scribe/dice
- Wire Bonding: K&S Wedge, Questar Wedge, K&S Ball Bonder
- Logitech Lapping/Polishing System
- Tresky T-3000-FC3-HF Flip Chip Bonder
- West-Bond Manual Epoxy Die Bonder

RESEARCH REPORTS

Astrophysical Sciences

Advisor: David McComas (Astrophysical Sciences, Space Physics Group)

Improving and Understanding the Flight Components for the Solar Wind and Pickup Ion (SWAPI) Instrument Onboard the IMAP Mission

Researcher: **John Teifert**

Sponsorship: N/A

The IMAP mission is a NASA-funded mission that aims to understand the acceleration of energetic particles and the interaction of the solar wind with the interstellar medium [1]. Professor David McComas from the Department of Astrophysical Sciences is leading this mission that constitutes of an international team of 24 partner institutions. The Princeton Space Physics Laboratory at 171 Broadmead is currently the home of the SWAPI instrument onboard the IMAP spacecraft. SWAPI is the first space instrument built by the Princeton Space Physics Laboratory and will provide simultaneous measurements of solar wind particles and pickup ions (PUIs), whose source is beyond our solar system, at 1 A.U. (the distance from the Earth to the Sun). See also figure 1.

To make quality measurements in space, it is crucial to understand the characteristics of the flight components, in which we are fortunate to have the facilities like MNFC and the expertise there to understand and improve our flight parts. Our team has benefited from the PDMS processing tool to perform the parylene coating on electronic boards. This step is crucial to ensure no leakage from the high voltage on the electronic boards and allow safe handling and testing of these boards. Because of the delicate nature of the components used in the construction of space instrumentation, handling is restricted to an extremely small number of qualified personnel. For similar reasons, components and assemblies are subject to extremely strict chain of possession protocols. These requirements sometimes make it unavoidable for team members to travel out of state to vendors with components in hand. The capacity of the MNFC to support SWAPI on the same campus as our lab provides tremendous savings in both travel expense and personnel time.

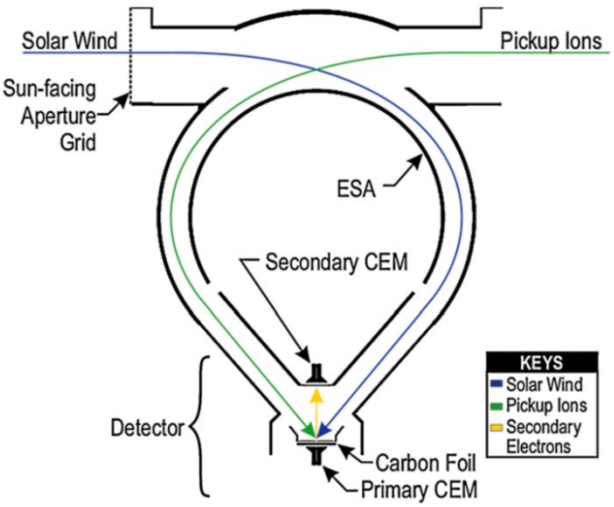

For more details about the IMAP mission and the Princeton Space Physics Laboratory, please visit our website (https://spacephysics.princeton.edu) or our recent news highlight (https://discovery.princeton.edu/2022/12/12/soaking-up-the-sun/).

Figure 1: Cross-sectional view of the SWAPI sensor with blue trajectories that highlight the incident solar wind and green that highlight PUIs. Yellow trajectories show the path of the secondary electrons generated from the foil to provide the coincidence timing.

CITATIONS

- [1] McComas, D.J., Christian, E.R., Schwadron, N.A. et al. Interstellar Mapping and Acceleration Probe (IMAP): A New NASA Mission. Space Sci Rev 214, 116 (2018). https://doi.org/10.1007/s11214-018-0550-1

Advisor: Philip Efthimion (Astrophysical Sciences, Princeton Program in Plasma Physics)

X-Ray Spectroscopy of Laser-Produced Plasmas

Researcher: **B. Frances Kraus** (Princeton Staff Research Physicist)

Sponsorship: Department of Energy

High intensity lasers incident on solid targets generate extreme states of matter. The plasma physics of such hot dense states is difficult to simulate or to study in the laboratory; one avenue of exploration involves x-ray spectroscopy, where line emission from highly ionized plasmas can be used to diagnose plasma parameters. We use the MNFC cleanroom to generate foil targets with embedded tracer layers of a different material, therefore isolating observed x-ray emission to thin regions. This work has allowed investigation of laser ablation at high intensities [1] as well as electron-ion equilibration in stationary, solid-density plasmas [2]. More recently, we have been awarded time in the Department of Energy Fusion Energy Science's LaserNetUS program to use lithographic targets, where tracer material is deposited in dots or stripes. These experiments will hone our understanding of radial gradients in laser-heated plasmas and also provide a window into plasma transport between a hot-dense laser-heated center and the radially surrounding warm-dense matter, where quantum coupling begins overriding ideal plasma physics effects in an understudied intermediate regime.

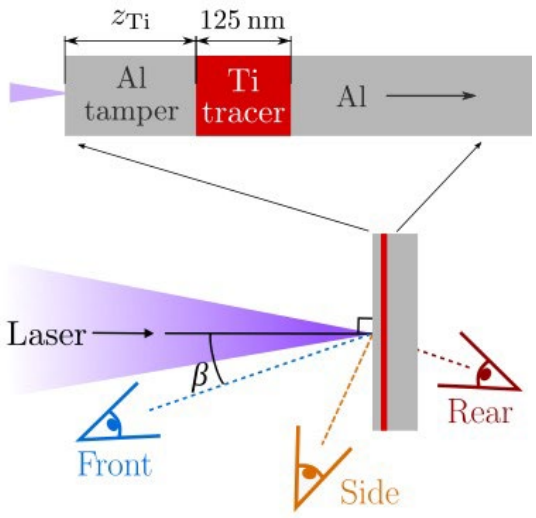

Figure 1: A typical experimental setup, where a high-intensity laser impinges on an aluminum foil target with a titanium tracer layer buried at some depth. The depth of the tracer layer determines the plasma region observed by the three x-ray spectrometers, placed at different viewing angles to isolate the effects of x-ray Doppler shifts and opacity effects. (Adapted from [1].)

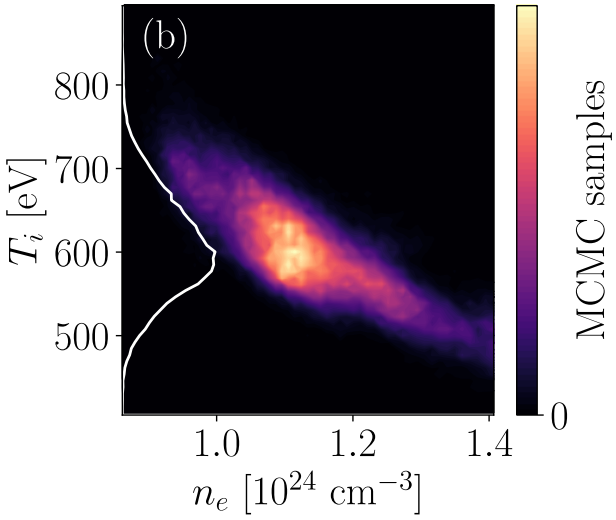

Figure 2: The results of fitting x-ray line shapes from measurements to advanced Stark broadening models. Older models make approximations that neglect penetrating collisions between ambient electrons and radiating ions in dense plasmas; when newer models drop these approximations, modeled line shapes are broadened and shifted with plasma density. Including this effect allows fitting of both plasma density and ion temperature. (Adapted from [2].)

CITATIONS

- [1] B. F. Kraus, L. Gao, W. Fox et al. "Ablating ion velocity distributions in short-pulse-heated solids via x-ray Doppler shifts." Physical Review Letters, accepted (2022).
- [2] B. F. Kraus, L. Gao, K. W. Hill et al. "Solid-Density Ion Temperature from Redshifted and Double-Peaked Stark Line Shapes." Physical Review Letters 127, 205001 (2021).

Chemical and Biological Engineering

Advisor: Clifford P. Brangwynne

Mechanochemical Induction of Nuclear Condensates During Invasive Cancer Cell Confined Migration

Researcher: **Jessica Zhao** (Princeton Graduate)

Sponsorship: HHMI

The physical process of cancer cell metastasis is rate-limited by squeezing the cell nucleus through interstitial spaces, with associated deformation of bulk nucleus material and its constituents. Compared to chromatin and nuclear peripheral lamina networks, proteinaceous membraneless nuclear bodies or condensates are much less understood in their response to mechanical stress. By combining microfluidics and live cell quantitative microscopy, we find that the DNA damage response protein 53BP1 undergoes a switch in phase behavior at the rear of migrating breast cancer cell nucleus, independent of DNA damage pathway. We hypothesize that 53BP1 and potentially other nuclear condensates can sense mechanical stimuli by changing their phase behavior, which is thereby closely coupled to the heterogeneity of the chromatin network they are embedded in. By quantitatively mapping the displacement field of chromatin, we found that chromatin forms spatially distinct domains of correlated motions as well as different strain magnitude. Our finding highlights the mechanical interplay between nuclear condensates and chromatin under physiological deformations and suggests the potential role of LLPS in mechanochemical transduction.

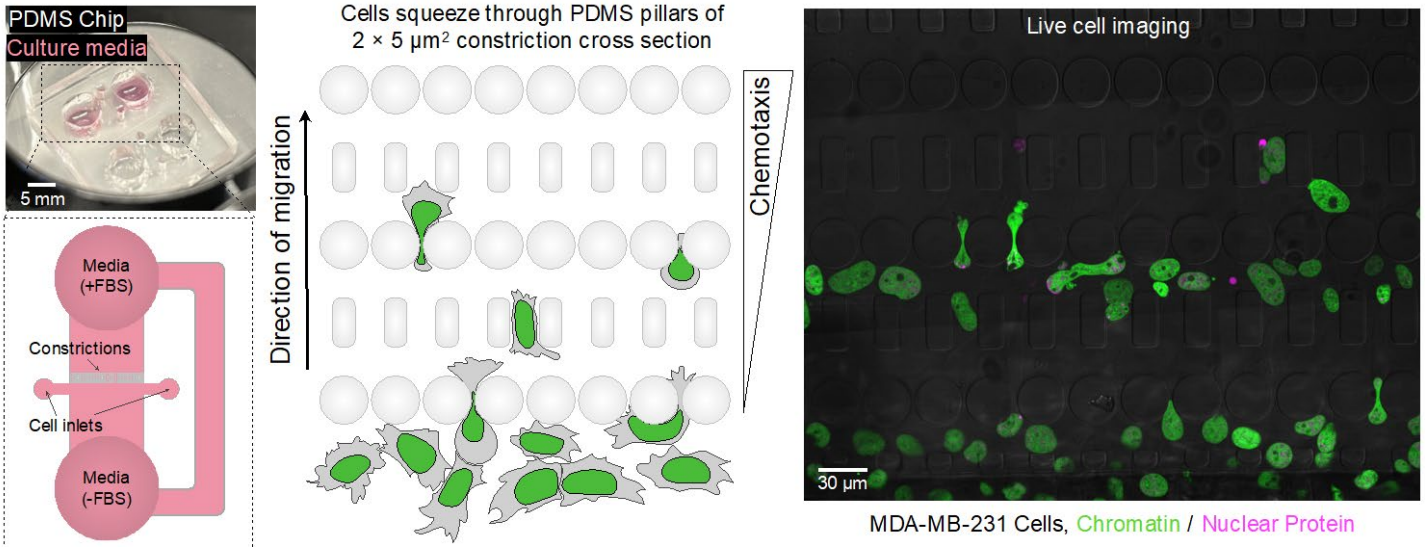

Figure 1: Invasive breast cancer cells migrate through 2-μm constrictions in a microfluidic device. (*Left*) Photo of a PDMS microfluidic device. This device[1, 2] contains cell culture media in the two large reservoirs (5-mm diameter), with and without growth serum FBS. The FBS gradient drives cells to move across the constrictions (indicated with arrow on the schematic) due to chemotaxis. Cells are seeded through the 1-mm diameter inlets. (*Middle*) Zoom in of a region of the constrictions with 2 × 5 μm² cross section area. Green: cell nucleus; Grey: cell cytoplasm. Control region with 15 × 5 μm² constrictions is not shown. (*Right*) Confocal microscopy image of breast cancer cells MDA-MB-231 migrating in the PDMS constrictions. Green: chromatin marker; magenta: nuclear protein 53BP1; grey: brightfield, PDMS.

CITATIONS

- Davidson PM, Sliz J, Isermann P, Denais CM, Lammerding J. (2015) Design of a microfluidic device to quantify dynamic intranuclear deformation during cell migration through confining environments. *Integr Biol* 7:1534-1546
- Keys JT, Windsor A, Lammerding J. (2018) Assembly and use of a microfluidic device to study cell migration in confined environments. *Methods in Molecular Biology*. (In press)

Advisor: Lynn Loo (Chemical and Biological Engineering)

Reliable and Efficient of UV-Absorbing Hexabenzocoronene Derivative Organic Solar Cells

Researcher: **Quinn Burlingame** (Princeton Postdoc)

Sponsorship: Arnold and Mabel Beckman Foundation, Andluca Technologies

UV-absorbing solar cells based on organic and perovskite materials are promising for building integrated smart window applications where transparency and color neutrality are critical. While many transparent electrode materials have been explored, there are tradeoffs to many of these materials. For example, nanowires and nanotubes cause haze, thin metal (i.e. Ag) electrodes have relatively low transparency and give a strong blue tint, and sputtered metal oxides have superior optical and electrical performance but can cause damage to underlying materials. In this work, we develop organic and perovskite absorbers with optimal absorption cutoffs to collect as much non-visible light as possible without noticeably degrading the aesthetic performance of the transparent solar cells. By optimizing sputtering deposition of indium tin oxide top electrodes, we were able to yield solar cells with no aesthetic compromise resulting in world record average visible transparencies (>82%), color rendering indices (>97), while generating sufficient power for IoT devices, and electrochromic devices.

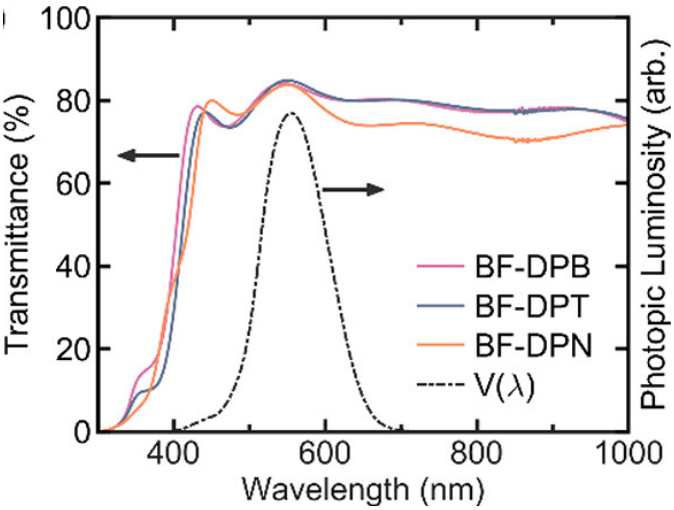

Figure 1. Transmission profiles for full-stack organic solar cells with sputtered top electrodes based on three different organic absorbing donor molecules. The photopic response of the eye is shown in black dashed line for reference, to highlight that the transmission maximum of the solar cells is well aligned.

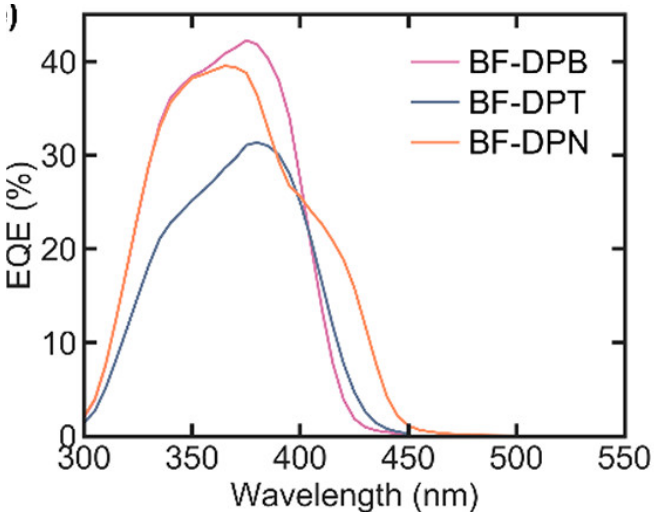

Figure 2. External quantum efficiencies of organic solar cells comprising three organic molecules—2 of which are designed at Princeton. The data show how efficiently the solar cells generate current for photons incident at each wavelength.

CITATIONS

- Melissa Ball, Quinnn Burlingame, Hannah Smith, Tianran Liu, Sean Parkin, Antoine Kahn, Yueh-Lin Loo "Design of UV-Absorbing Donor Molecules for Nearly Imperceptible Organic Solar Cells" ACS Energy Letters, 2022
- Quinn Burlingame, Yueh-Lin Loo "Optical Simulations to Inform the Design of UV-absorbing Organic Materials and Solar Cells" Solar Energy Materials & Solar Cells, 2021
- Tianran Liu, Xiaoming Zhao, Ping Wang, Quinn Burlingame, Junnan Hu, Kwangdong Roh, Zhaojian Xu, Barry Rand, Minjie Chen, Yueh-Lin Loo "Highly Transparent, Scalable, and Stable Perovskite Solar Cells with Minimal Aesthetic Compromise" Advanced Energy Materials, 2022.

Advisor: Lynn Loo (Chemical and Biological Engineering)

Highly Transparent Perovskite Solar Cells for Building Integrated Applications

Researcher: **Tianran Liu** (Princeton Graduate)

Sponsorship: Princeton Intellectual Property Accelerator Fund

Transparent photovoltaics (TPV) have the unique potential to electrify glass surfaces on buildings, vehicles, and electronic devices without impacting aesthetics. UV absorbing TPVs can be far more transparent and color-neutral than their IR counterparts, making them an ideal match for driving low-power applications such as electrochromic windows (ECWs), internet-of-things (IoT) sensors, heads-up displays, and other electronics within smart homes and energy-efficient buildings. Previously, fellow members in my group demonstrated and patented NUV-absorbing organic solar cells that can power variable tint smart windows for lighting and temperature control. However, these organic-based solar cells face a number of challenges before they are ready for practical applications. Critically, the chemically and mechanically fragile organic absorbers are often damaged during the deposition of transparent metal oxide top electrodes deposition, which has in turn limited fabrication yield, and the operational lifetimes of these devices remain low. To circumvent these issues, we proposed to replace the fragile organic absorbers with inorganic metal halide perovskites. These materials are chemically and photochemically stable, they can be easily evaporated to form dense films that are robust and mechanically stable during top electrode deposition. The resulting functional TPV exhibits a record high average visible transmittance and a nearly perfect color rendering index with an extrapolated outdoor lifetime of over 20 years, while maintaining enough power for specific applications.

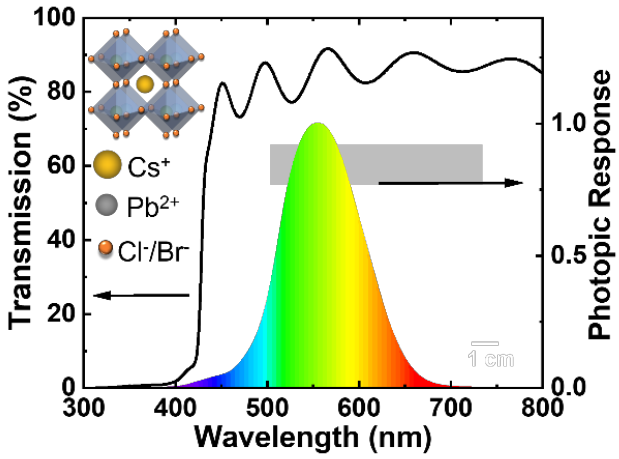

Figure 1. The transmittance spectrum of a $CsPbCl_{2.5}Br_{0.5}$ inorganic TPV with the photopic response of the human eye shown for reference, and the structure of inorganic perovskites as inset.

Figure 2. Photographs taken outdoors of a 25 cm^2 TPV and its photovoltage shown on a multimeter under ambient sunlight.

CITATIONS

- Liu, T.; Zhao, X.; Wang, P.; Burlingame, Q. C.; Hu, J.; Roh, K.; Xu, Z.; Rand, B. P.; Chen, M.; Loo, Y. Highly Transparent, Scalabl and Stable Perovskite Solar Cells with Minimal Aesthetic Compromise. *Adv. Energy Mater.* **2022**, 2200402.

Advisor: Celeste M. Nelson (Chemical and Biological Engineering)

DBiT-seq Platform Development

Researcher: **Pengfei Zhang** (Princeton Postdoc)

Sponsorship: NIH

Spatial omics study is an important tool for developmental biology and tumor biology. DBiT seq is a microfluidic-enabled, highly sensitive platform for spatial omics study with a resolution down to single- cell resolution (10 μm). We used both traditional soft lithography and microPG direct writing and fabricated the microfluidic devices. As a proof-of-concept, we showed the in-situ reverse transcription and ligation worked using the microfluidic device. The current plan is to use the device for embryonic lung development study.

CITATIONS

- Liu, Yang, et al. "High-spatial-resolution multi-omics sequencing via deterministic barcoding in tissue." Cell 183.6 (2020): 1665-1681. Su, Graham, et al. "Spatial multi-omics sequencing for fixed tissue via DBiT-seq." STAR protocols 2.2 (2021): 100532.

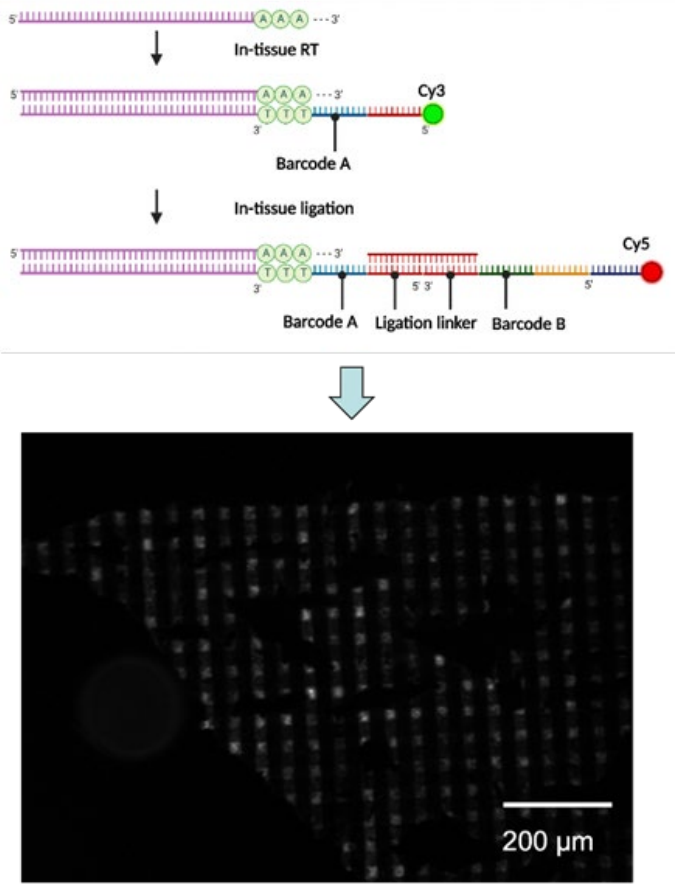

Figure 2: The proof-of-concept for in-situ reverse transcription (RT) and ligation. The resulted tissue section showed expected fluorescent pixel array after in-situ RT and ligation, demonstrating bioassays worked in the tissue section.

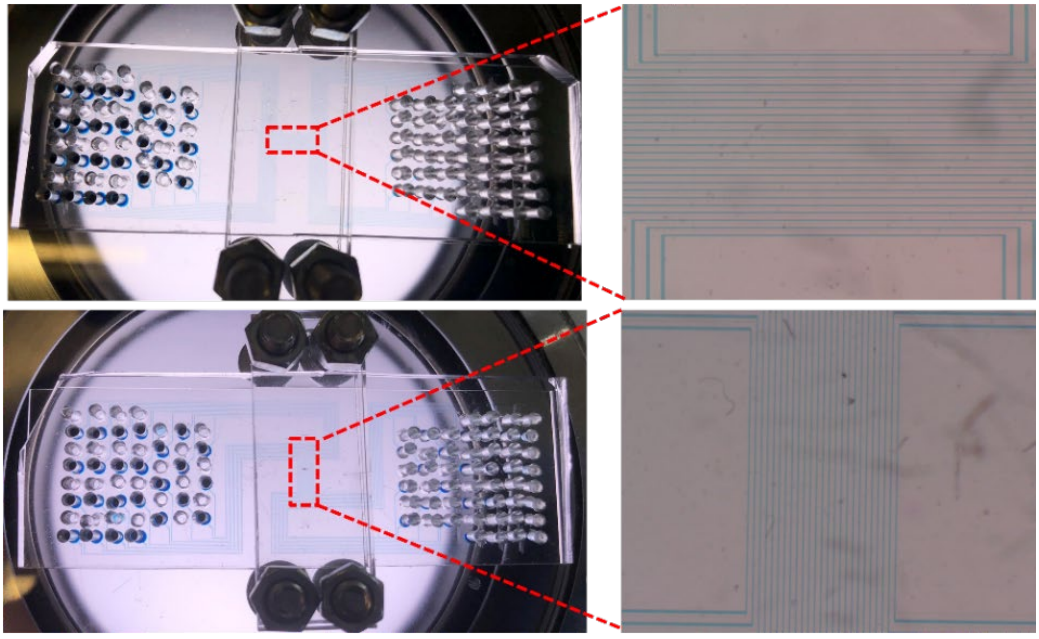

Figure 1: DBiT-seq PDMS chip. Top: PDMS chip 1 of parallel direction was loaded with food dye and PBS, showing the expected alternative pattern. Bottom: PDMS chip 2 of vertical direction was loaded food dye with food dye and PBS, showing the expected alternative pattern as well.

Chemistry

Advisor: Gregory D. Scholes (Chemistry)

Singlet Fission Dynamics in Strong Light-Matter Coupling

Researcher: **Ava Hejazi** (Princeton Graduate)

Sponsorship: Princeton University

This proposal aims to elucidate how the exceptionally low entropy of highly coherent states in strong-coupled systems can be harnessed to control chemical reactivity. We thus propose to study important and well-characterized photophysical processes, such as electron transfer and singlet fission, within systems in microcavities under collective strong light-matter coupling. We specifically aim to investigate how entropy can be leveraged in cavities to accomplish a desired photophysical transformation with less input energy than would be required without strong-coupling. Prior theoretical work predicts that such a transformation would be accomplished through the flow of population from the LP to the dark states, enabled by the large entropic difference between the highly delocalized LP state and the more localized dark states. The realization of this entropy leveraging could provide a new avenue for optimizing photophysical processes, including that underlying solar photochemistry.

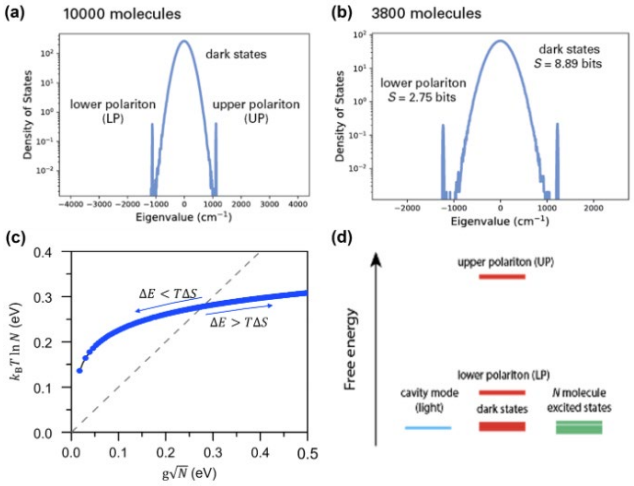

Figure 1. (a) Monte Carlo sampling over 500 samples of 10,000 molecules coupled to the common cavity mode with energy disorder in the molecular lineshape 200 cm-1 and (unitless) cavity strength factor Λ=40 resulting in a coupling strength of g=18cm-1 (b) Similar sampling to panel a, 4,000 molecules in the cavity with only 3,800 effectively coupling to the cavity mode with a cavity strength factor Λ=60 and the von Neumann entropy, S, calculated, (c) The entropy (k_gTlnN) against the electronic energy difference (g\N) between the LP and dark states for varying number of molecules (blue dots) at room temperature (T=300K) with a coupling strength of g=1.24 meV (10cm-1). Gray dashed line indicates the entropic term is equal to the electronic energy difference in Equation 2. In the regime where entropic gain surpasses the energy (left arrow) the dark states are located below the LP state in the free energy scale as seen in Panel (d).

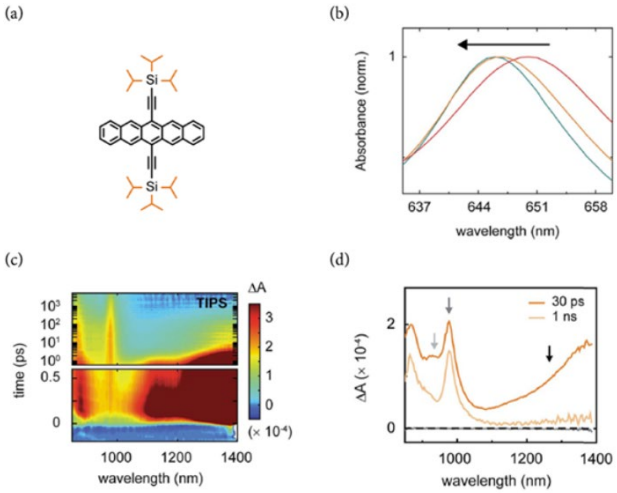

Figure 2. (a) Structure of TIPS-pentacene. (b) Absorbance of three pentacene derivatives (blue curve represents 6,13-bis-(trisecbutylsilylethynyl)pentacene (TSBS-Pn), orange curve represents 6,13-bis-(triisopropylsilylethynyl)pentacene (TIPS-Pn), red curve represents 6,13-bis (triethylsilylethynyl)pentacene (TES-Pn). (c) Transient absorption spectra over time of TIPS-pentacene. (d) Transient absorption spectra of TIPS-pentacene at 30 ns and 1 ns after singlet pumping, with arrows indicating peaks corresponding to singlet (black arrow) and triplet (grey and light grey arrows) excited state absorption.

.

CITATIONS

- DelPo, C. A.; Kudisch, B.; Park, K. H.; Khan, S. U.; Fassioli, F.; Fauusti, D.; Rand, B. P.; Scholes, G. D., Polariton Transitions in Femtosecond Transient Absorption Studies of Ultrastrong Light-Molecule Coupling. J. Phys. Chem. Lett. 2020, 11, 2667-2674

Advisor: Gregory D. Scholes (Chemistry)

Cavity Controlled Reverse Intersystem Crossing

Researcher: **Jessica Gaetgens** (Princeton Graduate)

Sponsorship: Moore Foundation

In the literature, the rate of reverse intersystem crossing (RISC) for thermal activated delayed fluorescence (TADF) molecules has been demonstrated to be both influenced and uninfluenced by electronic strong coupling to a cavity mode. The rate of RISC has been proven to change only for two molecules that undergo phosphorescence at room temperature in addition to TADF. This proposal would seek to (1) confirm room-temperature phosphorescence is a necessary characteristic for influencing the rate of RISC in a cavity and (2) understand what characteristics related to room-temperature phosphorescence lead to the change in rate (i.e. the effect on polariton lifetime, coupling strength, symmetry, etc.).

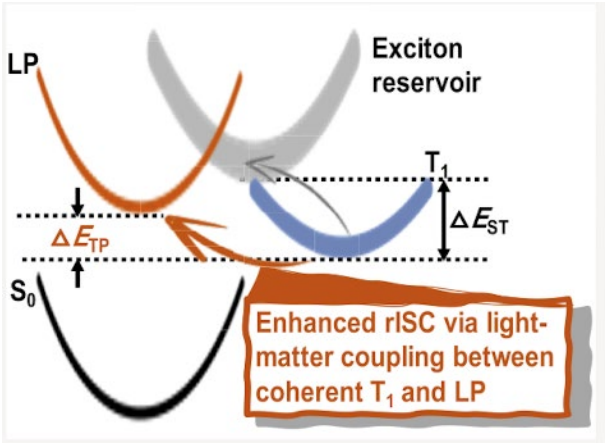

Figure 1. The energy differences between the RISC from the T1 to the lower polariton (LP) state vs the RISC to the singlet when light-matter coupling is present.

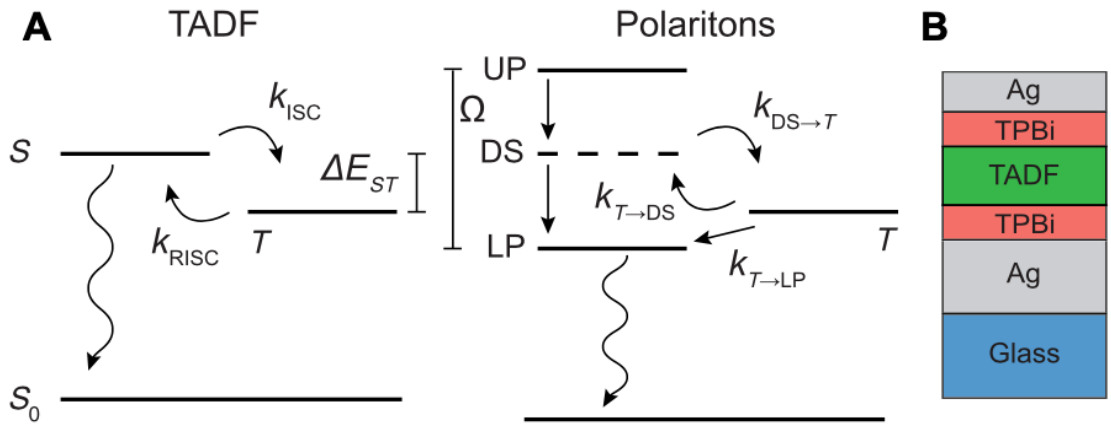

Figure 2. Energy diagrams showing TADF and RISC with polaritons (A). The structure of a cavity (B).

CITATIONS

- https://pubs.acs.org/doi/10.1021/acs.jpclett.1c02644
- Ou, Q.; Shao, Y.; Shuai, Z. Enhanced Reverse Intersystem Crossing Promoted by Triplet Exciton–Photon Coupling; Journal of the American Chemical Society 2021, 143 (42), 17786–17792.
- Eizner, E.; Martínez-Martínez, L. A.; Yuen-Zhou, J.; Kéna-Cohen, S. Inverting Singlet and Triplet Excited States Using Strong Light-Matter Coupling. Science Advances 2019, 5 (12).

Advisor: Gregory D. Scholes (Chemistry)
Controlling Biological Systems using the Quantum Vacuum
Researcher: **Avery Cirincione-Lynch** (Princeton Graduate)
Sponsorship: The Gordon and Betty Moore Foundation

We will transfer our current method of studying microtubule tryptophan fluorescence decay quenching as a function of AMCA label density, see picture below. However, the sample will be in a Fabry-Perot cavity tuned to resonance with tryptophan absorption. The microtubules are long, and will lay down parallel to the cavity mirrors. In recent theoretical work we predict a strong change of the energy transfer rate owing to strong light-matter coupling, where chromophores have this orientation.

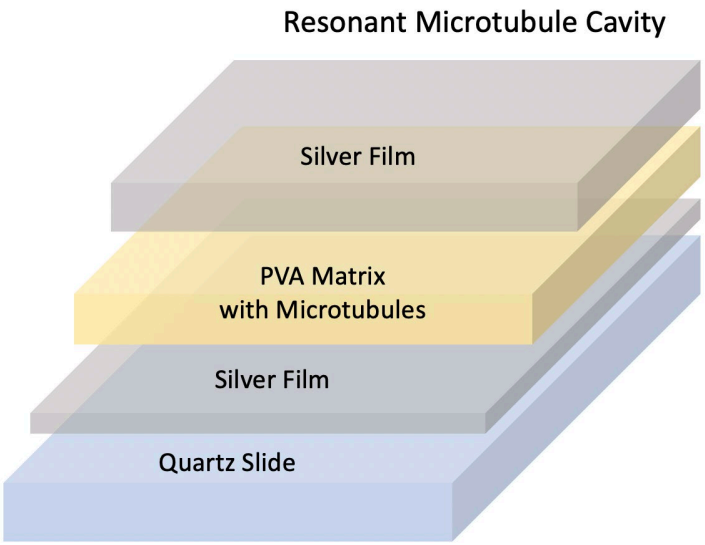

Figure 1: Design for a Fabry-Perot cavity resonant with the absorption of microtubules.

CITATIONS

- J. Phys. Chem. Lett. 2020, 11, 7, 2667 2674
- J. Phys. Chem. Lett. 2021, 12, 40, 9774 9782

Advisor: Gregory D. Scholes (Chemistry)

Cavity Coupling of Molecular Systems

Researcher: **Courtney DelPo** (Princeton Graduate)

Sponsorship: Gordon and Betty Moore Foundation

Electronic strong coupling enabled through the careful design of Fabry-Perot type cavity structures leads to the formation of hybrid light-matter states called polaritons. As hybrid light-matter states, polaritons adopt new and desirable properties that are not accessible with purely matter states. Among this list is enhanced delocalization, a property that can increase the efficiency of bilayer organic photovoltaics by providing a mechanism for transporting excitations outside of the exciton diffusion limit of the absorbing material to the charge-generating donor-acceptor interface. The often-fast decay of the polariton to the ground state, however, can be a significant barrier to the utilization of the hybrid light-matter properties including the enhanced delocalization. We employed femtosecond pump-probe spectroscopy to address the key question of whether or not the decay pathway for the polariton through charge transfer is fast enough to outcompete the decay pathway of the polariton to the ground state in a bilayer donor-acceptor cavity system.

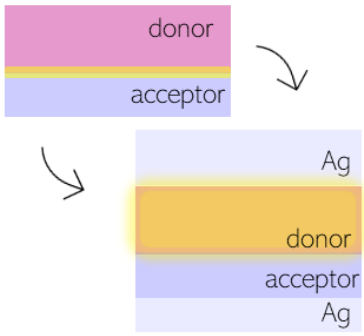

Figure 1: The delocalization of the polariton provides an alternative and more efficient method for bringing excitations to the charge-generating interface in an organic bilayer solar cell structure. The new structure could enable a higher power conversion efficiency of the organic bilayer photovoltaic.

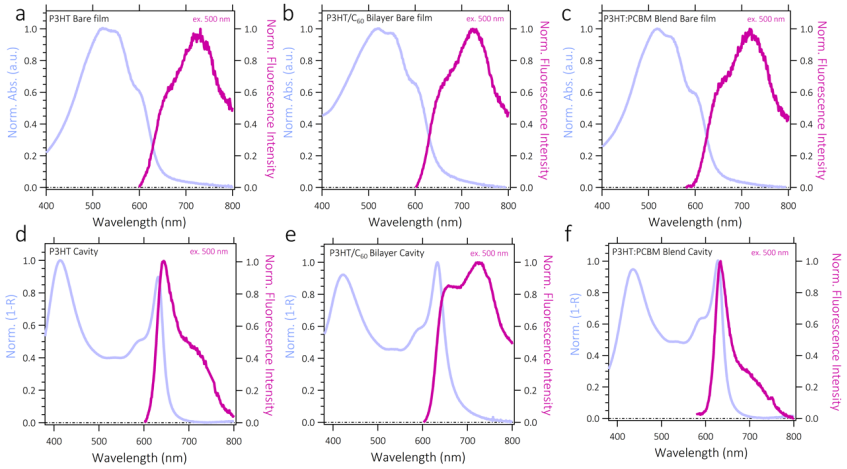

Figure 2: Steady state characterization of the cavity systems and bare film controls. Absorption and fluorescence of the bare P3HT film (a), the bare P3HT/C60 bilayer film (b), the bare P3HT:PCBM blend film (c), and the corresponding cavity systems (d-f) The fluorescence of the P3HT/C60 bilayer cavity (e) displays prominent contribution from uncoupled molecules (UM) which is in contrast to the LP dominated fluorescence of the P3HT cavity (d) and the P3HT:PCBM blend cavity (f). Charge transfer can occur in the bilayer and quench the lower polariton fluorescence, but is too slow to compete with the charge transfer from the uncoupled molecules in the blend.

CITATIONS

- DelPo et al., J. Phys. Chem. Lett. 2021, 12, 40, 9774–9782
- DelPo et al., J. Phys. Chem. Lett. 2020, 11, 7, 2667–2674

Advisor: Leslie M. Schoop (Chemistry)

Physical Properties of Novel 2D Materials

Researcher: **Nitish Mathur** (Princeton Postdoc)

Sponsorship: The Gordon and Betty Moore foundation

Our research focus on synthesis and physical property characterization of layered magnetic and novel two-dimensional (2D) materials to explore the layer dependent properties of quantum materials.1 Currently, we are working on a 2D van der Waals (vdW) high mobility metal, $TaCo_2Te_2$, which has shown potential for high temperature magnetic ordering.2 We were able to exfoliate a thin flake of $TaCo_2Te_2$ and fabricated electron beam lithography patterned device shown in Figure 1 using MNFC fabrication facilities. Preliminary transport measurements collected on the nanodevice clearly show highly anisotropic magnetoresistance (MR%) when the direction of applied current is parallel ($\rho_{\parallel}$) and perpendicular ($\rho_{\perp}$) to the applied magnetic field (Figure 2). This transport behavior could result from interaction of charge carrier with long range spin ordering in $TaCo_2Te_2$ thin flake. Further, we are trying to exfoliate $TaCo_2Te_2$ down to few layers (1-3 layers) to study magnetic ordering even down to monolayer limit.

Figure 1: Optical image of electron beam lithography patterned device on $TaCo_2Te_2$ thin flake (10 nm thickness).

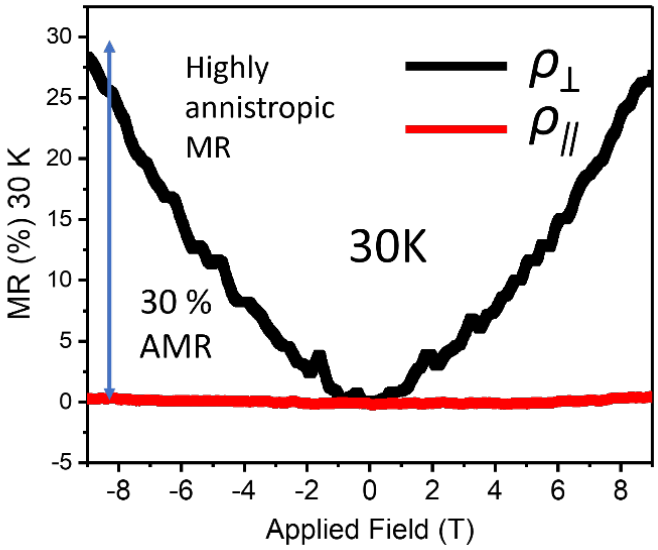

Figure 2: Anisotropic magnetoresistance (AMR) of $TaCo_2Te_2$ nanodevice when the direction of current flow is parallel and perpendicular to applied magnetic field.

CITATIONS

- X. Song, F. Yuan, and L. M. Schoop. The properties and prospects of chemically exfoliated nanosheets for quantum materials in two dimensions. Invited Review & Featured Article: Applied Physics Review 8, 011312 (2021)
- Singha, R., Yuan, F., Cheng, G., Salters, T. H., Oey, Y. M., Villalpando, G. V., Jovanovic, M., Yao, N., Schoop, L. M., $TaCo_2Te_2$: An Air-Stable, High Mobility Van der Waals Material with Probable Magnetic Order. Adv. Funct. Mater. 2022, 32, 2108920.

Advisor: Marissa L. Weichman (Chemistry)

Polariton Reaction Dynamics: Fundamental Mechanisms and Applications to Photocatalysis

Researcher: **Adam D Wright** (Princeton Postdoc)

Sponsorship: DOE

In our study, we have formed gas-phase molecular polaritons in a low-temperature, low-pressure regime. By thermalizing methane within a cryogenic buffer gas cell, we are able to create a molecular sample that is both cold and dense, enabling us to access the strong coupling regime within a Fabry-Pérot cavity constructed around the cell. The cavity mirrors were made by depositing 11nm of Au onto planoconcave CaF_2 substrates using the Angstrom Engineering Nexdep electron beam evaporator in the MNFC cleanroom.

When we tune the cavity length such that the v3 J=3⟶4 transition of methane at 3057.687423 cm^{-1} is resonant with a cavity fringe, flowing methane into the intracavity cell results in a splitting of the resonant cavity fringe. Using a classical Lorentz oscillator model, we simulate the observed transmission spectra. We confirm that the dependence of splitting on molecular number density and cavity detuning is consistent with that expected for Rabi splitting in the strong coupling regime. Therefore, our experimental setup has great potential for investigating how chemical reactivity is modified by the formation of molecular polaritons.

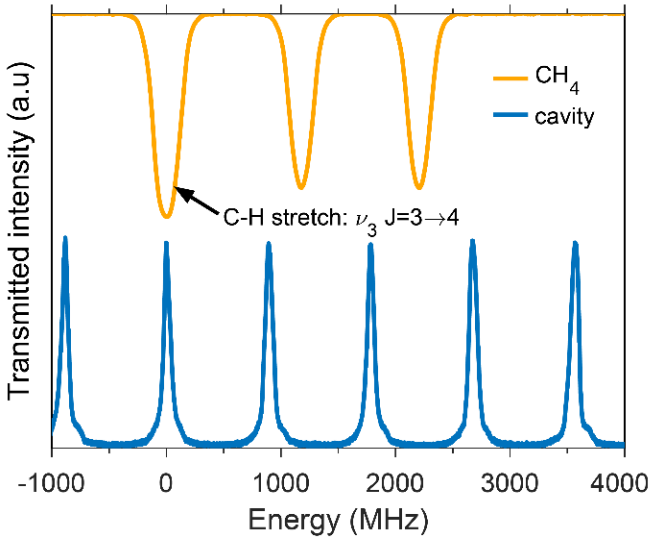

Figure 1: Transmission spectra of the Fabry-Pérot cavity and methane at 120 K, referenced against 3057.687423 cm^{-1} (corresponding to 0 MHz)

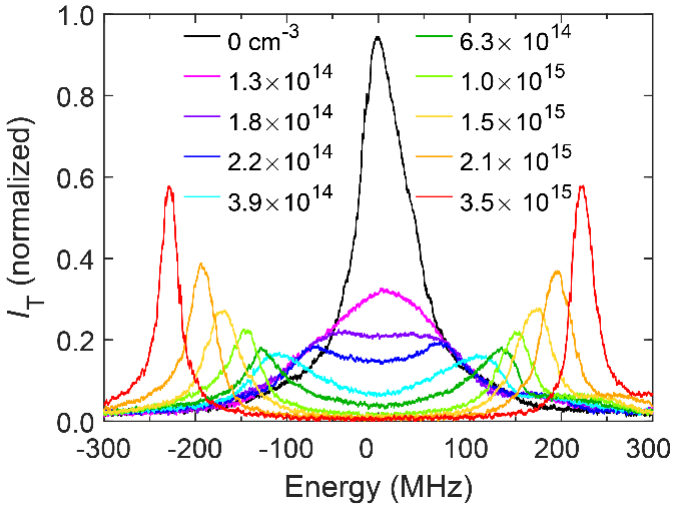

Figure 2: Dependence of the cavity transmission spectrum (I_T) on the number density of methane, demonstrating the Rabi splitting expected for the strong coupling regime.

CITATIONS

- N/A

Advisor: Marissa L. Weichman (Chemistry)

Condensed Phase Polaritons

Researcher: **Alexander Mckillop** (Princeton Graduate)

Sponsorship: Princeton Catalysis Initiative (PCI)

Matching one mode of an optical cavity with the molecular transition of a species within the cavity can create a hybrid light-matter state called a polariton. While we have, so far, been able to create flow cells to harbor vibrational polaritons, the same cannot be said when coupling to electronic transitions. By fabricating nanometer-scale optical cavities with the resources available in the cleanroom, we aim to create electronic polaritons in a flow cell environment and study chemistry within this regime.

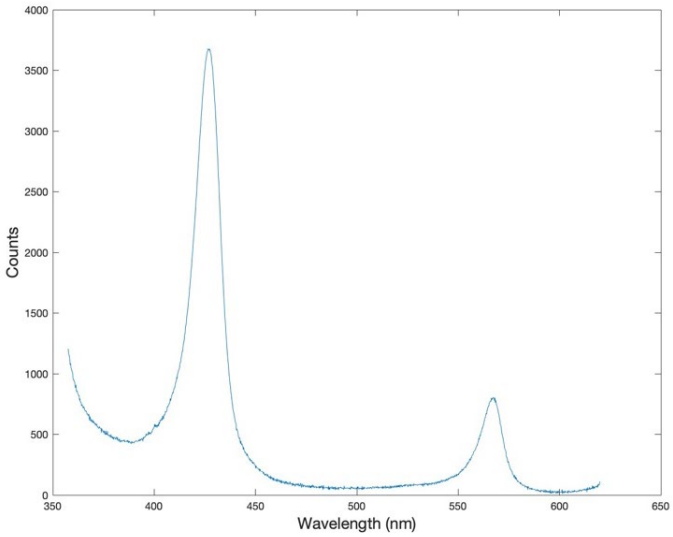

Figure 1: Cavity modes of a nanometer-scale etalon when placed in the path of a white light continuum.

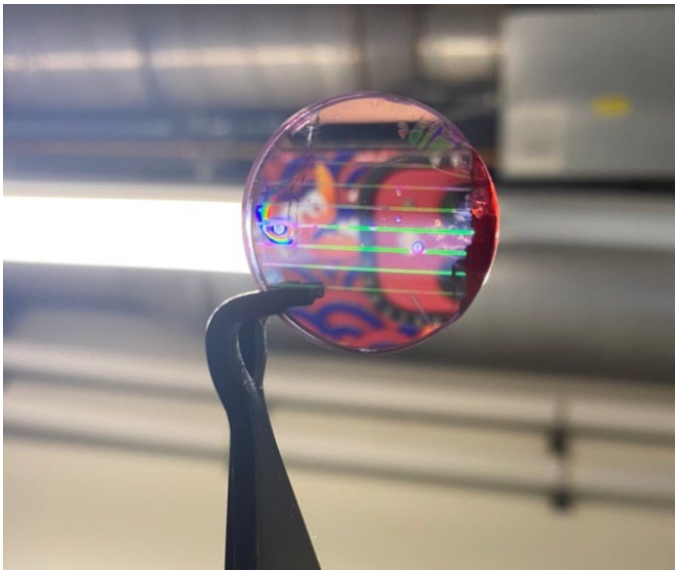

Figure 2: Optical cavities seen etched into borosilicate windows. Here, a laser dye has been brought into the cavities via capillary action.

CITATIONS

- N/A

Advisor: Marissa L. Weichman (Chemistry)

Quantum Control of Chemical Reactions via Vibrational Strong Coupling in Optical Microcavities

Researcher: **Ashley Fidler** (Princeton Postdoc)

Sponsorship: Princeton Catalysis Initiative

Quantum control of chemical reactions via light-matter interactions promises to revolutionize transformational chemistry, providing new avenues to generate desirable products or useful energy for a plethora of industrial and research applications. Polaritons, or delocalized hybrid light-matter states that arise due to strong coupling interactions between a molecular ensemble and a confined electromagnetic field of an optical microcavity, may facilitate command over the chemical reaction energetics, dynamics, and products. In this research endeavor, we will build a first-principles understanding of molecular reactivity under vibrational strong coupling by measuring the ultrafast kinetics and dynamics of benchmark condensed phase reactions, including elementary hydrogen abstractions of simple radicals (CN, Cl, and F) with small molecules (chloroform, acetonitrile, cyclohexane, acetone, and tetrahydrofuran), and excited state electron transfer reactions of organometallic donor-acceptor complexes. To interrogate these systems under strong coupling, we will design and manufacture robust optical microcavity architectures that permit the measurement of state-dependent chemical dynamics in situ using ultrafast transient absorption and femtosecond stimulated Raman spectroscopies. These critical experiments will not only augment the growing body of chemical transformations considered under strong coupling, but also provide tractable model systems for theoretical analysis, informing prospects for using the new degrees of freedom afforded by cavity coupling to steer increasingly complex chemistry.

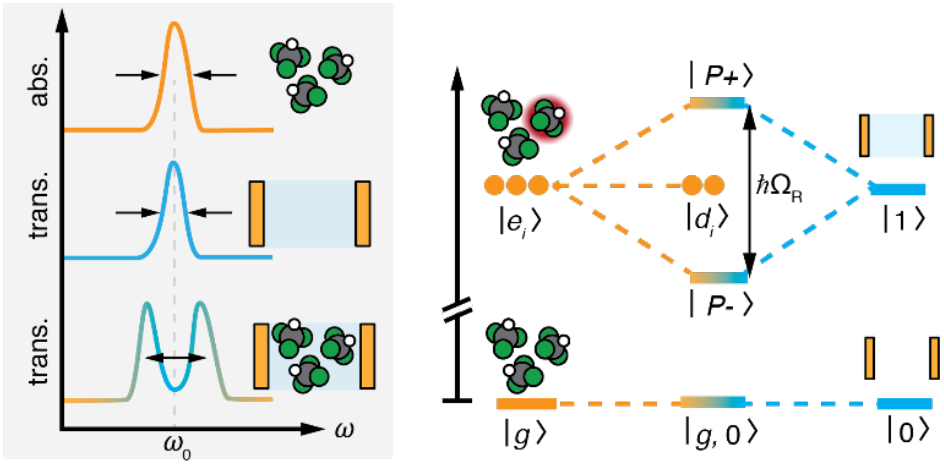

Figure 1: Polariton formation in Fabry-Pérot cavities.

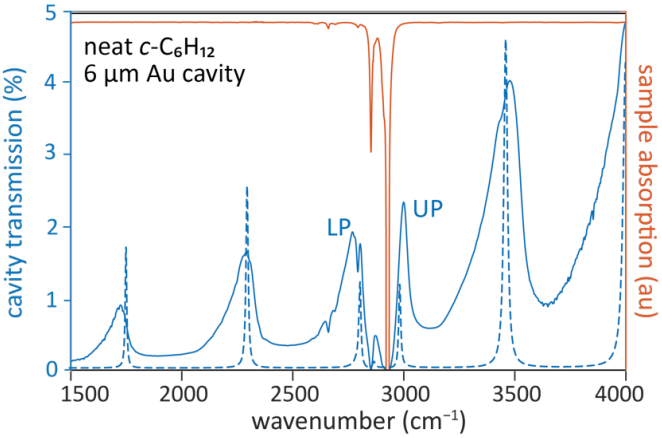

Figure 2: Strong light-matter coupling of the C-H stretch of cyclohexane in a cavity composed of fabricated Au mirrors.

CITATIONS

- N/A

Advisor: Marissa L. Weichman (Chemistry)

Cold Molecular Polaritons: Low-Temperature Reaction Kinetics under Strong Light-Matter Coupling

Researcher: **Jane Nelson** (Princeton Graduate)

Sponsorship: Startup

Polaritons are hybrid light-matter quantum states that pose a unique avenue of physical chemistry exploration because of their prospects of altering reaction speeds and outcomes. Polaritons in the condensed phase have been observed and their reactivity continues to be probed but the complexity of solvation effects limits the connection of current experimental work to quantum chemical theory. The gas phase is the next frontier for observing and probing these quantum states with careful experimental control and limited environmental effects. To achieve strong light-matter coupling in gases, we construct a Fabry-Perot optical cavity with sufficiently reflective mirrors around a cryogenic buffer gas cell. The allowed energies of transmission through the cavity, cavity modes, are approximately evenly spaced in a small range of wavelengths. By sweeping a continuous wave laser aligned through the cavity and centered near molecular transitions of interest, we observe the splitting of a cavity mode when it is on-resonance with an excitation of the sample. To align this laser with the cavity to maximize coupling with the molecular mode of interest, custom Au-coated mirrors produced in the MNFC Cleanroom are required. We have demonstrated molecular vibrational polaritons in the gas phase for the first time in a forthcoming paper using methane gas and future work will probe reaction kinetics in this novel regime.

.

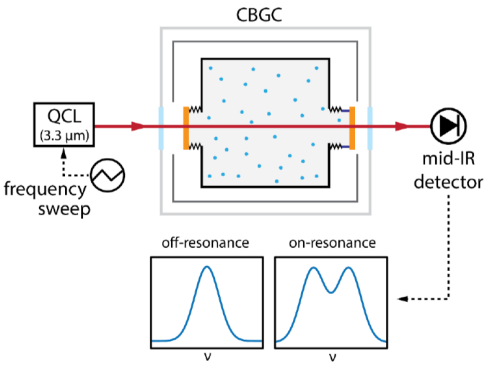

Figure 4: Spectroscopic scheme to measure the achieved Rabi splitting for CH_4 in the cryogenic buffer gas cell (CBGC). A distributed feedback quantum cascade laser (QCL) operating near 3.3 μm will be aligned through the cavity and onto a HgCdTe mid-infrared detector. A sawtooth voltage signal is applied to the QCL chip to slowly sweep the lasing frequency through resonance with the cavity. When the cavity is tuned off-resonance with the molecular absorption, the cavity transmission will show the ~50 MHz fwhm cavity lineshape. When the cavity is on-resonance, the Rabi splitting should appear in the cavity transmission.

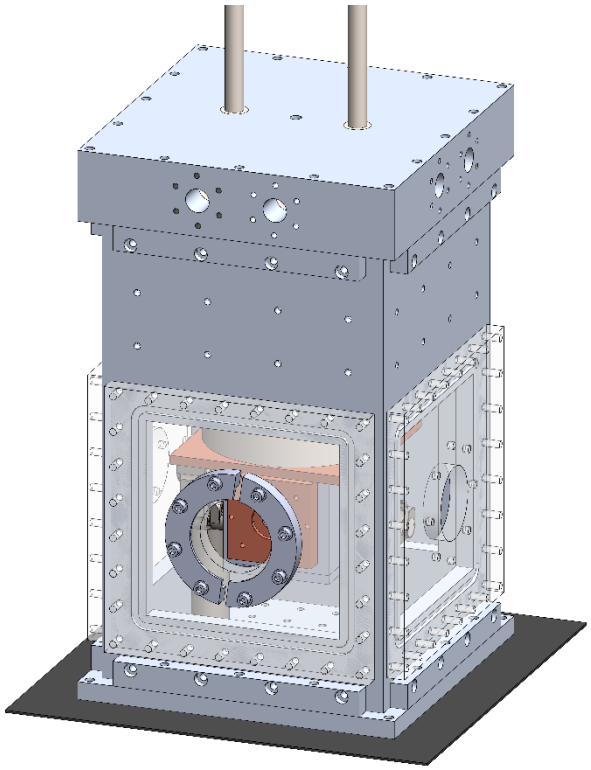

Figure 2: Full assembly of the gas cell enclosure

Figure 1: Spectroscopic scheme to measure the achieved Rabi splitting for CH_4 in the cryogenic buffer gas cell.

CITATIONS

- N/A

Advisor: Marissa L. Weichman (Chemistry)

Polariton Reaction Dynamics: Fundamental Mechanisms and Applications to Photocatalysis

Researcher: **Liying Chen** (Princeton Graduate)

Sponsorship: Start-up Budget

The emerging field of polaritonics using strong light-matter interactions to fine-tune molecular and material properties and behavior offers a potentially paradigm-changing means to direct chemical processes and functionalize materials. Polaritonic devices which engineer strong light-matter interactions in molecules have promise for rationally steering chemistry and energy transfer, while semiconductor exciton-polaritons have myriad applications for photonic devices, the demonstration of Bose-Einstein condensates, and low-threshold lasing. These technologies typically rely on planar microcavities or plasmonic nanostructures to encapsulate material within confined fields of light. Not only must cavity devices be delicately constructed, they also impede physical and optical access to intracavity material, limiting their practical applications. Strong and even ultrastrong light-matter coupling have recently been achieved for molecules embedded in slab cavities composed of layered dielectric films designed to partially confine light. This proposal investigates strong light- matter coupling at slab cavity interfaces to enable flexible and accessible polaritonic platforms for surface chemistry and functionalization of 2D materials.

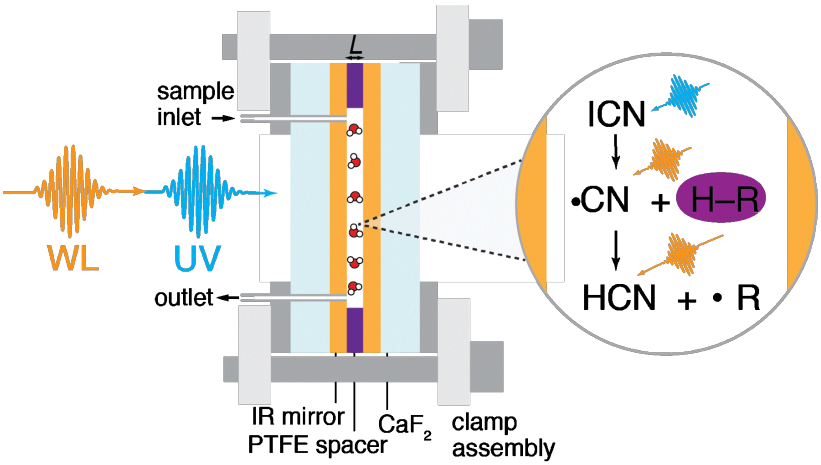

Figure 1: UV pump (250nm): Ultrafast photolysis of ICN to generate cyanide radicals.

White Light (WL) probe: Records the progress of the chemical reaction.

IR monitor: Establishes strong coupling of the C-H stretch of $CHCl_3$.

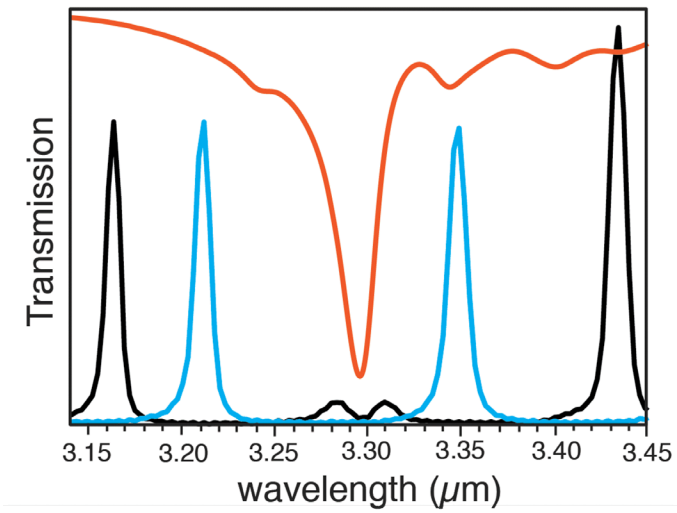

Figure 2. Tuning the cavity length shifts the frequency of the cavity mode on and off resonance with the CH stretch of $CHCl_3$.

CITATIONS

- N/A

Civil and Environmental Engineering

Advisor: Sigrid M. Adriaenssens (Civil and Environmental Engineering)
Multimaterial Freeform Micromanufacturing Enabled by Origami
Researcher: **Derosh George** (Princeton Postdoc)
Sponsorship: Princeton University Grant - HMEI Urban Challenge

In recent years, origami has gained the attention of the microfabrication community as it has enabled applications, including micromirrors, encapsulation devices, and microgrippers. However, origami-based fabrication methods available for millimeter and sub-millimeter objects are often confined to a narrow scope with product-specific synthesis strategies and limited control over the final shape. Therefore, generalized fabrication methods for origami at these scales are of great interest, preferably a method that takes a soft model as input and produces the corresponding physical model, as illustrated in Figure 1. The small length scales of these systems demand the implementation of self-folding or assisted folding methods as the fabrication approaches, contrary to a manual folding method often seen at large scales.

In this work, we demonstrate an origami microfabrication strategy involving a self-folding method to achieve complex bi-directionally folded shapes, as shown in Figures 1 and 2. Single-layer films of photopolymer with patterned properties along their in-plane domain and across the thickness are used to create the planar precursor films of the origami structures. The precursor film is devised such that the developer solution that removes the non-crosslinked polymer chains is inhomogeneously absorbed throughout the cross-section of the fold regions. This inhomogeneity in concentration and the resulting selective removal of the non-crosslinked polymer chains cause a targeted local bending when the developer is removed via heating. This diffusion-based self-folding method exhibits fold-angle tunability, allowing for the programming of the folds to attain targeted fold angles. By combining this programmability with one of the origami unfolding methods, this study establishes an end-to-end microfabrication method for three-dimensional shapes. This method, enabled by patterned films produced using multi-exposure photolithography, shows promise for the freeform fabrication of millimeter and submillimeter origami systems.

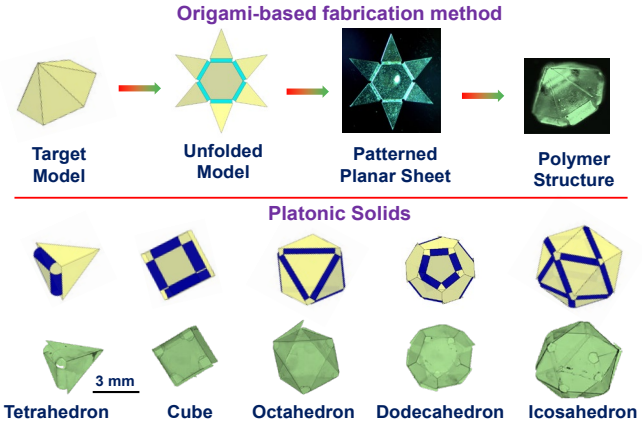

Figure 1: Origami-based fabrication method: An end-to-end fabrication method starting with a target model and ending with the corresponding physical model. **Platonic solids:** Examples of shapes with positive Gaussian curvature involving only unidirectional folding.

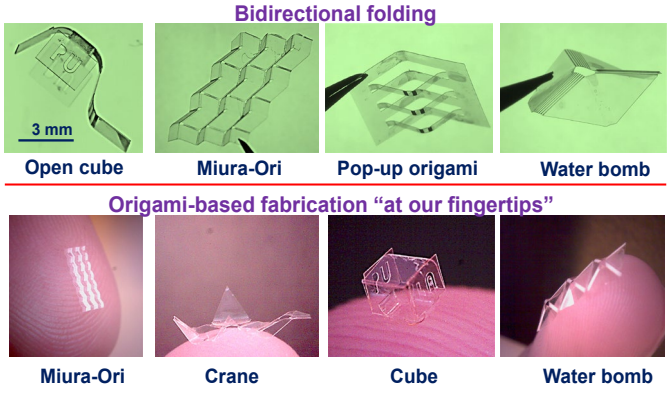

Figure 1: Bidirectional folding: Sample shapes fabricated using bidirectional self-folding of the polymer film. Millimeter and submillimeter shapes fabricated using Origami-based fabrication are placed on the fingertip for scale reference.

CITATIONS

- N/A

Electrical Engineering

Advisor: Robert J. Cava (Electrical Engineering)
Transduction
Researcher: **Chen Yang** (Princeton Graduate)
Sponsorship: Brookhaven

Recently, using the strong microwave and optical transitions of a cloud of Rydberg atoms at microkelvin temperatures, a conversion efficiency of 0.3% was achieved with a 4-MHz bandwidth [23]. Collective spin excitations within a ferromagnet (magnons) have also been suggested. These resonances interact strongly with microwave cavity fields because of the very high density of spins. Low-efficiency upconversion has been demonstrated in a ferromagnetic crystal of yttrium iron garnet (YIG), limited by the weak coupling of the magnons to the optical field [24 27]. Everts, Jonathan R., Matthew C. Berrington, Rose L. Ahlefeldt, and Jevon J. Longdell. *Microwave to Optical Photon Conversion via Fully Concentrated Rare-Earth-Ion Crystals*. Physical Review A 99, no. 6 (June 21, 2019).

Figure 1: The crystal growth technique called floating zone that is used commonly to grow oxides with high melting temperature.

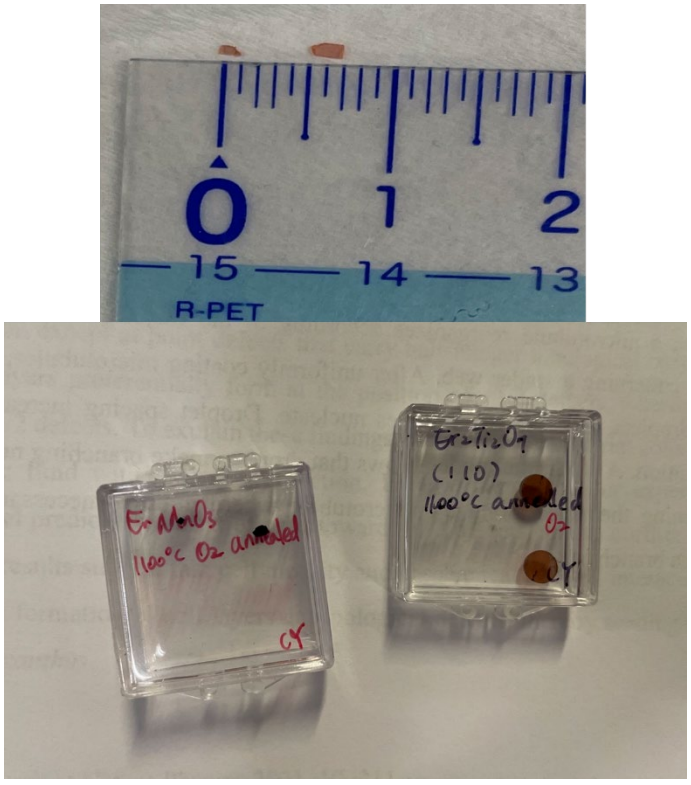

Figure 2: Upper: 1~2mm sized $ErVo_4$ double-side polished crystals. $ErVO_4$ is a anti-ferromagnetic crystal. Lower: $ErMnO_3$ (left) and $Er_2Ti_2O_7$ (Right) crystals. Both double-side polished. $ErMnO_3$ is a ferrimagnetic perovskite. $Er_2Ti_2O_7$ is a pyrochlore with frustrated magnetism.

CITATIONS

- Everts, Jonathan R., Matthew C. Berrington, Rose L. Ahlefeldt, and Jevon J. Longdell. Microwave to Optical Photon Conversion via Fully Concentrated Rare-Earth-Ion Crystals. Physical Review A 99, no. 6 (June 21, 2019)

Advisor: Nathalie P. de Leon (Electrical Engineering)

Observation Hybrid III-V Diamond Photonic Platform for Quantum Nodes Based on Neutral Silicon Vacancy Centers in Diamond

Researcher: **Sean Karg** (Princeton Graduate)

Sponsorship: AFOSR; NSF; DARPA

Integrating atomic quantum memories based on color centers in diamond with on-chip photonic devices would enable entanglement distribution over long distances. However, efforts towards integration have been challenging because color centers can be highly sensitive to their environment, and their properties degrade in nanofabricated structures. Here, we describe a heterogeneously integrated, on- chip, III-V diamond platform designed for neutral silicon vacancy (SiVo evanescent coupling to SiVo centers near the surface of diamond, the platform will enable Purcell enhancement of SiVo emission and efficient frequency conversion to the telecommunication C-band. The proposed structures can be realized with readily available fabrication techniques.

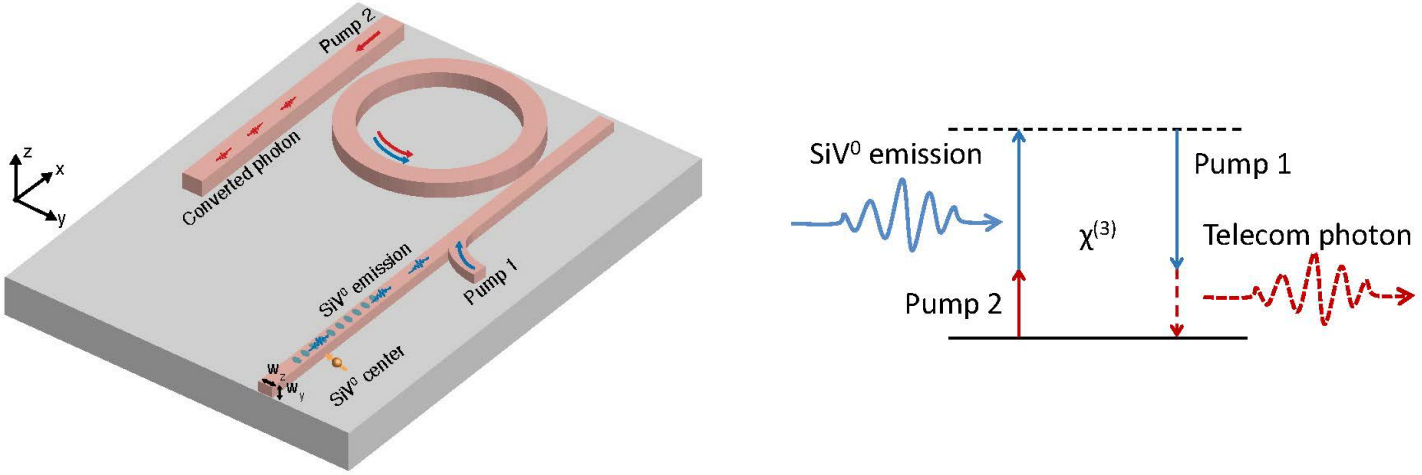

Figure 1: Schematic illustration of the hybrid III-V diamond photonic platform. III-V material (pink) is patterned on top of the diamond substrate (grey). The SiVo center near the diamond surface is evanescently coupled to a nanobeam photonic crystal cavity with a width of *wy* and a thickness of *wz*. The emitted photon is routed to an on-chip frequency conversion module, where FWM-BS scheme is used to translate the signal to single photon at the telecommunication C-band.

CITATIONS

- Ding Huang, Alex Abulnaga, Sacha Welinski, Mouktik Raha, Jeff D. Thompson, and Nathalie P. de Leon, "Hybrid III-V diamond photonic platform for quantum nodes based on neutral silicon vacancy centers in diamond," Opt. Express 29, 9174-9189 (2021).

Advisor: Nathalie P. de Leon (Electrical Engineering)

A Telecom O-band Emitter in Diamond

Researcher: **Sounak Mukherjee** (Princeton Graduate), **Zi-Huai Zhang** (Princeton Graduate),

Sponsorship: DOE, AFOSR, Office of Science, National Quantum Information Science Research Centers, Co-design Center for Quantum Advantage

Color centers in diamond are promising platforms for quantum technologies. Most color centers in diamond discovered thus far emit in the visible or near-infrared wavelength range, which are incompatible with long-distance fiber communication and unfavorable for imaging in biological tissues. We report the experimental observation of a new color center that emits in the telecom O-band, which we observe in silicon-doped bulk single crystal diamonds and microdiamonds. Combining absorption and photoluminescence measurements, we identify a zero-phonon line at 1221 nm and phonon replicas separated by 42 meV. Using transient absorption spectroscopy, we measure an excited state lifetime of around 270 ps and observe a long-lived baseline that may arise from intersystem crossing to another spin manifold.

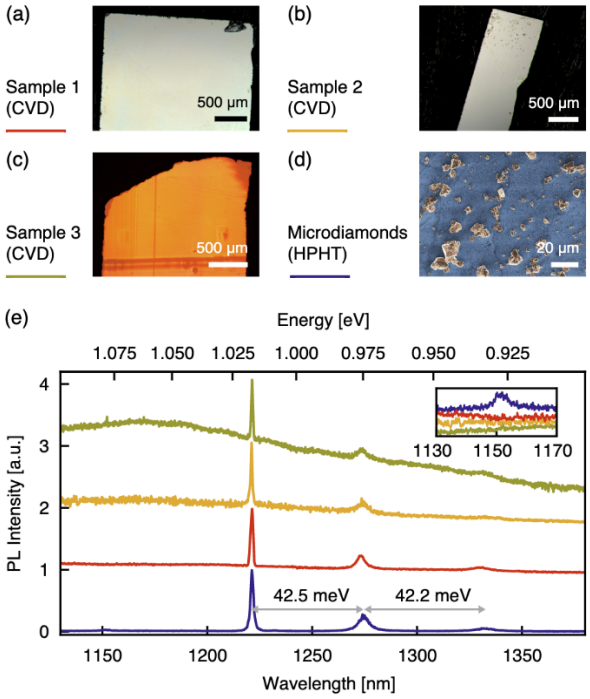

Figure 1: Low temperature photoluminescence (PL) spectroscopy. (a), (b), (c) Optical images of bulk-doped diamonds grown by CVD. (d) False-colored scanning electron microscope image of HPHT microdiamonds. (e) Comparison of the PL emission spectra in different samples with 850 nm excitation. Color coding of the spectra corresponds to samples shown in (a) to (d). Inset shows PL intensity from 1130 nm to 1170 nm where we observe an additional peak at 1152 nm for the microdiamonds. The PL spectra corresponding to samples 1 and 3 have been measured at 8.5 K. For sample 2 and the microdiamonds, the temperature was 5.8 K.

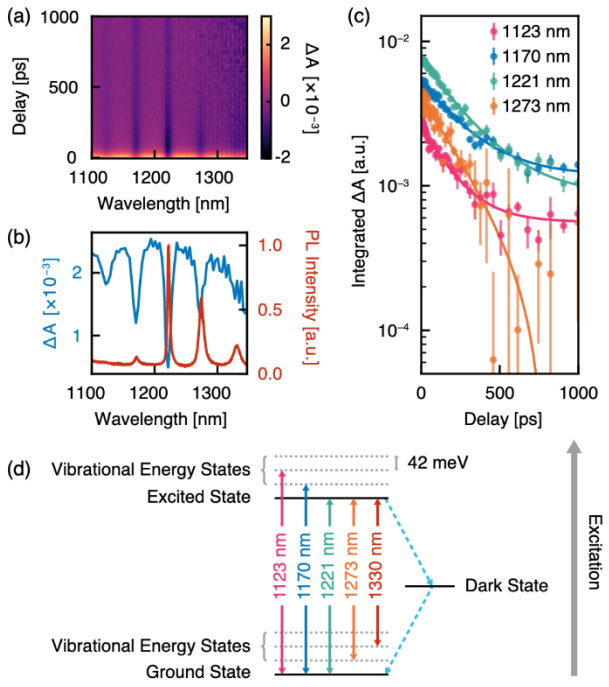

Figure 2: Transient absorption spectroscopy. (a) 2D map of transient absorption ΔA as functions of time delay and wavelength measured at 4.2 K. A series of approximately evenly spaced lines originating from the telecom emitter are observable. (b) Comparison between the PL spectrum (red) at 225 K and the transient absorption spectrum (blue) at a delay of 5 ps. (c) Decay of integrated ΔA for different transitions. The decays are fitted to a single exponential and we observe an excited state lifetime of ~270 ps. (d) Level diagram of the telecom emitter deduced from PL emission, absorption, and transient absorption.

CITATIONS

- Sounak Mukherjee, Zi-Huai Zhang, Daniel G. Oblinsky, Mitchell O. de Vries, Brett C. Johnson, Brant C. Gibson, Edwin L. H. Mayes, Andrew M. Edmonds, Nicola Palmer, Matthew L. Markham, Ádám Gali, Gergő Thiering, Adam Dalis, Timothy Dumm, Gregory D. Scholes, Alastair Stacey, Philipp Reineck, and Nathalie P. de Leon, "A telecom O-band emitter in diamond," arXiv:2211.05969 (2022)

Advisor: Nathalie P. de Leon (Electrical Engineering)

Observation of an Environmentally Insensitive Solid-State Spin Defect in Diamond

Researcher: **Alex Abulnaga** (Princeton Graduate)

Sponsorship: NSF, PCCM

Engineering coherent systems is a central goal of quantum science. Color centers in diamond are a promising approach, with the potential to combine the coherence of atoms with the scalability of a solid-state platform. We report a color center that shows insensitivity to environmental decoherence caused by phonons and electric field noise: the neutral charge state of silicon vacancy (SiV0). Through careful materials engineering, we achieved >80% conversion of implanted silicon to SiV0. SiV0 exhibits spin-lattice relaxation times approaching 1 minute and coherence times approaching 1 second. Its optical properties are very favorable, with ~90% of its emission into the zero-phonon line and near transform-limited optical linewidths. These combined properties make SiV0 a promising defect for quantum network applications.

In MNFC, we fabricate photonic devices with a high-index photonic layer on top of the diamond substrate such that photons can evanescently couple to color centers that are close to the diamond surface.

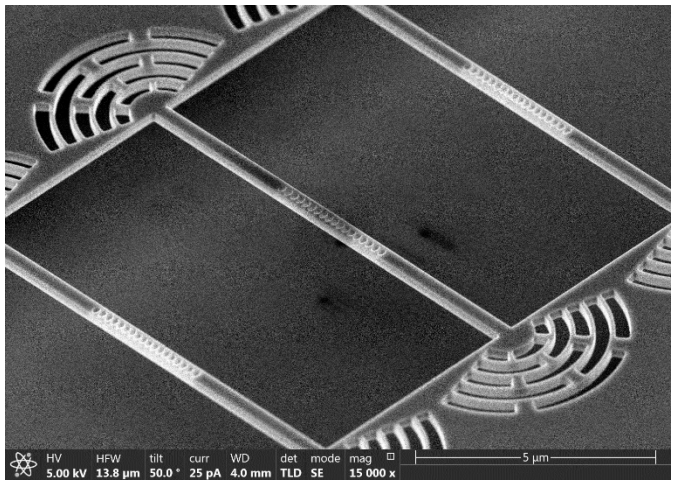

Figure 1. A photonic crystal cavity fabricated in MNFC.

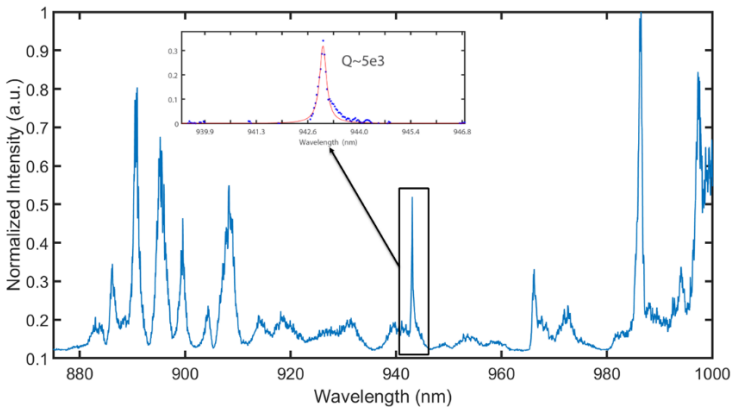

Figure 2. The measured transmission spectrum of a photonic crystal cavity.

CITATIONS

- Rose, Brendon C., et al. "Observation of an environmentally insensitive solid-state spin defect in diamond." Science 361.6397 (2018): 60-634877.
- Huang, Ding, et al. "Hybrid III-V diamond photonic platform for quantum nodes based on neutral silicon vacancy centers in diamond." Optics Express, 29(6), 9174-9189.

Advisor: Nathalie P. de Leon (Electrical Engineering)

Diamond and Electronic and Photonic Nano/Micro Fabrication

Researcher: **Alexander Pakpour-Tabrizi** (Princeton Postdoc)

Sponsorship: DARPA, NSF

Integrating atomic quantum memories based on color centers in diamond with on-chip photonic devices would enable entanglement distribution over long distances. However, efforts towards integration have been challenging because color centers can be highly sensitive to their environment, and their properties degrade in nanofabricated structures. Here, we describe a heterogeneously integrated, on-chip, III-V diamond platform designed for neutral silicon vacancy (SiV0) centers in diamond that circumvents the need for etching the diamond substrate. Through evanescent coupling to SiV0 centers near the surface of diamond, the platform will enable Purcell enhancement of SiV0 emission and efficient frequency conversion to the telecommunication C-band. The proposed structures can be realized with readily available fabrication technique.

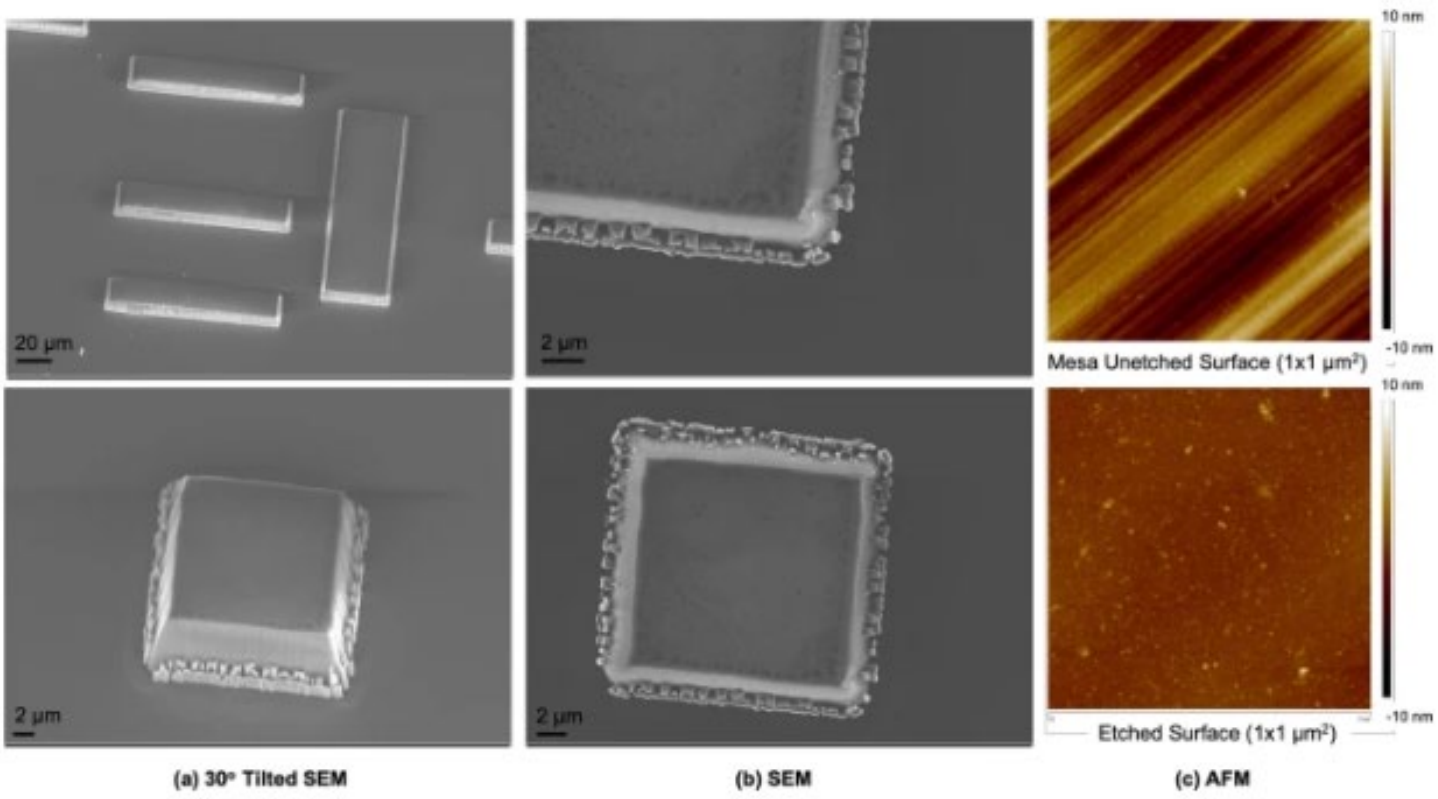

Figure 1: 8 μm Deep Etch with Near-Zero Micromasking after Cyclic Ar/O_2 - Ar/Cl_2 ICP RIE: (**a**) 30° tilted SEM, (**b**) no tilt SEM and (**c**) AFM scans of the unetched mesa surface with 1.7 nm roughness and etched surface with 0.47 nm roughness. The etched surface was smooth, with micromasking only observed within a 1-micron radius around the base of the mesa. The mesa sidewalls were also smooth with defects observed at the base and without trenching.

CITATIONS

- Marie-Laure Hicks, Alexander C. Pakpour-Tabrizi, Richard B. Jackman; Diamond Etching Beyond 10 µm with Near-Zero Micromasking, Scientific Reports volume 9, Article number: 15619 (2019)

Advisor: Nathalie P. de Leon (Electrical Engineering)

Quantum Sensing with Nitrogen-Vacancy Centers

Researcher: **Hilal Saglam** (Princeton Postdoc)

Sponsorship: DOE

Nitrogen vacancy centers in diamond are promising for nano-scale quantum sensing due that that they exhibit spin-dependent fluorescence and they can interact with weak magnetic fields, enabling a sensitive form of spectroscopy. Our goal will be to use NV centers in order to understand the physics of various material systems.

Figure 1: Diamond sample.

CITATIONS

- N/A

Advisor: Nathalie P. de Leon (Electrical Engineering)
Microwave Striplines for Diamond
Researcher: **Lila Rodgers** (Princeton Graduate)
Sponsorship: NSF

My research involves using nitrogen-vacancy (NV) centers in diamond for nanoscale quantum sensing. NV centers are point defects in the diamond lattice that can be used to detect small magnetic signals from their environment with nanoscale spatial resolution. Additionally, these defects offer long spin coherence times at room temperature, making them an attractive platform for nanoscale sensing of biological materials. For these experiments, we need to be able to image through a glass coverslip to opitically inititialize and collect fluorescence from individual NV centers (Fig. 1). We also need to apply microwaves to manipulate the spin state (Fig. 1). I am fabricating microwave striplines on a glass coverslip that allow us to accomplish these tasks (Fig. 2). We place our diamonds on top of these striplines to efficiently deliver microwaves to diamonds, and optically initialize and read out the spin state.

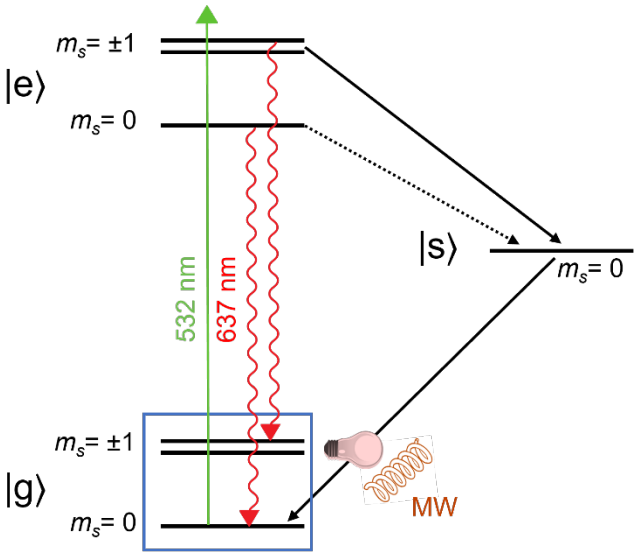

Figure 1: Energy structure of nitrogen vacancy centers in diamond, reproduced from [1]. The ground state is a triplet with a zero field splitting of 2.87 GHz. This spin state can be manipulated by applying microwaves to the NV centers and can be read out optically through a spin-dependent fluorescence measurement.

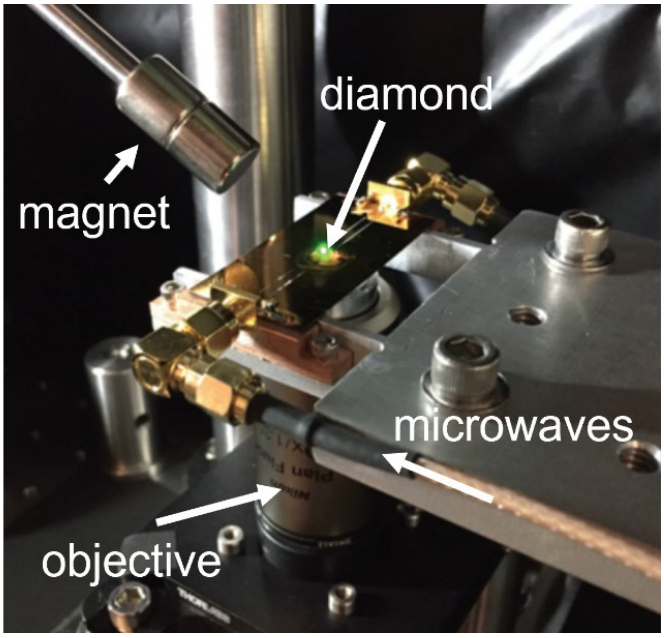

Figure 2 : Diamond sample with shallow NV centers sits on top of a microwave stripline. These striplines are fabricated using the photolithography facilities at MNFC. Diamond is 2x2mm in size.

CITATIONS

- [1] L. V. H. Rodgers, L. B. Hughes, M. Xie, P. C. Maurer, S. Kolkowitz, A. C. B. Jayich, N. P. de Leon, Materials Challenges for Color Centers in Diamond. MRS Bulletin 46.7 (2021)
- [2] S. Sangtawesin*, B.L. Dwyer*, S. Srinivasan, J.J. Allred, L.V.H. Rodgers, K. De Greve, A. Stacey, N. Dontschuk, K.M. O'Donnell, D. Hu, D.A. Evans, C. Jaye, D.A. Fischer, M.L. Markham, D.J. Twitchen, H. Park, M.D. Lukin, N.P. de Leon. Origins of diamond surface noise probed by correlating single-spin measurements with surface spectroscopy. Physical Review X 9, 031052. (2019)

Advisor: Nathalie P. de Leon (Electrical Engineering)
Quantum Sensing With Nitrogen Vacancy Centers
Researcher: **Marjana Mahdia** (Princeton Graduate)
Sponsorship: DOE

Nitrogen Vacancy (NV) centers are promising quantum bits in the field of quantum sensing, and quantum computing, as the spins in these centers can be modulated efficiently which results in various interesting quantum phenomenon. We have the goal to manipulate, and to understand these centers to contribute to the field of quantum electronics.

NV centers can be stable in various charge states; most common ones are NV^0, and NV^- charge states. For many quantum applications, NV^- charge state is preferred and is used because of easy and efficient manipulation of electron triplet spin state. My research goal is to convert NV charge state through implantation of donor in diamond, and to make sure the coherence of spin is not compromised at the same time. To measure coherence time through spin manipulation, we use MW signal, and we apply the MW signal to our NV centers through a stripline, which we fabricate on a glass coverslip.

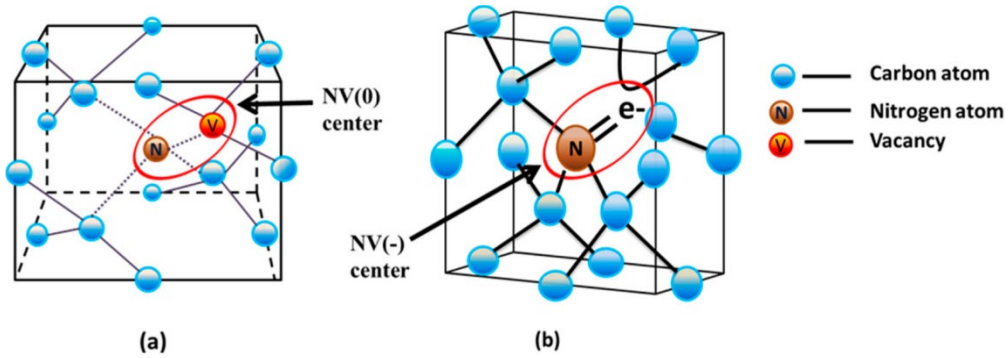

Figure 1: Diamond lattice with NV center.

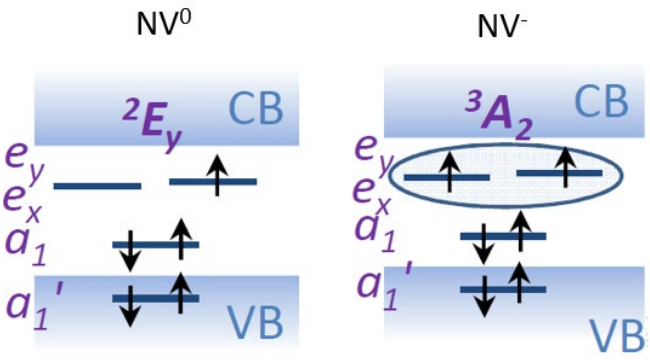

Figure 2: Zeeman splitting of energy levels in a magnetic field.

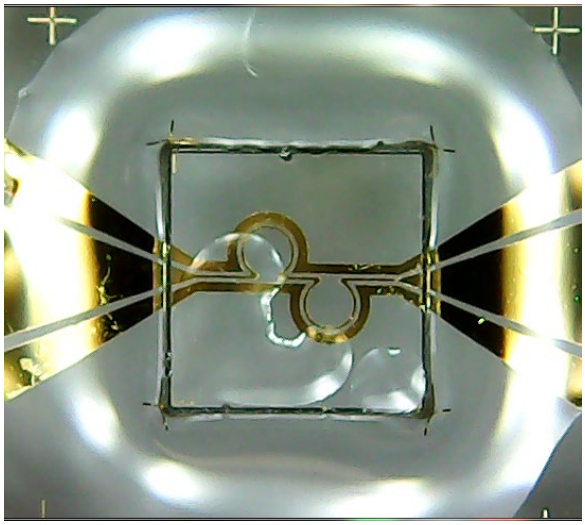

Figure 3: Diamond on a stripline ready for oil confocal microscope.

CITATIONS

- Nitrogen Vacancy Centers: Robust Magnetic Field Sensors https://www.findlight.net/blog/nitrogen-vacancy-centers-sensors/

Advisor: Nathalie P. de Leon (Electrical Engineering)

Measuring Spatiotemporal Correlations Between Two Nitrogen Vacancy Centers

Researcher: **Jared Rovny** (Princeton Postdoc)

Sponsorship: DOE, NSF, DARPA

Nitrogen vacancy (NV) centers in diamond are atom-scale defects that can be used to sense magnetic fields with high sensitivity and spatial resolution. Typically, the magnetic field is measured by averaging sequential measurements of single NV centers, or by spatial averaging over ensembles of many NV centers, providing mean values containing no nonlocal information about the relationship between two points separated in space or time. Here we propose and implement a sensing modality whereby two or more NV centers are measured simultaneously, and we extract temporal and spatial correlations in their signals that would otherwise be inaccessible. We demonstrate measurements of correlated applied noise using spin-to-charge readout of two NV centers, and implement a spectral reconstruction protocol for disentangling local and nonlocal noise sources.

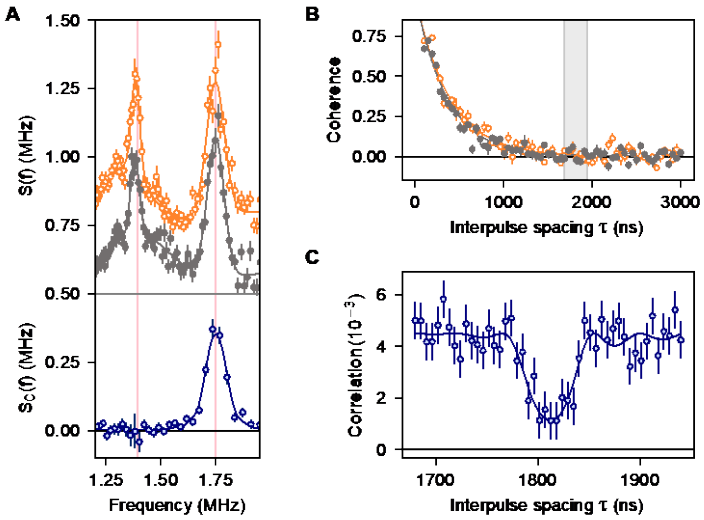

Figure 1: (A) Single-NV noise spectra derived from conventional XY8 variance magnetometry (top) of two NV centers (orange open markers and gray filled markers. Spectral decomposition (bottom) using covariance magnetometry reveals that the higher frequency peak is caused by a shared noise source. (B) In a broadband correlated noise environment, the two NV centers rapidly decohere (orange open markers and gray filled markers). (C) Covariance magnetometry for evolution times indicated by the gray rectangle in (B) reveals a dip in the Pearson correlation due to the local ^{15}N spins intrinsic to each NV center.

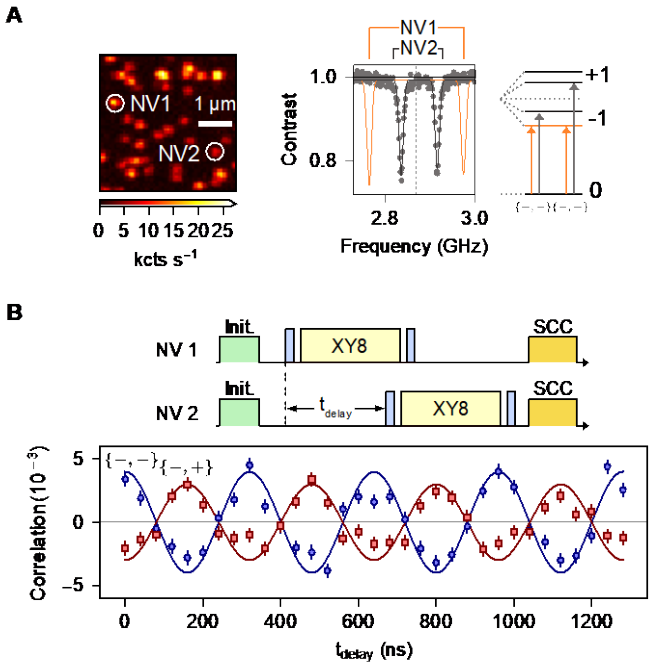

Figure 2: (A) Covariance magnetometry enables simultaneous independent control of two NV centers (NV1 and NV2, left image) by addressing the two centers on different spin transitions (right). By manipulating the two NV centers independently, we can choose when to start the sensing protocols independently (B). By sweeping the delay between starting times, we demonstrated unprecedented resolution of a signal measured at two points separated in space and time, where correlations are positive (blue circles) or negative (red squares) depending on the magnetic orientation of the transitions we choose to address.

CITATIONS

- J. Rovny, M. Fitzpatrick, Z. Yuan, A. I. Abdalla, L. Futamura, C. Fox, M. C. Cambria, Shimon Kolkowitz, and N. P. de Leon, Nanoscale covariance magnetometry with diamond quantum sensors (2022), arXiv:2209.08703

Advisor: Nathalie P. de Leon (Electrical Engineering)

Charge State Dynamics and Optically Detected Electron Spin Resonance Contrast of Shallow Nitrogen-Vacancy Centers in Diamond

Researcher: **Zhiyang Yuan** (Princeton Graduate)

Sponsorship: NSF

Nitrogen-vacancy (NV) centers in diamond can be used for nanoscale sensing with atomic resolution and sensitivity; however, it has been observed that their properties degrade as they approach the diamond surface. Here we report that in addition to degraded spin coherence, NV centers within nanometers of the surface can also exhibit decreased fluorescence contrast for optically detected electron spin resonance (OD-ESR). We demonstrate that this decreased OD-ESR contrast arises from charge state dynamics of the NV center, and that it is strongly surface-dependent, indicating that surface engineering will be critical for nanoscale sensing applications based on color centers in diamond.

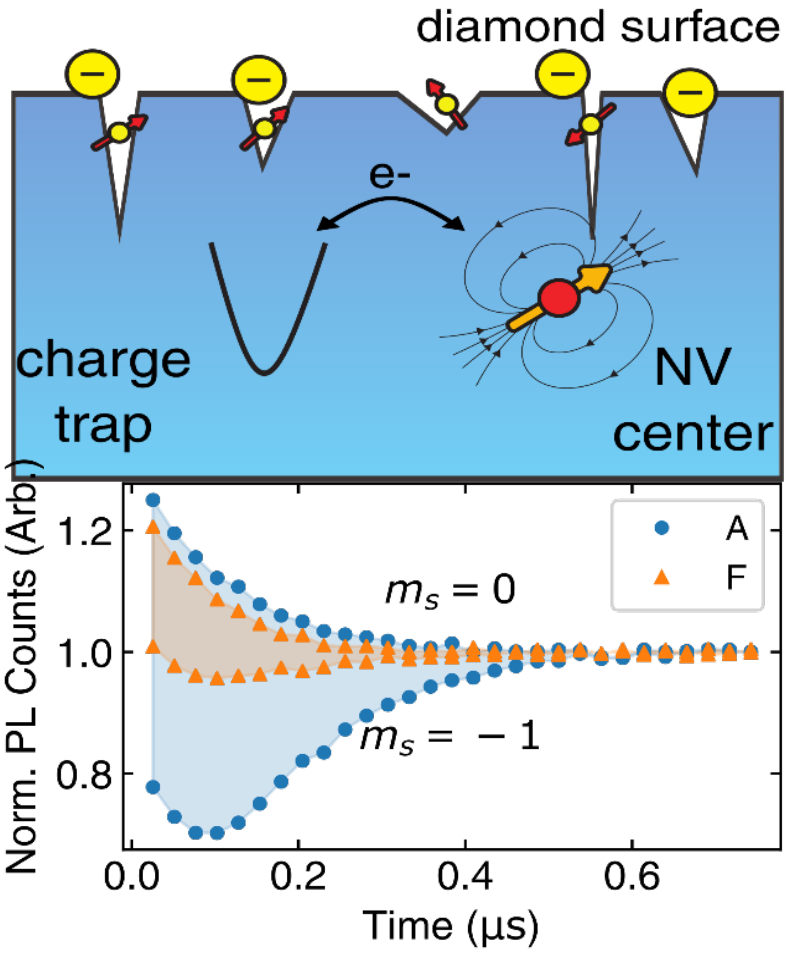

Figure 1: Cartoon depicting the interaction between shallow NV centers and defects at the diamond surface. Defects can act as charge traps, leading to changes in ionization and recombination kinetics for nearby NV

Figure 2: Comparison of photoluminescence traces for representative NV centers from the two samples, A (blue) and F (orange), under 664 μW of green illumination. Charge state instability in sample F gives rise to the lower contrast in the NV photoluminescence signal.

CITATIONS

- Yuan, Zhiyang, et al. "Charge state dynamics and optically detected electron spin resonance contrast of shallow nitrogen-vacancy centers in diamond." Physical Review Research 2.3 (2020): 033263.

Advisor: Nathalie P. de Leon (Electrical Engineering)

2D Material Device Fabrication on Diamond

Researcher: **Kai-Hung Cheng** (Princeton Graduate)

Sponsorship: DOE

Fabrication of 2D material (graphene, hBN, and etc.) for transport measurement on top of diamond to study the noise using NV centers.

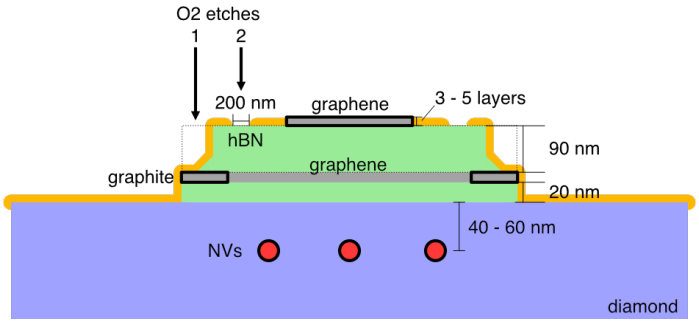

Figure 1: A device structure.

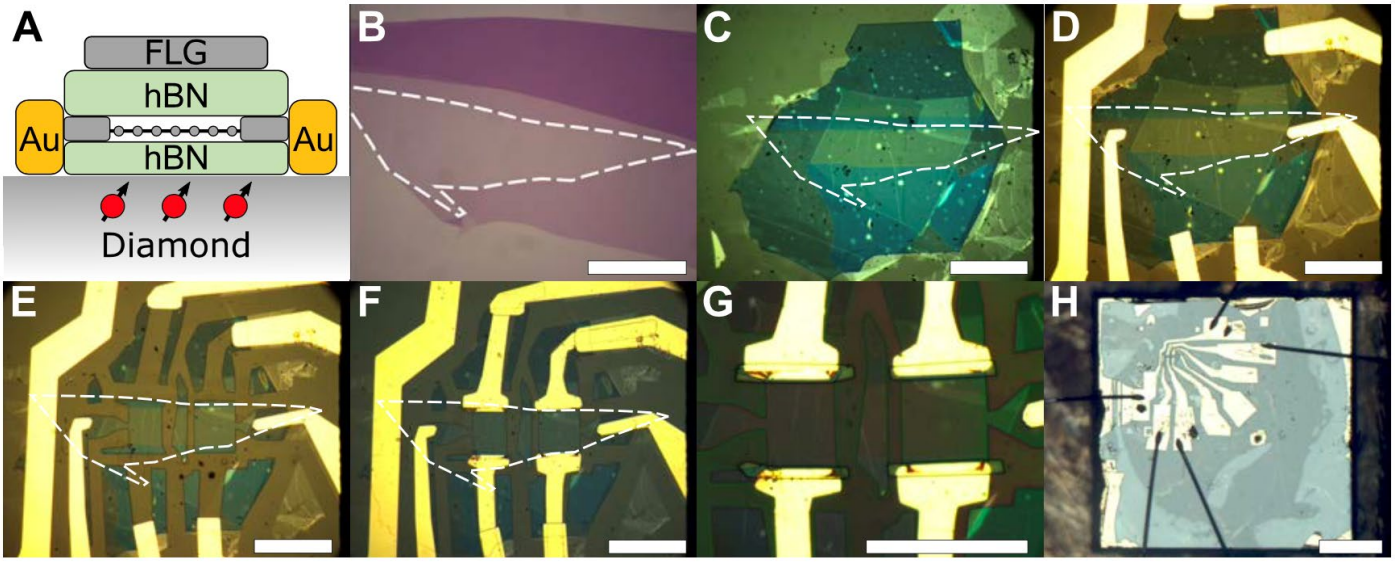

Figure 2: Device fabrication on diamond substrate. (A) Device schematic: Monolayer graphene (grey chain) was graphite contacted and encapsulated with hexagonal boron nitride (hBN). Few-layer graphene (FLG) was used as topgate. (B-H) Micrographs of device fabrication, with 40 μm scalebar in (B)-(G) and 500 μm in (H). (B) Exfoliated graphene. White dashed line indicates monolayer region. (C) Complete stack on diamond substrate with shallow implanted (40 – 60 nm deep) NV centers. (D) Initial contacts and wire for delivering reference noise (left-most electrode). (E) Device after etch to define geometry. (F) Edge contacts constructed through etching and subsequent thermal evaporation. (G) Device with etch mask for disconnecting topgate from edge contacts. The left device is the source of data for Figure 2D-E in the main text (Device C2). Note that ripples visible in the image are entirely contained in the top gate graphene and are not expected to affect the transport properties of the channel graphene, due to the thick (~ 90 nm) hBN dielectric. (H) Entire (2×2 mm2) single crystal diamond, with wire bonded device.

CITATIONS

- Andersen et al., Science 364, 154–157 (2019)

Advisor: Nathalie P. de Leon (Electrical Engineering)

Superconducting Qubits

Researcher: **Aveek Dutta** (Princeton Postdoc)

Sponsorship: NSF

The superconducting transmon qubit is a leading platform for quantum computing. Building large, useful quantum systems based on transmon qubits will require significant improvements in qubit relaxation and coherence times. Recently we have demonstrated that by replacing niobium (Nb) with tantalum (Ta) as the material of choice in 2D superconducting transmons, it is possible to achieve qubit lifetimes exceeding 0.3 ms [1]. In order to understand the sources of loss in Ta transmon qubits, we performed temperature and microwave power dependent quality factor measurements of tantalum resonators. Our measurements indicate two-level-systems residing in metal surfaces as a significant source of loss in Ta transmons. We also performed energy dependent X-ray photoelectron spectroscopy of tantalum films to obtain a chemical depth profile of the tantalum surface. We found that the native oxide on top of metallic Ta consists of a tantalum oxide in the +5 oxidation state, tantalum sub-oxides in the +3 and +1 oxidation state and Ta atoms at the interface of bulk metal and surface oxide. By chemically treating the Ta surface with 10:1 Buffered Oxide Etch, we were able to reduce the oxide on top of bulk metallic Ta and achieve an improvement in Ta resonator quality factor.

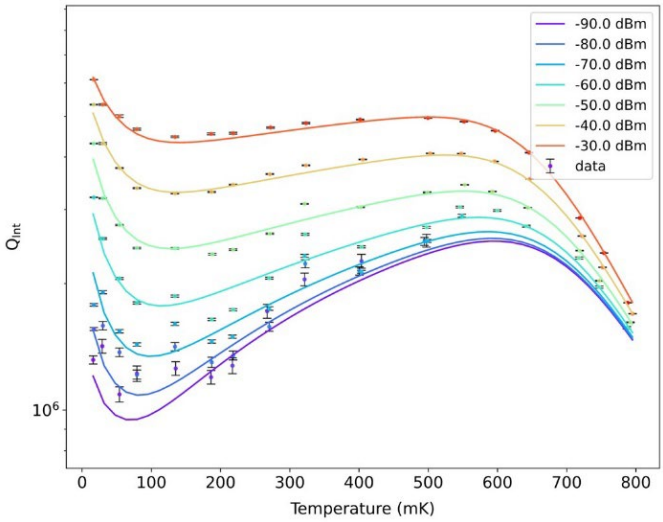

Figure 1: Internal quality factor Q_{int} of a tantalum resonator as a function of temperature measured at different microwave powers. In the high temperature range above 500 mK, Q_{int} decreases with increasing temperature, irrespective of microwave power, due to thermal quasiparticle induced losses. Between 100 and 500 mK, Q_{int} increases with temperature due to thermal saturation of two-level-systems. Below 100 mK, Q_{int} decreases with increasing temperature due to increased losses associated with an increase in saturation power of two-level-

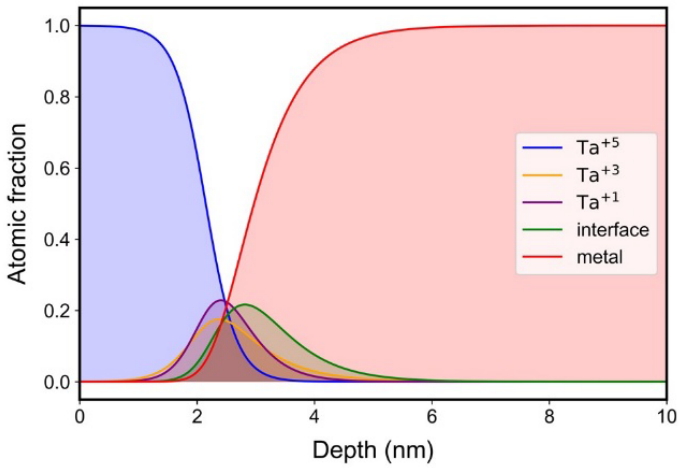

Figure 2: Chemical depth profile of the surface of tantalum films as obtained from energy-dependent X-ray photoelectron spectroscopy. The tantalum film has ~2.2 nm thick Ta_2O_5 on top of the bulk tantalum metal. However, the interface of the pentoxide and bulk metal is a complex one due to the presence of Ta +3 and +1 sub-oxides and also tantalum atoms at the interface of bulk metal and surface oxide.

CITATIONS

- A. P. M. Place et al "New material platform for superconducting transmon qubits with coherence times exceeding 0.3 milliseconds," Nat. Comm. 12, 2021.

Advisor: Nathalie P. de Leon (Electrical Engineering)

Exploring New Materials to Construct Superconducting Qubits

Researcher: **Esha Umbarkar** (Princeton Undergraduate)

Sponsorship: DOE

The superconducting transmon qubit is a leading platform for quantum computing and quantum science. Building large, useful quantum systems based on transmon qubits will require significant improvements in qubit relaxation and coherence times, which are orders of magnitude shorter than limits imposed by bulk properties of the constituent materials. This indicates that relaxation likely originates from uncontrolled surfaces, interfaces, and contaminants. Previous efforts to improve qubit lifetimes have focused primarily on designs that minimize contributions from surfaces. However, significant improvements in the lifetime of two-dimensional transmon qubits have remained elusive for several years. Here, we fabricate two-dimensional transmon qubits that have both lifetimes and coherence times with dynamical decoupling exceeding 0.3 milliseconds by replacing niobium with tantalum in the device. We have observed increased lifetimes for seventeen devices, indicating that these material improvements are robust, paving the way for higher gate fidelities in multi-qubit processors

.

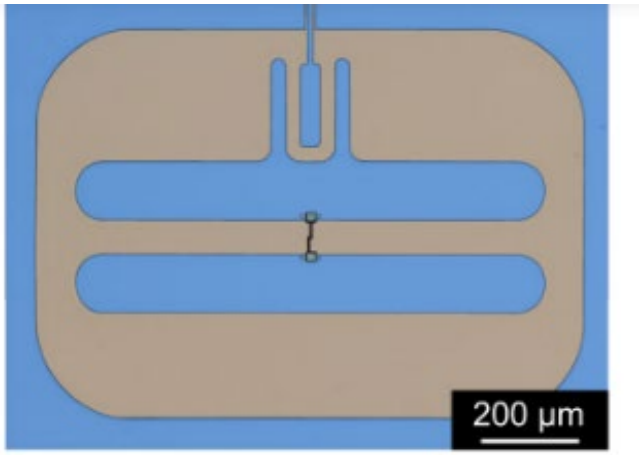

Figure 1. Tantalum-based transmon superconducting qubit. a False-colored optical microscope image of a transmon qubit. The transmon consists of a Josephson junction shunted by two large capacitor islands made of tantalum (blue) on sapphire (gray).

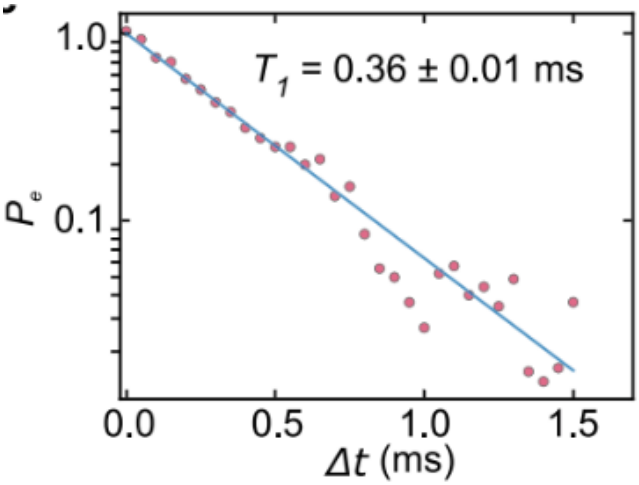

Figure 2. T1 measurement of Device 18, showing the excited state population Pe as a function of delay time Δt. Line represents a single exponential fit with a characteristic T1 time of 0.36 ± 0.01 ms.

CITATIONS

- Place, A.P.M., Rodgers, L.V.H., Mundada, P. et al. New material platform for superconducting transmon qubits with coherence times exceeding 0.3 milliseconds. Nat Commun 12, 1779 (2021). https://doi.org/10.1038/s41467-021-22030-5

Advisor: Claire F. Gmachl (Electrical Engineering)

Metal Halide Perovskite Thin Film Lasers: A Disruptive Technology Platform

Researcher: **Manuel Gallego** (Princeton Graduate)

Sponsorship: Internal Funding

Disordered Hyperuniform Structures (DHU) are a novel type of metamaterial with the potential for optical spatial differentiation of light at angles away from normal incidence. The isotropic nature of DHU structures comes from the patterning itself; at large scales it behaves like a crystal, while at smaller scales it doesn't have any recognizable pattern. This property can be used to create a photonic band gap akin to those encountered in photonic crystals.

Current work on DHU structures is composed of polarization dependent transmission, and angle resolved reflection measurements on an InP substrate with quantum cascade (QC) layers. From these measurements not only is the isotropy of the sample visible, but also the photonic band gap can be observed. Previous work on DHU structures was based on a pillar design created via a combination of photolithography and dry etching processes. Meanwhile, Current work uses the same nanofabrication techniques to instead make hole structures. Future measurements of the sample spectra will use the QC as a potential gain medium to aid in the spatial differentiation (edge detection) process.

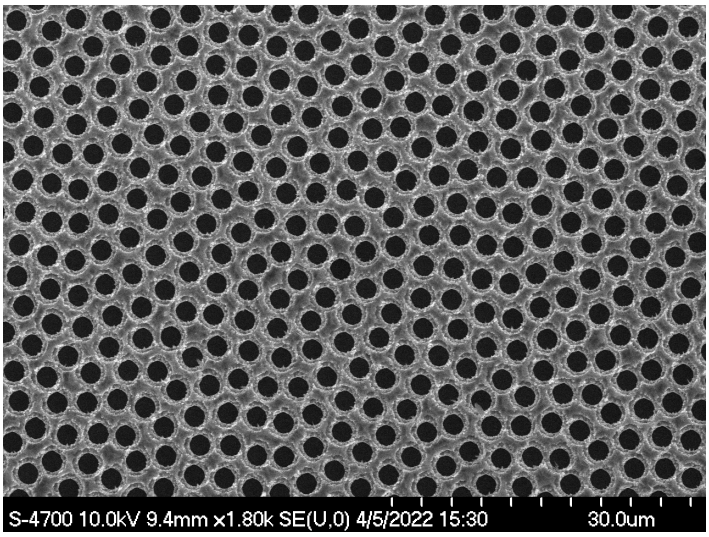

Figure 1: Scanning electron microscope image of the top-down view of hole structure DHU sample

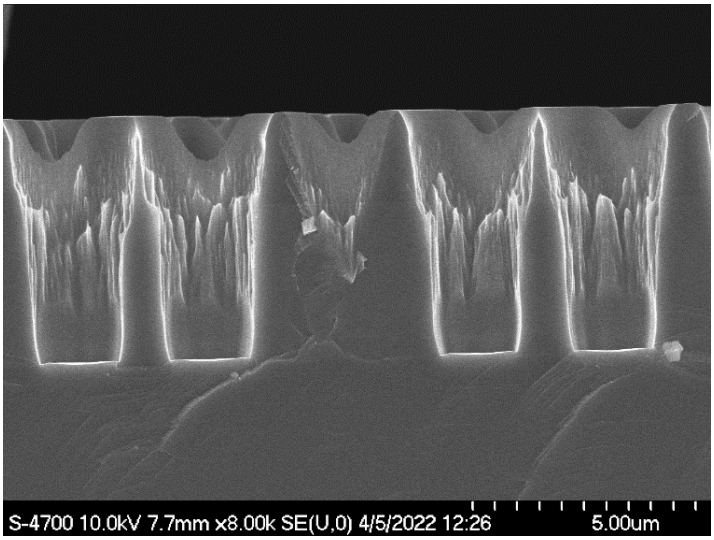

Figure 2: Scanning electron microscope image of the cross-section view of hole structure DHU sample

CITATIONS

- Zhang, Yezhezi. "Novel Material Engineering in III-IV Semiconductor Platforms: Metamaterials with Quantum Cascade Structures." PhD diss., Princeton University, 2022.

Advisor: Claire F. Gmachl (Electrical Engineering)

Monolithically Integrated Mid-Infrared Systems Based on Coupled Quantum Cascade Ring Lasers

Researcher: **Sara Kacmoli** (Princeton Graduate)

Sponsorship: Internal Funding

Quantum cascade lasers (QCLs) are a prominent light source in the mid-infrared. They find applications in absorption spectroscopy, IR countermeasures, free space optical communication systems. Monolithic integration of QCLs with other elements of a photonic circuit such as waveguides and detectors may unlock opportunities in realizing miniaturized sensing and spectroscopy systems. In our work we fabricate and study the performance of small systems based on ring QCLs. In addition to evaluating system-wide performance, we also study mode dynamics in single and coupled QCLs focusing on aspects such as unidirectionality, bistability, mode competition and frequency comb operation. All fabrication and packaging steps for our devices are performed in the MNFC facility.

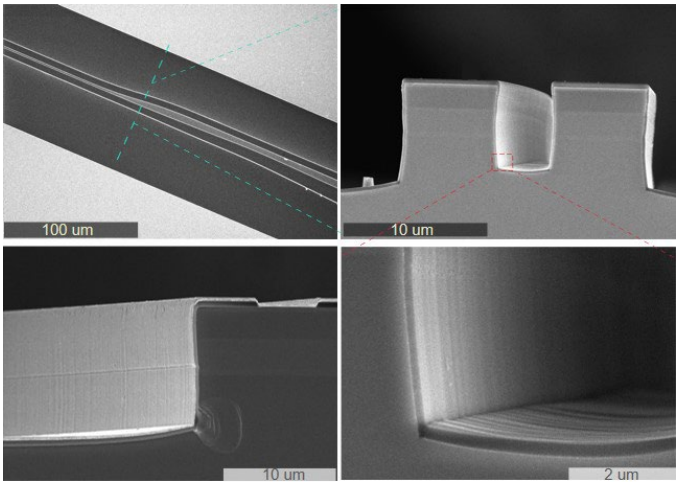

Figure 1: Scanning electron microscope (SEM) images depicting details of a small mid-infrared system built on a quantum cascade laser wafer (InGaAs/AlInAs epi layers on InP), focusing on a directional coupler. Top left: A top-view of the tapered coupling region. Top right: Cross-sectional view along the taper. The darker contour along the ridges is the insulating SiNx layer. The coupling region is kept free of metal. Bottom left: Cross-sectional view of the ridge waveguide elsewhere in the device with a dielectric window and Ti/Au metal layer for electrical contact. Bottom right: Magnified view showing the etch profile and minimal, highly sub-wavelength roughness on the waveguide sidewalls.

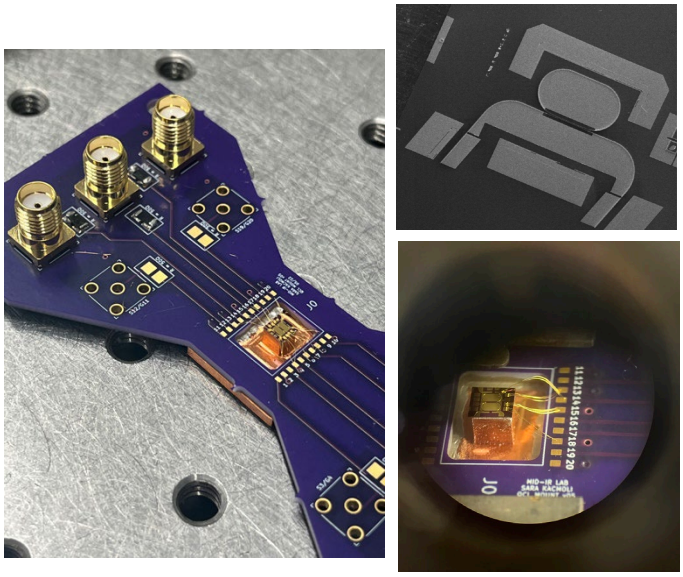

Figure 2: Packaging of the mid-infrared quantum cascade laser-based system. Left: Custom made high-frequency PCB. The device is mounted on a copper mount with silver epoxy and wire bonded to gold electrodes using a ball bonder. Bottom right: A magnified view of a partially wire bonded device. The device sits on a "pedestal" to allow detection of the emitted signal. Top right: SEM of one "unit" of the system ready for mounting once cleaved. It is comprised of a laser, active waveguide and two integrated photodetectors. The image shows the device after metallization.

CITATIONS

- S. Kacmoli, D. L. Sivco, and C. F. Gmachl, "Unidirectional mode selection in bistable quantum cascade ring lasers." arXiv:2205.07156, 2022.
- S. Kacmoli and C. F. Gmachl, "Monolithic integration of quantum cascade lasers, detectors and active waveguides," 2022 Conference on Lasers and Electro-Optics (CLEO), 2022

Advisor: Claire F. Gmachl (Electrical Engineering)

Quantum Cascade Lasers

Researcher: **Richard Brun** (Princeton Graduate), **Danxian Liu** (Princeton Undergraduate)

Sponsorship: Internal Funding

Quantum cascade lasers are well known for their tunable emission wavelengths in the mid infrared region. This is of particular interest for the sensing of trace gases Quantum cascade lasers derive their name from the intersubband transition that occurs between alternating materials forming wells and barriers, producing eigenmodes of electron states leading to a large design space. Long wavelength quantum cascade lasers (12-20 μm) are difficult to fabricate on conventional InP substrates due to two photon absorption. With a lack of commercially viable options, there is a demand for such lasers. Using GaAs/AlGaAs material system, we design, fabricate and characterize 14 and 18 μm mesas and Fabry Perot lasers to probe their characteristics.

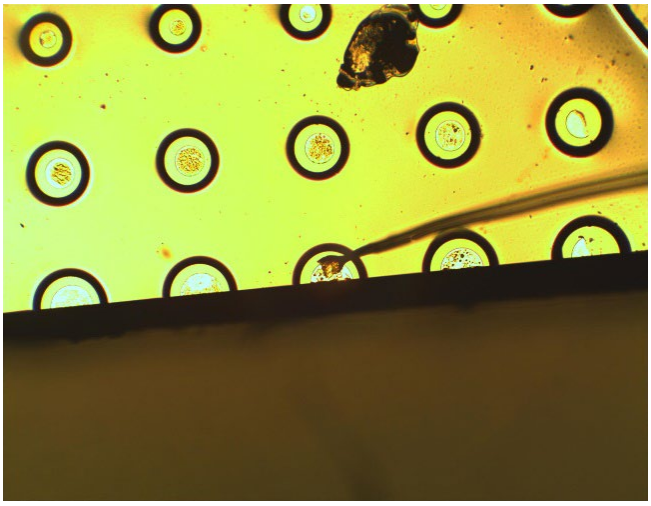

Figure 1: Microscope image of a wire bonded quantum cascade material mesa fabricated using GaAs/AlGaAs system.

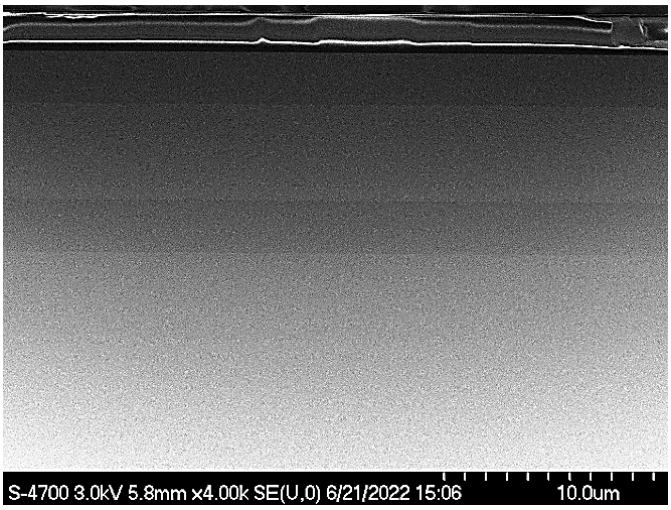

Figure 2: Scanning electron microscope image of the cross section of quantum cascade material.

CITATIONS

- Faist Jérôme. (2018). *Quantum Cascade Lasers*. Oxford University Press.

Advisor: Andrew A. Houck (Electrical Engineering)

Granular Aluminum Kinetic Inductors

Researcher: **Alex Place** (Princeton Graduate)

Sponsorship: ARO

This project explores a novel material with an anomalously large kinetic inductance, granular aluminum. High kinetic inductance materials may be used to realize the next generation of qubits, including qubits with topological protection against decoherence. Further, granular aluminum behaves nonlinearly. Almost every qubit requires a nonlinear element- most qubits use Josephson junctions to provide their nonlinearity, but the junctions introduce a significant amount of noise. This project pursues several junctionless-qubit designs which could eliminate this common source of decoherence.

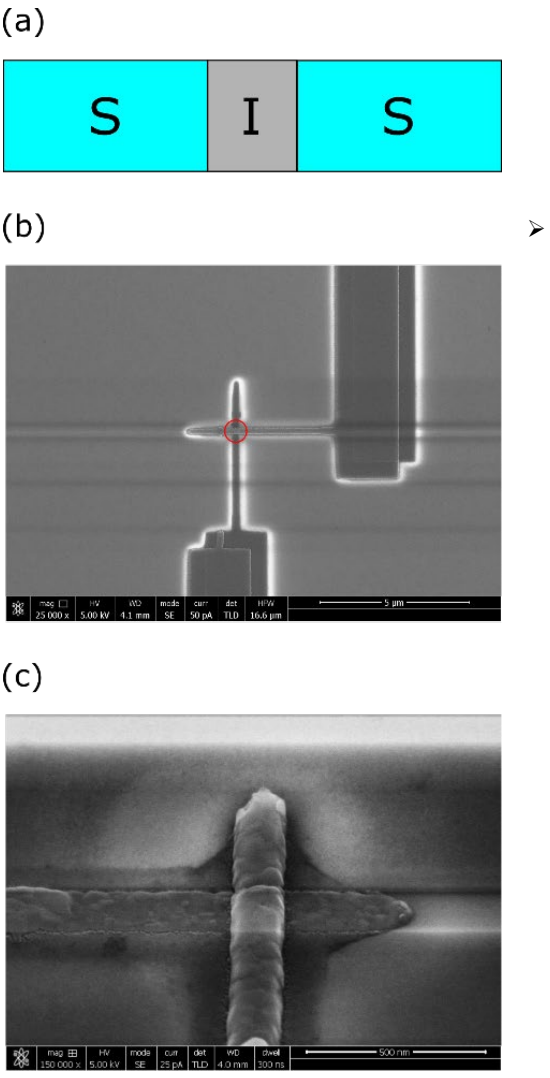

Figure 1: Josephson junctions made out of aluminum on sapphire.

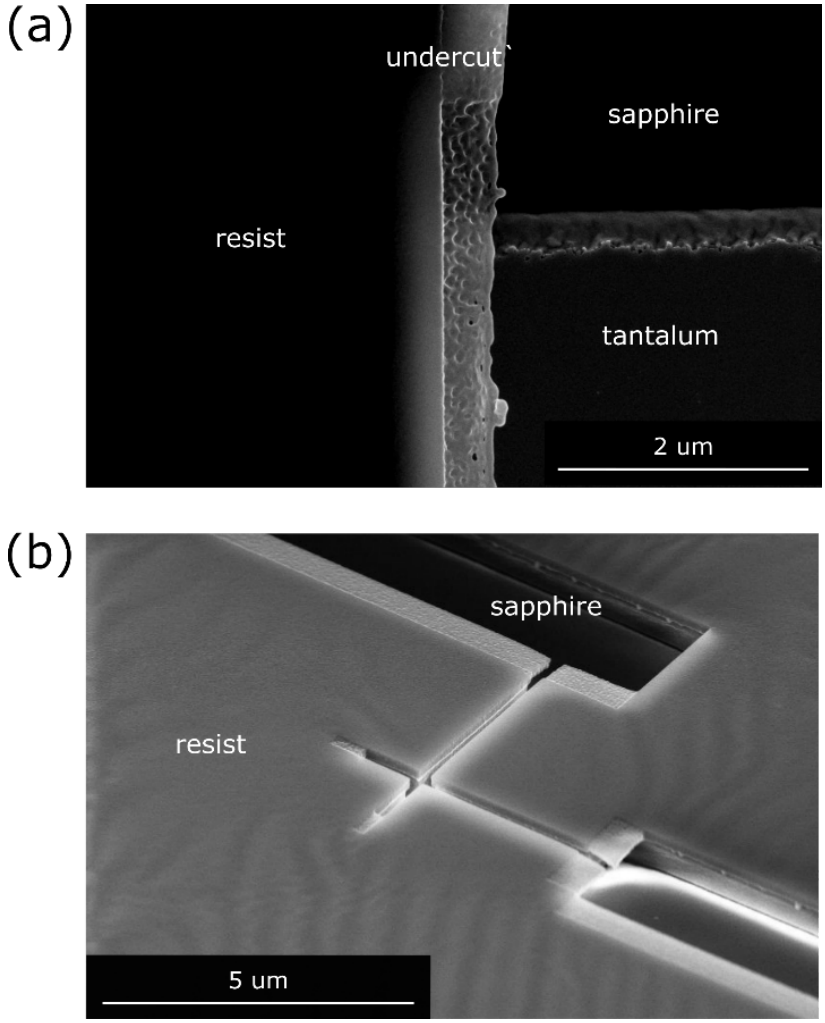

Figure 2: Developed resist on top of a patterned tantalum on sapphire substrate. The resist is used in a double angle evaporation to make Josephson junctions, the nonlinear inductor in a transmon superconducting qubit.

CITATIONS

- A. Place, et al., New material platform for superconducting transmon qubits with coherence times exceeding 0.3 milliseconds; Nature Communications volume 12, Article number: 1779 (2021)

Advisor: Andrew A. Houck (Electrical Engineering)

Microscopic Relaxation Channels in Materials for Superconducting Qubits

Researcher: **Anjali Premkumar** (Princeton Graduate)

Sponsorship: ARP

Researchers across academia and industry are exploring superconducting qubits as a promising implementation of quantum computing. While there is growing evidence that loss in constituent materials is limiting qubit performance, the microscopic details of that loss is poorly understood. In this work [1], we explore the connections between microscopic material properties and qubit performance. We fabricated superconducting transmon qubits using polycrystalline niobium thin films deposited using three different sputtering techniques, resulting in a spread of relaxation times (Figure 1) and materials properties. Collaborators at Brookhaven National Lab used spatially-resolved x-ray spectroscopy and microscopy to characterize the structural and electronic properties of the niobium thin films used in fabrication. Ultimately, we showed correlations between relaxation times in transmon qubits and several properties of the niobium thin films used in fabrication, including grain size, oxide thickness, oxide quality, and residual resistance ratio. This work gives some clues to the microscopic sources of relaxation, and it paves the way for future studies to use a materials-based approach to enhance qubit coherence.

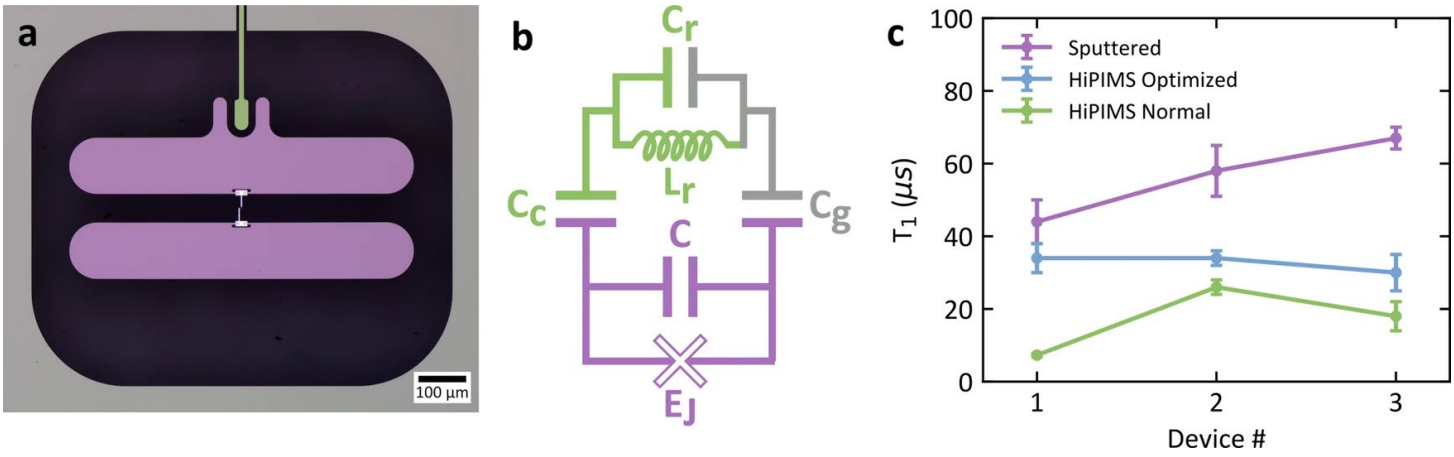

Figure 1: Transmon qubit design and performance.

a False color optical image of a representative transmon qubit from our study. Niobium regions include the center-pin of the coplanar waveguide resonator (green), the transmon capacitor pads (purple), and the ground plane (gray). The aluminum Josephson junction is shown in white. Black areas indicate where the metal has been etched away, and the sapphire substrate is exposed. **b** Effective circuit diagram of a transmon qubit coupled to a resonator. Each circuit element is schematically colored as in (**a**). The resonator is comprised of a center-pin coupled to ground via a capacitor (C_r) and an inductor (L_r). E_J and C refer to the Josephson energy and the capacitance of the qubit respectively. The qubit is capacitively coupled to the center-pin of the resonator (C_c) and to ground (C_g). **c** Measured relaxation times (T_1) for three rounds of devices fabricated with sputtered (purple circles), HiPIMS optimized (blue diamonds), and HiPIMS normal (green squares) niobium films, for a total of nine devices. Error bars indicate standard deviation across all T_1 measurements taken on a particular device.

CITATIONS

- (1) Premkumar, A. et al. Microscopic relaxation channels in materials for superconducting qubits. *Commun Mater* **2**, 72 (2021).

Advisor: Andrew A. Houck (Electrical Engineering)

Superconducting-Circuit Device Design and Quantum Simulation

Researcher: **Basil Smitham** (Princeton Graduate)**, Jeronimo Martinez** (Princeton Graduate)**, Christie Chiu** (Princeton Postdoc)

Sponsorship: NSF

Superconducting circuits are perhaps most well-known for their use in quantum computing. There, a superconducting quantum processor may look like an array of qubits, with lines and resonators coupled to each qubit for control and readout.

The same toolbox used for quantum computing applications, however, can also be applied to directly emulate quantum models motivated by condensed matter physics. For example, a lattice of transmon qubits implements the Bose-Hubbard model: excitations can "hop" between capacitively coupled qubits much like electrons hop between adjacent lattice sites in a crystalline material, and the transmon nonlinearity maps onto electron-electron on-site interactions. In this sense, superconducting circuits can be used for "quantum simulation" of real materials.

For scalability of these circuits, it is desirable to create wideband on-chip filters that can be used with multiple qubit readout resonators and provide robustness to possible device fabrication imperfections. The bottom left figure shows a novel filter design by graduate student Basil Smitham, which preliminary data suggests has a relatively flat admittance profile from 7 to 8 GHz.

At the same time, condensed matter models with qualitatively interesting single- and many-particle dynamics are already within reach. The bottom right figure shows a device prototype by graduate student Jeronimo Martinez, used to develop superconducting-circuit quantum simulation of flat electronic bands. In lattice models with flat bands, particles have infinite effective mass and any nonzero interaction is sufficient to reach the strongly interacting regime.

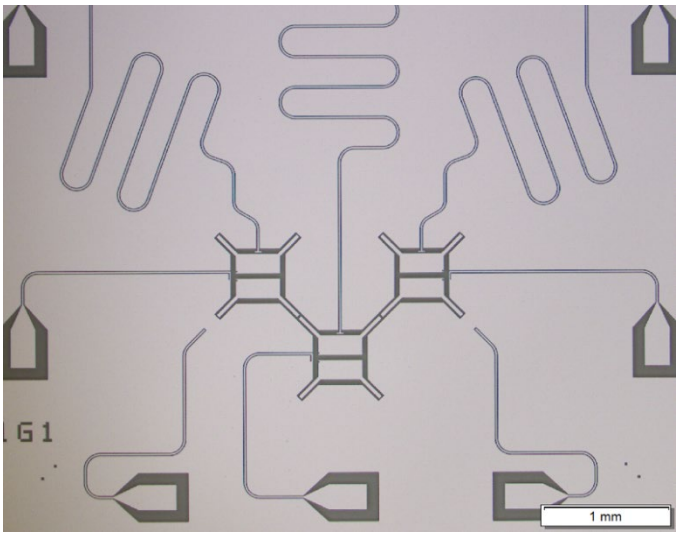

Figure 1. Towards flat-band lattices for superconducting circuits: We leverage the flexible geometry of superconducting circuits to study lattices with flat bands. However, this requires precise and accurate control over device and qubit parameters, which we began developing using this prototype. Device & image by Jeronimo Martinez.

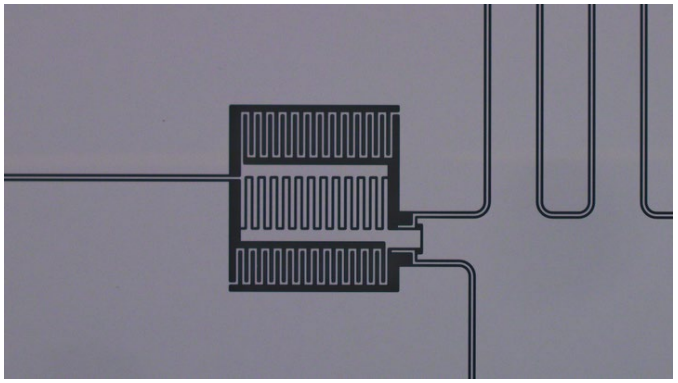

Figure 2. A novel wideband Purcell filter: Through a new design methodology for Purcell filters, we create a novel wideband Purcell filter with compact size (approx. 500 μm x 600 μm), while also maintaining large bandwidths of frequencies for both qubits and readout resonators. Device & image by Basil Smitham.

CITATIONS

- N/A

Advisor: Andrew A. Houck (Electrical Engineering)
Quantum Simulation With Superconducting Circuits
Researcher: **Jacob Bryon** (Princeton Graduate)
Sponsorship: NSF, DOD

Recent theoretical work has highlighted that quantizing a superconducting circuit in the presence of time- dependent flux Φ(t) generally produces Hamiltonian terms proportional to dΦ/dt unless a special allocation of the flux across inductive terms is chosen. Here, we present an experiment probing the effects of a fast flux ramp applied to a heavy-fluxonium circuit. The experiment confirms that naïve omission of the dΦ/dt term leads to theoretical predictions inconsistent with experimental data. Experimental data are fully consistent with recent theory that includes the derivative term or equivalently uses "irrotational variables" that uniquely allocate the flux to properly eliminate the dΦ/dt term.

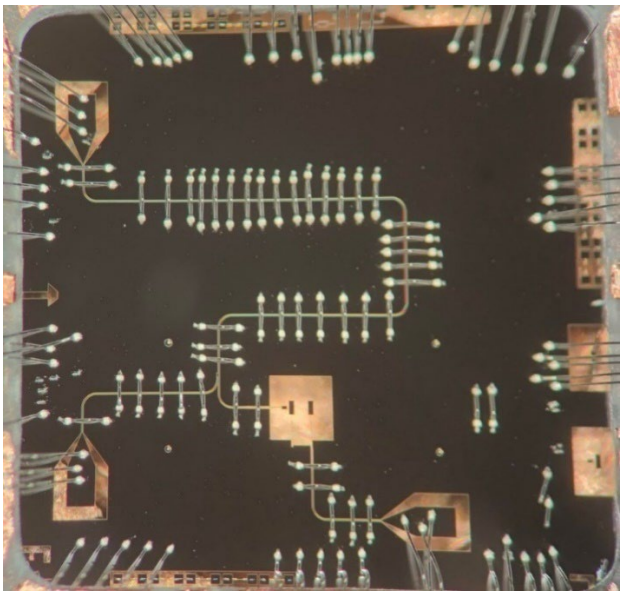

Figure 1: Image of device fabricated in the MNFC for exploring qubit interactions for superconducting quantum computing and simulation.

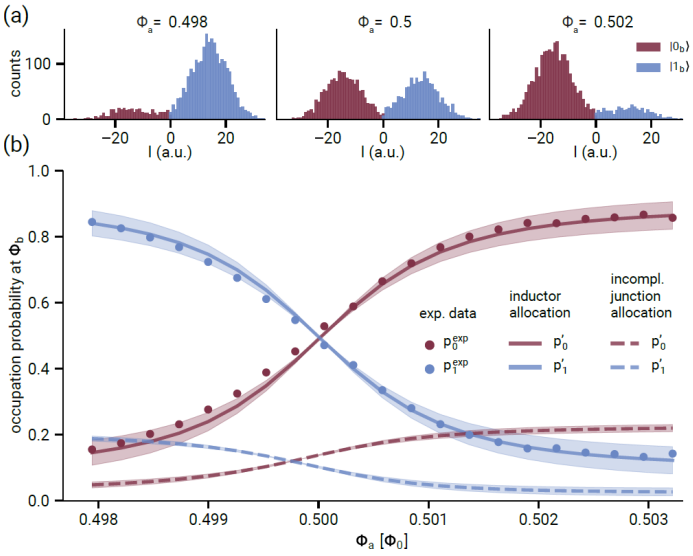

Figure 2: Occupation probabilities pm = | ⟨mb|oa⟩ |2 after a sudden flux ramp from initial flux Φa ∈ [0.498, 0.503] to final flux Φb = 0.812 Φo, starting in state |oa⟩ . (a) Representative single-shot data of ground state (red) and first-excited state (blue) occupation probability when pulsed from Φa = 0.498, 0.5, 0.502 Φo to Φb = 0.812 Φo. (b) Occupation probability as a function of initial flux point Φa. Points represent measured data, solid lines signify inductor allocation, and dashed lines the incomplete junction allocation. The ground (first-excited) state is represented in red (blue). Experimental error bars are plotted on the data points, but are small enough to be enclosed within the size of the markers. Simulation curves are plotted accounting for measurement infidelity and state preparation errors as described in Sec. III, with α = 0.05 as the center and shaded region showing range α ∈ [0.0, 0.1]. For the inductor allocation the occupation probability primarily remains in the qubit subspace, while for incomplete junction allocation most of the occupation probability would leak into higher-lying states (not shown).

CITATIONS

- Jacob Bryon, D. K. Weiss, Xinyuan You, Sara Sussman, Xanthe Croot, Ziwen Huang, Jens Koch, Andrew Houck; Experime verification of the treatment of time-dependent flux in circuit quantization (https://arxiv.org/abs/2208.03738)

Advisor: Andrew A. Houck (Electrical Engineering)

Improving T1 in Dielectric-Loss-Limited Fluxonium Qubits

Researcher: **Parth Jatakia** (Princeton Graduate)

Sponsorship: ARO, NSF, AFOSR

Superconducting qubit is a leading platform for the development for quantum computers and quantum science. The long coherence times and high anharmonicity of fluxonium qubits make it an attractive candidate for a superconducting quantum computer. However, past generations of high coherence fluxonium qubits [1,2] have been limited by the dielectric loss associated with lossy capacitors. Recent studies on tantalum-based transmons have shown improvement in dielectric-loss-limited coherence times, realizing new records in device coherence [3]. Utilizing the same approach, we study the coherence properties of fluxonium while being informed by the material surface participation ratio of the electric field in tantalum. As a result of our study, we have observed improvements in the coherence times of current 2D fluxonium qubits.

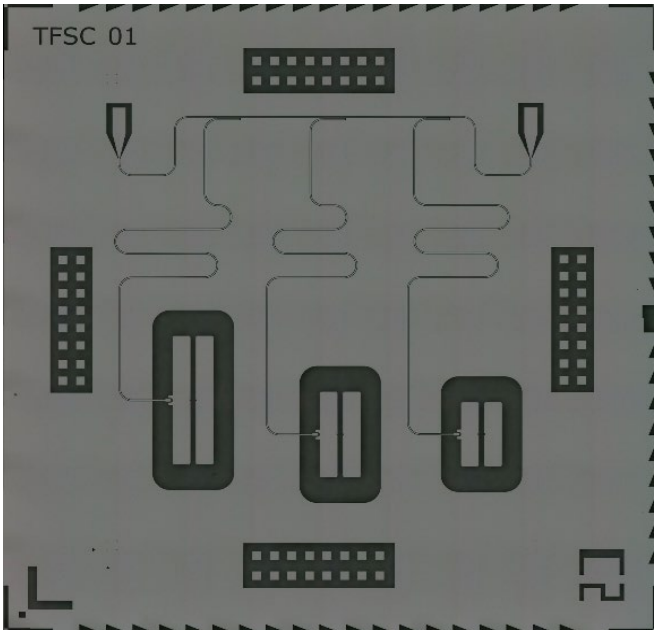

Figure 1: Optical Image of a device containing three tantalum based fluxonium superconducting qubits. The device design principles were based on the solutions on the recent work in improving coherence in transmons [3].

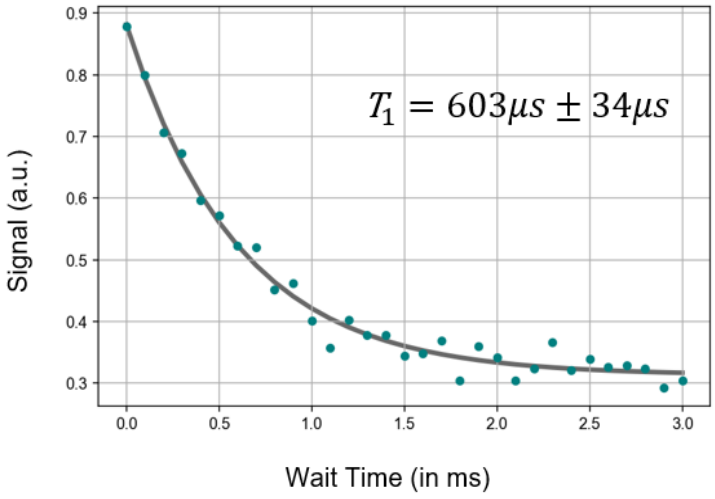

Figure 2: The qubit lifetime or decay measurement of the qubit showed in Figure 1. The measured lifetime is 603 μs which is the highest lifetime measured for a 2D fluxonium qubit.

CITATIONS

- [1] Nguyen, L. B., Lin, Y. H., Somoroff, A., Mencia, R., Grabon, N., & Manucharyan, V. E. (2019). High-Coherence Fluxonium Qubit. Physical Review X, 9(4).
- [2] Zhang, H., Chakram, S., Roy, T., Earnest, N., Lu, Y., Huang, Z., Weiss, D. K., Koch, J., & Schuster, D. I. (2021). Universal Fast-Flux Control of a Coherent, Low-Frequency Qubit.
- [3] A. P. M. Place, L. V. H. Rodgers, P. Mundada, B. M. Smitham, M. Fitz- patrick, Z. Leng, A. Premkumar, J. Bryon, S. Sussman, G. Cheng, T. Madhavan, H. K. Babla, B. Jaeck, A. Gyenis, N. Yao, R. J. Cava, N. P. de Leon, and A. A. Houck, New material platform for superconducting transmon qubits with coherence times exceeding 0.3 milliseconds, arXiv:2003.00024v1 (2020).

Advisor: Andrew A. Houck (Electrical Engineering)

Superconducting Circuits for Quantum Device Applications

Researcher: **Sara Sussman** (Princeton Graduate)

Sponsorship: ARO

Two-qubit gate error is a major limiting factor for today's large superconducting quantum processors at Google and IBM. Designing an architecture to optimize two-qubit gates requires both strong interactions and fast gate speeds while minimizing coupling to the environment. In the MNFC cleanroom at Princeton, the Houck lab developed and is optimizing an architecture that uses a generalized flux qubit to couple two far-detuned fixed-frequency transmon qubits. After fitting the device spectrum and minimizing the crosstalk between the two qubits, the Houck lab team tunes up and characterizes the resulting two-qubit gate.

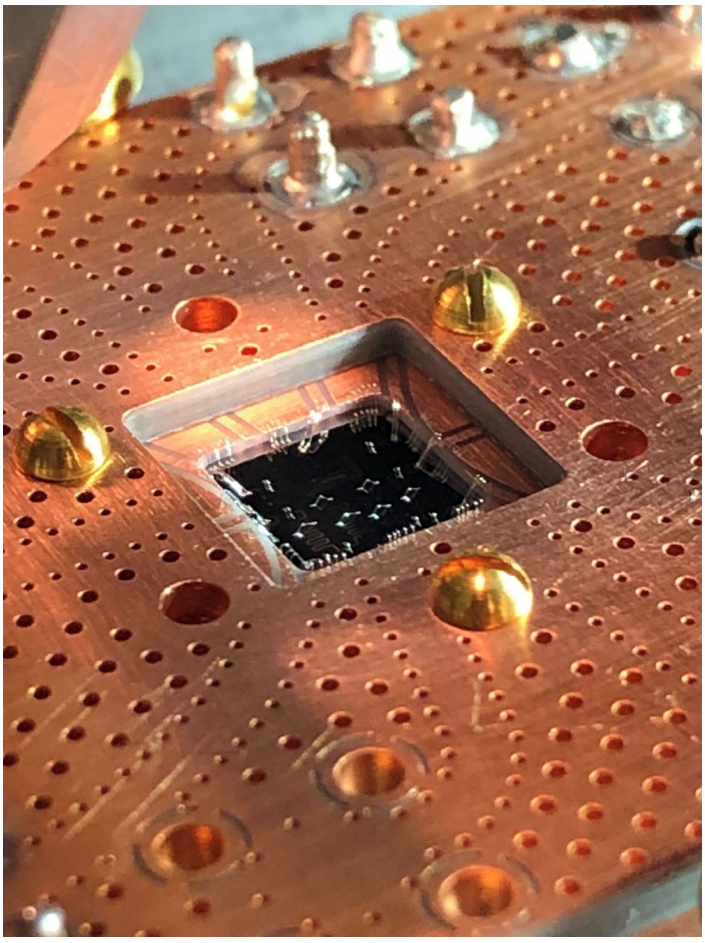

Figure 1: A two-qubit entangling device, fabricated and packaged at MNFC.

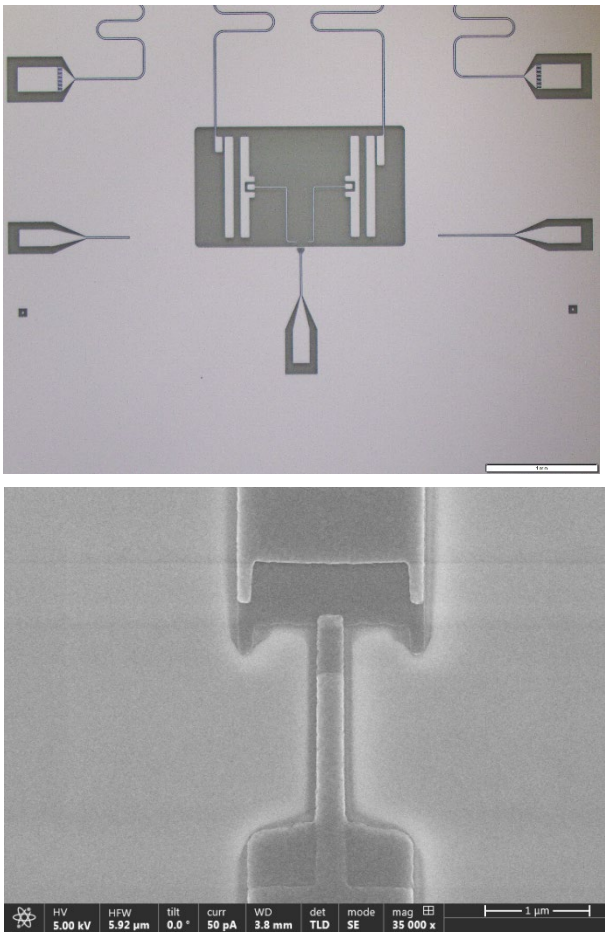

Figure 2 (Top) A two-qubit entangling device photolayer fabricated at MNFC, (Bottom) A qubit Josephson junction fabricated at MNFC.

CITATIONS

- "Let Each Quantum Bit Choose Its Basis Gates", arXiv:2208.13380; In MICRO 2022: 55th IEEE/ACM International Symposium on Microarchitecture.

Advisor: Andrew A. Houck (Electrical Engineering)

Protomon: Prototype for a Protected Superconducting Qubit

Researcher: **Shashwat Kumar** (Princeton Graduate)

Sponsorship: ARO, NSF, Co-design Center for Quantum Advantage

Protection against depolarization and pure dephasing processes is desirable for long coherence times in qubits. The disjoint support of the logical wavefunctions and sweet spots in the qubit energy splitting protect against spontaneous qubit relaxation and pure dephasing, respectively. We employ a fluxonium molecule [1] circuit to engineer protection against noise in a novel subspace having disjoint support and a sweet spot. At MNFC, Houck-lab engineers protected superconducting qubit, Protomon, and measure coherence times in the lab.

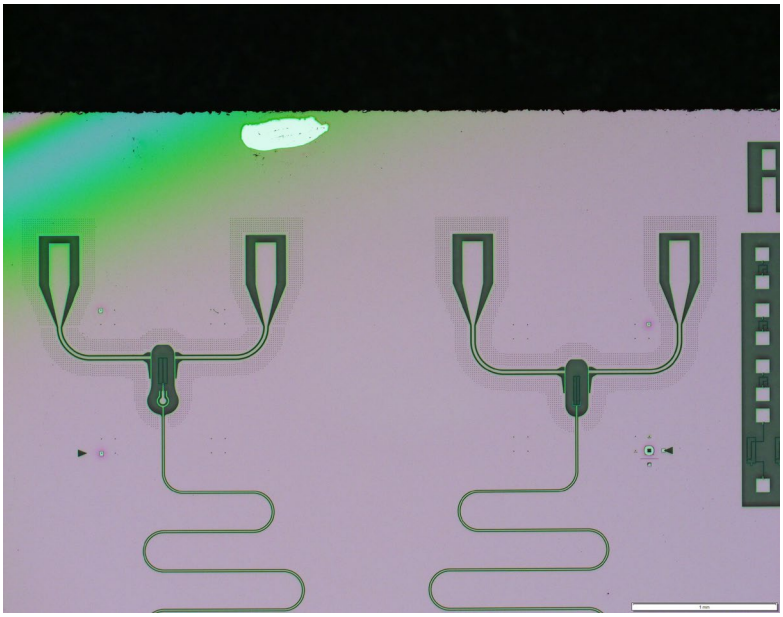

Figure 1: MNFC E-Beam developed two-protomon-qubit device. The qubit is shown in the figure on right.

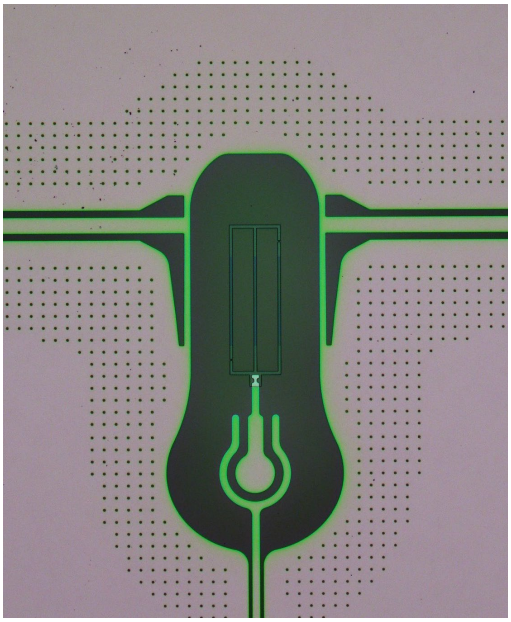

Figure 2: An E-Beam developed protomon qubit at MNFC.

CITATIONS

- [1] A. Kou, W. C. Smith, U. Vool, R. T. Brierley, H. Meier, L. Frunzio, S. M. Girvin, L. I. Glazman, and M. H. Devoret, Phys. Rev. X 7, 031037 (2017)

Advisor: Andrew A. Houck (Electrical Engineering)

Characterizing Sources of Loss in Tantalum-Based Transmon Qubits

Researcher: **Nishaad Khedkar** (Princeton Undergraduate)

Sponsorship: DOE

The superconducting transmon qubit ('transmon') is a leading platform for quantum computing and other applications in quantum information science. Building useful systems based on transmons requires significant improvements in qubit lifetimes, which are typically ~0.1-0.2 ms, orders of magnitude shorter than limits imposed by bulk properties of the constituent materials. This indicates that decoherence likely originates from contaminants and other non-idealities on uncontrolled surfaces and interfaces. Our group has fabricated transmons with lifetimes exceeding 0.3 ms by replacing niobium with tantalum as the primary conductive component; we hypothesize this is partially due to reduction in non-idealities from the better-structured oxide growth on tantalum surfaces. Analysis of these devices has indicated that the impact of non-idealities on lifetime scales with the transmon's energy levels. To further reduce decoherence, we have used the MNFC cleanroom facilities to fabricate several novel transmon designs with reduced energy levels that can be analyzed to determine the validity of these claims.

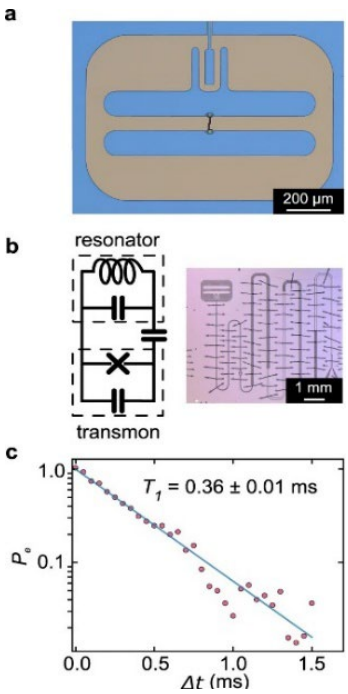

Figure 1. Original tantalum-based transmon. (A) False-colored optical microscope image of a transmon qubit. The transmon consists of a nonlinear Josephson junction shunted by two large capacitor islands made of tantalum (blue). (B) Corresponding circuit diagram of the transmon coupled to a resonator, used for reading out the quantum state of the transmon indirectly, via a capacitor. (C) Peak T1 measurement, showing the excited state population Pe as a function of delay time Δt. Line represents a single exponential fit with a characteristic time of 0.36 ± 0.01 ms.

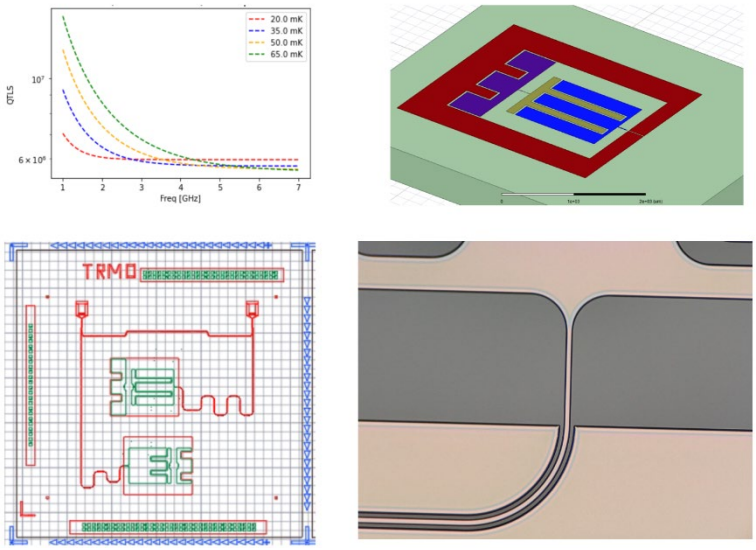

Figure 2. Design of a lower-energy transmon. (A) Simulation of dependence of the non-idealities Q factor and the resonance frequency (energy) of the transmon for select superconducting temperatures. (B) Computerized design of lower-frequency transmon. Compared to Fig 1a, capacitances were designed significantly larger to achieve resonances lower by a factor of ~4, requiring elongated design (dimensions of the red block are >2mm) and finger capacitor structure. (C) Novel transmons coupled to their readouts, to be fabricated on a chip. (D) Post-fabrication microscopic image of transmon-resonator coupling.

CITATIONS

- A. P. M. Place et al "New material platform for superconducting transmon qubits with coherence times exceeding 0.3 milliseconds," Nat. Commun. 12, 2021.

Advisor: Andrew A. Houck (Electrical Engineering)

Decoherence and Relaxation in New Qubits

Researcher: **Hoang Le** (Princeton Undergraduate), and **Youqi Gang** (Princeton Undergraduate)

Sponsorship: ARO

We are exploring the limiting factors of qubits made from new types of materials and new processing techniques.

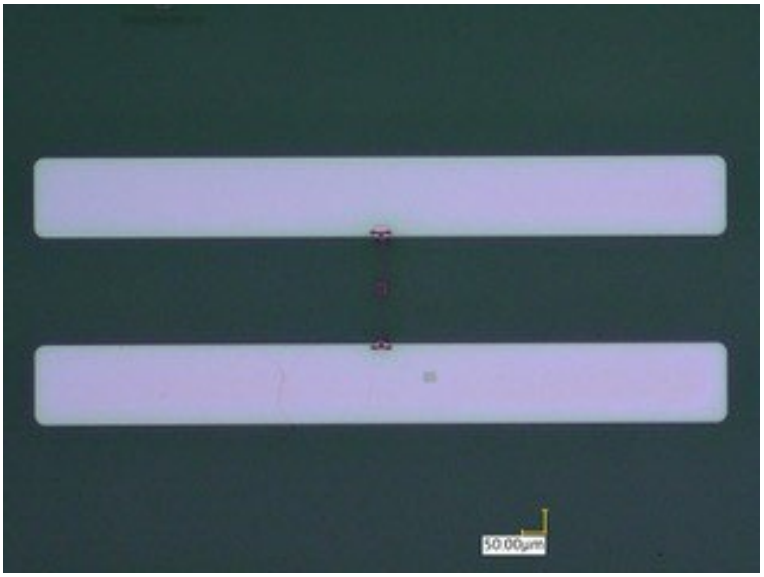

Figure 1: 3D transmon qubit. The big white pads are the tantalum, and in between them runs an aluminum Josephson junction.

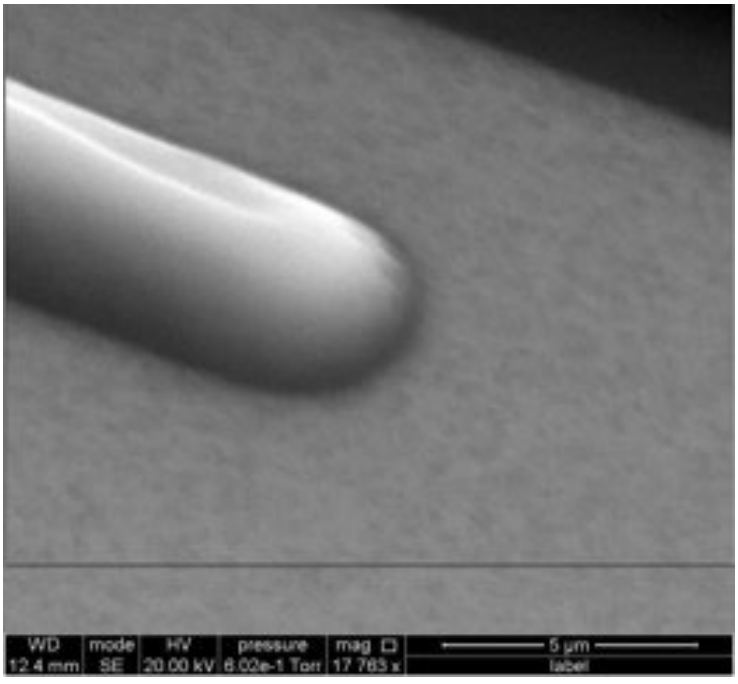

Figure 2: Photoresist on top of tantalum. We use the photoresist to protect the tantalum that we don't want to etch away.

CITATIONS

- Place, A.P.M., Rodgers, L.V.H., Mundada, P. et al. New material platform for superconducting transmon qubits with coherence times exceeding 0.3 milliseconds. Nat Commun 12, 1779 (2021). https://doi.org/10.1038/s41467-021-22030-5

Advisor: Stephen A. Lyon (Electrical Engineering)
Electron Thermometry of Helium Surface States Above a Resistive Metal
Researcher: **Matt Schulz** (Princeton Graduate)
Sponsorship: DOE

This project attempts to carry out thermopower-based helium surface-state electron thermometry above a resistive metal. Thermopower-based thermometry has been shown to be effective in measuring electron temperatures for hot electrons using thicker helium channel depths. This work attempts to carry out the thermometry for thin helium channel depths, where the man dissipative power mechanism is the image charge interaction in the resistive metal.

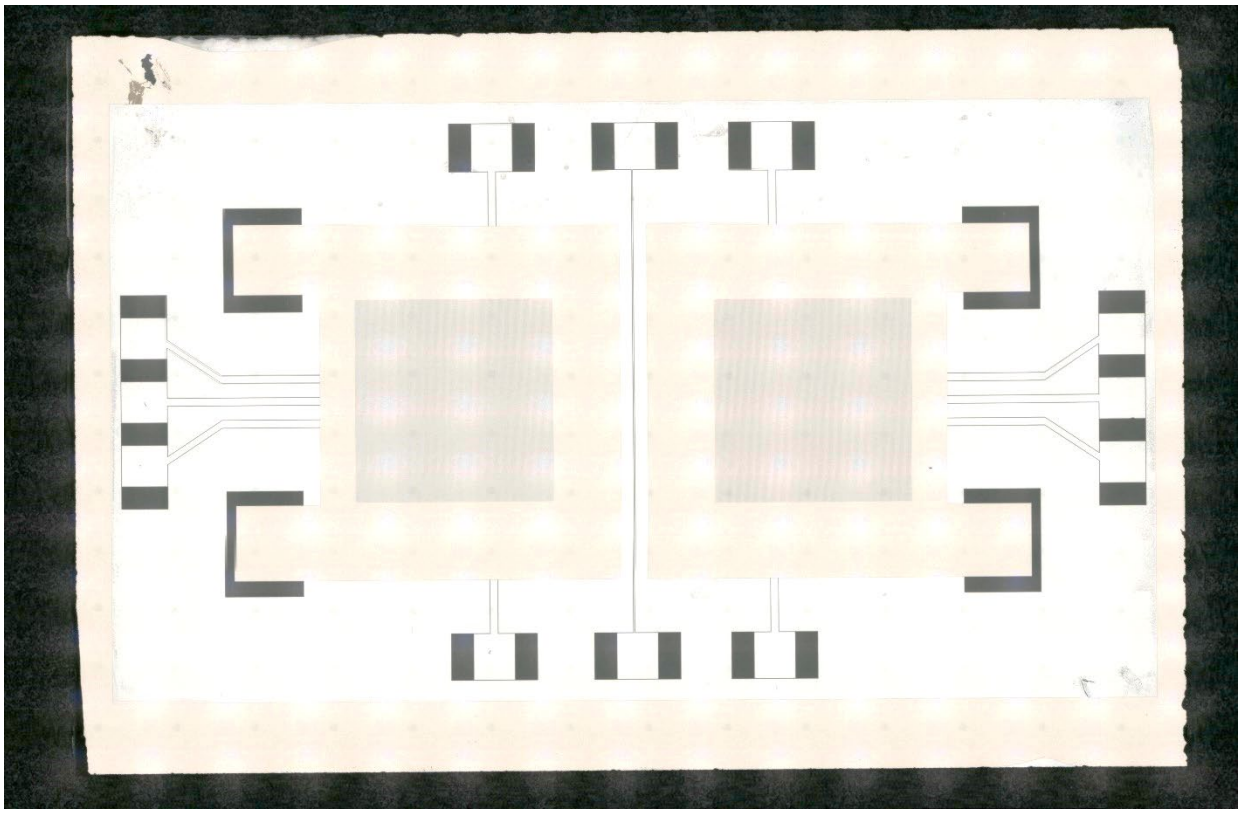

Figure 1: A real-space image of a completed chip (carrying two devices) taken with a Keyence VHX-6000. The processes used to complete this chip were all done on devices in the MNFC cleanroom (predominantly including the EBPG 5150, the Heidelberg DWL 66+, the Savannah ALD, and the APEX Metal Etcher).

CITATIONS

- Thermopower-Based Hot Electron Thermometry of Helium Surface States at 1.6 K. E. Kleinbaum and S. Lyon, Phys. Rev. Lett. 121, 236801 (2018).

Advisor: Stephen A. Lyon (Electrical Engineering)

Electrons on Helium

Researcher: **Mayer Feldman** (Princeton Graduate)

Sponsorship: Lawrence Berkeley Lab

Electrons on Helium are a promising platform for quantum computing due to their high mobility and absence of noise. However, fine electrical control of the electron wavefunction as well as control of the spin degree of freedom is still an outstanding problem. Our goal is to fabricate new devices (e.g.: a photonic bandgap resonator, a lumped element LC oscillator) that can probe the coherence properties of the spin degree of freedom of electrons floating on Helium.

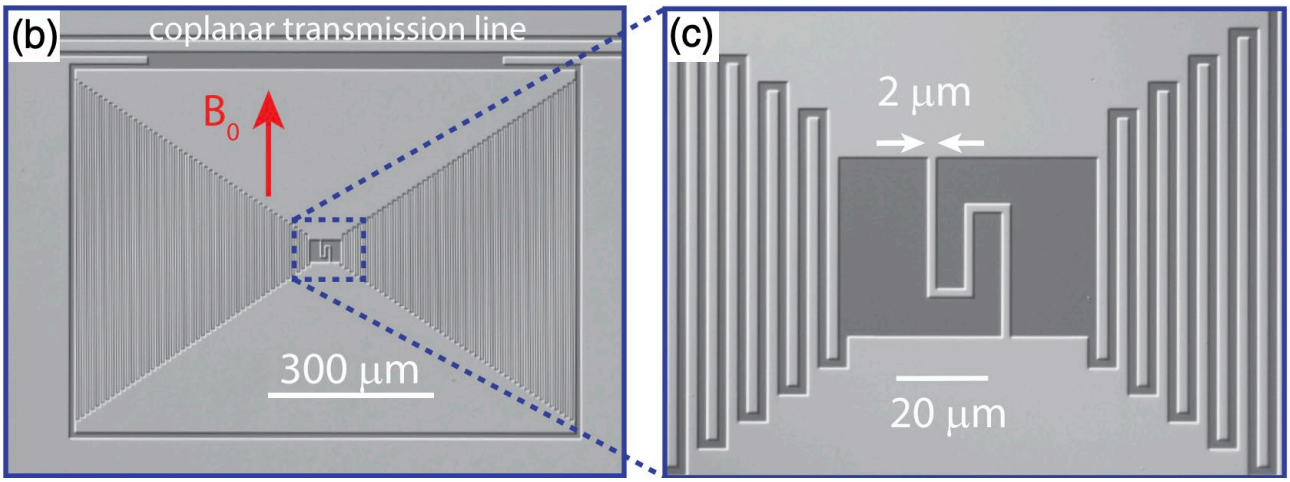

Figure 1: A photonic bandgap resonator for probing the coherence properties of electrons floating on liquid helium.

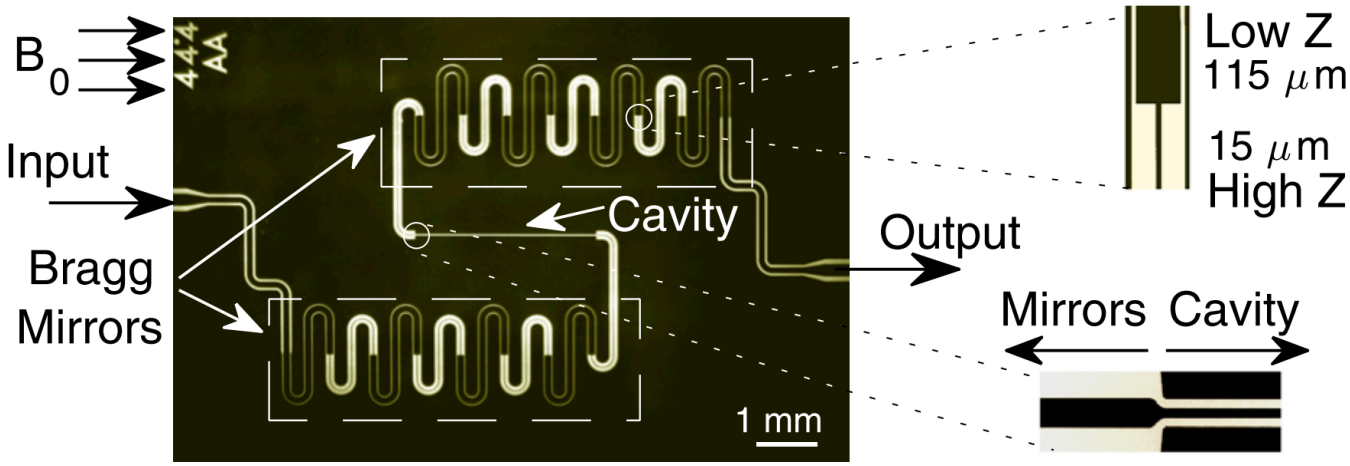

Figure 2: A lumped element LC oscillator.

CITATIONS

- N/A

Advisor: Stephen A. Lyon (Electrical Engineering)

Electron Transport on Variable Superfluid Helium Thickness

Researcher: **Tiffany Liu** (Princeton Graduate)

Sponsorship: NSF

This project will study electron transport on superfluid Helium. The device will include interdigitated capacitors which sandwich the electron transport line. When a DC voltage is applied, the capacitors will generate electric fields which alter the superfluid Helium film thickness. Electron density and mobility will be measured to understand electron transport with varying levels of Helium.

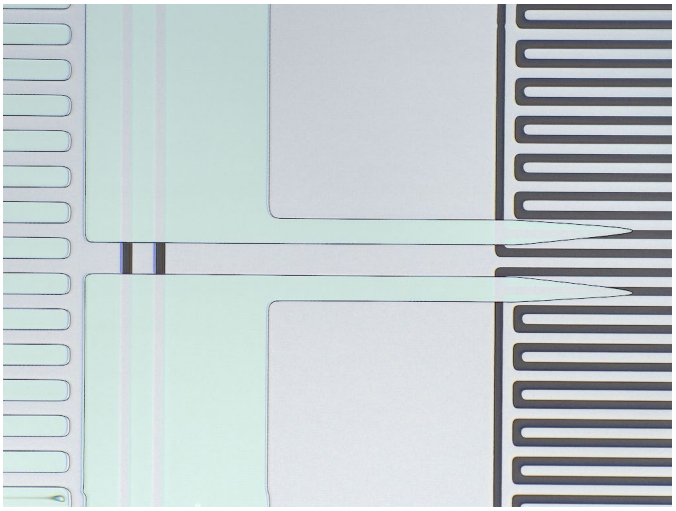

Figure 1: Confocal image of the electron transport line made of sputtered NbSi into one of the Sommer Tanner measurement zones which consists of 650 nm tall helium filled channels. These channels sit above 3 gates which allow us to measure electron density. Electrons are transported between this 5um wide line sandwiched between interdigitated capacitors, fabricated using Heidelberg, acting to both measure and vary the helium level.

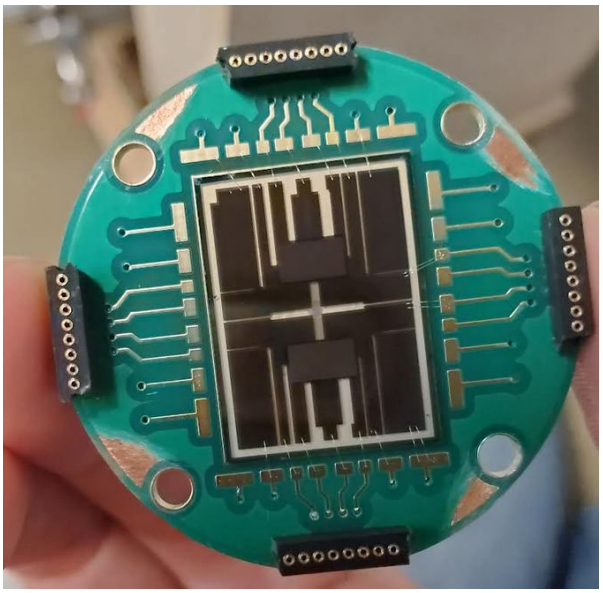

Figure 2: A completed electron on helium transport device wirebonded to a printed circuit board. The device is 15 x 20um consisting of two measurement zones on both sides connected by a thin transport line for electrons to travel across. The device is placed in a copper cell filled with helium and cooled to 1.6K to achieve a thin superfluid helium film for electrons to move across.

CITATIONS

- N/A

Advisor: Stephen A. Lyon (Electrical Engineering)
Coupling Electron Spin to Superconducting Resonator
Researcher: **Weiheng Fu** (Princeton Graduate)
Sponsorship: SEAS

We would like to explore the possibilities of measuring ESR for electrons on Helium. The device will consist of an LC resonator with holes in the inductor and a positive 'plunger' gate below attracting electrons to those locations.

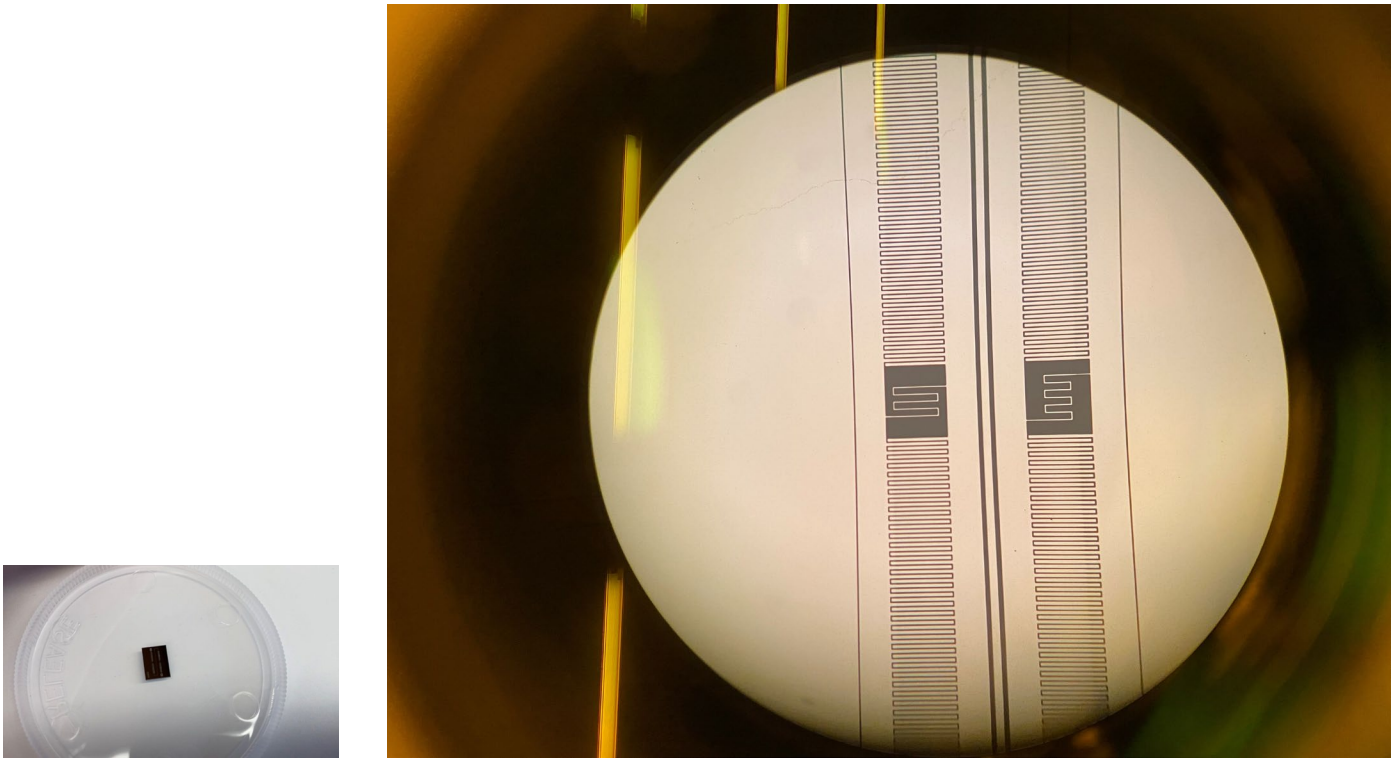

Figure 1: The chip 6x8mm with the LC resonator etched in MNFC.

CITATIONS

- https://doi.org/10.1103/PhysRevLett.118.037701

Advisor: Stephen A. Lyon (Electrical Engineering)

Measure and Study the EPR Signal for Electrons on Liquid Helium

Researcher: **Emil Joseph** (Princeton Postdoc)

Sponsorship: DOE

I would like to work on the experiments to measure the decoherence time of electron spin for electrons on liquid helium. The spin states of electrons on liquid helium are expected to remain coherent for at least 100 seconds[1] which is several orders of magnitude higher than for electrons in semiconductors. If experimentally we could demonstrate such a long spin decoherence time for electrons on liquid helium, then the spin of electron on liquid helium could be used effectively as a qubit for quantum computation. Thin film of helium on a substrate is known to support higher electronic densities than on bulk liquid. The higher densities in such systems should give a better signal to noise ratio to detect electron spin resonance (ESR) of electrons on helium. This could pave the way for measuring the decoherence time of electron spin for electrons on liquid helium.

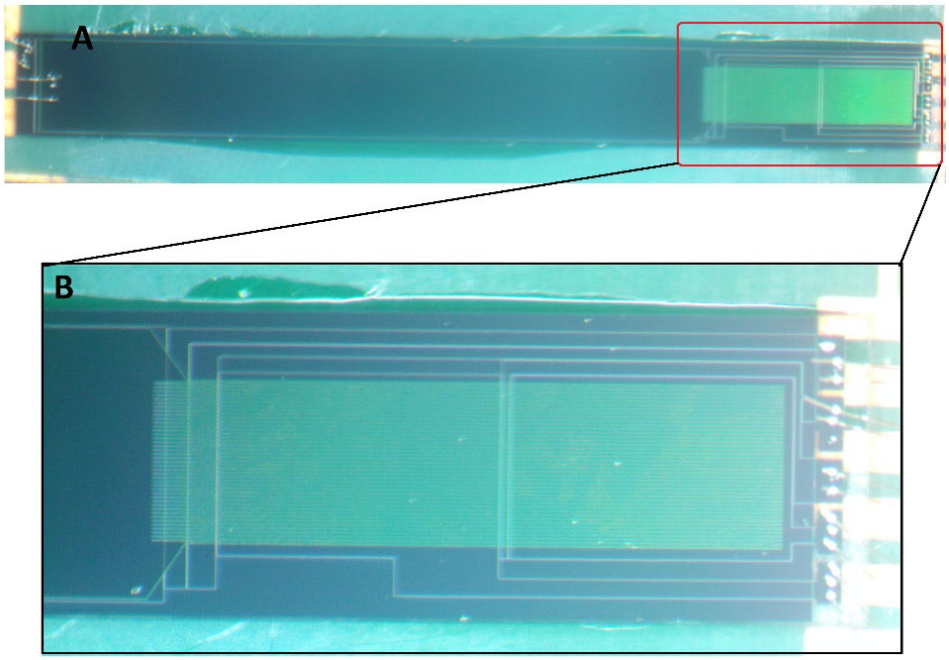

Figure 1: (A) Shows a device mounted on a PCB which was used to confine an ensemble of electrons on a Van Der Waals film of liquid helium condensed on a smooth amorphous film of TaWSi (the left side of the device). A thin film of helium can hold a high density of electrons (about 10^11 per cm^2) which helps to get a measurable ESR signal. (B) Enlarged view of the Sommer-Tanner device with micro-channeled top-metal used to measure the electron density [2].

CITATIONS

- [1] S. A. Lyon. Spin-based quantum computing using electrons on liquid helium. Phys. Rev. A 74, 052338 (2006). https://doi.org/10.1103/PhysRevA.74.052338
- [2] Asfaw, A.T., Kleinbaum, E.I., Henry, M.D. et al. Transport Measurements of Surface Electrons in 200-nm-Deep Helium-Filled Microchannels Above Amorphous Metallic Electrodes. J Low Temp Phys 195, 300–306 (2019). https://doi.org/10.1007/s10909-018-02139-6

Advisor: Paul R. Prucnal (Electrical Engineering)

Photonic Neural Processing

Researcher: **Eli Doris** (Princeton Graduate), **Simon Bilodeau** (Princeton Graduate), **Aashu Jha** (Princeton Graduate), **Josh Lederman** (Princeton Graduate), **Weipeng Zhang** (Princeton Graduate)

Sponsorship: ONR

Spiking neural networks are known to be superior over artificial neural networks for their computational power efficiency and noise robustness. The benefits of spiking coupled with the high- bandwidth and low-latency of photonics can enable highly-efficient, noise-robust, high-speed neural processors. The landscape of photonic spiking neurons consists of an overwhelming majority of excitable lasers and a few demonstrations on nonlinear optical cavities. The silicon platform is best poised to host a scalable photonic technology given its CMOS-compatibility and low optical loss. Silicon, however, does not support native spiking lasers due to the lack of optical gain. To address this, hybrid integration seeks to optically couple fibers to chips or chips of disparate material using 2-photon 3D printed structures. This will enable high-performance low-loss connections that will in turn allow us to create spiking systems that are impossible with silicon alone.

Additionally, 2-photon 3D printing can create complex networks of waveguides to enable novel 3D interconnection networks. These networks will bring photonic integrated circuits beyond the constraints of planar geometry, enabling new classes of optical processing devices

.

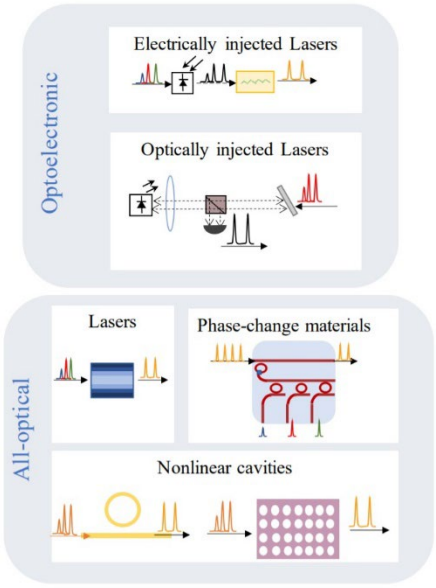

Figure1: Implementations of photonic spiking neurons, categorized into (top) optoelectronic devices including semiconductor lasers, and (bottom) all-optical devices, including lasers, phase-change material-based devices and nonlinear cavities. Additionally, the operational principles of each class of devices is also illustrated, showing incoming and output spikes, where colors represent optical wavelengths.

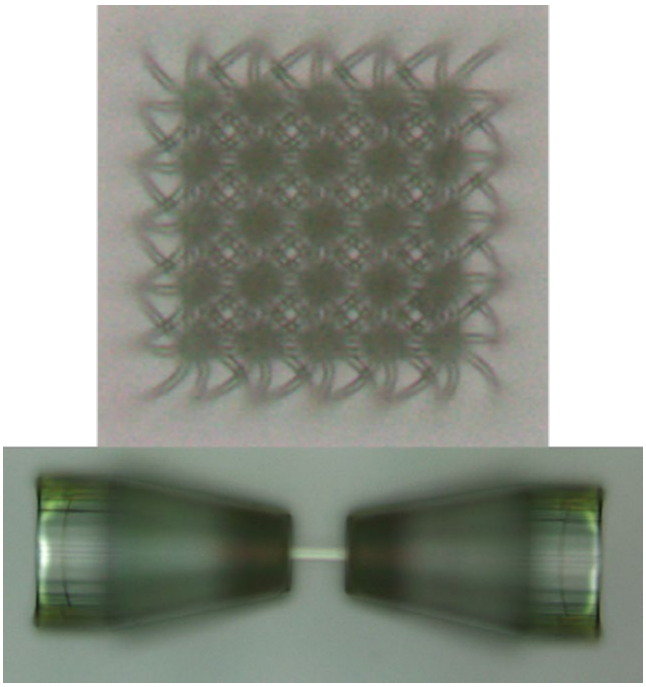

Figure 2: (top) cross section of a 3D-printed interconnection network implementing a 3x3 all-to-all convolutional kernel, (bottom) 3D-printed fiber-waveguide-fiber coupling test structure. Fibers will be plugged into either end to test efficacy and transparency of 3D-printed waveguides.

CITATIONS

- C. Huang, et al., Silicon photonic neural network for fiber nonlinearity impairment compensation., Nature Electronics, 4, (2021)
- A. Jha, et al., Photonic spiking neural networks and CMOS- compatible graphene-on-silicon spiking neurons, (2021)
- A Jha, C. et al. Reconfigurable Nonlinear Activation Functions for Neuromorphic Photonics, Opt. Lett. 23, 12758 (2020)
- C. Huang, et al. Programmable Silicon Photonic Optical Thresholder, IEEE PTL 31 (22), 1834-1837 (2020)
- C. Huang, et al. Demonstration of scalable microring weight bank control for large-scale photonic integrated circuits, APL Photonics 5 (4), 040803 (2020)
- A. Jha, et al., High-speed All-optical Thresholding via Carrier-Lifetime Tunability, Opt. Lett. 45 (8), 2287-2290 (2020)
- A. Jha, et al. Lateral Bipolar Junction Transistor on a Silicon Photonic Platform, Opt. Exp.28 (8), 11692-11704 (2020)
- C. Huang, et al. On-Chip Programmable Nonlinear Optical Signal Processor and Its Applications, IEEE JSTQE (2020)

Advisor: Paul R. Prucnal (Electrical Engineering)

Photonic Integrated Circuits for Neuromorphic and Microwave Processing

Researcher: **Simon Bilodeau** (Princeton Graduate), **Eli Doris** (Princeton Graduate), **Jesse Wisch** (Princeton Graduate), **Manting Gui** (Princeton Graduate)

Sponsorship: Universal Display Corporation

Thin-film dielectric and planar silicon leverage high refractive index contrasts to support subwavelength-scale, low-loss optical structures that can exploit economies of scale for their manufacture. However, means of controlling the optical properties of thin-film and silicon in-situ to create reconfigurable devices and circuits are limited. On the other hand, organic polymers and molecules support a much richer space of tunability, but a lower index contrast results in low-performance integrated photonic platforms. In this collaboration between the Prucnal and Rand research groups, we are exploring the hybrid integration of various organic systems with thin-film and silicon nanophotonic circuits to combine the best of both materials for novel reconfigurable integrated photonic platforms. MNFC supports this effort by enabling the fabrication, characterization, and co-integration of these disparate technologies into a single platform.

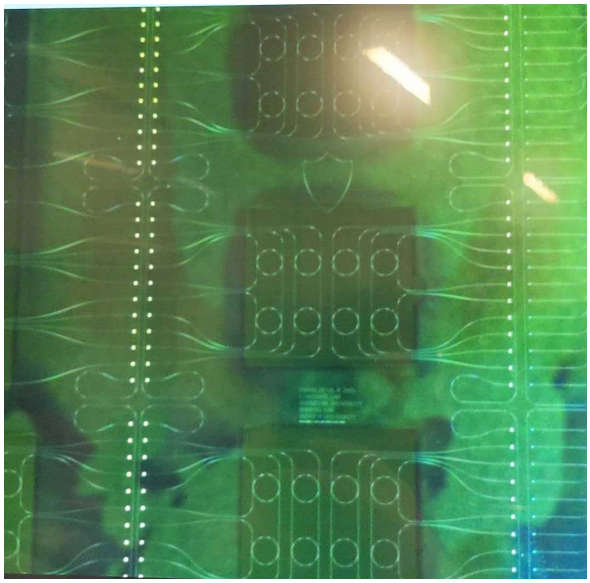

Figure 1: Flip-chip bonder alignment of silicon nitride nanophotonic devices with a custom silicon shadow mask for selective evaporation of organic molecules.

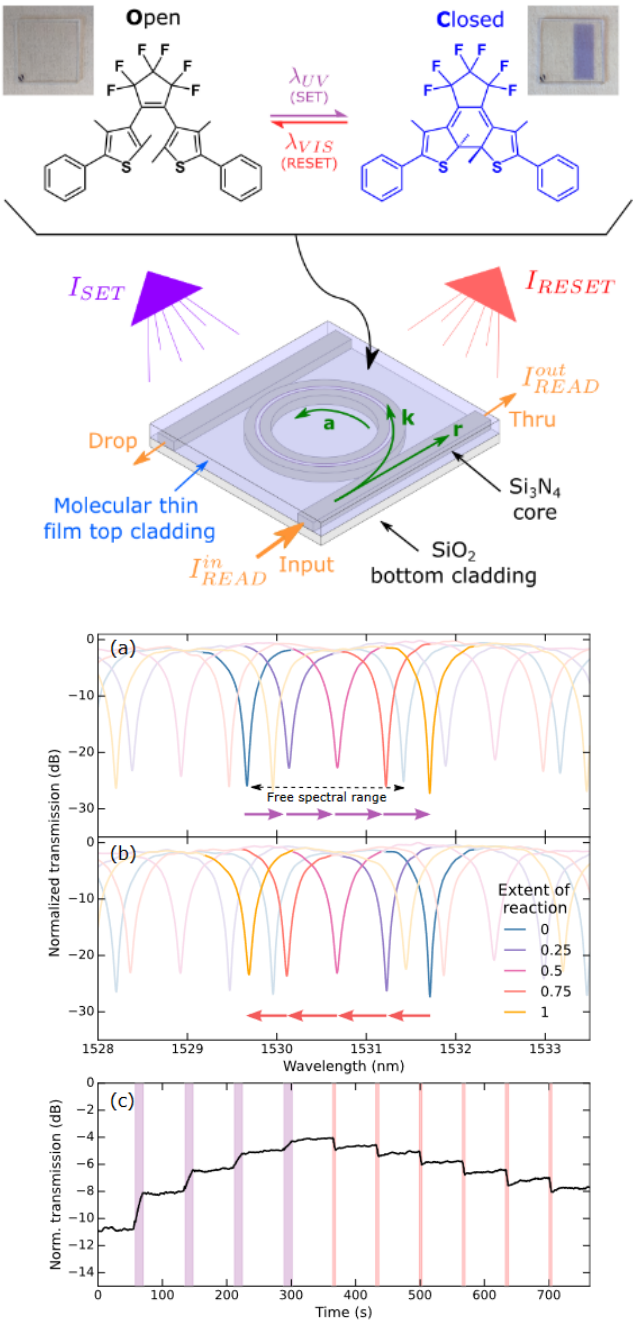

Figure 2: Photochemical reprogrammation of a silicon nitride microring resonator. Under UV and visible illumination, the infrared resonance wavelength of a nanophotonic silicon nitride resonator over which organic photochromic molecules were evaporated can be non-volatilely and reversibly tuned with low loss.

CITATIONS

- S. Bilodeau et al. All-optical organic photochemical integrated nanophotonic memory: lossless, continuously-tunable, non-volatile. (under review)
- S. Bilodeau, et al., Dynamics of a Photochromic-Actuated Slot Microring Photonic Memristor," IEEE JSTQE (2022)
- S. Bilodeau et al., "Stacked Reconfigurable Optical Cavities for Smart Sensing Pixels," IEEE JSTQE (2022)
- S. Bilodeau et al., "Thin film photonic resonator weight stacks," IEEE Summer Topicals (2022)

Advisor: Paul R. Prucnal (Electrical Engineering)

Photonic Integrated Circuits for Neuromorphic and Microwave Processing

Researcher: **Eric Blow** (Princeton Graduate)

Sponsorship: Samsung Research, NSF

The Lightwave Laboratory develops integrated photonic circuits for optical signal processing applications. This technology uses light to process broadband radio-frequency signals, achieving tunable processors with tens of GHz in bandwidth and sub-nanosecond latencies. Specifically, the laboratory focuses on developing microwave linear photonic systems and neuromorphic photonic systems. The MNFC serves the critical need of post-processing foundry-made photonic chips and packaging these chips.

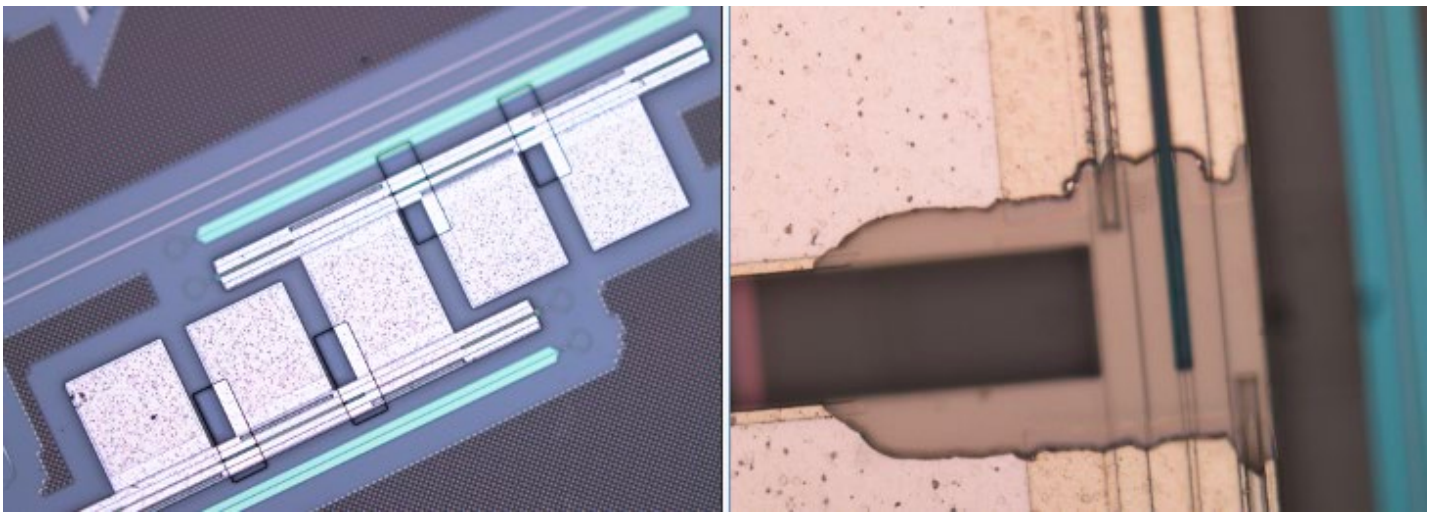

Figure 1: This figure demonstrates a required micrometer etch essential to optimize performance of an on-chip modulator of a foundry-fabrication photonic integrated circuit. Source: Simon Bilodeau

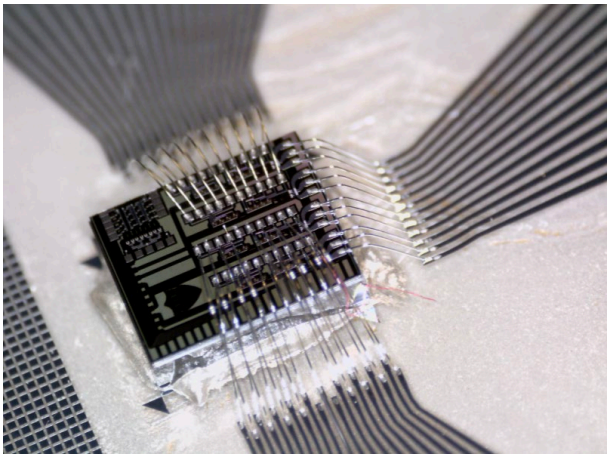

Figure 2: This figure demonstrates the large-scale photonic packaging capabilities developed for this research within the MNFC. DC wire bonds interface with the photonic neural network

CITATIONS

- Shastri, B. J., Tait, A. N., Ferreira de Lima, T., Pernice, W. H., Bhaskaran, H., Wright, C. D., & Prucnal, P. R. (2021). Photonics for artificial intelligence and neuromorphic computing. Nature Photonics, 15(2), 102-114.

Advisor: Barry P. Rand (Electrical Engineering)

Perovskite LEDs and Lasers

Researcher: **Kwangdong Roh** (Research Collaborator)

Sponsorship: Schmidt Award

Metal halide perovskite semiconductors show considerable promise as an efficient coherent light source, but the extent of their spectral tunability and optical gain bandwidth have not been established. Here, we demonstrate continuously tunable single-mode lasing from halide perovskite thin films over a wide spectral range (758 804 nm for $CH_3NH_3PbI_3$, 653 684 nm for $Cs_{0.4}(CH_3NH_3)_{0.6}Pb(Br_{0.4}I_{0.6})_3$, and 520 542 nm for $CsPbBr_3$) at room temperature for the first time. The large optical gain bandwidth (90 meV) and high modal gain coefficient (533 cm 1) are key enabling factors for this achievement. Period-varying chirped Bragg gratings utilized for optical feedback allow fine-tuning of the lasing output, with a minimum spectral tuning spacing, lasing 1.4 nm. This precise tuning control allows us to obtain the lowest possible lasing threshold throughout the gain bandwidth, useful for designing highly efficient electrically pumped laser.

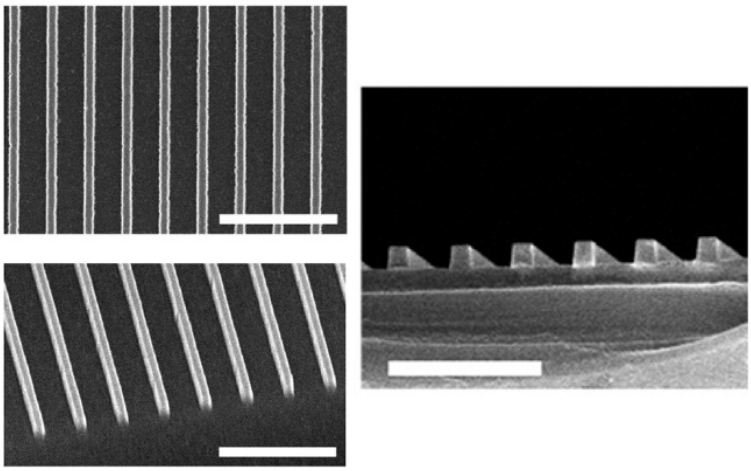

Figure 1: SEM images of quartz Bragg grating for optical feedback structure. Scale bars are 1 μm.

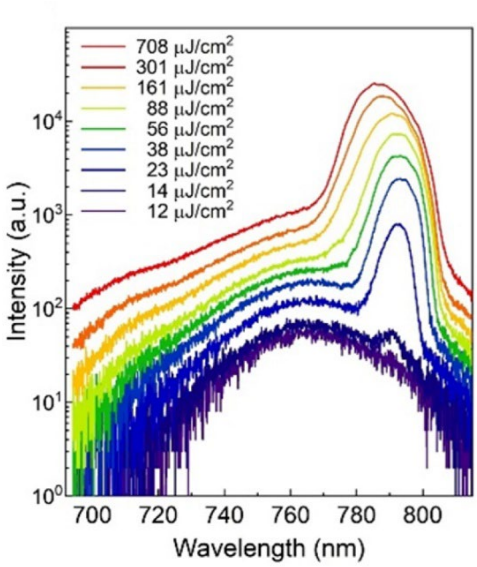

Figure 2: Emission spectra from metal halide perovskite thin film showing high optical gain property.

CITATIONS

- Roh, Kwangdong, Lianfeng Zhao, and Barry P. Rand. "Tuning Laser Threshold within the Large Optical Gain Bandwidth of Halide Perovskite Thin Films." ACS Photonics 8.8 (2021): 2548-2554

Advisor: Barry P. Rand (Electrical Engineering)
Efficient and Stable Organic-Inorganic Hybrid Perovskite Light Emitting Diodes
Researcher: **Lianfeng Zhao** (Princeton Postdoc)
Sponsorship: AFOSR

Hybrid organic inorganic perovskite semiconductors have shown potential to develop into a new generation of light emitting diode (LED) technology. Herein, an important design principle for perovskite LEDs is elucidated regarding optimal perovskite thickness. Adopting a thin perovskite layer in the range of 35 40 nm is shown to be critical for both device efficiency and stability improvements. Maximum external quantum efficiencies (EQEs) of 17.6% for Cs0.2FA0.8PbI2.8Br0.2, 14.3% for $CH_3NH_3PbI_3$ ($MAPbI_3$), 10.1% for formamidinium lead iodide ($FAPbI_3$), and 11.3% for formamidinium lead bromide ($FAPbBr_3$) based LEDs are demonstrated with optimized perovskite layer thickness. Optical simulations show that the improved EQEs source from improved light outcoupling. Furthermore, elevated device temperature caused by Joule heating is shown as an important factor contributing to device degradation, and that thin perovskite emitting layers maintain lower junction temperature during operation and thus demonstrate increased stability.

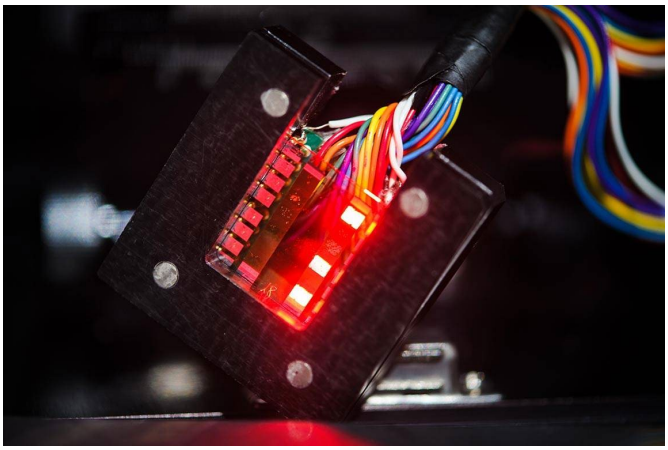

Figure 1: Perovskite Light-Emitting Diodes

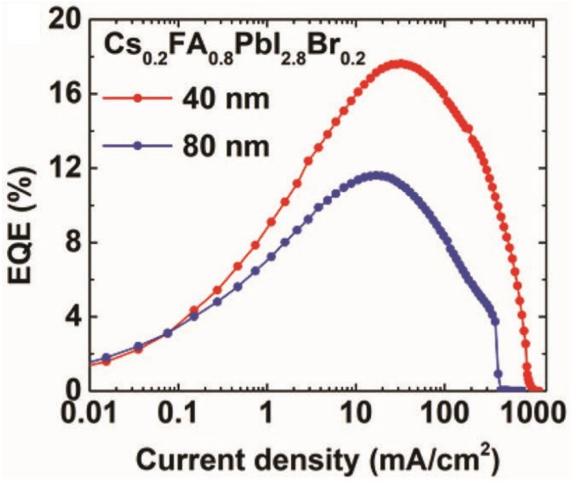

Figure 2: EQE versus current density of perovskite LEDs based on Cs0.2FA0.8PbI2.8Br0.2 thin films with 40nm, and 80 nm thicknesses.

CITATIONS

- L. Zhao, et al, Improved Outcoupling Efficiency and Stability of Perovskite Light Emitting Diodes using Thin Emitting Layers, Advanced Materials 31, 1805836, 2019.

Advisor: Kaushik Sengupta (Electrical Engineering)

Deep Learning Aided mmWave Circuit Design

Researcher: **Emir Karahan** (Princeton Graduate)

Sponsorship: DOD

Deep learning and artificial intelligence, in general, is advancing scientific discovery and technological inventions through its ability to extract inherently hidden features and map it to output in a highly complex multi-dimensional space. Synthesis of electromagnetic (EM) structures with nearly arbitrary with desired functional properties is such an example of a high dimensional optimization space. In this article, we employ deep convolutional neural network (CNN) to allow robust and rapid prediction of scattering properties of nearly arbitrary planar electromagnetic structures on chip.

Utilizing this, the work reports an mm-wave PA in 90-nm SiGe with a novel deep learning-enabled inverse design of low-loss, broadband output matching network that achieves a PAE of 16% 24.7%, a saturation power of 16.7 19.5 dBm across P sat, 3 dB bandwidth of 30 94 GHz (103.2%), while supporting both single- carrier high-speed modulation and concurrent multiband multi-Gb/s non-constant amplitude modulation. The P sat, 3 dB bandwidth covers from 5G band up to W-band and is higher than all reported mm-wave silicon PAs which have peak PAE > 20% and demonstrates for the first time concurrent multiband (triple-band) transmission with superior performance at multi-Gb/s.

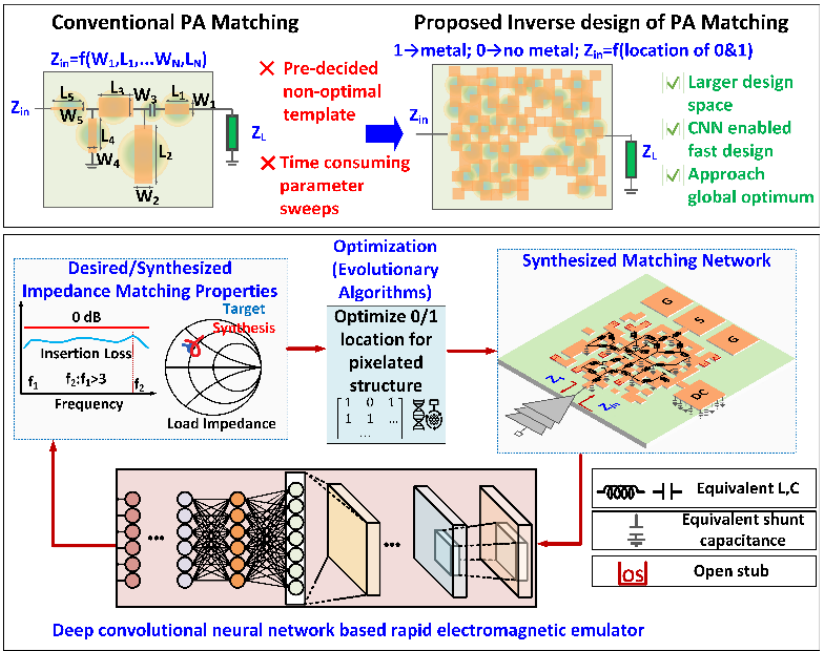

Figure 1: Concept and method of inverse design of PA, utilizing a deep CNN-based EM predictor, compared with the traditional template

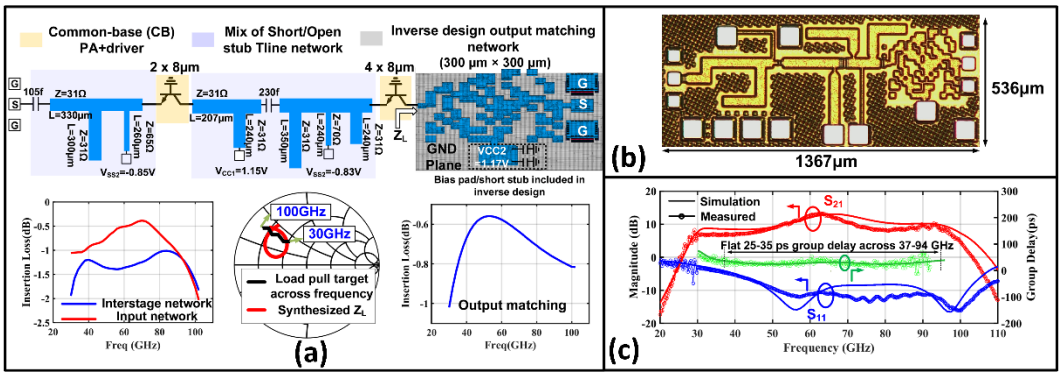

Figure 2: (a) PA schematic, (b) chip micrograph, and (c) small-signal measurement results.

CITATIONS

- DOI: 10.1109/LMWC.2022.3161979

Advisor: Kaushik Sengupta (Electrical Engineering)

mm-Wave Integrated Circuit Design for 5G

Researcher: **Zheng Liu** (Princeton Graduate)

Sponsorship: Industrial

The proliferation of millimeter-wave (mmWave) bands across 24-90 GHz and the strict spectral efficiency requirements demand future transmitter front ends to operate across multiple bands with simultaneously back-off efficiency and high linearity characteristics that typically trade off strongly with each other. In this article, we propose a simultaneously broadband, back-off efficient and linear mmWave Doherty power amplifier (PA) architecture with a quadrature hybrid, and a non-Foster inspired impedance tuner on-chip. The combination of transformer-based hybrid and the quasi-non-Foster tuner allows the architecture to synthesize optimal impedances to the PA across the 2-D variations of power back-off and frequency, enabling high back-off efficiency across a broad frequency range. In addition, the unique location of the tuner at the isolation port of the hybrid allows us to exploit its benefits while shielding the architecture from effects of tuner non-linearity, power losses, and typical stability concerns of traditional non-Foster circuits. For high linearity, we implement an emitter follower-based class C bias network with boosting effect. The PA is implemented in a 130-nm SiGe BiCMOS process. Across 44-64 GHz, the PA achieves 18.5-21.5-dBm Psat, the peak collector efficiency of 26%-34.7% and 14%-23.2% at 6-dB back-off, maintaining back-off enhancement ratio of 2.77/2.53/2.37 (1.39/1.27/1.19) at 46/52/62 GHz compared to the class-A (class-B) operation. It supports 6-gigabit-per-second (Gb/s) 64-QAM signal with -26.5-dB/-28.3-dBc error vector magnitude (EVM)/adjacent channel leakage ratio (ACLR) at average Pout/power added efficiency (PAE) of 14.6 dBm/15% at 54 GHz. This work achieves the state-of-the-art bandwidth among silicon-based mmWave PAs where higher than class-B back-off efficiency is achieved. The designed integrated circuit is wire bonded for testing in MNFC package lab.

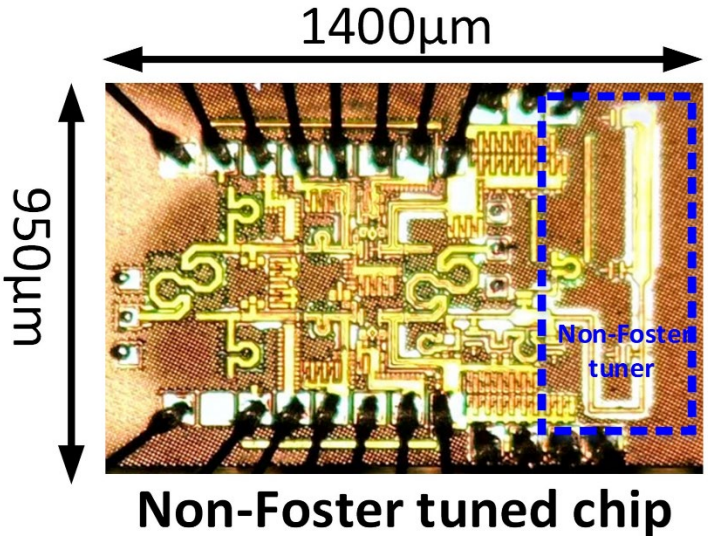

Figure 1: Wire bonded chip micrograph. The wirebond is done in the packaging lab.

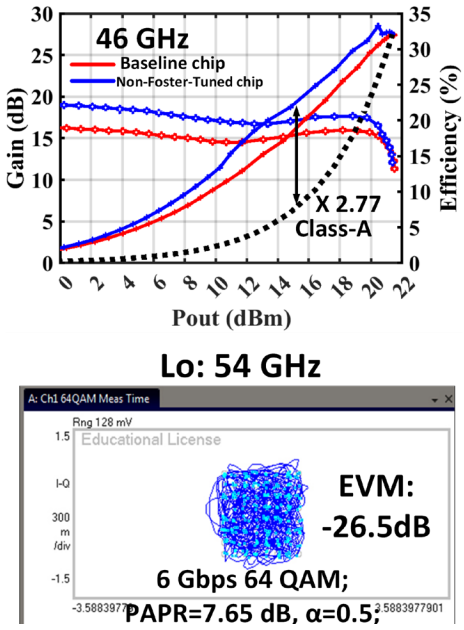

Figure 2: Measurement results Back-off efficiency enhancement over conventional class B at 46 GHz.

CITATIONS

- Zheng Liu and K. Sengupta, "A 44-64-GHz mmWave Broadband Linear Doherty PA in Silicon With Quadrature Hybrid Combiner and Non-Foster Impedance Tuner," in IEEE Journal of Solid-State Circuits, vol. 57, no. 8, pp. 2320-2335, Aug. 2022

Advisor: Mansour Shayegan (Electrical Engineering)

Limits to Mobility in Ultrahigh-Mobility GaAs Two-Dimensional Electron Systems

Researcher: **Adbhut Gupta** (Princeton Postdoc)

Sponsorship: NSF, DOE, Industrial

Two-dimensional electron systems (2DESs) residing in GaAs quantum wells formed at interface of GaAs/AlGaAs are some of the cleanest materials that can be grown in a lab. Over the last few decades, efforts to improve their quality (mobility) using advances in molecular beam epitaxy has led to emergence of several exotic many-body phases such fractional quantum Hall states (FQHSs), stripe/nematic phases, Wigner solids, and Bose-Einstein exciton condensates. Recently, a growing interest has been seen in GaAs 2DESs due to potential applications in topological quantum computing and history has demonstrated that numerous unexpected interaction-driven phases materialize with better GaAs 2DES quality. Hence, there is a strong incentive to continue efforts on this front while trying to understand what limits the mobility in modern ultrahigh-mobility 2DESs. Using experimental mobility data collected over several years for a wide variety of state-of-the-art GaAs 2DESs, and analyzing various scattering mechanisms that set the limits to mobility [1], we answer this question. Ultraclean GaAs 2DESs with densities ranging from ~ 0.2 to 3 x 1011/cm2 exhibit an interesting trend in mobility rising with density, up to a new world record of ~57 x 106 cm2/Vs at a density of 1.55 x 1011/cm2, and then dropping. A careful comparison of experimental data and models explains the trends while providing guidelines to achieving 100 x 106 cm2/Vs mobility and beyond.

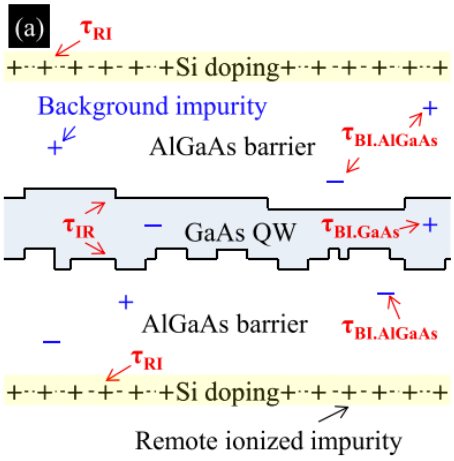

Figure 1: A schematic diagram depicting the various scattering mechanisms for 2DESs hosted in modulation-doped GaAs QWs. The scattering times from background impurities in the GaAs channel (τBI,GaAs) as well as the AlGaAs barrier (τBI,AlGaAs), remote ionized impurities that are generated by doping (τRI), and layer fluctuation driven interface roughness (τIR) all contribute to the total amount of scattering and are each shown in red. The charged species from residual background impurities are marked in blue, while those from intentional ionized dopants are marked in black.

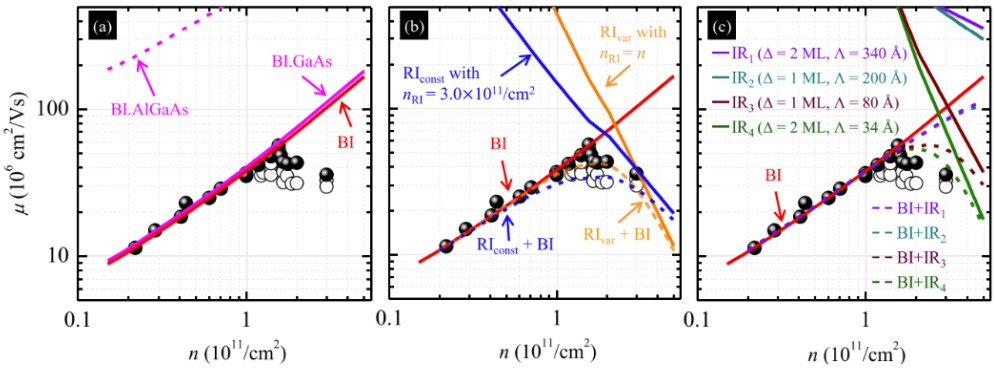

Figure 2: Experimental μ vs n data (T = 0.3 K) for our ultrahigh-quality GaAs 2DESs and their comparison with simple models (a) only background impurities (b) background impurities and remote ionized impurities (c) background impurities and interface roughness.

CITATIONS

- Y. J. Chung, A. Gupta, K. W. Baldwin, K. W. West, M. Shayegan, and L. N. Pfeiffer, Phys. Rev. B 106, 075134 (2022).

Advisor: Mansour Shayegan (Electrical Engineering)

Probing Exotic Phases of Two-Dimensional Hole Systems

Researcher: **Casey Calhoun** (Princeton Graduate)

Sponsorship: Schmidt

At low temperature and under a perpendicular magnetic field, two-dimensional electron and hole systems have been observed to form a variety of exotic quantum states. Thanks to recent advances in growth techniques, the fabrication of high-quality two-dimensional charge carrier systems with record-breaking high mobilities is now possible. This has enabled the observation of exciting new features including an unusual even-denominator fractional quantum hall state at filling factor 3/4. Measurements in these ultra-high-quality samples have also revealed a new feature: oscillations at extremely low magnetic fields. These oscillations exhibit a distinctively lower frequency than the well-known Shubnikov-de Haas (SdH) oscillations and appear to continue down to very low fields where the SdH oscillations have disappeared. Further study of these oscillations via low-temperature magneto-transport measurements of similar high-mobility, two-dimensional hole systems should help to characterize these features in order to determine their physical mechanism.

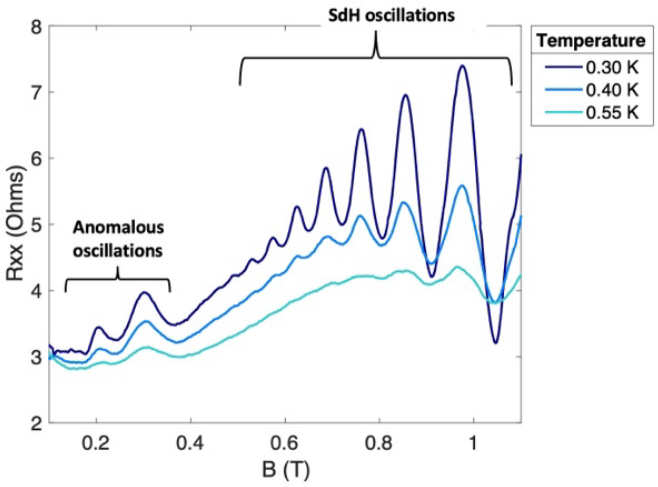

Figure 1: Low field magneto-resistance oscillations for ultra-high mobility, 2D hole system in a 20nm wide GaAs quantum well for three different temperatures. The expected SdH oscillations exist down to between 0.5T at lower temperatures before they die out (this occurs at slightly higher field at higher temperatures). Then the anomalous low-field oscillations show up around 0.3T.

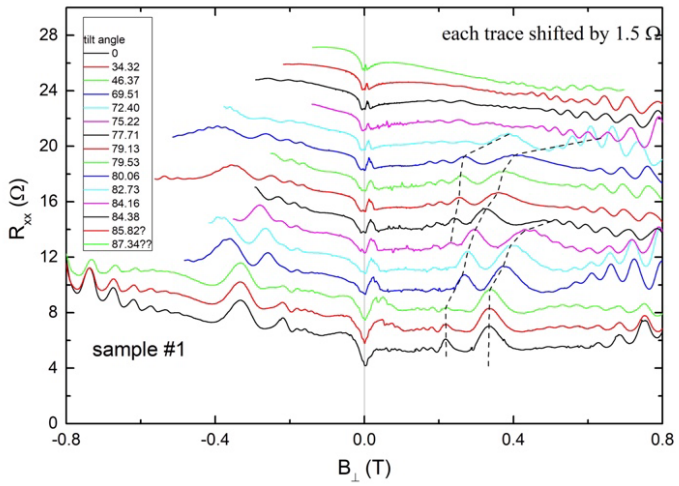

Figure 2: Evolution of the low-field features with varying tilt angle for the same sample as in Figure 1, plotted as magneto-resistance against perpendicular field. The peaks from the anomalous oscillations appear to shift to higher perpendicular fields as the tilt angle increases, while the SdH oscillations do not, indicating that an additional physical mechanism may be present.

CITATIONS

- Yoon Jang Chung, C. Wang, S. K. Singh, A. Gupta, K. W. Baldwin, K. W. West, R. Winkler, M. Shayegan, and L. N. Pfeiffer, Record-quality GaAs two-dimensional hole sys- tems, Phys. Rev. Mater. 6, 034005 (2022).

Advisor: Mansour Shayegan (Electrical Engineering)

Study of Exotic, Many-Body phases in Two-Dimensional Hole Systems

Researcher: **Chengyu Wang** (Princeton Graduate)

Sponsorship: NSF, ECCS

In a low-disorder two-dimensional electron system, when two Landau levels of opposite spin or pseudospin cross at the Fermi level, the dominance of the exchange energy can lead to a ferromagnetic, quantum Hall ground state whose gap is determined by the exchange energy and has skyrmions as its excitations. This is normally achieved via applying either hydrostatic pressure or uniaxial strain.

In our latest work [1], we study a very high-quality, low-density, two-dimensional hole system, confined to a 30-nm-wide (001) GaAs quantum well, in which the two lowest-energy Landau levels can be gate tuned to cross at and near filling factor $\nu = 1$. To tune the 2D hole density while keeping the charge distribution symmetric, we placed the sample on melted In to make a back gate and deposited Ti/Au on the top surface as the front gate. We measure the longitudinal resistance R_{xx} vs magnetic field B at different temperatures ranging from 0.03 K to 1 K, and extract the energy gap of the $\nu = 1$ quantum Hall state from the Arrhenius plot (Fig. 1). As we tune the field position of the crossing from one side of $\nu = 1$ to the other by changing the hole density, the energy gap for the quantum Hall state at $\nu = 1$ remains exceptionally large, and only shows a small dip near the crossing (Fig. 2). The gap overall follows a square root of B dependence, expected for the exchange energy. Our data are consistent with a robust quantum Hall ferromagnet as the ground state.

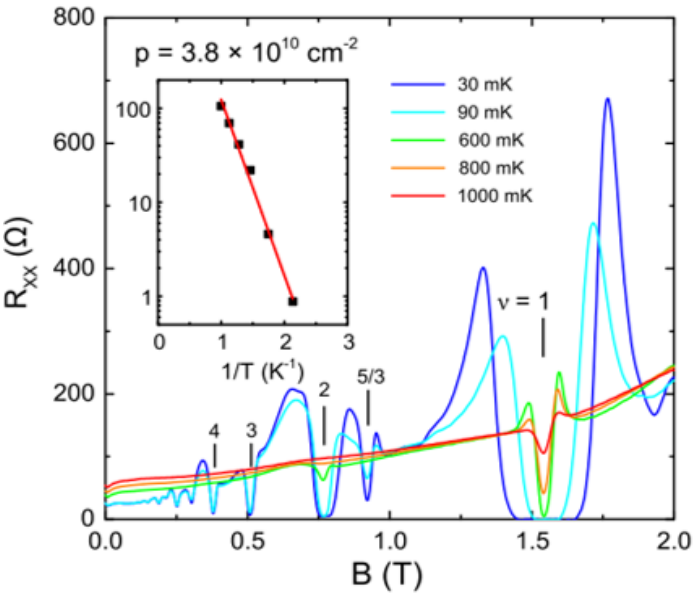

Figure 1: Temperature dependence of the longitudinal resistance R_{xx} vs magnetic field B.

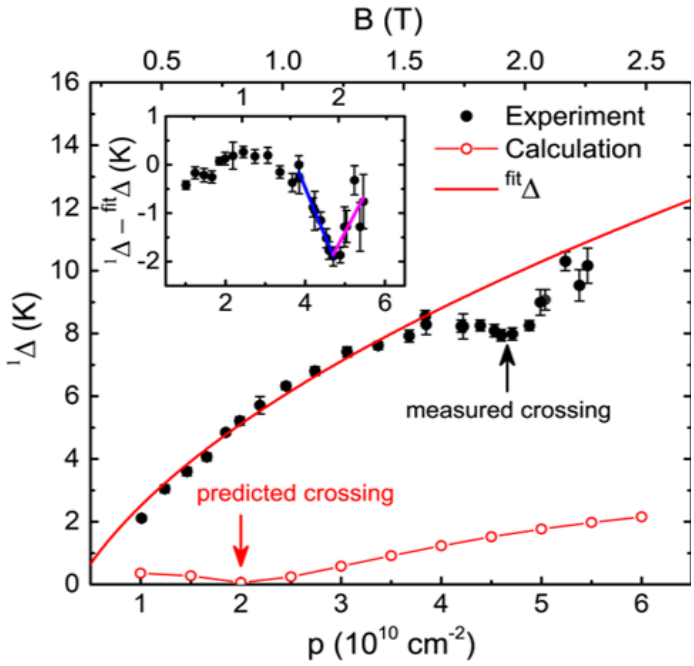

Figure 2: Summary of the $\nu = 1$ gap ($^1\Delta$) as a function of density (lower scale), or equivalently, magnetic field (upper scale).

CITATIONS

- 1. Meng K. Ma, Chengyu Wang, Y. J. Chung, L. N. Pfeiffer, K. W. West, K. W. Baldwin, R. Winkler, and M. Shayegan, Robust Quantum Hall Ferromagnetism near a Gate-Tuned $\nu = 1$ Landau Level Crossing, Phys. Rev. Lett., 129, 196801 (2022).

Advisor: Mansour Shayegan (Electrical Engineering)

Probing Exotic Phases of Two-dimensional Electrons in Unconventional Systems.

Researcher: **Chia-Tse Tai** (Princeton Graduate)

Sponsorship: Schmidt Fund

Memory or transistor devices based on electron s spin rather than its charge degree of freedom offer certain distinct advantages and comprise a cornerstone of spintronics. Recent years have witnessed the emergence of a new field, valleytronics, which seeks to exploit electron s valley index rather than its spin. An important component in this quest would be the ability to control the valley index in a convenient fashion. Here we show that the valley polarization can be switched from zero to one by a small reduction in density, simply tuned by a gate bias, in a two-dimensional electron system. This phenomenon arises fundamentally as a result of electron-electron interaction in an itinerant, dilute electron system. Essentially, the kinetic energy favors an equal distribution of electrons over the available valleys, whereas the interaction between electrons prefers single-valley occupancy below a critical density. The gate-bias-tuned transition we observe is accompanied by a sudden, two-fold change in sample resistance, making the phenomenon of interest for potential valleytronic transistor device applications. Our observation constitutes a quintessential demonstration of valleytronics in a very simple experiment. We demonstrate the high quality of our sample by showing the zero field commensurability.

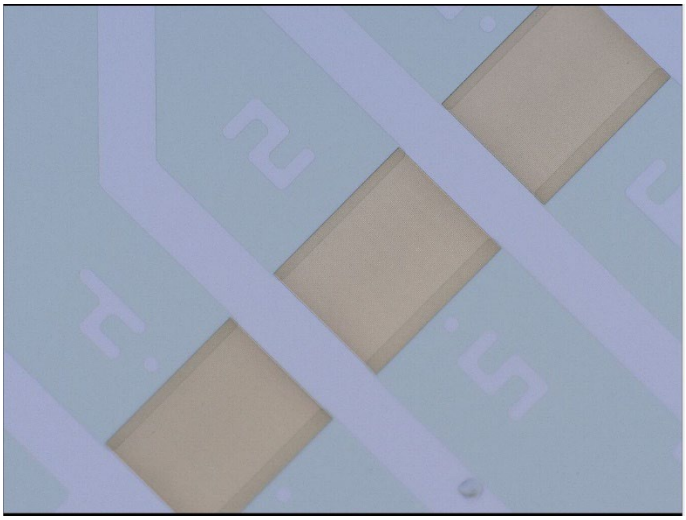

Figure 1: An optical microscopic view of magnetic stripe on top of the hallbar structure.

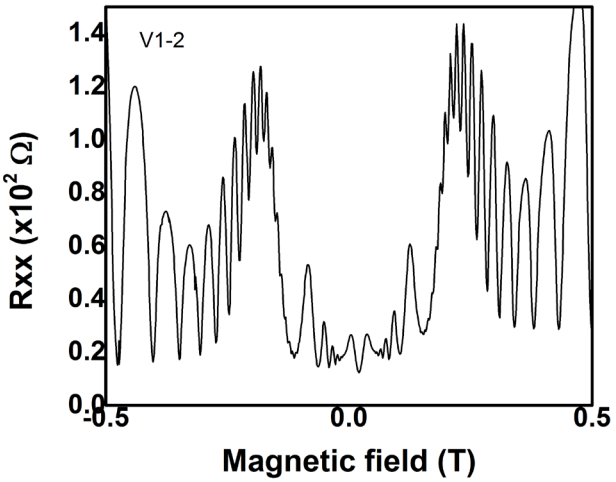

Figure 2: Zero field commensurability oscillations, showing the high quality of sample.

CITATIONS

- Md. S. Hossain, M. K. Ma, K. A. Villegas-Rosales, Y. J. Chung, L. N. Pfeiffer, K. W. West, K. W. Baldwin, and M. Shayegan Phys. Rev. Lett. 127, 116601
- Hossain, M.S., Ma, M.K., Rosales, K.V., Chung, Y.J., Pfeiffer, L.N., West, K.W., Baldwin, K.W. and Shayegan, M., 2020. Proceedings of the National Academy of Sciences, 117(51), pp.32244-32250.

Advisor: Mansour Shayegan (Electrical Engineering)

Exotic Phases of Electrons in Interacting 2D Systems

Researcher: **Siddharth Singh** (Princeton Graduate)

Sponsorship: MOORE

In selectively-doped semiconductor structures, the electrons are spatially separated from the dopant atoms to reduce scattering by the ionized impurities. Thanks to the reduced disorder and scattering, such clean structures provide nearly ideal systems for studies of electron- electron interaction phenomena, especially at low temperatures and high magnetic fields where the thermal and kinetic energies of the electrons are quenched. The dominant electron interaction leads to various fascinating and exotic ground states that are often unexpected. Studies of such states are at the forefront of condensed matter research. They could lead to a better fundamental understanding of interaction phenomena, and they might help advance new concepts such as topological quantum computing. We experimentally investigate electron interaction physics in high-quality, quantum-confined semiconductor structures. The program will include studies of the electronic transport properties at low temperatures and high magnetic fields where electron correlation phenomena dominate. The emphasis of the work will be on several systems, including high-quality two- dimensional electron systems (2DESs) confined to selectively-doped AlAs quantum wells (QWs), and electron and hole systems confined to wide or to double QWs of GaAs. The 2DESs in AlAs have parameters that are very different from those of the standard 2DESs in GaAs: they have a much larger and anisotropic effective mass, a much larger effective g-factor, and they occupy multiple conduction band valleys. The electron or hole systems in wide or double GaAs QWs, on the other hand, possess an additional subband or layer degree of freedom. Both AlAs and bilayer systems provide crucial and important test-beds for new many-body physics. Several exotic phases of these systems will be studied during the course of this project, including the fractional quantum Hall effect (FQHE), composite fermions, Wigner crystal, and stripe phases.

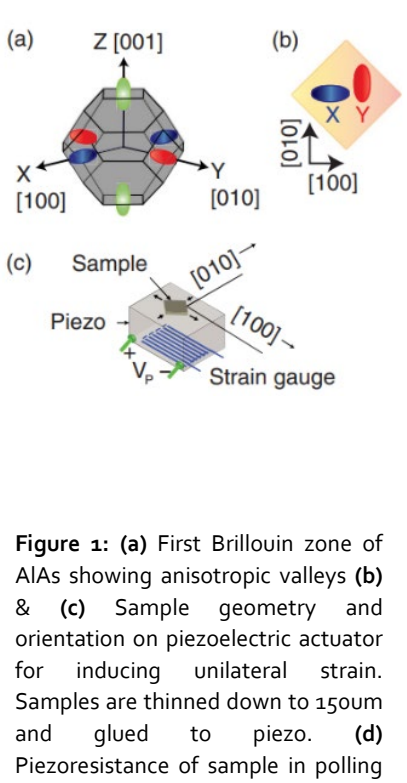

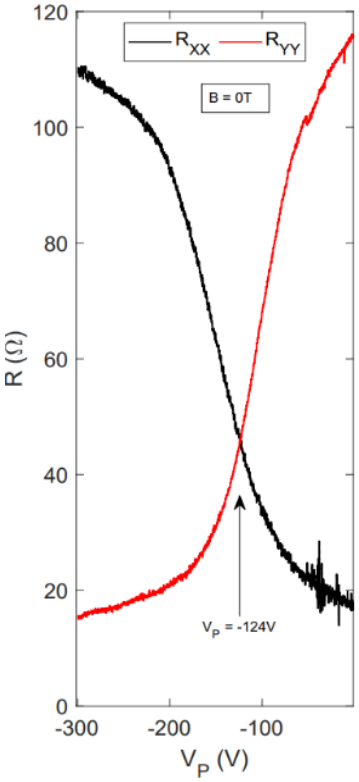

Figure 1: (a) First Brillouin zone of AlAs showing anisotropic valleys **(b)** & **(c)** Sample geometry and orientation on piezoelectric actuator for inducing unilateral strain. Samples are thinned down to 150um and glued to piezo. **(d)** Piezoresistance of sample in polling direction indicating precise control of valley occupation in device.

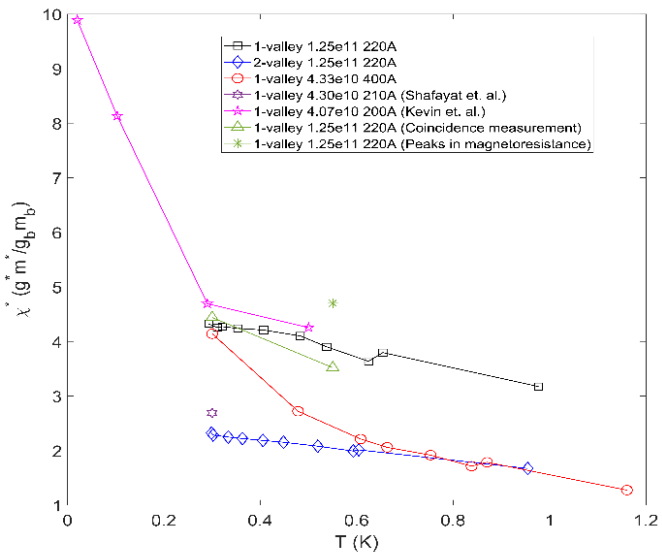

Figure 2: Spin susceptibility of 2D electron gas confined to AlAs quantum well. Here, we study the trend of spin susceptibility in different samples of varying sheet electron density and valley occupation both of which change the Fermi energy of the 2DEG. We see that to make an accurate spin susceptibility measurement, the 2DEG temperature must be << than Fermi energy of the system.

CITATIONS

- N/A

Advisor: James C. Sturm (Electrical Engineering)
Microfluidic Flow control via Transistor Like Devices
Researcher: **David Bershadsky** (Princeton Undergraduate)
Sponsorship: ECE Independent Research

We are attempting to design and fabricate solid state microfluidic fluidic valves that can be used to digitally control the flow in a microfluidic channel. These devices will use the surface tension forces as well as a parallel plate capacitor located around the channel to restrict the flow in the channel. We hope that these electrically actuated solid-state gates can eventually be used to replace Quake valves in large Microfluidic systems.

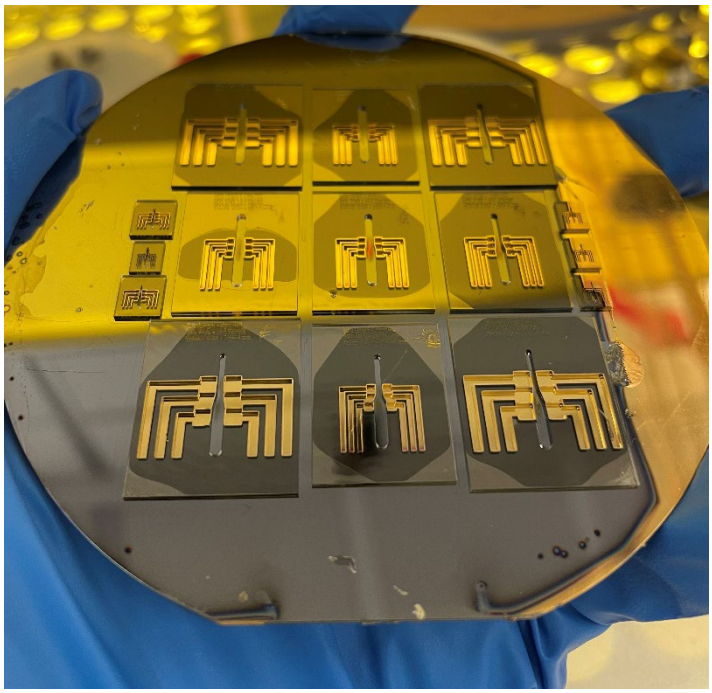

Figure 1: Test Structures after Metallization in 100-micron thick SU-8.

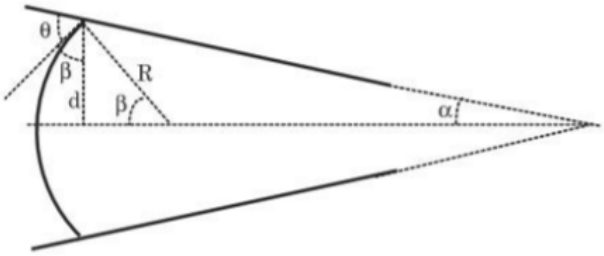

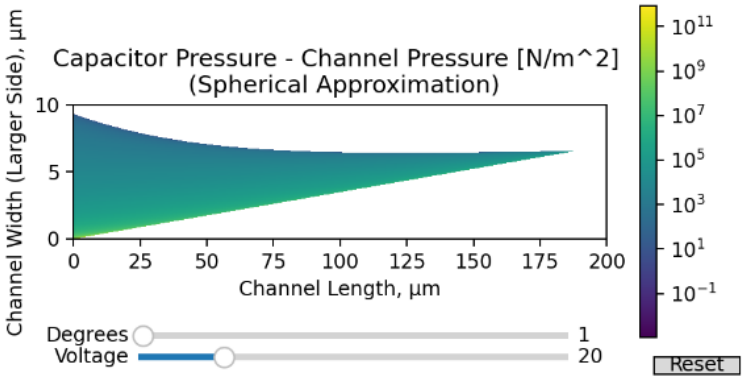

Figure 2: The Colored Area Shows the range of allowable Channel Dimensions for a gate at 20 volts and an angle (alpha) of 1 degree. The Dimensions discussed above can be seen on the diagram above the graph taken from Vowell, Schuyler. "Microfluidics: The Effects of Surface Tension," 2009.

CITATIONS

- N/A

Advisor: James C. Sturm (Electrical Engineering)

Microfluidic CAR-T Cell Processing Device

Researcher: **Miftahul Jannat Rasna** (Princeton Graduate)

Sponsorship: GPB Scientific, LLC

The focus of our work at Princeton is on increasing the throughput of DLD array chip structures by ~36 X to enable the processing of a complete 500 ml leukapheresis unit in one hour for CAR-T and related cell therapies, and then addressing issues related to transferring the know-how to plastic chips amenable to low-cost high-volume production, such as quality control and the impact of different parameters on ultimate chip and chip-stack performance.

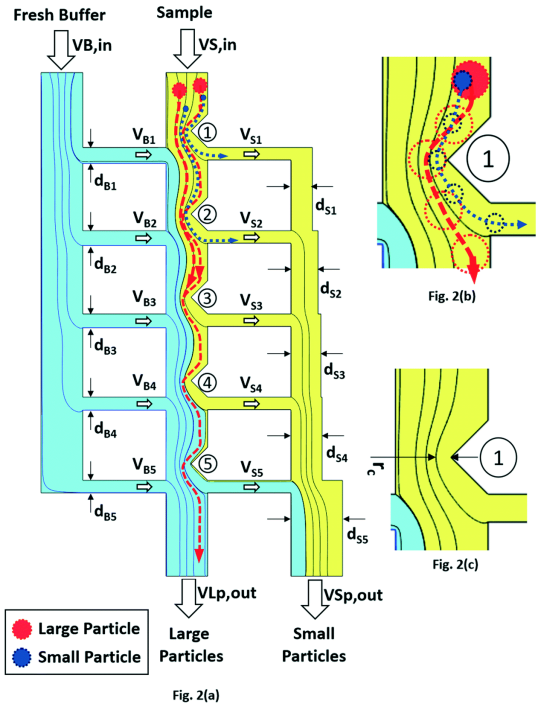

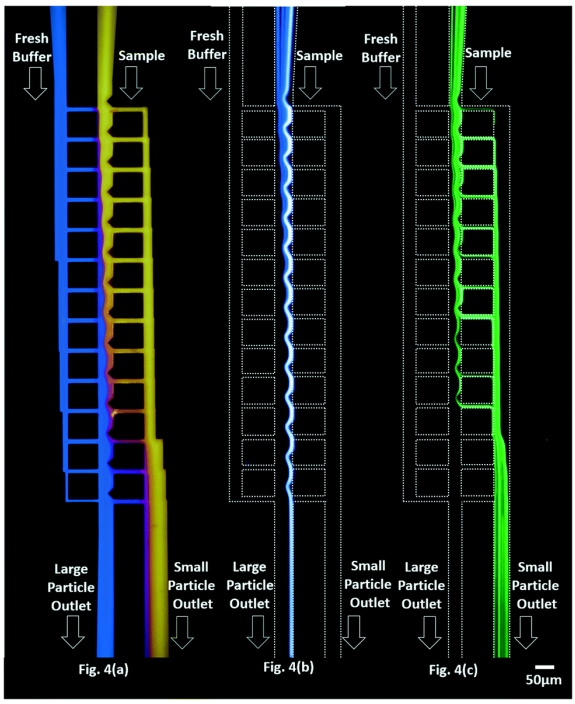

Figure 1. Schematic of single-column DLD device. The overall schematic of the single-column DLD device with 5 rows of bumping obstacles. The thin black lines represent streamlines. The particle-containing "Sample" fluid (yellow) and a buffer without particles (blue) enter from the top. By the end (bottom) of the device, in the central column the original fluid is completely replaced by the fresh buffer, small particles (blue circles) flow along the stream tubes (dashed blue lines) and exit the device from the small particle outlet on the bottom. The red circles represent the particles larger than the critical diameter and the red dashed line with arrow shows their trajectories. All bumping occurs on the protruding obstacles in the central column. Large particles in the stream tube adjacent to the obstacles are "displaced" by the obstacles and remain in the central column, exiting the device from the large particle outlet.

Figure 2: Fluorescent images showing fluid flow patterns and microparticle trajectories. The dotted lines indicate the approximate channel locations. (a): Flow pattern (overlay figures), exposure time: 1.3 s; (b) 9.9 µm microparticle trajectories, exposure time 1/30 s; (c) 4.8 µm microparticle trajectories, exposure time 1/30 s

CITATIONS

- K.C. Lin, G. Torga, Y.S. Sun, K.J. Pienta, J.C. Sturm, R.H. Austin, Generation of Heterogeneous Drug Gradients Across Cancer Populations on a Microfluidic Evolution Accelerator for Real-Time Observation, Jove-Journal of Visualized Experiments, 151, e60185 (2019).
- K.C. Lin, G. Torga, Y.S. Sun, R. Axelrod, K.J. Pienta, J.C. Sturm, R.H. Austin, The role of heterogeneous environment and docetaxel gradient in the emergence of polyploidy, mesenchymal and resistant prostate cancer cells, Clinical & Experimental Metastasis, 36, 2, 97-108 (2019).
- L.E. Aygun, P. Kumar, Z.W. Zheng, T.S. Chen, S. Wagner, J.C. Sturm, N. Verma, Hybrid System for Efficient LAE-CMOS Interfacing in Large-Scale Tactile-Sensing Skins via TFT-Based Compressed Sendsing, 2019 IEEE International Solid State Circuits Conference, 62, 280, (2019).

Advisor: James C. Sturm (Electrical Engineering)

Cancer Cell Dynamics on a Complex Drug Landscape

Researcher: **Kumar Mritunjay** (Princeton Graduate)

Sponsorship: James C. Sturm Unrestricted Fund

We are working on patterning rat hippocampal neurons (in vitro) over a patterned electrode substrate to interface individual cells with individual electrodes for one-cell to one-electrode interface. We use various lithography, deposition and etching tools to create our device.

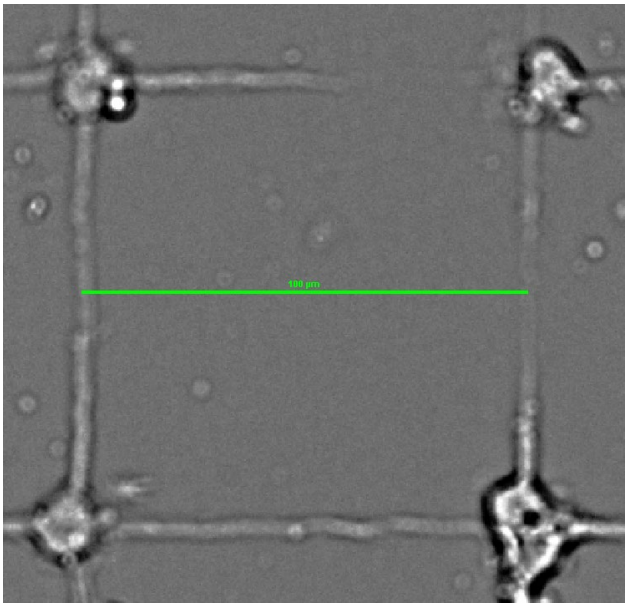

Figure 1: Individually patterned hippocampal cells over a silicon dioxide substrate.

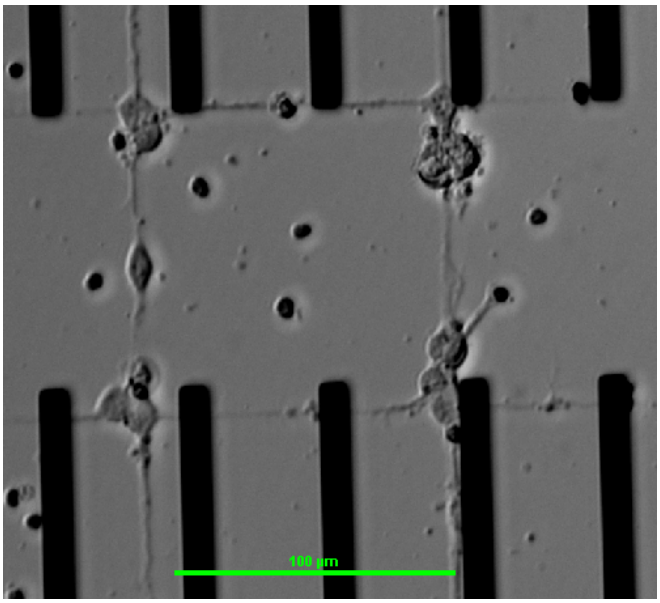

Figure 2: Neurons patterned over gold electrodes.

CITATIONS

- N/A

Advisor: James C. Sturm (Electrical Engineering)

High Performance ZnO TFTs

Researcher: **Nicholas Fata** (Princeton Graduate)

Sponsorship: Industrial

This project is concerned with the fabrication of self-aligned, passivated ZnO thin-film transistors (TFTs), using plasma-enhanced atomic layer deposition (PEALD), for use in large-area electronics applications. ZnO, a metal oxide, is suited for this particular application due to its scalability to large areas and because it has a similar fabrication process to amorphous silicon. These ZnO TFTs have a bottom-gate staggered geometry, which means that the gate metal is at the bottom of the stack, and the source and drain metal are on the opposite side of the semiconductor as the gate. The materials used in these TFTs include: a glass substrate, Cr for the gate metal, aluminum oxide (Al_2O_3) for the gate dielectric, ZnO for the active semiconducting layer, and Ti as the source/drain metal.

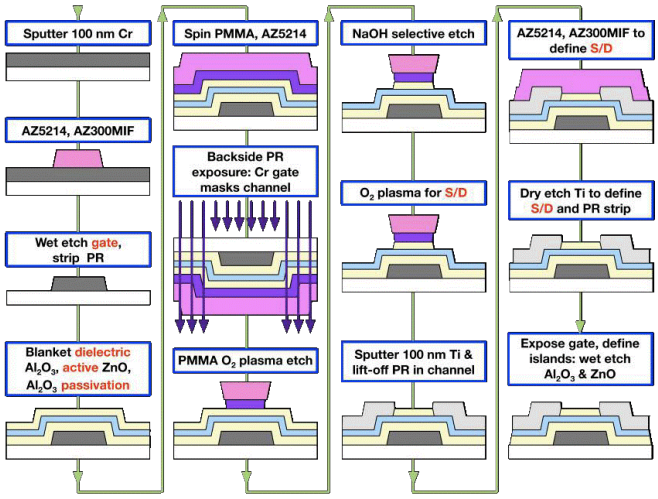

Figure 1: Diagram of fabrication process for passivated, self-aligned ZnO TFTs.

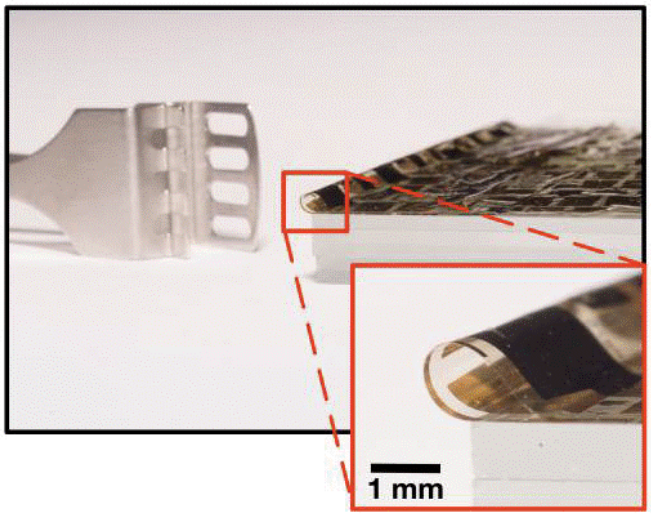

Figure 2: Picture of ZnO TFTs on flexible substrate folded over itself.

CITATIONS

- Yasmin Afsar, Tiffany Moy, Nicholas Brady, Sigurd Wagner, James C. Sturm, and Naveen Verma, An Architecture for Large-Area Sensor Acquisition Using Frequency-Hopping ZnO TFT DCOs, IEEE Journal of Solid-State Circuits, vol. 53 (1), 297-308 (2018).
- Yasmin Afsar, Jenny Tang, Warren Rieutort-Louis, Liechao Huang, Yingzhe Hu, Josue Sanz-Robinson, Naveen Verma, Sigurd Wagner, and James C. Sturm, "Impact of bending on flexible metal oxide TFTs and oscillator circuits," Journal of the Society for Information Display 24/6, pp. 371-380 (2016).

Advisor: James C. Sturm (Electrical Engineering)
Large-area Thin Film Transistors for Sensing Applications
Researcher: **Yue Ma** (Princeton Graduate)
Sponsorship: NSF

The tremendous value artificial intelligence (AI) is showing across a broad range of applications is driving it from cyber-systems to systems pervading every aspect of our lives. But real-world data challenges the efficiency and robustness with which AI systems of today can perform, due to the highly dynamic and noisy scenarios they face. While algorithmic solutions are required, this paper also explores technological solutions based on large- scale sensing. Specifically, Large-Area Electronics (LAE) is a technology that can make large-scale, form-fitting sensors possible for broad deployment in our lives. System-design principles, architectural approaches, supporting circuits, and underlying technological concerns surrounding LAE and its use in emerging systems for intelligent sensing are explored. Fig. 1 shows the schematic of a bottom-gate ZnO TFT, which is the building block for the circuit and/or system demonstration. Fig. 2 shows the schematic of a directional antenna with tunability in direction of radiation beams, which is a representative wireless sensing/communication system built by LAE technology.

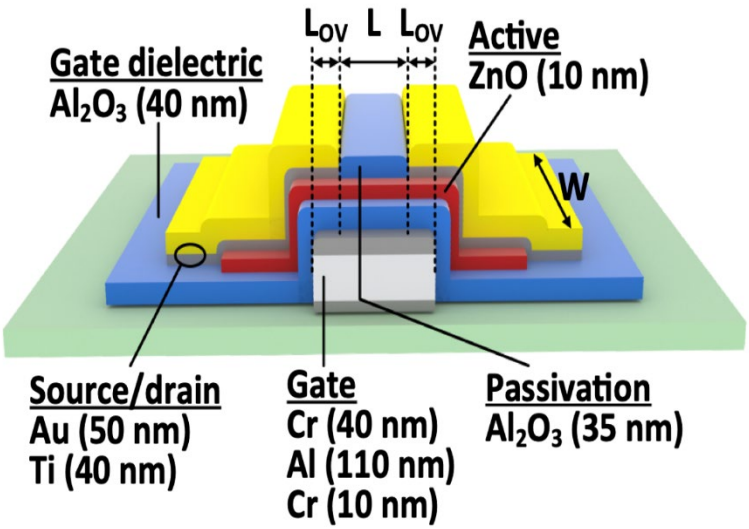

Figure. 1 Schematic of a bottom-gate ZnO TFT (L = TFT's channel length; W = TFT's channel width; L_{OV} = length of overlap between source/drain to gate).

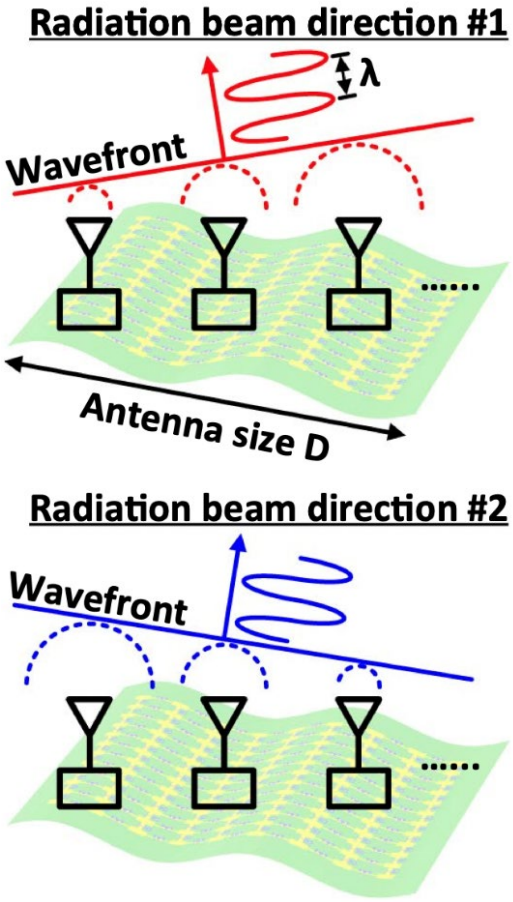

Figure 2. Schematic of a multi-element directional antenna with direction of radiation beams controlled through tuning the relative phase of each individual radiative antenna element.

CITATIONS

- Ozatay M, Aygun L, Jia H, et al. Artificial intelligence meets large-scale sensing: Using Large-Area Electronics (LAE) to enable intelligent spaces[C]//2018 IEEE Custom Integrated Circuits Conference (CICC). IEEE, 2018: 1-8.

Advisor: James C. Sturm (Electrical Engineering)
A Phased Array Based on Large-Area Electronics That Operates at Gigahertz Frequency
Researcher: **Zili Tang** (Princeton Graduate)
Sponsorship: NSF

Large-aperture electromagnetic phased arrays can provide directionally controlled radiation signals for use in applications such as communications, imaging and power delivery. However, their deployment is challenging due to the lack of an electronic technology capable of spanning large physical dimensions. Furthermore, applications in areas such as aviation, the Internet of Things and healthcare require conformal devices that can operate on shaped surfaces. Large-area electronics technology could be used to create low-cost, large-scale, flexible electromagnetic phased arrays, but it employs low-temperature processing that limits device- and system-level performance at high frequencies. Here we show that inductor capacitor oscillators operating at gigahertz frequencies can be created from large-area electronics based on high-speed, self-aligned zinc-oxide thin-film transistors. The oscillator circuits incorporate frequency locking and phase tuning, which are required for electromagnetic phased arrays. We integrate our phase-tunable oscillators in a 0.3-m-wide aperture, creating a phased array system that operates at ~1 GHz and is capable of beamforming.

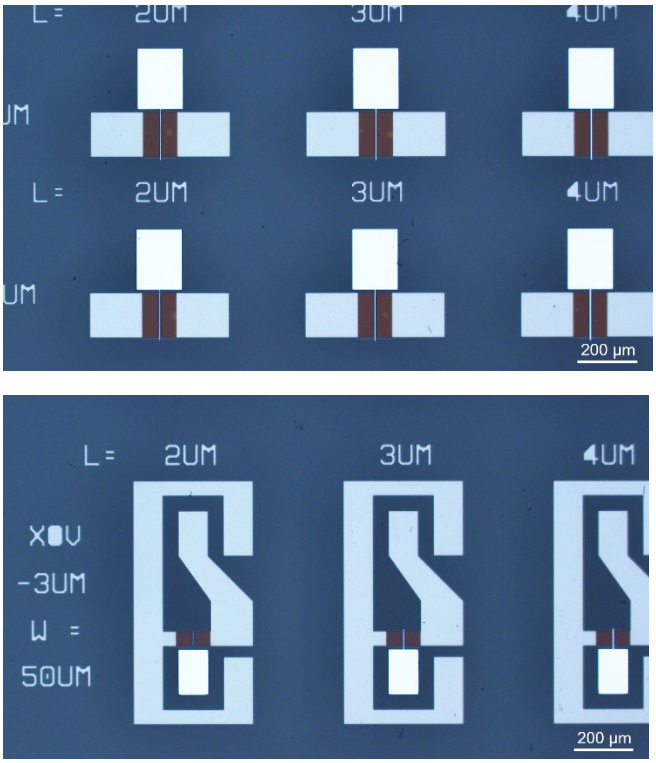

Figure 1. Microscope images of top gate ZnO TFTs fabricated on glass for DC (Top image: width, WTFT= 150.0 µm; length, LTFT= 2, 3, 4 µm) and high frequency analysis up to 3 GHz (Bottom image: width, WTFT= 50.0 µm; length, LTFT= 2, 3, 4 µm).

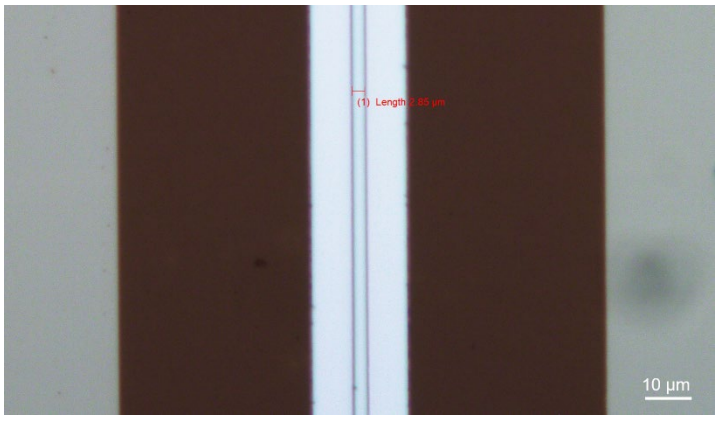

Figure 2: Zoomed-in microscope image of the gate region of a top gate ZnO TFT, where the gate width WTFT is measured to be 2.85 µm.

CITATIONS

- Can Wu et al., *A phased array based on large-area electronics that operates at gigahertz frequency Nature Electronics | VOL 4 | October 2021 | 757–766;* https://doi.org/10.1038/s41928-021-00648-z

Advisor: James C. Sturm (Electrical Engineering)

TFT Fabrication for Reconfigurable Antenna

Researcher: **Cindy Pan** (Princeton Graduate)

Sponsorship: N/A

The development of reconfigurable antennas serves a vital role in modern wireless technology such as 5G, IoT, and holographic display. Its reconfigurability in specific electromagnetic properties provides great versatility in various applications. While considerable efforts have been contributed regarding the hardware design and fabrication of reconfigurable antennas, a robust and efficient computational solution for inverse design has yet to be discovered. This project consists of my preliminary research exploring the relationship between the antenna switch configuration and current distribution with graph modeling and graph neural networks. While the proposed message-passing-based graph neural network model is subject to further improvements, it demonstrates the ability to emulate the general current propagation direction as well as the identification of patches with accumulating current density.

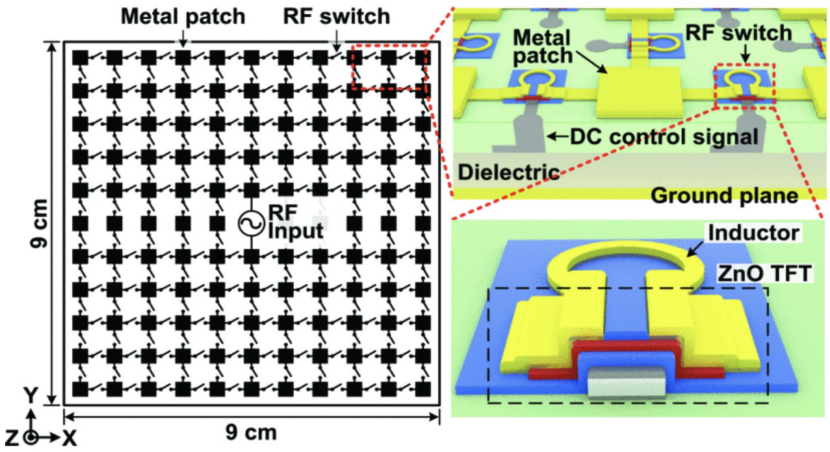

Figure 1: Left: System schematic of the reconfigurable antenna a single external RF source connected in the middle. Top right: the antenna cross-section, with a ground plane to direct radiation towards the upper hemisphere, the metal patches as sub-radiators, and a dielectric layer to improve radiation efficiency. Bottom right: resonant RF switch, consisting of a ZnO TFT and a loop inductor made of Au.

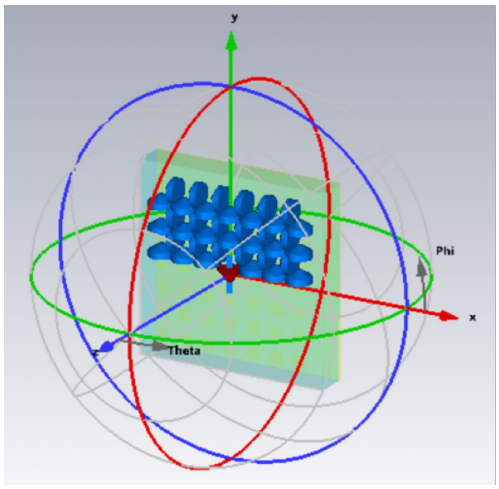

Figure 2: Reconfigurable antenna constructed in CST Simulations.

CITATIONS

- N/A

Advisor: James C. Sturm (Electrical Engineering)
Silicon-Based Quantum Computing: Enhancement-Mode Undoped 2DEG
Researcher: **Zoe Cyue** (Princeton Graduate)
Sponsorship: Princeton University Internal Funds

Single-electron quantum dot (QD) devices fabricated from Si/SiGe two-dimensional electron gases (2DEGs) are attractive due to the weak hyperfine interaction, weak spin-orbit coupling, and resulting long relaxation time. Recently, a metal-oxide-semiconductor (MOS) gated undoped enhancement-mode Si/SiGe heterostructure was demonstrated as a promising approach to realize a single-electron QD in silicon due to its capability to tune the 2D electron density (n2D) in a strained Si 2DEG to a very low level, which in turn facilitates the process to isolate a single electron. Currently, the main challenge of this Si/SiGe QD used in quantum computing is its small valley splitting since the intervalley scattering degrades spin coherence and operation fidelity. To resolve this problem, we grew ultra-flat quantum well layers with surface roughness of below 0.2 nm using our home-built ultra-high vacuum CVD chamber. The layer structure is shown in Fig.1. However, field effect cannot be observed in our devices, which could be attributed to poor Si/oxide interface. To optimize the MOS interface, we fabricated typical MOSFET devices with different gate insulators, including thermal SiO_2, PECVD SiO_2, ALD Al_2O_3, and PEALD Al_2O_3. Among these gate insulators, ALD Al_2O_3 was demonstrated as our best choice in terms of its low growth temperature, low interface trapped states, high mobility up to 300 $cm^2/V\text{-}s$, and low threshold voltage (~0.5 V). The field effect and gate-dependent drain current of MOSFETs with ALD Al_2O_3 are shown in Fig.2. This facilitates using ALD Al_2O_3 as our gate insulators in undoped enhancement-mode Si/SiGe QDs.

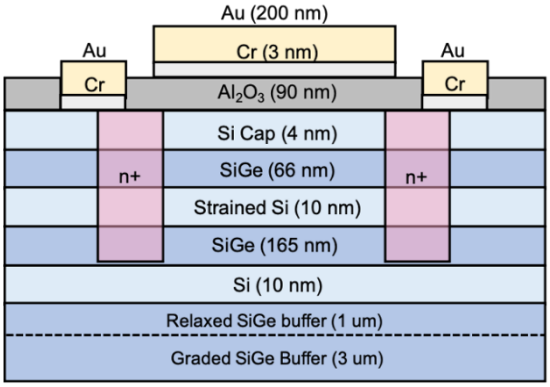

Figure 1: The schematic of an undoped enhancement-mode Si/SiGe heterostructure. A 2DEG in the strained Si quantum well (QW) by a positive gate voltage.

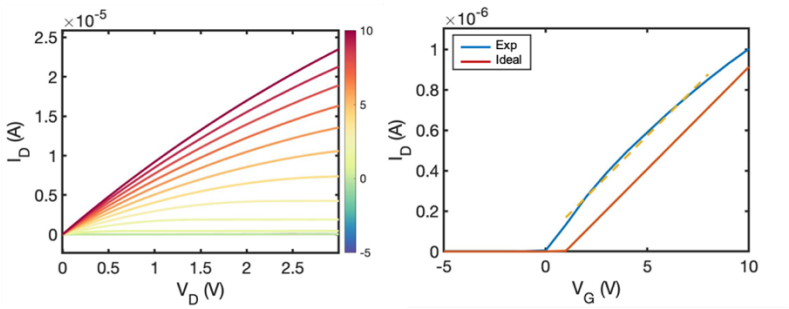

Figure 2: (a) The field effect of MOSFET devices with ALD Al_2O_3 as gate insulators, and (b) the gate dependence of measured drain current. From this curve, the mobility and threshold voltage are estimated as 300 cm2/V-s and 0.5V, respectively.

CITATIONS

- Huang, Chiao-Ti, Jiun-Yun Li, and James C. Sturm. "Very low electron density in undoped enhancement-mode Si/SiGe two-dimensional electron gases with thin SiGe cap layers." ECS Transactions 53.3 (2013): 45.

Advisor: Jeffrey D. Thompson (Electrical Engineering)

New Color Centers for Quantum Computing and Quantum Networks

Researcher: **Isaiah Gray** (Princeton Postdoc)

Sponsorship: PCI

Er^{3+} ions embedded in crystalline hosts are promising candidates for nodes in quantum networks, since their $4f$ transitions can form the basis of coherent spin-photon interfaces operating at telecom wavelengths. While much work has focused on Er ions implanted or doped into bulk crystals, Er doped into thin films may offer distinct advantages, such as increased flexibility of the host crystal structure by strain tuning and more natural on-chip integration with other quantum devices. In this work, we investigate structural and optical properties of Er-doped anatase TiO_2 thin films on $LaAlO_3$ substrates. We show that the Er^{3+} substitutes for the Ti^{4+} ion. We demonstrate inhomogeneous optical linewidths as narrow as 5.4 GHz for concentrations < 100 ppm, and we show that the addition of buffer layers of undoped TiO_2 decreases the linewidth in a 4000 ppm-doped sample, offering a path to further optimization of Er:TiO_2.

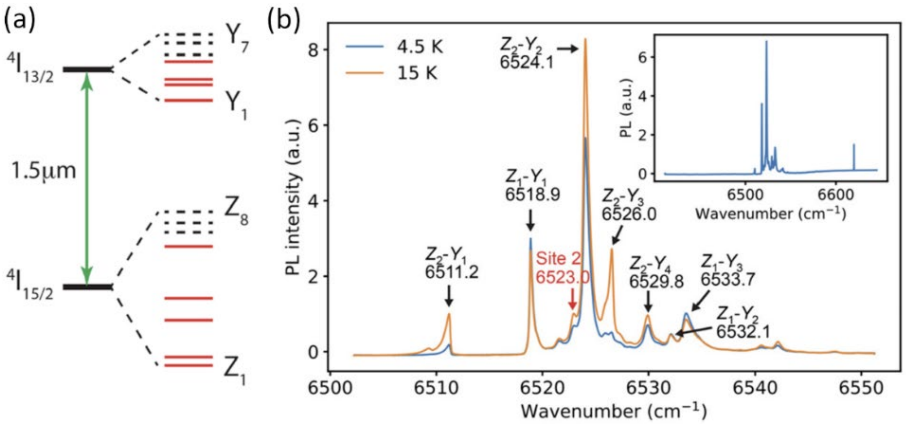

Figure 1: Er^{3+} ion level structure in TiO_2. (a) Schematic illustration of the ground (Z) and first excited (Y) state manifolds of the Er^{3+} ion, split by the crystal field of a host crystal. (b) Measured photoluminescence excitation spectra of Er^{3+} incorporated into 18 nm-thick anatase TiO_2, epitaxially grown on $LaAlO_3$ in a molecular beam epitaxy system at Yale, at 4.5 K and 15 K. From level energies, emission spectroscopy (not shown) and a crystal field model, we deduce that Er^{3+} substitutes for Ti^{4+}. Several representative transition energies are labeled.

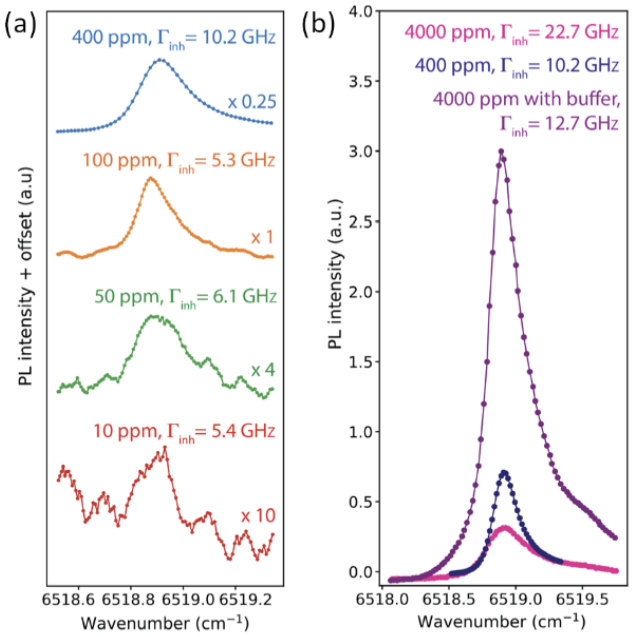

Figure 2: $Z_1 - Y_1$ linewidths vs doping concentration and buffer layer. (a) Inhomogeneous optical linewidths of the $Z_1 - Y_1$ transition at 4.5 K at different doping concentrations. Concentrations lower than 400 ppm result in narrower linewidths. (b) $Z_1 - Y_1$ transitions of samples with and without a buffer layer of undoped TiO_2 above and below the Er:TiO_2 layer. The addition of a buffer layer improves the linewidth from 22.7 GHz to 10.2 GHz and increases the photoluminescence intensity by a factor of 10.

CITATIONS

- K. Shin*, I. Gray* et al., Er-doped anatase TiO_2 thin films on $LaAlO_3$(001) for quantum interconnects (QuICs), Appl. Phys. Lett. 121, 081902 (2022)

Advisor: Jeffrey D. Thompson (Electrical Engineering)

Parallel Single-Shot Measurement and Coherent Control of Solid-State Spins Below the Diffraction Limit

Researcher: **Mehmet Tuna Uysal** (Princeton Graduate)

Sponsorship: DOE, DARPA, AFOSR

Solid-state spin defects are a promising platform for quantum science and technology. The realization of larger-scale quantum systems with solid-state defects will require high-fidelity control over multiple defects with nanoscale separations, with strong spin-spin interactions for multi-qubit logic operations and the creation of entangled states. We demonstrate an optical frequency-domain multiplexing technique, allowing high-fidelity initialization and single-shot spin measurement of six rare-earth (Er3+) ions, within the subwavelength volume of a single, silicon photonic crystal cavity. We also demonstrate subwavelength control over coherent spin rotations by using an optical AC Stark shift. Our approach may be scaled to large numbers of ions with arbitrarily small separation and is a step toward realizing strongly interacting atomic defect ensembles with applications to quantum information processing and fundamental studies of many-body dynamics.

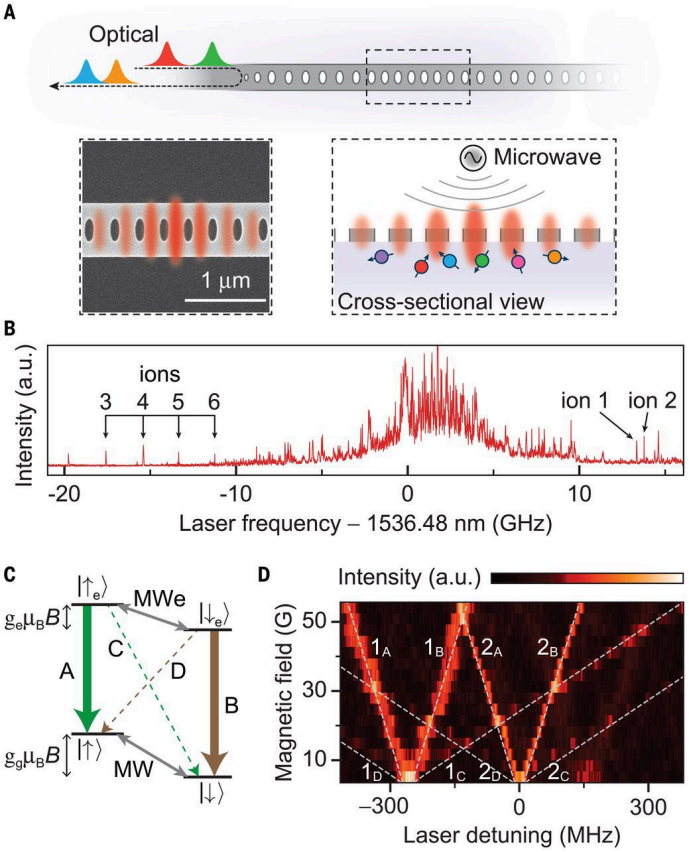

Figure. 1 Spectrally addressing multiple ions in a diffraction-limited volume.
(**A**) Schematic of the device, showing multiple ions with different transition frequencies (colors) coupled to the cavity. (Inset) Scanning electron microscope image of a representative cavity, showing the extent of the optical mode.
(**B**) PLE spectrum of Er^{3+} ions in a single device with magnetic field B=0. Arrows indicate the six ions used in this work.
(**C**) Level structure of Er^{3+}:YSO in a magnetic field, with optical (A to D) and microwave (MW, MWe) transitions indicated. g_g (g_e) denotes the ground- (excited-) state magnetic g-factor.
(**D**) PLE spectrum of ion 1 and ion 2 in the presence of a magnetic field (oriented along the D_2 axis of the YSO crystal). (1A,1B) and (2A,2B) correspond to the spin-conserving optical transitions (A, B) of the two ions, respectively. Zero detuning in this panel and subsequent figures refers to the ion 2 resonance when B=0. a.u., arbitrary units.

CITATIONS

- Chen et al.; Parallel single-shot measurement and coherent control of solid-state spins below the diffraction limit; Science 30 Oct 2020 Vol 370, Issue 6516, pp. 592-595, DOI: 10.1126/science.abc782

Advisor: Jeffrey D. Thompson (Electrical Engineering)

Magnetic DiPole Mediated Purcell Enhancement of Single Erbium Emitter

Researcher: **Sebastian Horvath** (Princeton Postdoc)

Sponsorship: DOE, DARPA, AFOSR, NSF

The interaction of electromagnetic radiation with matter is of fundamental importance and underlies numerous current and future technologies. The ability to control absorption and emission through engineering the environment is particularly relevant for quantum technologies requiring efficient light-matter interfaces, and has been demonstrated using optical cavities and a range of emitters from atoms and ions to quantum dots and atom-like defects in the solid state.

Light-matter interaction can be mediated through several mechanisms, including electric dipole (ED) or magnetic dipole (MD) transitions. The scale of the ED transition is the by far the largest, and therefore most often utilized for controlling light-matter interactions. However, in certain atoms the ED transition is suppressed, and higher-order processes play a considerable role. As a consequence, it has been a long-standing goal to realize control over the magnetic density of states and emission of magnetic dipole emitters.

In a nanophotonic resonator, the maximum value of electric and magnetic mode volume, V_e and V_m, are comparable, with a slight deviation from equality due to dielectric boundary conditions that affect E and B differently. Therefore, for an optimally positioned emitter, a comparable Purcell enhancement factor would be expected for a purely ED or purely MD emitter.

Phenicie et al engineered a new material, ion implanted Er:MgO, which due to the crystalline symmetry has ED transitions strictly forbidden. By coupling this emitter to a silicon nanophotonic device, with a simulated mode volume of V_m = 0.068 μm³, a magnetic Purcell factor of 1100 +/- 90 was realized. In Fig. 1(d) we show a high-resolution scan of an individual ion, yielding a single-ion linewidth of 690 kHz at 500 mK. We note that this is more than 10x narrower than single Er^{3+} ions observed in nanophotonic devices in non-centrosymmetric crystals such as Y_2SiO_5 or $LiNbO_3$. This is likely a consequence of the absence of a permanent electric dipole-moment and illustrates an advantage of being able to interface to Er^{3+} through an MD transition. To unambiguously establish single ion emission, a second-order autocorrelation measurement of the fluorescence was performed (Fig. 1(e)). This work opens the door to using nanophotonic structures to control MD emission and enables the use of a wider class of atoms and atom-like systems for quantum technologies.

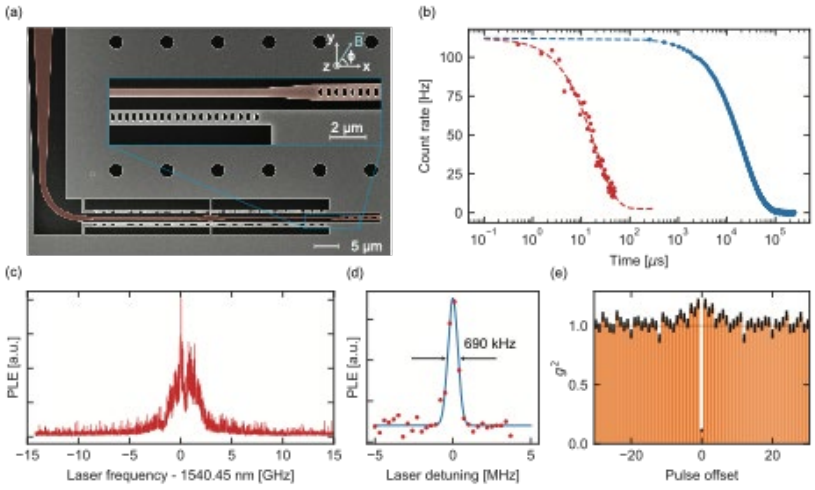

Figure. 1 Purcell enhancement of MD mediated optical transition.

(a) Scanning electron micrograph image of the nanophotonic circuit for enhancing and collecting the Er3+ ion emission. (b) Time-resolved emission from a single cavity-coupled ion (red). The emission time trace is fit to an exponential indicating an optical lifetime of 19.2 ± 1.5 μs. For comparison, the bare lifetime (blue, amplitude re-scaled) is 21.04 ± 0.02 ms showing a magnetic Purcell enhancement of Pm = 1100 ± 90 for the cavity-coupled ion. (c) Single-ion photoluminescence excitation spectrum of the ions coupled to a photonic crystal cavity at 4 K. (d) A single Er3+ ion observed in the same sample at 500 mK with a linewidth of 690 kHz. (e) The second-order autocorrelation function of fluorescence photons from the ion shown in (d). Fluorescence from individual excitation pulses are combined into a single bin, such that the pulse offset axis consists of fluorescence from consecutive excitation periods.

CITATIONS

- Phenicie et al.; Magnetic Dipole Mediated Purcell Enhancement of Single Erbium Emitter, In Preparation

Mechanical and Aerospace Engineering

Advisor: Daniel J. Cohen (Mechanical and Aerospace Engineering)

Electron Transfer Through Entrained DNA Strands

Researcher: **Anamika** (Princeton Postdoc)

Sponsorship: NIH

Geometric cues are known to control the behavior of the cells like proliferation, migration, differentiation etc. 3D printing is an efficient technology to develop materials with simple to complex geometries, macro to nano size dimensions, natural to synthetic polymers with high precision. We are interested in developing such geometric cues in 2D and 3D objects which could modify cellular behavior. Using Nanoscribe Photonic Professional GT2 system, we have fabricated micro size "Arch" for promoting self-contact and membrane fusion in mammalian cells. We are further exploring these microstructures as potential implant surfaces to induce self-membrane fusion and understand its mechanism in mammalian cells.

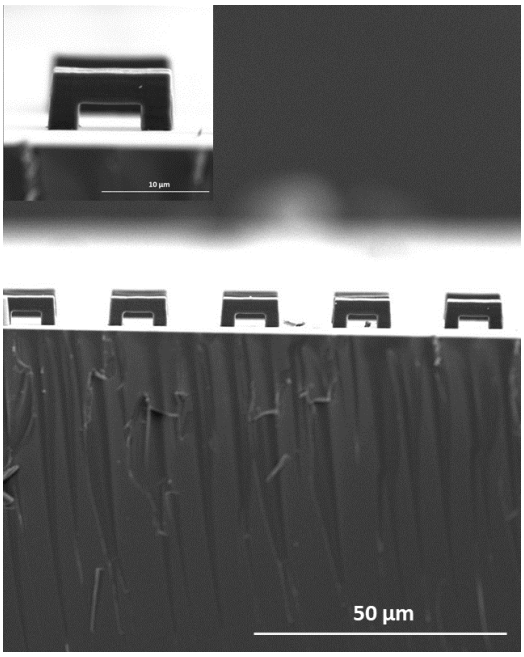

Figure 1: Scanning electron microscopic image of the array of 3D printed arches.

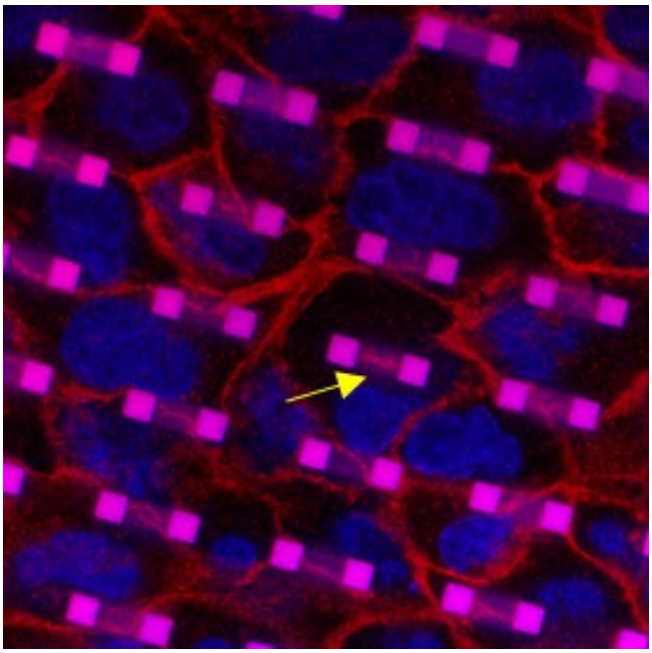

Figure 2: RFP Ecad-MDCK cells cultured on array of arch. The red fluorescent signal (yellow arrow) indicates the self-contact made by the cell membrane on the 3D printed arch.

CITATIONS

- Sumida, G. M., & Yamada, S. (2013). Self-contact elimination by membrane fusion. *Proceedings of the National Academy of Sciences*, *110*(47), 18958-18963.
- Hohmann, J. K., & von Freymann, G. (2014). Influence of Direct Laser Written 3D Topographies on Proliferation and Differentiation of Osteoblast-Like Cells: Towards Improved Implant Surfaces. *Advanced functional materials*, *24*(42), 6573-6580.

Advisor: Daniel J. Cohen (Mechanical and Aerospace Engineering)

3D Nano-printing of Complex Materials for Biomedicine and General Use

Researcher: **Lauren Rawson** (Princeton Undergraduate)

Sponsorship: Cohen Lab

The MNFC recently acquired a Nanoscribe printer that can print intricate structures down to 200 nm feature sizes in a variety of polymeric and silica-based materials using extremely precise two-photon technology. This opens entirely new possibilities in a variety of fields both due to the resolution and the fact that any arbitrary 3D structure can be produced (not possible with standard 2.5D photolithography). This project seeks to characterize and apply the Nanoscribe for biomedical applications. The primary goal involves introducing different printable materials and nanostructures to living cells and to enhance the cell-material interface and engineer cell behaviors. As the Nanoscribe is a relatively new technology with few established recipes for biological application, there are a number of practical design challenges that will be addressed during this project.

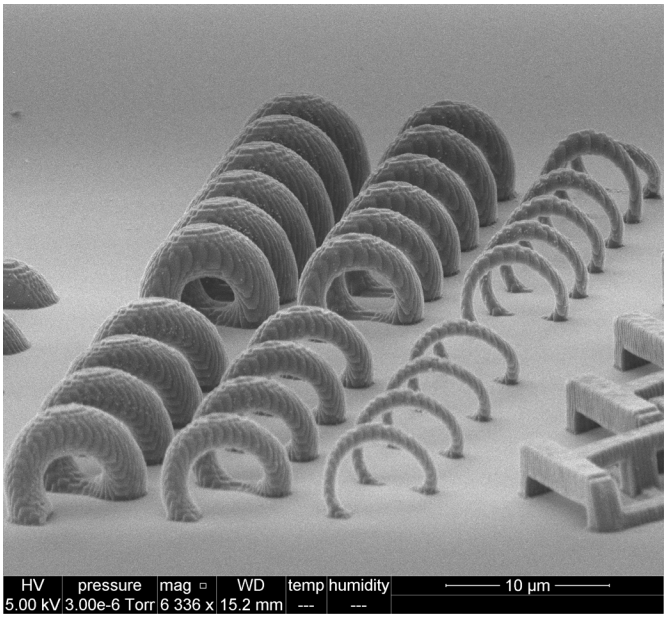

Figure 1. Scanning Electron Microscope (SEM) image that shows an array of coils printed in MNFC with the NanoScribe PPGT2 3D Printer. They vary in turns per unit length and diameter of material.

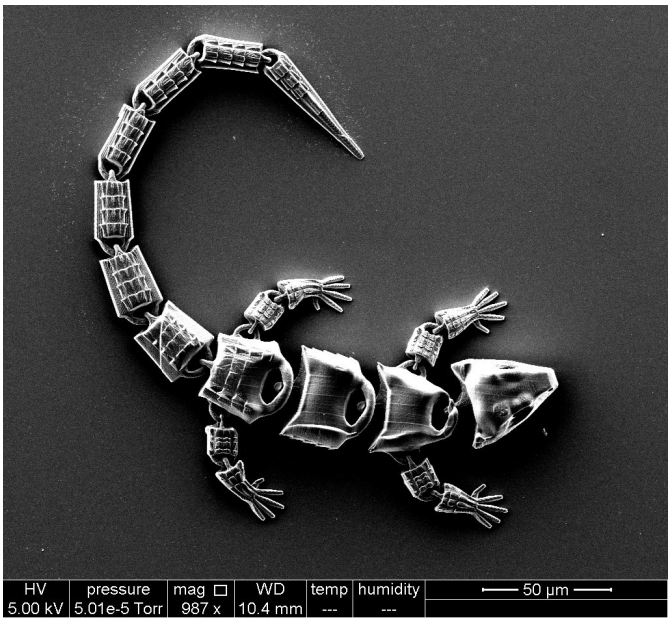

Figure 2. SEM image of an articulated skink printed in MNFC with the NanoScribe PPGT2 3D Printer as form of resolution testing.

CITATIONS

- N/A

Advisor: Marcus N. Hultmark (Mechanical and Aerospace Engineering)

Nanoscale Thermal Anemometry Probes (NSTAP) for Supersonic Applications

Researcher: **Alexander Piqué** (Princeton Graduate)

Sponsorship: NSF

The nanoscale thermal anemometry probe (NSTAP) has been used with a great degree of success for the analysis of high Reynolds number flows. Recent applications include the investigations of wind turbine wakes and pressure gradient effects on canonical pipe flow. In addition, recent work using MNFC facilities has led to design improvements of an NSTAP for supersonic flows (SNSTAP). Varying levels of gold were added to SNSTAP stubs to reduce "end-conduction" effects, which arise due to the temperature difference between the large thermal mass of the platinum stubs and the small thermal mass of the platinum sensing element. It was shown that increasing levels of gold led to an increased temporal response of the SNSTAP. An improved temporal response will enable the SNSTAP to sample and probe some of the smallest turbulent length scales that are present in high Reynolds number compressible flows.

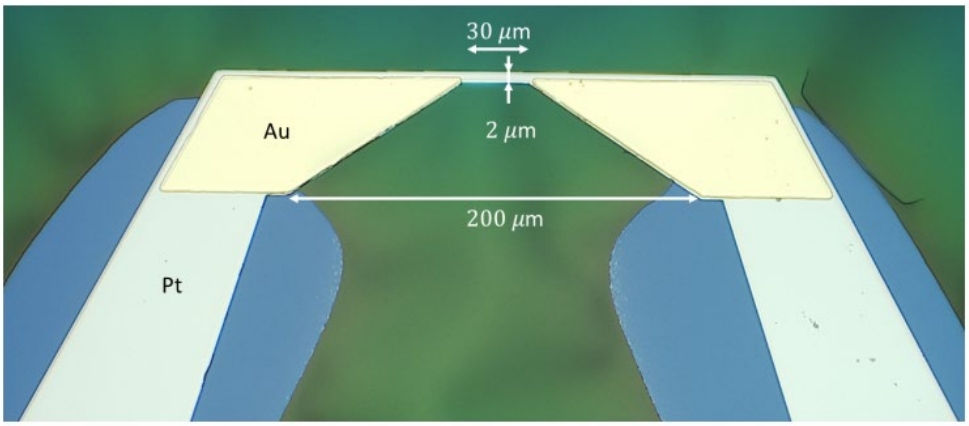

Figure 1: Gold-plated SNSTAP probe. Gold layer thicknesses of 200 nm and 360 nm were studied.

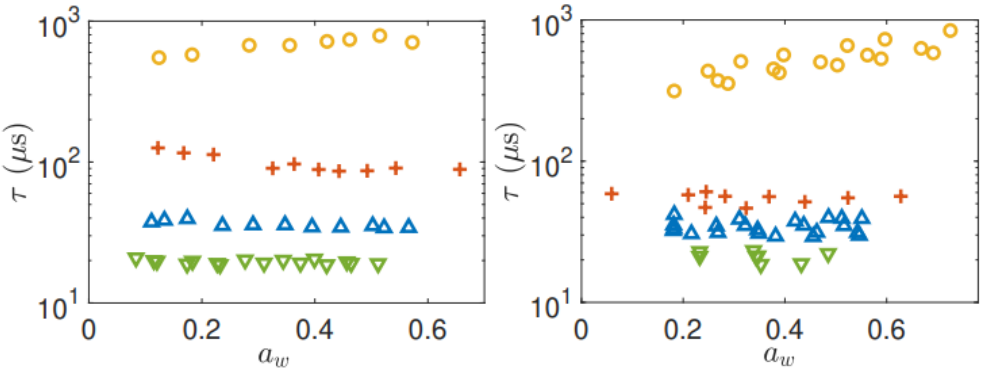

Figure 2: Temporal response of NSTAP probes (tau) in subsonic (left) and supersonic (right) conditions for different overheat ratios (a_w). Yellow circles represent commercial hot-wires, orange crosses represent SNSTAP without gold, blue upward triangles represent SNSTAP with 200 nm of gold, and green upside-down triangles represent SNSTAP with 360 nm of gold.

CITATIONS

- Brunier-Coulin, F., Barros, D.C., Piqué, A., Hultmark, M., Dupont, P., "Thermal response of a nanoscale hot-wire in subsonic and supersonic flows", *Experiments in Fluids* (Under Review), 2022
- Piqué, A., Miller M.A., Hultmark, M., "Dominant flow features in the wake of a wind turbine at high Reynolds numbers", Journal of Renewable and Sustainable Energy Vol 14 (033304), 2022
- Piqué, A., Miller M.A., Hultmark, M., "Laboratory investigation of the near and intermediate wake of a wind turbine at very high Reynolds numbers", *Experiments in Fluids* Vol 63 (106), 2022.
- Gunady, I.E., Ding, L., Hultmark, M., Smits, A.J. "Response of high Reynolds number turbulent pipe flow to the presence of an axisymmetric body", Proceedings of the 12th International Symposium on Turbulence and Shear Flow Phenomena, 2022.

Advisor: Marcus N. Hultmark (Mechanical and Aerospace Engineering)

Heat transfer enhancement over motion-inducing surfaces

Researcher: **Lena Sabidussi** (Princeton Graduate)

Sponsorship: Princeton Center for Complex Materials

Fouling significantly diminishes the performance of applications that rely on heat transfer. The widespread use of these applications, alongside this constant diminution of their operational performance, has spurred decades of research into methods to combat fouling. Currently, anti-fouling polymer coatings are often applied; however, these coatings typically have low thermal conductivity, resulting in reduced performance. Liquid Infused Surfaces (LIS) are presented as an interesting option for such coatings. LIS are surfaces that create a mobile interface between an internal liquid and external flow. This motion has been shown to reduce drag in both laminar and turbulent flows, and has been shown to have significant anti-fouling properties. We study this internal flow for its potential to enhance convection within the surface material. Due to an increase in heat exchange by convection in the internal liquid, these surfaces have the potential to yield anti-fouling effects without loss of thermal performance. An experimental study is performed to measure both drag reduction and heat transfer over LIS. Several surface designs and modifications are explored to better enhance these features. The experiments and surfaces are further designed to mimic canonical surfaces used in a numerical study that suggests significant heat transfer enhancement over similar surfaces. Microfluidic channels are used to study drag reduction and heat transfer in laminar external flows. The retention of the internal liquid is also studied, along with surfaces modifications to enhance retention.

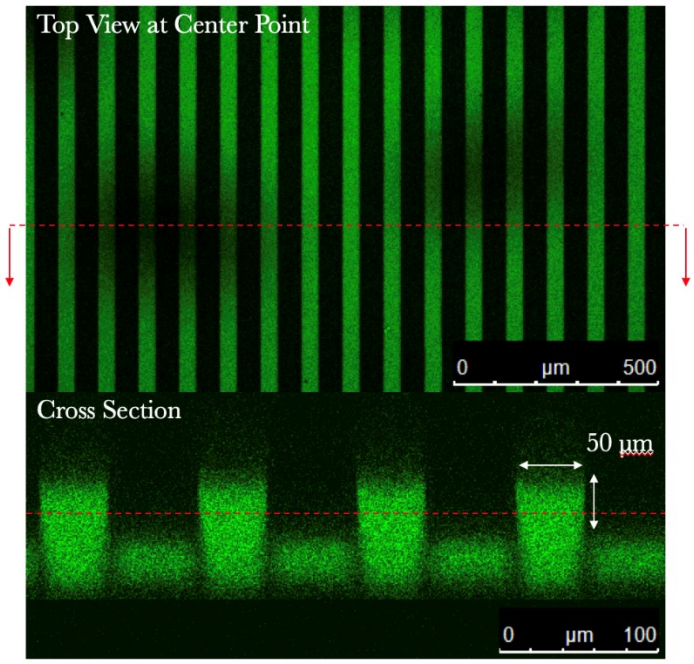

Figure 1: Images of LIS taken with a confocal microscope, with fluorescence imbued in silicone oil. Silicone oil is used as the internal fluid in these experiments.

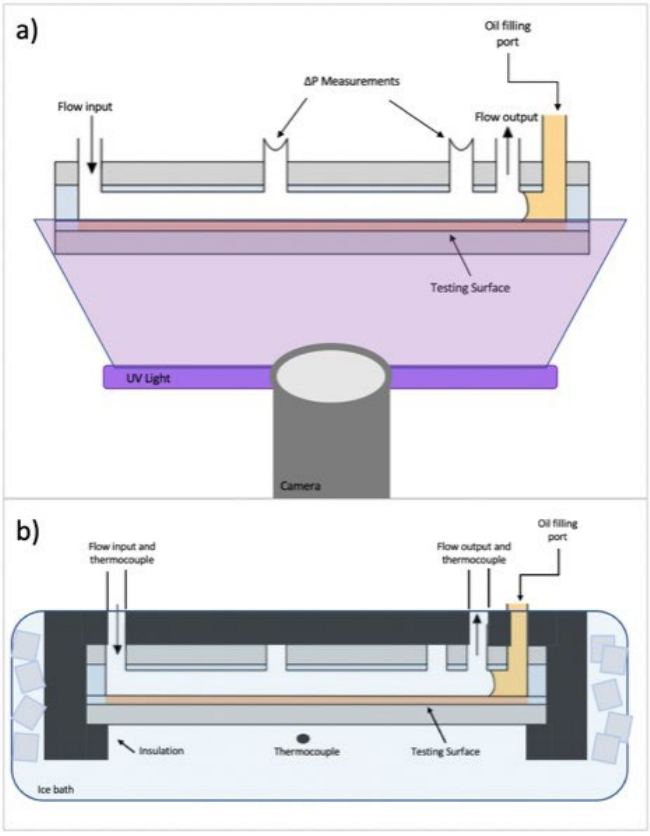

Figure 2: a) Experimental design for drag reduction and oil retention measurements in a microfluidic device with a LIS testing surface and b) experimental design for heat exchange over a LIS.

CITATIONS

- N/A

Advisor: Marcus N. Hultmark (Mechanical and Aerospace Engineering)

Development and Evaluation of Flexible MEMS Hot-Film Arrays for Real-Time Stall Sensing With Unprecedented Temporal and Spatial Resolution

Researcher: **Nicholas Conlin** (Princeton Graduate)

Sponsorship: Army

The primary research objective of the proposed research is to reveal and characterize early spatiotemporal signatures of dynamic stall at high Reynolds numbers, with a focus on signatures of these structures that can be measured on, or close to, the skin of the lifting surface for on-board real- time control. The combination of a one-of-a-kind flow facility and novel instrumentation will enable unique insight into the details of a phenomenon that is of utmost importance to a large number of aeronautical applications and industrial processes.

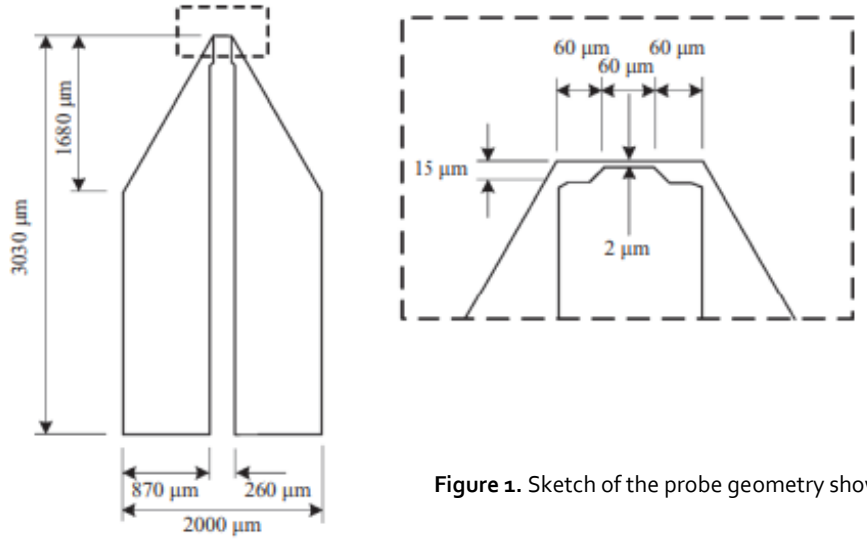

Figure 1. Sketch of the probe geometry showing dimensions of contact pads and wire.

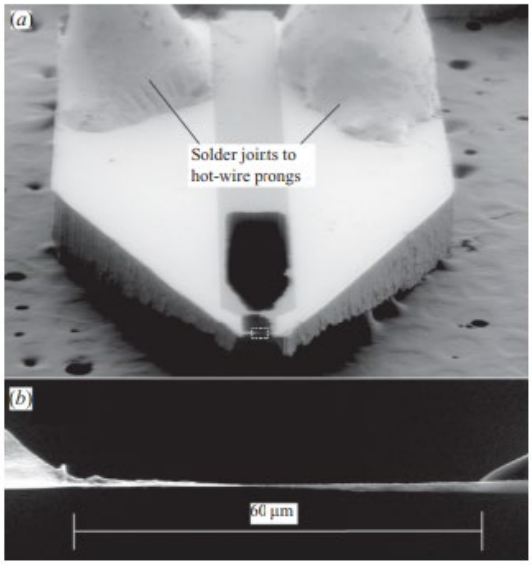

Figure 2. A scanning-electron microscope image of the completed NSTAP showing (a) the whole probe and (b) a close-up of the region indicated by a dashed box showing wire sensing length.

CITATIONS

- Fan, Y., Arwatz, G., Van Buren, T.W. et al. Nanoscale sensing devices for turbulence measurements. Exp Fluids 56, 138 (2015).
- Kunkel, G. J., Arnold, C. B. & Smits, A. J. 2006 Development of NSTAP: nanoscale thermal anemometry probe. In 36th AIAA Fluid Dynamics Conference and Exhibit, San Francisco, CA, June 5 8, 2006, AIAA Paper 2006-3718. Probe. Journal of Fluid Mechanics, vol. 663, 2010, pp. 160 179.

Advisor: Marcus N. Hultmark (Mechanical and Aerospace Engineering)

Highly Sensitive Elastic Filament Velocimetry Probe

Researcher: **Yuyang Fan** (Princeton Researcher)

Sponsorship: NSF

We introduce a novel, strain-based sensor for both gaseous and liquid flows, named the Elastic Filament Velocimetry (EFV) probe. The sensor consists of a free-standing, electrically conductive, nanoscale ribbon suspended between silicon supports. Due to its size, the nanoribbon deflects in flow under viscously dominated fluid forcing, which induces axial strain and a resistance change in the sensing element. The change in resistance can then be measured by a Wheatstone bridge, resulting in straightforward design and operation of the sensor. Since its operating principle is based on viscous fluid forcing, the sensor has high sensitivity especially in liquid or other highly viscous flow. Recent focuses have been towards optimizing this physical phenomenon with different sensing ribbon materials such as a semiconductor, which has the potential to significantly increase both accuracy and sensitivity.

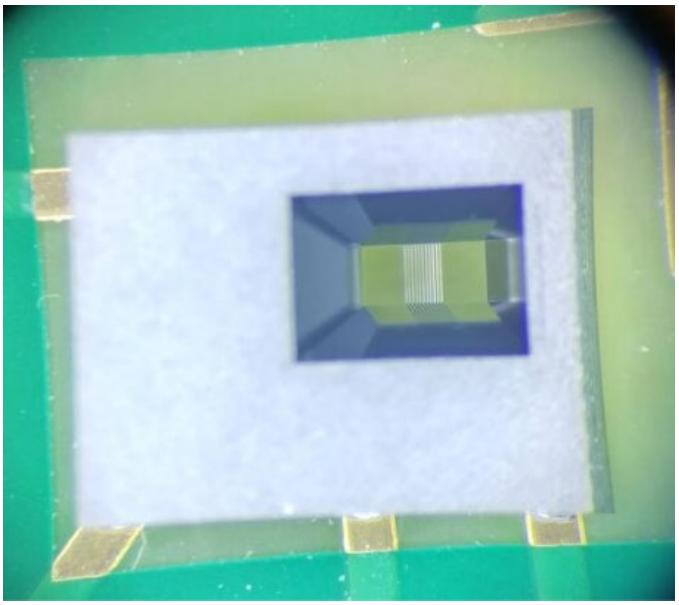

Figure 1: Example of an EFV probe mounted on a piece of printed circuit board (PCB). The nanoscale ribbons can be seen through the rectangular opening on the silicon substrate.

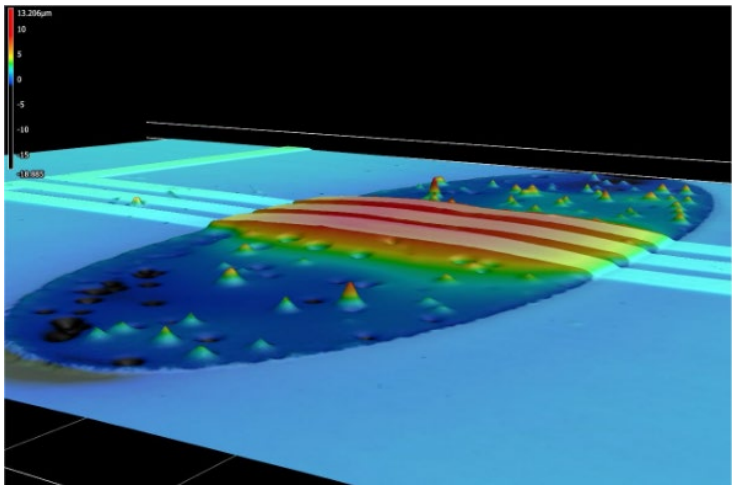

Figure 2: Confocal microscopic image of the semiconductor sensing ribbons under fluid forcing, where a parabolic shaped sensing ribbon profile can be seen with the color contour.

CITATIONS

- Hultmark M, Fan Y, Byers CP, Fu MK, System and Method for Monitoring Injection Site Pressure, **2022** U.S. Patent No. 11,351,313 B2
- Hultmark M, Fan Y, Byers CP, Fu MK, Multi-component Fast-response Velocity Sensor, **2021** U.S. Patent No. 11,187,715 B2
- Hultmark M, Byers CP, Fu MK, Fan Y, Elastic Filament Velocimetry, **2020** U.S. Patent No. 10,539,443 B2; **2021** U.S. Patent No. 11,054,290 B2
- Byers CP, Fu MK, Fan Y, Hultmark M (**2018**) Development of Instrumentation for Measurements of Two Components of Velocity with A Single Sensing Element, Measurement Science and Technology, 29(2), 025304
- Fu MK, Fan Y, Byers CP, Chen T-H, Arnolds CB, Hultmark M (**2016**) Elastic Filament Velocimetry, Measurement Science and Technology, 28(2), 025301

Advisor: Anirudha Majumdar (Mechanical and Aerospace Engineering)

Real-time Control of UAVs in Extreme Wind Conditions using High-Frequency Flow Sensors

Researcher: **Nathaniel Simon** (Princeton Graduate)

Sponsorship: Princeton University - Project X Innovation Fund

Autonomous unmanned aerial vehicles (UAVs) have the potential for transformative impact in numerous applications. However, current systems struggle to maintain precise control in high winds and gusty conditions. Our hypothesis is that the ability to make high-resolution measurements of wind speed will allow us to maintain stability in the face of significantly higher wind gusts than currently possible (e.g., gusts of 40-50mph) and allow for improved maneuverability in very cluttered environments (e.g., when performing infrastructure inspection applications around tall structures). Conventional anemometry techniques are unsuitable for wind estimation: either too slow, insensitive, or bulky. The goal of this project is to design a novel omnidirectional flow sensor, exploiting recent advances in MEMS flow sensing devices for turbulent airflow measurements [1], to enable UAV robustness and maneuverability in extreme winds. The sensing element used is the MEMS Hotwire, developed by PI Marcus Hultmark's group. The MNFC Packaging Lab is used to bond the MEMS Hotwires to custom printed circuit boards (PCBs), to make our sensor: the MAST (MEMS Anemometry Sensing Tower). We show the MAST to be a fast and accurate flow sensor that enables improvements in UAV performance [2].

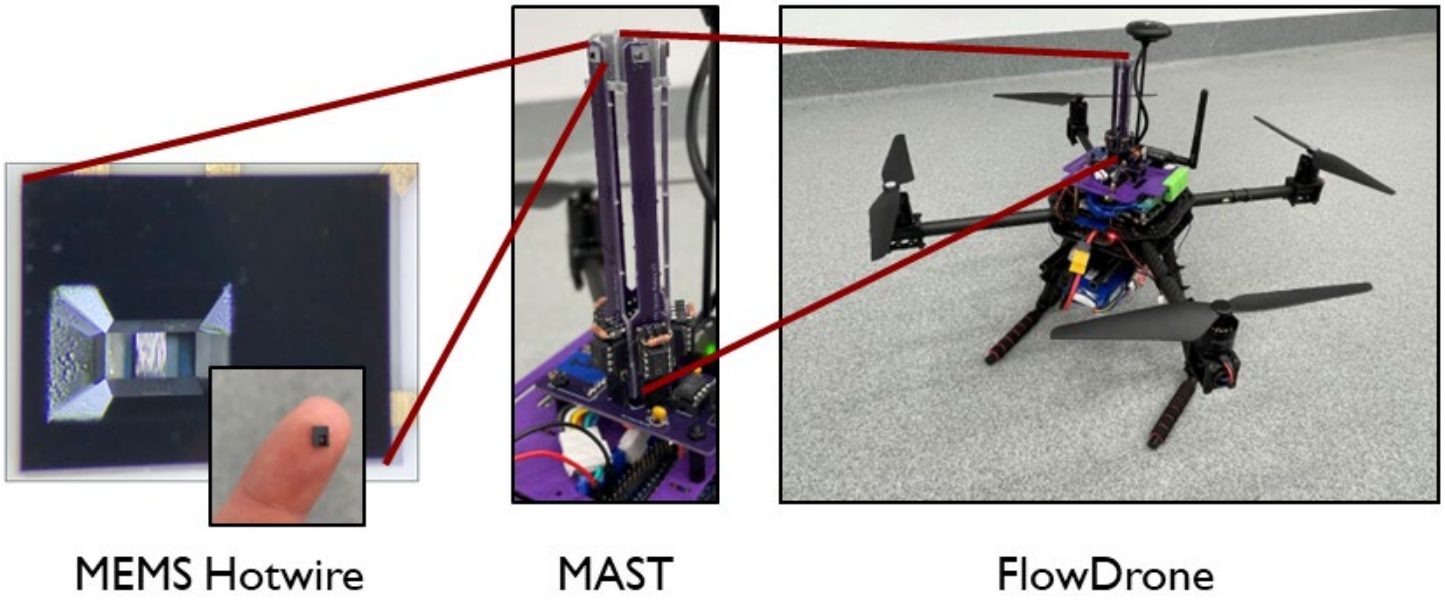

Figure 1: (Left) The MEMS Hotwire is a microscale fast-response hot-wire anemometry device. (Center) The MAST uses numerous MEMS Hotwires for omnidirectional flow sensing. (Right) The MAST mounted on a UAV for wind-aware control using real-time wind estimates.

.

CITATIONS

- (1) M. K. Fu, Y. Fan, C. P. Byers, T.-H. Chen, C. B. Arnold and M. Hultmark Elastic filament velocimetry, Measurement Science and Technology. 28.2 (2016): , 28, 2, 025301
- (2) N. Simon, A. Piqué, D. Snyder, K. Ikuma, A. Majumdar and M. Hultmark Fast-response hot-wire flow sensors for wind and gust estimation on UAVs, 2023 Meas. Sci. Technol. 34 025109

Advisor: Howard A. Stone (Mechanical and Aerospace Engineering)

Co-Axial Nozzle Droplet Formation

Researcher: **Richard Zhu** (Princeton Undergraduate)

Sponsorship: N/A

This project focus on the behaviour of fluids moving through nozzles with both 2 and 3 conduits (respectively 2- and 3-nozzles). We are specifically interested in atomization behavior of suspensions, and a key aspect of the project involves fabrication of nozzles using the Nanoscribe Photonic Professional GT2 device in the cleanroom. Classified as the world's highest resolution 3-D printer, we hope to use the device to fabricate nozzle opening parameters within a tolerance of plus-minus 1 micron in the vertical direction, and 500nm in the x and y-axes. The fabrication process involves making devices with exfoliated crystal of quantum spin liquid candidates, preparing substrates for experiments involving 3D topological insulators and Weyl/Dirac semimetals, and more.

Currently, Rubio et al. uses a 75 micron inner diameter for the outer nozzle. We propose a larger, 200 micron outer nozzle and also investigate a novel connection type.

I hope to investigate droplet formation from a coaxial nozzle, building on previous research. For the 3-nozzle, two fluids (one air, the other liquid with surfactant (potentially with suspended particles)) will be pushed through the three inlets of the nozzle, forming droplets as the fluids meet and exit. The inner nozzle may have an inner diameter of 100 microns, while the middle and outer nozzles may have inner diameters of 200 and 300 microns, respectively.

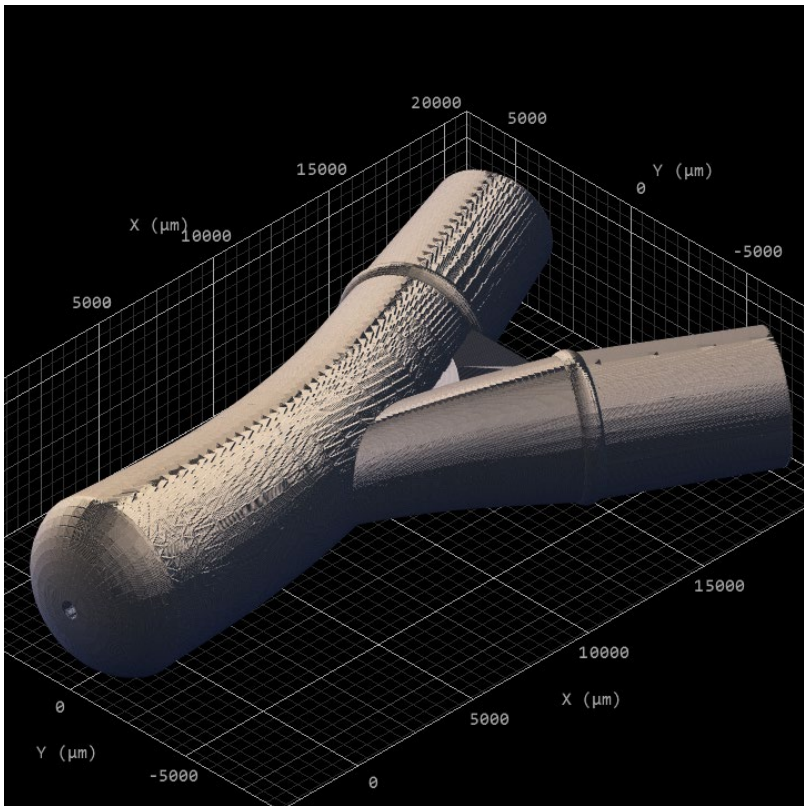

Figure 1: Nanoscribe DeScribe render of 2-nozzle.

CITATIONS

- Viscoelastic transition in transonic flow focusing by Rubio et al.

Advisor: Howard A. Stone (Mechanical and Aerospace Engineering)

Microtubule-Enabled NanoTechnology (MENT): Pulling, Pushing and Separating on the Nanoscale

Researcher: **Ryungeun Song** (Princeton Postdoc)

Sponsorship: Schmidt Funding

We will combine our expertise on building the microtubule cytoskeleton to further our understanding of how it works in a cell (Petry), with microfluidics, fluid mechanics, bioengineering and theory (Stone), to create a next-generation nanotechnology that we coin Microtubule-Enabled NanoTechnology (MENT). We hypothesize that the spindle, Nature s machine for separating chromosomes every time cells divide, can be repurposed for innovative new forms of programmed and targeted molecular separations, sequestering, and/or assembly. We will apply our ability to build cellular structures in order to create nanosystems ranging from a bio-actuator in various sizes and strengths, to a molecular conveyer belt, a distribution center, and ultimately biomolecular factories.

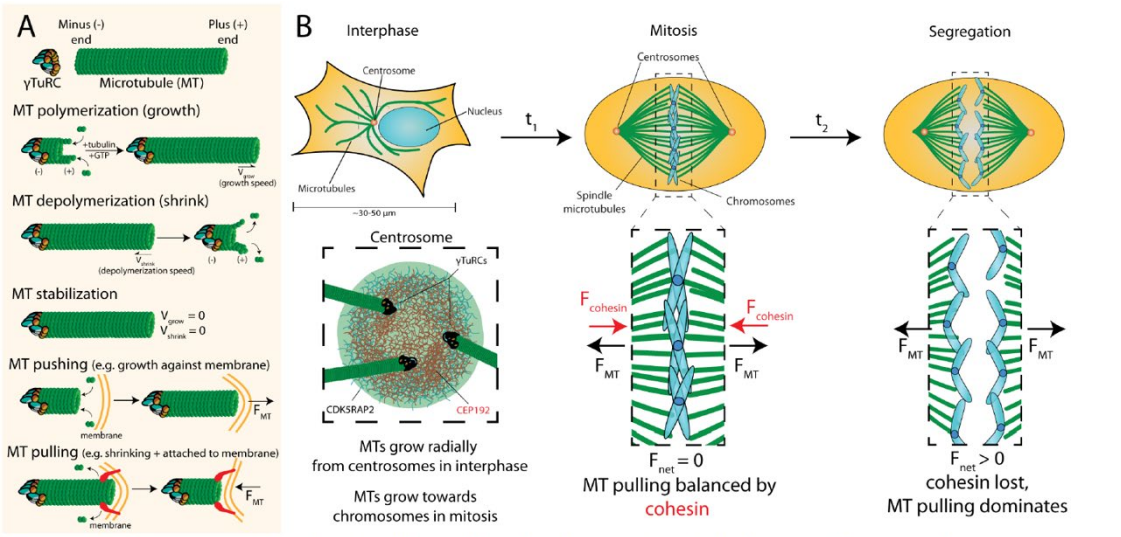

Figure 1: Our proposal is inspired by cells, which use microtubules as a framework to grow, shrink, push, pull, and move materials. We will build upon these concepts in our nanotechnology.

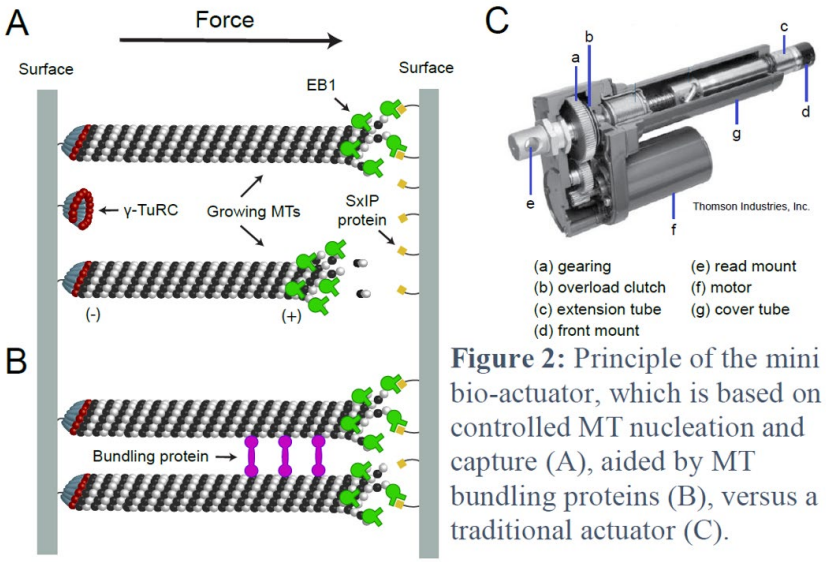

Figure 2: Principle of the mini bio-actuator, which is based on controlled MT nucleation and capture (A), aided by MT bundling proteins (B), versus a traditional actuator (C).

CITATIONS

- N/A

Advisor: Howard A. Stone (Mechanical and Aerospace Engineering)

Exxon Microfluidics

Researcher: **Samantha McBride** (Princeton Postdoc)

Sponsorship: NSF

We are fabricating fluidic devices with micro-scale porosity in order to understand how one fluid phase may be trapped within those pores while another fluid flows past them. The goal of this work is to understand the trade-offs between stability and maximal volume of the trapped phase in order to increase kinetics of adsorption or other reaction between the two fluids.

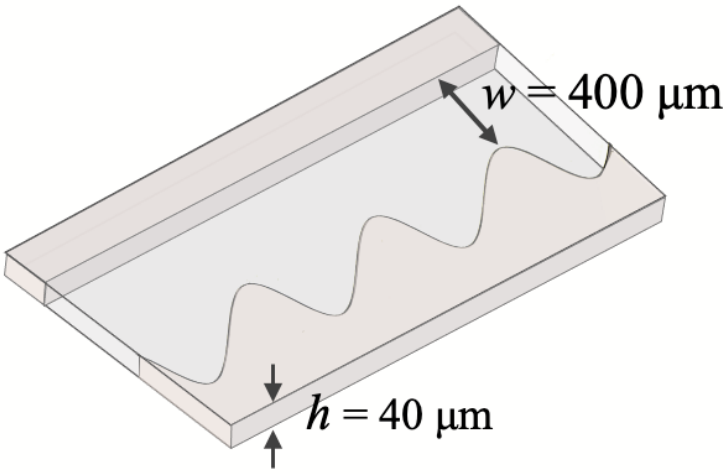

Figure 1: Schematic of the microfluidic devices with micro-scale sinusoidal pores. The devices are 40 um thick and were fabricated out of PDMS using a silicon master template. The silicon template was fabricated in the cleanroom using the Heidelberg direct laser write to pattern photoresist with the microfluidic pattern, before using the SAMCO 800 to etch into the master template to a depth of 40 um.

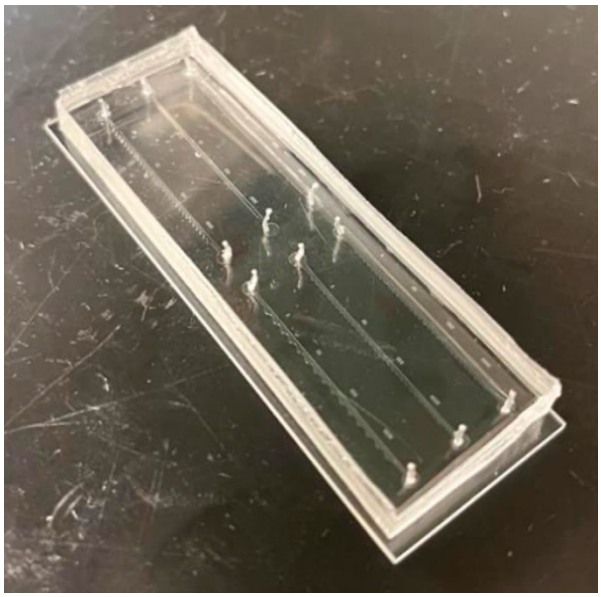

Figure 2: Image of one of the micro-porous microfluidic devices. The device has two components: the PDMS patterned with the channels was created from the silicon master mold, and a glass slide is used to seal the channels. Each device has 6 channels in total with different sine geometries so we can test the influence of different pore geometries on trapping of different fluid phases within the pores.

CITATIONS

- McBride, S.A., Coleto, F.T., Kaneelil, P.R., Knopp, R., Taylor, A.J., Storey-Matsutani, M.A., Wilson, J.L., Stone, H.A. Effect of Capillary Number on Drainage from Microscale Sinusoidal Pores. Presented on Nov 22nd at the American Physical Society Division of Fluid Dynamics 74th Annual Meeting in Indianapolis
- McBride, S.A., Kaneelil, P.R., Coleto, F.T., Knopp, R., Taylor, A.J., Storey-Matsutani, M.A., Wilson, J.L., Saleh, S., Konicek, A.R., Yeganeh, M.S., Stone, H.A. Effect of Capillary Number on Liquid Entrapment/Displacement in Microscale Pores. In preparation for publication.

Physics

Advisor: M. Zahid Hasan (Physics)
Sample Preparation for Ultrafast Study
Researcher: **Zijia Cheng** (Princeton Graduate)
Sponsorship: DOE

Ultrafast x-ray and optical study of topological materials and devices.

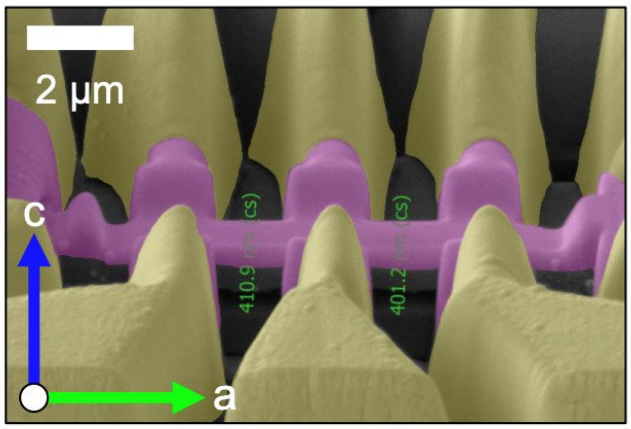

Figure 1: A device of the microscopic sample made by focus ion beam technique [1].

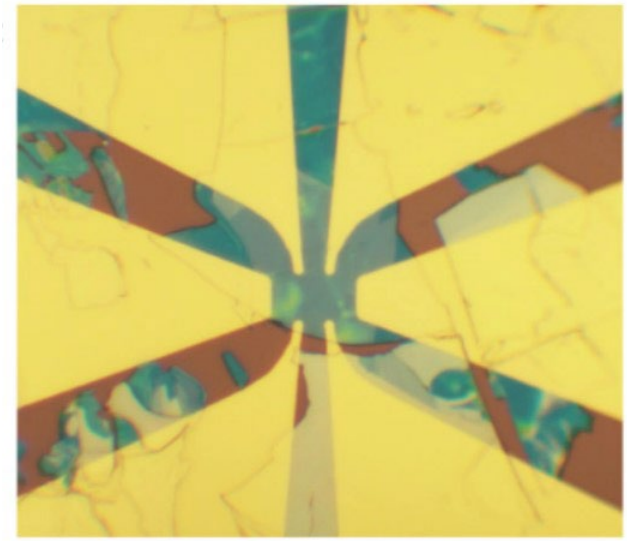

Figure 2: A device of an exfoliated sample [2].

CITATIONS

- [1] Osterhoudt, Gavin B., et al. "Colossal mid-infrared bulk photovoltaic effect in a type-I Weyl semimetal." Nature materials 18.5 (2019): 471-475.
- [2] Deng, Yujun, et al. "Quantum anomalous Hall effect in intrinsic magnetic topological insulator MnBi2Te4." Science 367.6480 (2020): 895-900.

Advisor: M. Zahid Hasan Physics)

Sample Device Preparation for Ultrafast Study

Researcher: **Qi Zhang** (Princeton Postdoc)

Sponsorship: DOE

The project focuses on exploring novel physics of quantum-many-body emergence, condensates, quantum coherence, and topological emergence by combining novel spectroscopy, microscopy and transport methods, such as room-temperature macroscopic quantum phenomena and engineered hetero-structures and artificial quantum matter for novel devices.

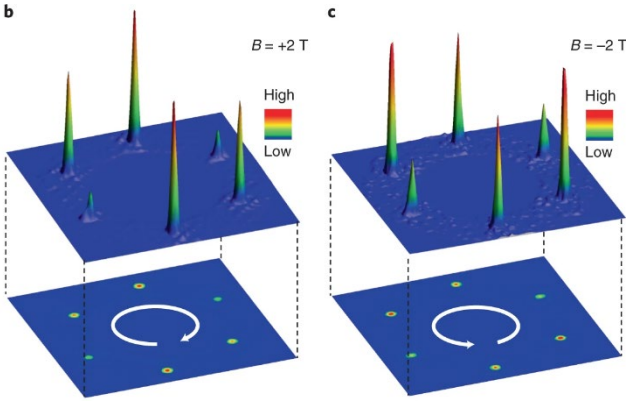

Figure 1: Magnetic response of the chiral charge order.

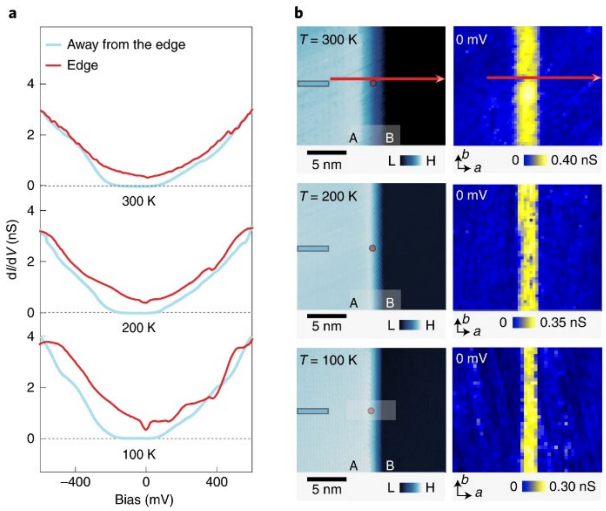

Figure 2: Room-temperature edge state.

CITATIONS

- Jiang, YX., Yin, JX., Denner, M.M. *et al.* Unconventional chiral charge order in kagome superconductor KV_3Sb_5. *Nat. Mater.* **20,** 1353–1357 (2021).
- Shumiya, N., Hossain, M.S., Yin, JX. *et al.* Evidence of a room-temperature quantum spin Hall edge state in a higher-order topological insulator. *Nat. Mater.* **21,** 1111–1115 (2022).

Advisor: Nai Phuan Ong (Physics)

Low Temperature Transport measurements on Topological Materials

Researcher: **Jiayi Hu** (Princeton Postdoc)

Sponsorship: NSF, DOE, Moore

Frontier of research on topological materials has uncovered many intriguing phenomena. I am measuring transport properties of (magnetic) Weyl and Dirac semimetals, topological superconductor candidates, and others at low temperature. To perform electrical device fabrication for exfoliated samples and prepare substrates, I am employing techniques including photo-/electron beam lithography and physical vapor deposition.

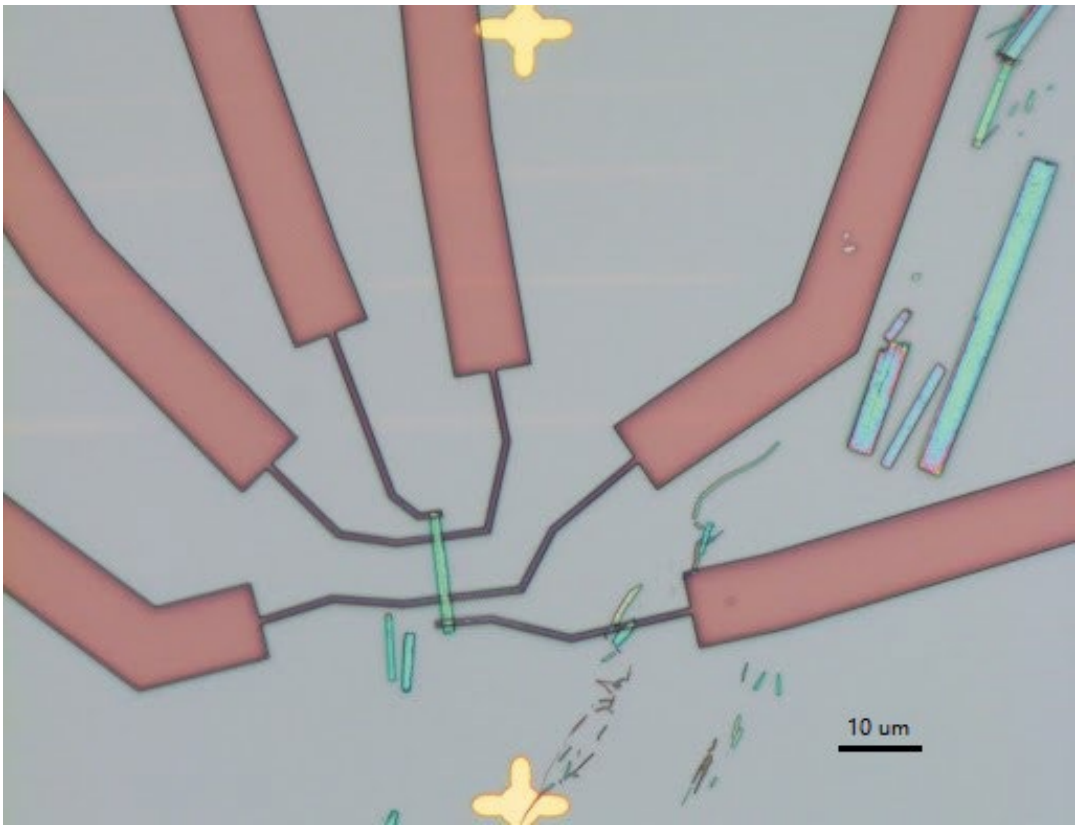

Figure 1: A photo of the device made in MNFC taken after the e-beam writing and before Au deposition.

CITATIONS

- Jun Ge, et al. Unconventional Hall effect induced by Berry curvature; National Science Review, Volume 7, Issue 12, December 2020, Pages 1879–1885, https://doi.org/10.1093/nsr/nwaa163.

Advisor: Nai Phuan Ong (Physics)

Electronic Devices Using Topological Materials

Researcher: **Zheyi Zhu** (Princeton Graduate)

Sponsorship: DOE

This project focus on the transport properties of topological material. We make asymmetric SQUID on thin flake of topological material to measure the phase dependent supercurrent in sample junction. A typical A-SQUID consists of a trivial Al tunneling junction with large critical current, which help to pin the superconducting phase, and a sample junction of interest made with two Al fingers. In our recent work, we observed multiple Andreev reflections with exceptional clarity and were able to determine the coherent fraction even at finite voltage regime.

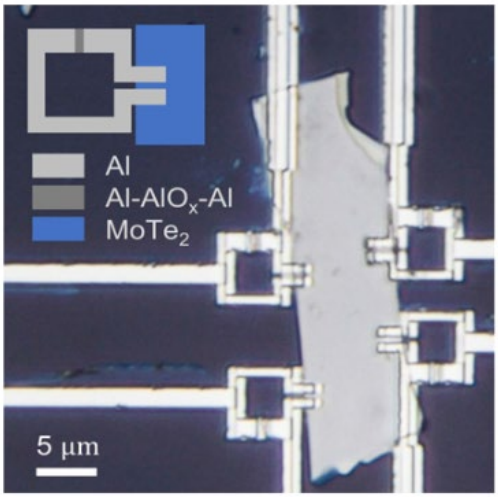

Figure 1: Asymmetric SQUID made on top of MoTe2 thin flake using Raith eline E-beam lithography.

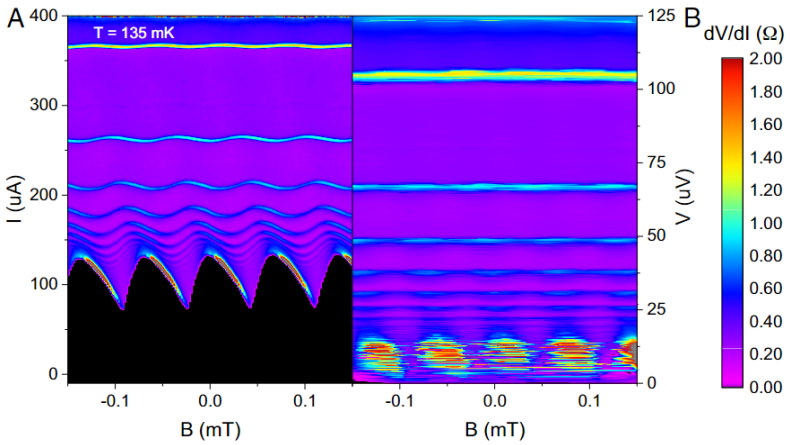

Figure 2: Observed subharmonic singularity in transport measurement, which is evidence for multiple Andreev reflection.

CITATIONS

- [1] Zheyi Zhu, Stephan Kim, Shiming Lei, Leslie M. Schoop, R. J. Cava, and N. P. Ong, Phase tuning of multiple Andreev reflections of Dirac fermions and the Josephson supercurrent in Al–MoTe2–Al junctions, Proceedings of the National Academy of Sciences of the United States of America 119, 28 (2022).

Advisor: Nai Phuan Ong (Physics)

Monolayer Graphene Quantum Hall Device Fabrication

Researcher: **Nicholas Quirk** (Princeton Graduate)

Sponsorship: NSF, Moore Foundation

Recently, I have focused on making devices out of two-dimensional materials, namely graphene-boron nitride heterostructures. I rely heavily on the Raith EBPG to do high-resolution electron-beam lithography. With the expert help of the MNFC staff, I have developed an optimized recipe that allows me to make a gap in a gold electrode on top of the graphene that is just 20 nm wide.

In the lab, I cool these devices down to 300 mK and apply strong magnetic fields of up to 13.5 T. The 20 nm gap creates a saddle-point potential through which quantum Hall edge states in the graphene can tunnel. This allows me to finely tune the conductance of the device and study the interesting physics of quasiparticles in various quantum Hall states in graphene.

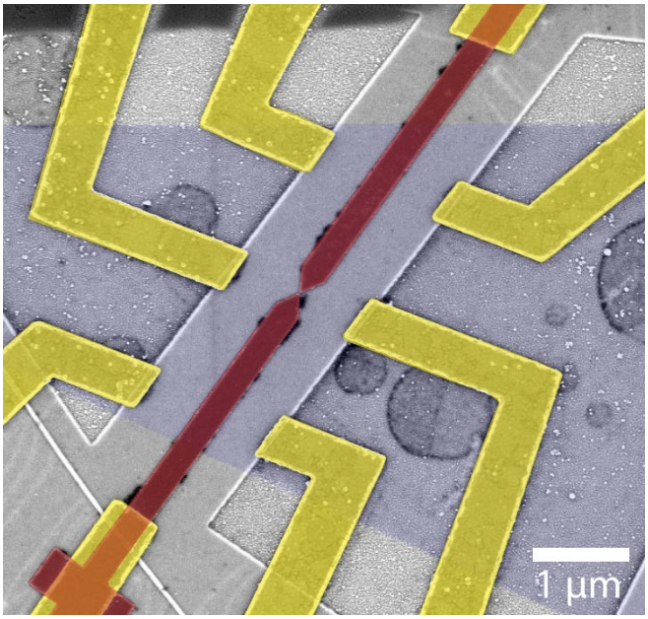

Figure 1: A triangular graphene flake (blue) is cut into a rectangular device with reactive ion etching. Chrome/gold edge contacts (yellow) are added as well as a palladium top gate (red). This gate has a 20 nm gap between its two triangular arms (quantum point contact).

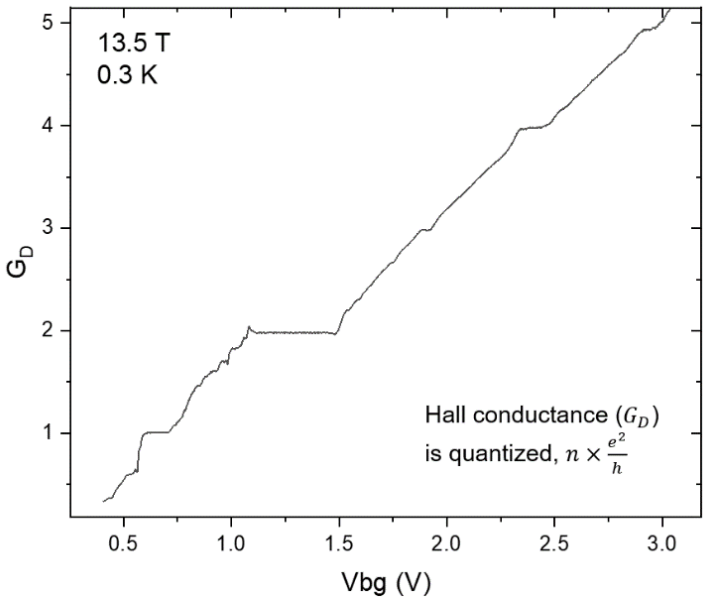

Figure 2: Sample quantum Hall effect data in a graphene device. In a perpendicular magnetic field (H = 13.5 T), the transverse conductance (G_D) has quantized values determined by the number of ballistic edge modes, which can be tuned with a global electrostatic gate (V_{BG}).

CITATIONS

- N/A

Advisor: Jason Petta (Physics)

Gate Microscopy of Si/SiGe Quantum Dot Devices

Researcher: **Gordian Fuchs** (Princeton Graduate)

Sponsorship: ARO

Conventional transport methods provide quantitative information on spin, orbital, and valley states in quantum dots but lack spatial resolution. Scanning tunneling microscopy, on the other hand, provides exquisite spatial resolution at the expense of speed. Working to combine the spatial resolution and energy sensitivity of scanning probe microscopy with the speed of microwave measurements, we couple a metallic tip to a Si/SiGe double quantum dot (DQD) that is integrated with a charge detector. We first demonstrate that the dc-biased tip can be used to change the occupancy of the DQD. We then apply microwaves through the tip to drive photon-assisted tunneling (PAT). We infer the DQD level diagram from the frequency and detuning dependence of the tunneling resonances. These measurements allow the resolution of 65 eV excited states, an energy consistent with valley splittings in Si/SiGe. This work demonstrates the feasibility of scanning gate experiments with Si/SiGe devices.

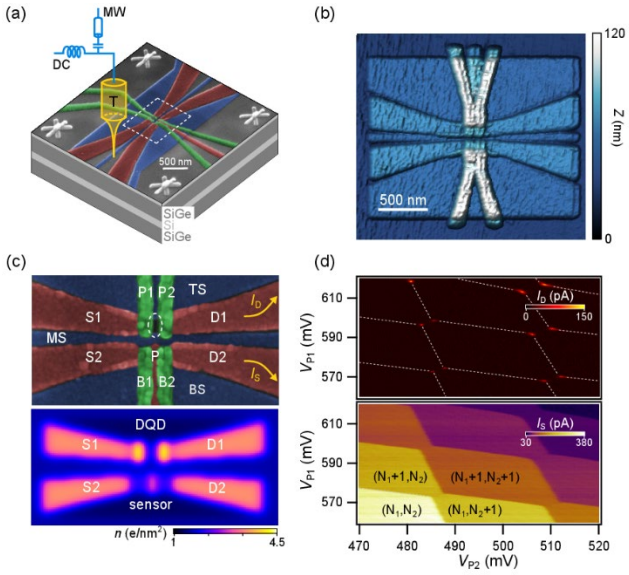

Figure 1. (a) Schematic of the Si/SiGe device being perturbed by an atomic force microscope (AFM) tip (T). A bias-T allows microwaves to be applied to a dc-biased tip. (b) Low-temperature AFM topography of a test structure that is adjacent to the device. (c) (Top) False-color SEM image of the device. The absence of metal between gates P1 and P2 allows the potential of the AFM tip to perturb the electronic wave function in the Si QW. (Bottom) Simulated charge density n in the Si QW. The charge sensor is used to probe the charge occupancy of the DQD. (d) DQD charge stability diagram extracted from the current I_D flowing through the DQD (top) and charge sensing measurements of I_S (bottom). The tip is pulled far from the device with V_T= 0.51 V.

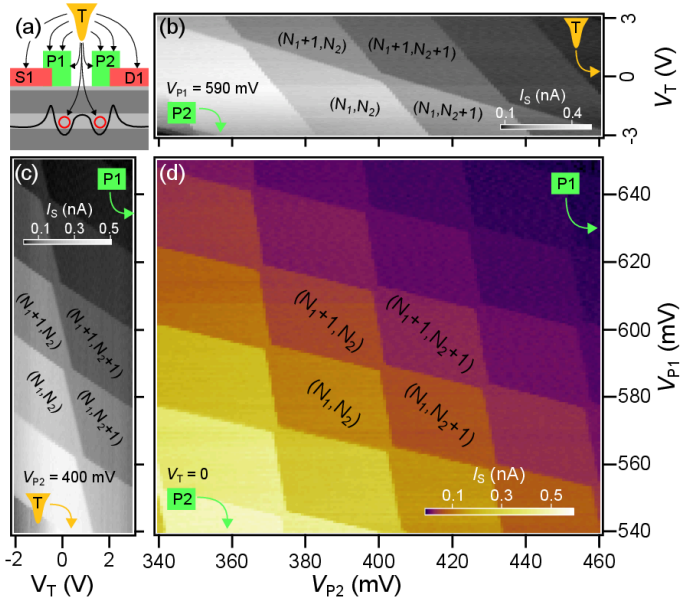

Figure 3. (a) Illustration showing symmetric coupling between the tip and the DQD confinement potential. The metallic gates vastly screen the electric field of the tip. The tip is placed ~100 nm above the Al gates. (b) Stability diagram plotted as a function of V_{P2} and V_T, with V_{P1}= 590 mV. (c) Stability diagram plotted as a function of V_T and V_{P1}, with V_{P2}= 400 mV. (d) Stability diagram as a function of V_{P1} and V_{P2}, with V_T=0V.

CITATIONS

- Denisov et al. Microwave-Frequency Scanning Gate Microscopy of a Si/SiGe Double Quantum Dot. Nano Lett. 2022, 22, 12, 4807-4813.

Advisor: Jason Petta **(Physics)**

High-Impedance Cavities With Gate-Defined Quantum Dots

Researcher: **Susanne Zhang** (Princeton Graduate)

Sponsorship: ARO

Circuit quantum electrodynamics (QED) employs superconducting microwave resonators as quantum buses. In circuit-QED with semiconductor quantum-dot-based qubits, increasing the resonator impedance is desirable as it enhances the coupling to the typically small charge dipole moment of these qubits. In an effort to move towards a new generation of devices with high-impedance cavities, we worked on a new niobium nitride (NbN) process using our new AJA sputtering tool. We recently reported our recent direct current (DC) resistivity study and microwave investigation of NbN films of different thickness. For 15 nm NbN thin films, we measured a high kinetic inductance of Lk ~ 41.2 pH/sq and sheet resistance of Rs ~ 274 Ohm/sq. Using this film, we fabricated half-wavelength microwave resonators and achieved high quality factors by reducing photon losses through low-pass LC filters on the gate bias lines. Looking ahead, the combination of a high-impedance superconducting resonator with low-pass filters and long-coherence qubits will enable an improved cQED platform for strong-coupling demonstration of two spin-qubits.

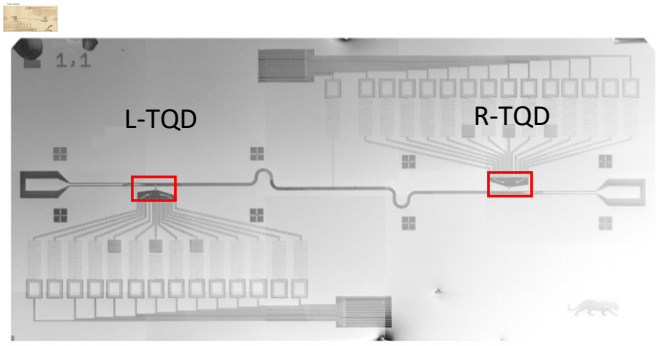

Figure 1: Full device substrate, with two distant triple quantum dots (TQDs) highlighted in red.

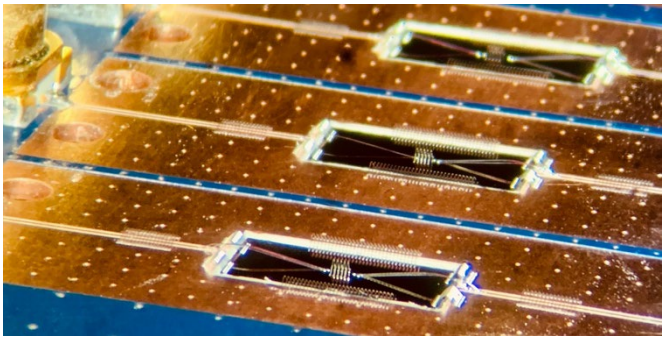

Figure 2: Test LC filter chips packaged using wire bonds for transmission measurement.

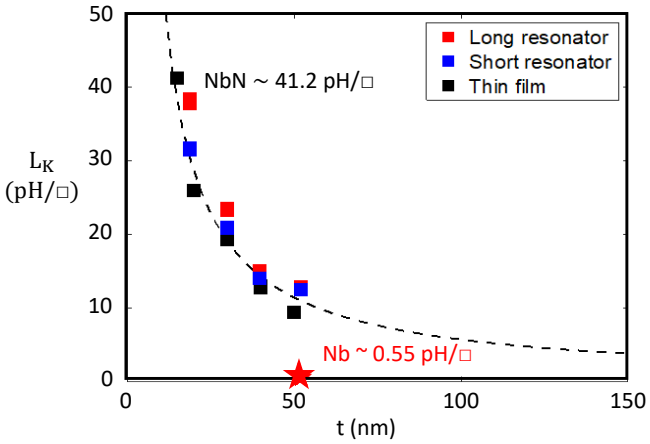

Figure 3: Kinetic inductances measured from NbN thin films of different thicknesses.

CITATIONS

- X. Mi, J. V. Cady, D. M. Zajac, J. Stehlik, L. F. Edge, and J. R. Petta, Applied Physics Letters 110, 043502 (2017).
- P. Harvey-Collard, G. Zheng, J. Dijkema, N. Samkharadze, A. Sammak, G. Scappucci, and L. M. Vandersypen, Physical Review Applied 14, 034025 (2020).
- X. Zhang, Z. Zhu, N.P. Ong, and J.R. Petta, Fortifying the strong-coupling regime of quantum dot circuit QED using high-impedance superconducting resonators, presented at APS March Meeting, Chicago, IL, 2022.

Advisor: Sanfeng Wu (Physics)

Quantum Devices Based on 2D Materials

Researcher: **Guo Yu** (Princeton Graduate)

Sponsorship: Startup Funding

This project aims to fabricate quantum devices based on 2D materials, such as graphene, boron nitride and Tungsten ditelluride (WTe2), for quantum transport measurements. We will study the topological phases and novel superconducting states in these materials. To accomplish that, we create nanoscale devices using equipment in MNFC including electron beam lithography, RIE, metal evaporation and so on.

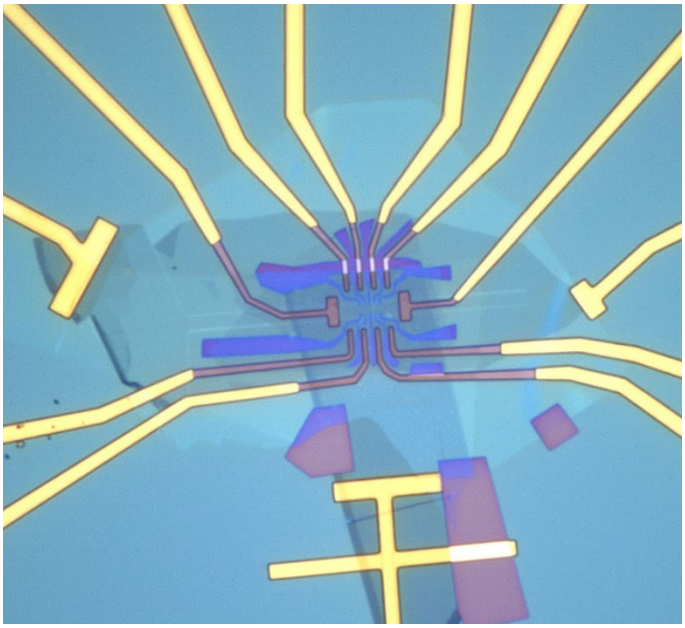

Figure 1: Optical image taken with Keyence Confocal in MNFC, of a twisted bilayer WTe2 device with selectively-etched edges.

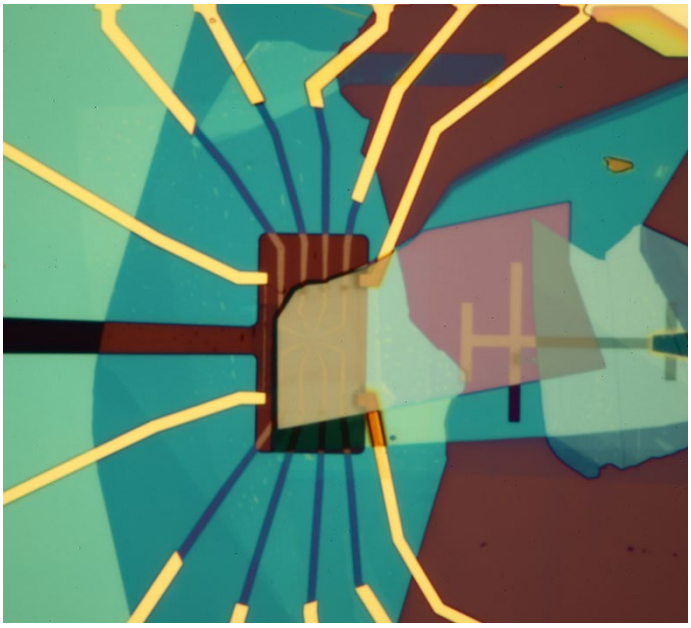

Figure 2: Optical image of a dual-metal-gated twisted bilayer WTe2 device, with all the EBL, metal deposition and etching done in MNFC.

CITATIONS

- Wang, P., Yu, G., Kwan, Y.H. *et al.* One-dimensional Luttinger liquids in a two-dimensional moiré lattice. *Nature* **605**, 57–62 (2022).

Advisor: Sanfeng Wu (Physics)

Moiré Luttinger Liquids in Two Dimensions

Researcher: **Pengjie Wang** (Princeton Postdoc)

Sponsorship: Startup Funding

This project aims to fabricate quantum devices based on 2D materials, such as graphene, boron nitride, tungsten ditelluride (WTe_2), and their moiré stacks, for quantum transport measurements. Figure 1 shows a twisted bilayer WTe_2 device (twist angle ~ 5°), which was fabricated in the MNFC cleanroom and had been discovered with a novel moiré Luttinger liquid phase.[1] The laser image (Fig. 2) is captured by the confocal imaging system, showing the selectively etched area for exposing the contacts. We create many nanoscale devices like this using equipment in MNFC, such as electron beam lithography, metal evaporation, confocal characterization, and RIE etcher.

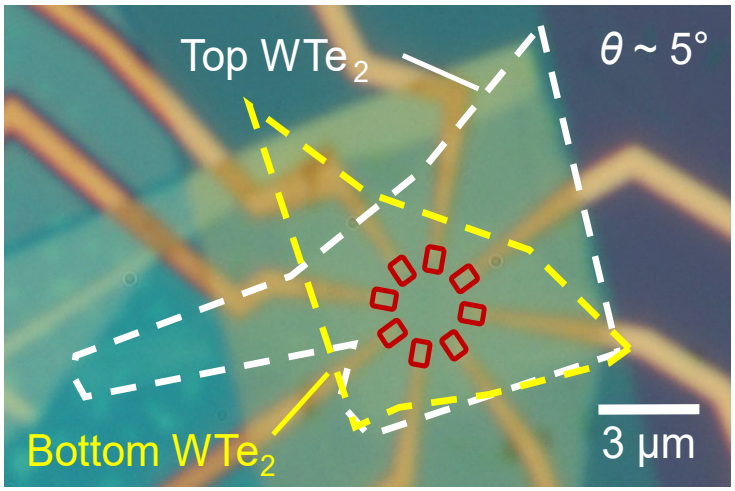

Figure 1: A cartoon image of a twisted bilayer WTe_2 device.[1] The dashed white (yellow) line highlights the top (bottom) monolayer WTe_2, and the red squares denote the contact regions.

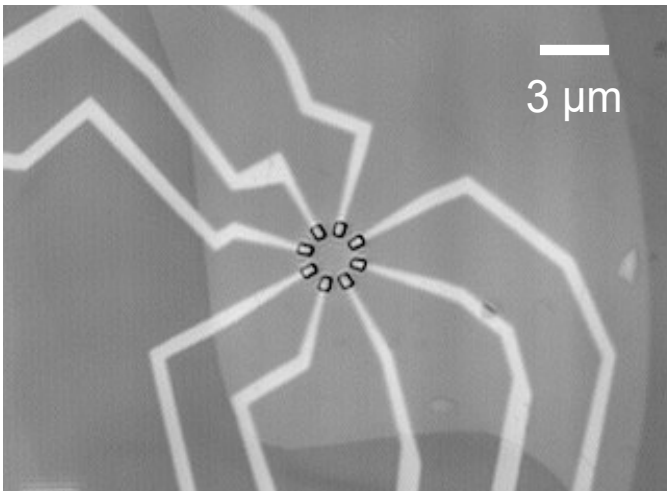

Figure 2: A laser image of a pre-pattern bottom stack captured by Keyence Confocal. The central part denotes the etching exposed contact regions.

CITATIONS

- [1} Wang, P. et al. One-dimensional Luttinger liquids in a two-dimensional moiré lattice. Nature 605, 57–62 (2022).

Advisor: Sanfeng Wu (Physics)

Topological Quantum Phases in 2D materials

Researcher: **Tiancheng Song** (Princeton Postdoc)

Sponsorship: Princeton Physics New Faculty Startup

This project aims to fabricate quantum devices based on 2D materials, such as graphene, boron nitride, and tungsten ditelluride (WTe2), for quantum transport measurements. We will study the topological phases and novel superconducting states in these materials. To accomplish that, we will create nanoscale devices using equipment in MNFC, such as E-beam lithography, dry etch, metal evaporator, and wire bonder.

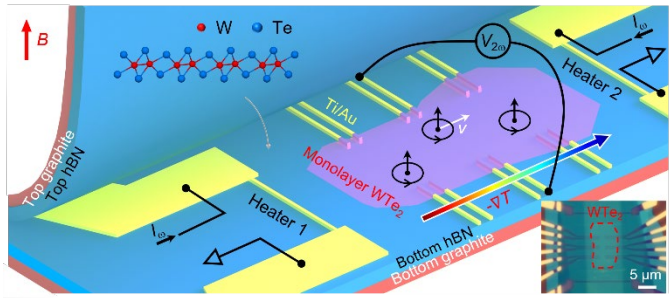

Figure 1. Cartoon illustration of the device structure for measuring thermoelectric signal. Current is applied to the two microheaters to produce a temperature gradient on monolayer WTe_2. The inset shows the optical microscope image of the device.

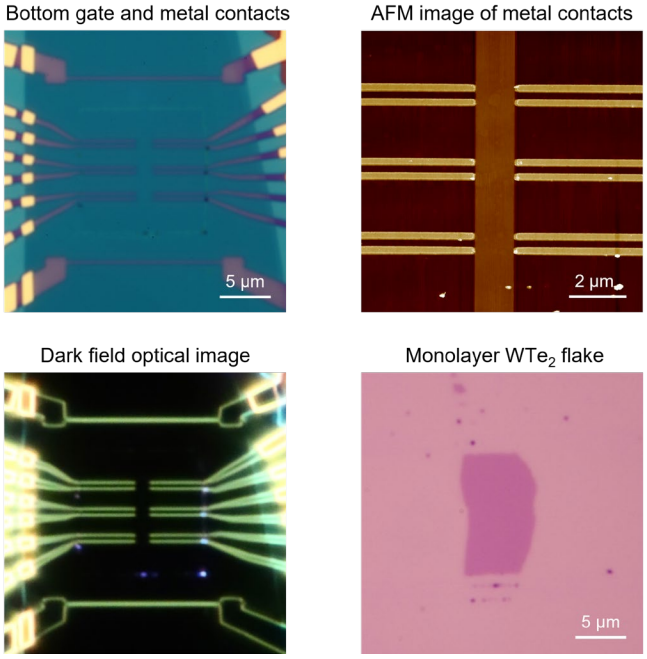

Figure 2. Microscope and AFM images during the device fabrication process. Bottom gate and metal electrodes after AFM tip clean. Dark field optical image of the bottom part. Tapping-mode AFM image of the metal electrodes. Microscope image of monolayer WTe_2 flake exfoliated in the glovebox.

CITATIONS

- T. Song, Y. Jia, G. Yu, Y. Tang, P. Wang, R. Singha, X Gui, A. J. Uzan, M. Onyszczak, K. Watanabe, T. Taniguchi, R. J. Cava, L. M. Schoop, N. P. Ong, S. Wu, "Unconventional Superconducting Quantum Criticality in Monolayer WTe2", under review (in preparation).

Advisor: Sanfeng Wu (Physics)

Topological Quantum Phases in 2D materials

Researcher: **Mike Onyszczak** (Princeton Graduate)

Sponsorship: ONR, NSF, and the Eric and Wendy Schmidt Transformative Technology Fund at Princeton

This project aims to fabricate quantum devices based on 2D materials, such as graphene, boron nitride, and transition metal dichalcogenides, for quantum transport measurements as well far infrared absorption spectroscopy. We will study the interplay between the topological phases and novel superconducting states in these materials.

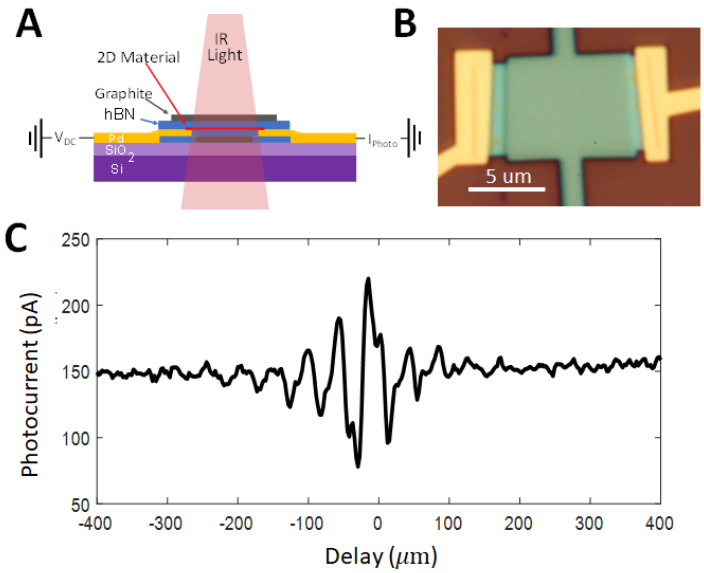

Figure 1: A: Cartoon schematic of far infrared absorption photocurrent spectroscopy. B: Optical image of h-BN encapsulated bilayer graphene device used in photocurrent spectroscopy. C: Photocurrent interferogram of landau level transitions in bilayer graphene.

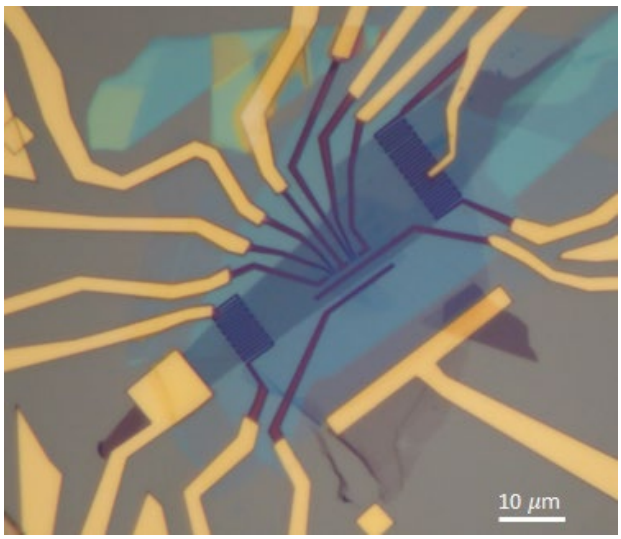

Figure 2: Optical image of a WTe_2 nanodevice containing heaters for thermoelectric measurements, tunable PN junction, and top and bottom graphite electrostatic gates.

CITATIONS

- N/A

Advisor: Sanfeng Wu (Physics)

Topological Quantum Phases in 2D materials

Researcher: **Yanyu Jia** (Princeton Graduate)

Sponsorship: Princeton Physics New Faculty Startup

This project aims to fabricate quantum devices based on 2D materials, such as graphene, boron nitride and Tungsten ditelluride (WTe2), for quantum transport measurements. We will study the topological excitonic insulating state and novel superconducting states in these materials. To accomplish that, we will create nanoscale devices using equipment in MNFC, such as E-beam lithography, dry etch, metal evaporator and wire bonder.

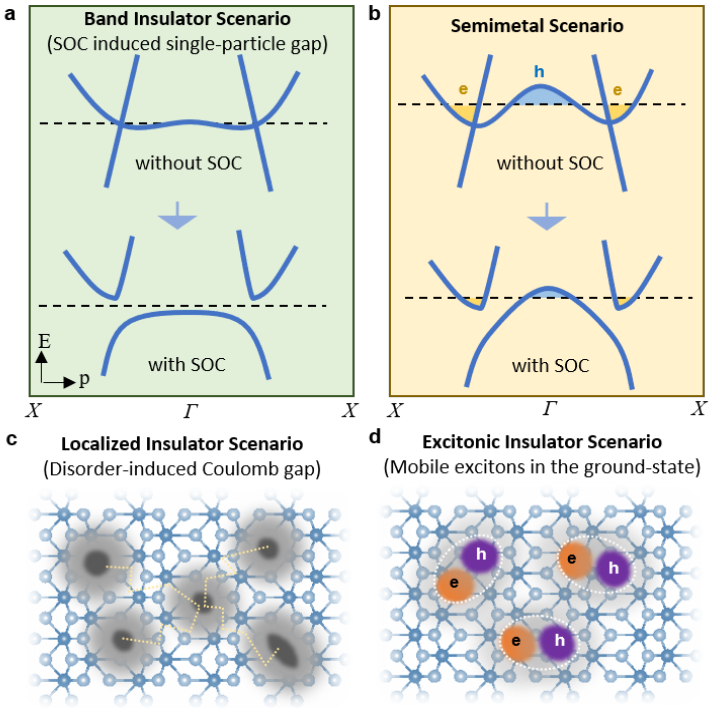

Figure 1. Possible scenarios of the ground states at CNP in monolayer WTe2.

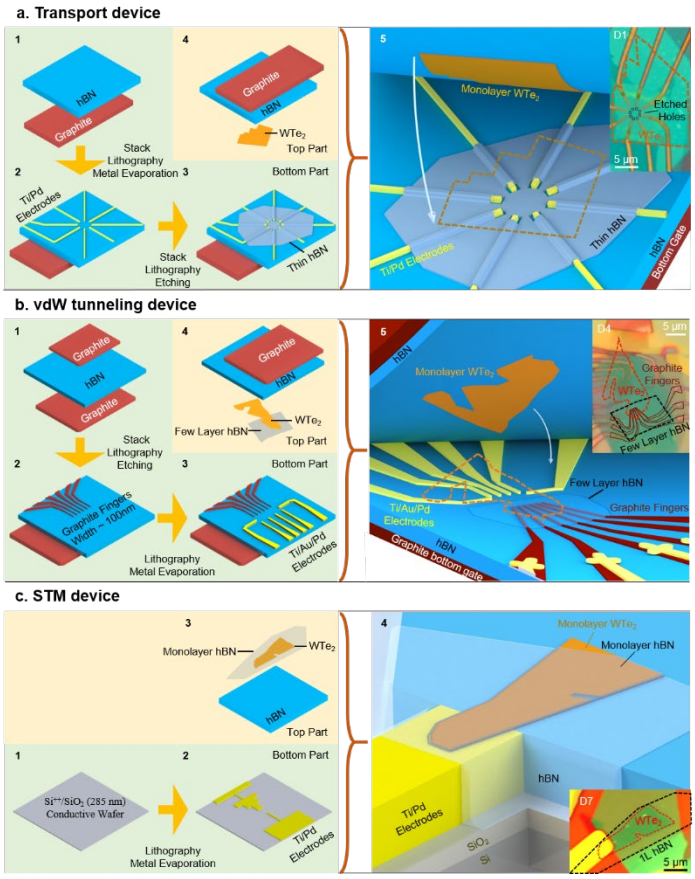

Figure 2. Device fabrication process.

CITATIONS

- Jia, Y. et al. Evidence for a monolayer excitonic insulator. Nat. Phys. 18, 87–93 (2022).

Advisor: Sanfeng Wu (Physics)

Topological Quantum Phases in 2D Materials

Researcher: **Yue Tang** (Princeton Graduate)

Sponsorship: NSF MRSEC

This project aims to fabricate quantum devices based on 2D materials, such as graphene, boron nitride, and tungsten ditelluride (WTe2), for quantum transport measurements. We will study the topological phases and novel superconducting states in these materials. To accomplish that, we will create nanoscale devices using equipment in MNFC, such as E-beam lithography, dry etch, metal evaporator, and wire bonder.

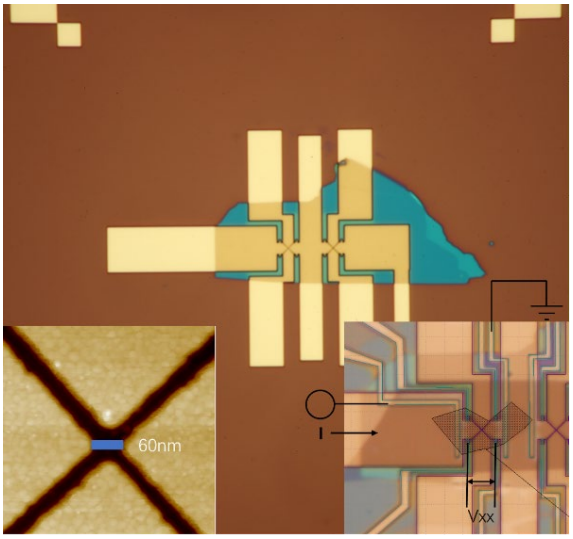

Figure 1: Quantum point contact device. A quantum point contact device is designed to investigate one-dimensional electron behaviors, which can also be used for probing electron tunneling effects.

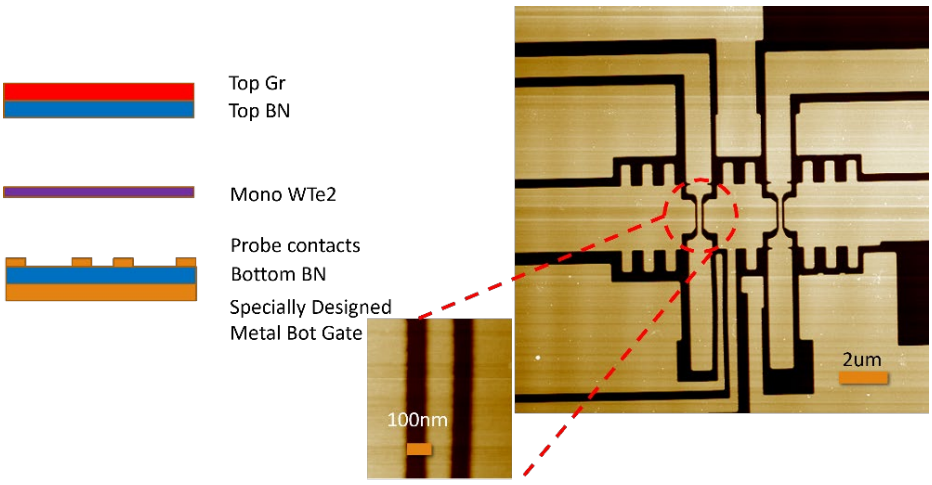

Figure 2: Joesphson junctions device. Two consecutive Joesphson junctions are designed to investigate unique properties of 2D materials. The side view of an electronic device is shown on the left.

CITATIONS

- [1] S. Wu, V. Fatemi, Q. D. Gibson, K. Watanabe, T. Taniguchi, R. J. Cava, and P. Jarillo-Herrero, Science 359, 76 (2018).
- [2] Y. Jia, P. Wang, C.-L. Chiu, Z. Song, G. Yu, B. Jäck, S. Lei, S. Klemenz, F. A. Cevallos, M. Onyszczak, N. Fishchenko, X. Liu, G. Farahi, F. Xie, Y. Xu, K. Watanabe, T. Taniguchi, B. A. Bernevig, R. J. Cava, L. M. Schoop, A. Yazdani, and S. Wu, Nature Physics 18, 87 (2022).
- [3] V. Fatemi, S. Wu, Y. Cao, L. Bretheau, Q. D. Gibson, K. Watanabe, T. Taniguchi, R. J. Cava, and P. Jarillo-Herrero, Science 362, 926 (2018).
- [4] S. Shapiro, Physical Review Letters 11, 80 (1963).
- [5] J. Wiedenmann, E. Bocquillon, R. S. Deacon, S. Hartinger, O. Herrmann, T. M. Klapwijk, L. Maier, C. Ames, C. Brüne, C. Gould, A. Oiwa, K. Ishibashi, S. Tarucha, H. Buhmann, and L. W. Molenkamp, Nat. Commun. 7, 10303 (2016).
- [6] T. Godfrey, J. C. Gallop, D. C. Cox, E. J. Romans, J. Chen, and L. Hao, IEEE Transactions on Applied Superconductivity 28, 1 (2018).

Advisor: Sanfeng Wu (Physics)

Far infrared Optical Studies of Monolayer WTe2 at Ultralow Temperatures

Researcher: **Ayelet Uzan** (Princeton Postdoc)

Sponsorship: NSF MRSEC Grant

Monolayer tungsten ditelluride (WTe2) has been established as a highly intriguing 2D material, which exhibits various topological and correlated quantum phases, such as the quantum spin Hall insulator, excitonic insulator, and gate-induced superconductivity. Yet theoretical understanding of this unique 2D crystal remains poorly developed, including even its basic band structure and the effects of electron correlations on it. In this project we aim to probe its electronic phases using our newly developed instrument that integrates far-infrared optical spectroscopy with a dilution refrigerator. With optics, we hope to reveal new information about monolayer WTe2 that is hidden from electronic transport.

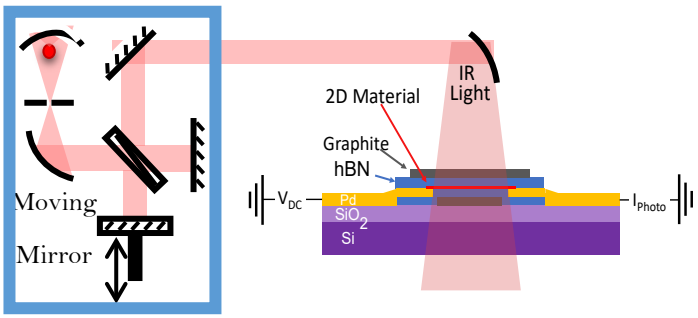

Figure 1: Schematic description of our FTIR photocurrent detection setup.

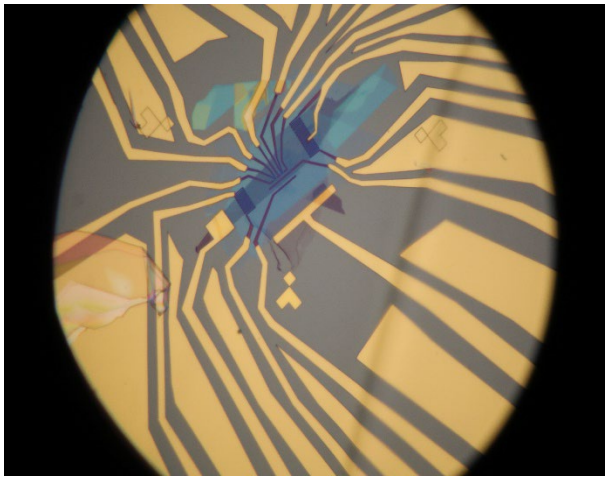

Figure 2: Fabricated monolayer tungsten ditelluride device using nanolithography methods.

CITATIONS

- Long,J. et al. Tunable excitons in bilayer graphene. Science. 358, 907-910(2017).
- Wu S. et al Observation of the quantum spin Hall effect up to 100 kelvin in monolayer crystal, Science, 359, 76-79 (2018)

Advisor: Suzanne T. Staggs (Physics)

Simon Observatory

Researcher: **Bert Harrop** (Princeton Staff), **Martina Macakova** (Princeton Staff), **Thomas Hanstein** (Princeton Staff), **Logan Ernst** (Princeton Staff)

Sponsorship: Simons Foundation and other smaller partners including Princeton University

The Simons Observatory (SO) is a new cosmic microwave background experiment being built on Cerro Toco in Chile. SO will measure the temperature and polarization anisotropy of the cosmic microwave background in six frequency bands centered at: 27, 39, 93, 145, 225 and 280 GHz. The initial configuration of SO will have three small-aperture 0.5-m telescopes and one large-aperture 6-m telescope, with a total of 60,000 cryogenic bolometers to achieve the detection sensitivity for the cosmological science goals. The optical coupling, detector array, and cold readout are packaged in a so-called Universal Focal-plane Module (UFM). At MNFC, we fabricate and assemble UFM components. Shown here is the so-called Routing Wafer in the low frequency, LF, (27/39 GHz) UFM, which distributes and interconnects the biasing and TES (Transition Edge Sensors) to the high-speed readout.

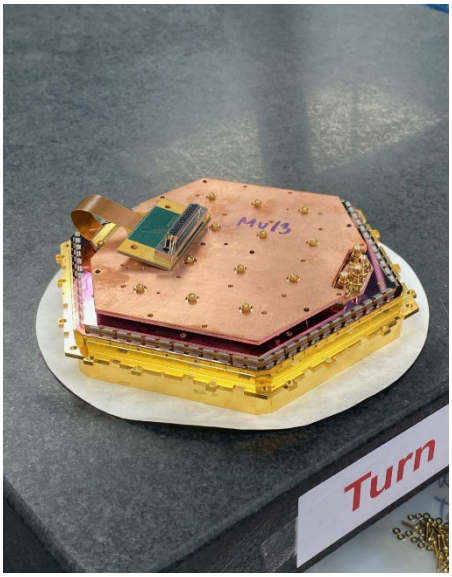

Figure 1: Universal Focal Plane Module (UFM).

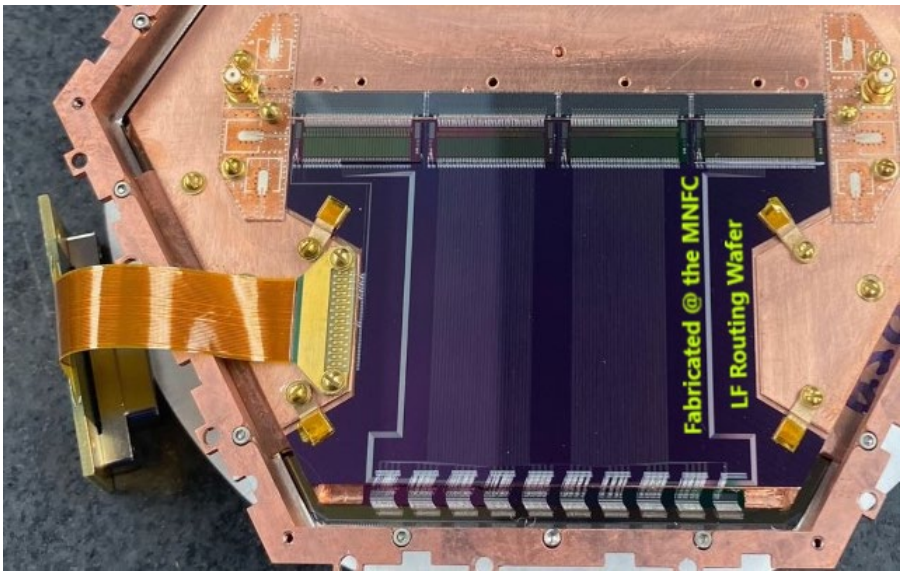

Figure2: Simons Low Frequency (LF) Silicon Routing Wafer. The SO LF Detector frequency bands are: 27/39 GHz.

CITATIONS

- Heather McCarrick et al. The Simons Observatory microwave SQUID multiplexing detector module design. 2021 ApJ 922 38
- The Simons Observatory: Science goals and forecasts JCAP 1902 (2019) 056

Advisor: Ali Yazdani (Physics)

Visualizing Unconventional Superconductivity in Twisted Bilayer Graphene

Researcher: **Kevin Nuckolls** (Princeton Graduate)

Sponsorship: DOE

We are interested in investigating unconventional superconductivity in 2D materials, with emphasis on the superconducting phases of twisted bilayer graphene (TBLG), which consists of two sheets of graphene rotated 1.1 deg with respect to one another.

This exciting new platform hosts an emergent low-temperature unconventional superconducting phase, but only at this very particular twist angle. While superconductivity in TBLG appears, in some ways, reminiscent of the high- temperature superconductivity in the cuprates, preliminary results describe signatures of a much more complex pairing mechanism, inducing "nematic superconductivity". In this previously undiscovered phase of matter, TBLG could be tuned using a very small, in- plane magnetic field to host highly directional superconducting channels. Utilizing the nematic superconducting phase in TBLG requires the atomic-scale insight of STM to determine exactly why electrons pair and why a magnetic field induces these directionally dissipationless current channels. Specifically, measurements of the local conductance surrounding a single atomic impurity in TBLG are expected to show distinguishable signatures of the spatial symmetries enforcing superconductivity, and the symmetries removed by a magnetic field to induce nematicity. Additionally, both theoretical calculations and numerical simulations predict strained TBLG devices to host another distinct, useful form of superconductivity known as "chiral superconductivity". Chiral superconductors are topologically protected and, thus, exhibit highly robust electronic behavior that would be ideal for large-scale production of 2D material devices.

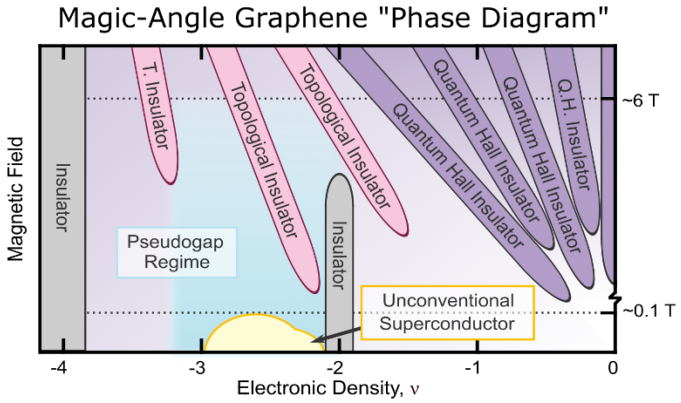

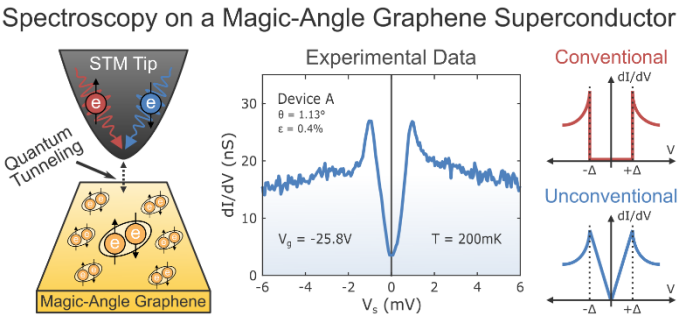

CITATIONS

- Oh, M.*, Nuckolls, K. P.*, Wong, D.*, et al. Evidence for unconventional superconductivity in twisted bilayer graphene. Nature 600, 240-245 (2021).
- Nuckolls, K. P.*, Oh, M.*, Wong, D.*, et al. Strongly correlated Chern insulators in magic-angle twisted bilayer graphene. Nature 588, 610-615 (2020).
- Wong, D.*, Nuckolls, K. P.*, Oh, M.* et al. Cascade of electronic transitions in magic-angle twisted bilayer graphene Nature 582, 198-202 (2020).

Advisor: Ali Yazdani (Physics)

Scanning Tunneling Microscopy of 2D Graphene

Researcher**: Minhao He** (Princeton Postdoc)

Sponsorship: Moore Foundation

The interaction between electrons in graphene under high magnetic fields drives the formation of a rich set of quantum Hall ferromagnetic (QHFM) phases with broken symmetry. Uniquely in Bernal stacked bilayer graphene, the lowest Landau level is eight-fold degenerate, with spin, valley and orbit degeneracy. More interestingly, electronic interaction at low temperature, high magnetic field is strong enough to additionally drive a variety of fractional quantum hall effect (FQHE) states at partial filling of individual Landau level.

In this study, we fabricate ultraclean graphene samples to study with scanning tunneling microscopy (STM). By visualizing atomic-scale electronic wave functions with scanning tunneling spectroscopy (STS), we can study microscopic signatures of the symmetry breaking in QHFM phases and the spectral feature of FQHE with potential anyonic feature. In MNFC cleanroom, we use a set of state of art nanofabrication tools to make these graphene samples.

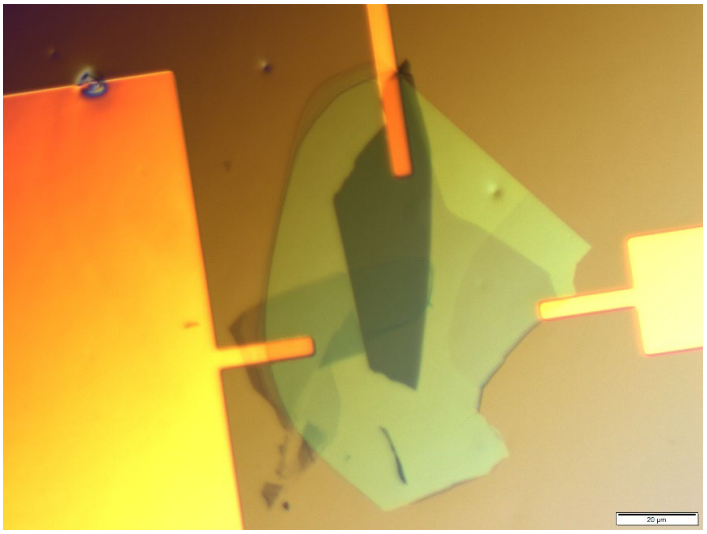

Figure 1: Optical image of a Bernal bilayer graphene STM sample. The sample structure (from top to down) is Bernal bilayer graphene, h-BN as the gate dielectric, and few-layer graphite as the bottom gate. The heterostructure is stacked on top of pre-patterned gold electrodes on a SiO_2/Si wafer.

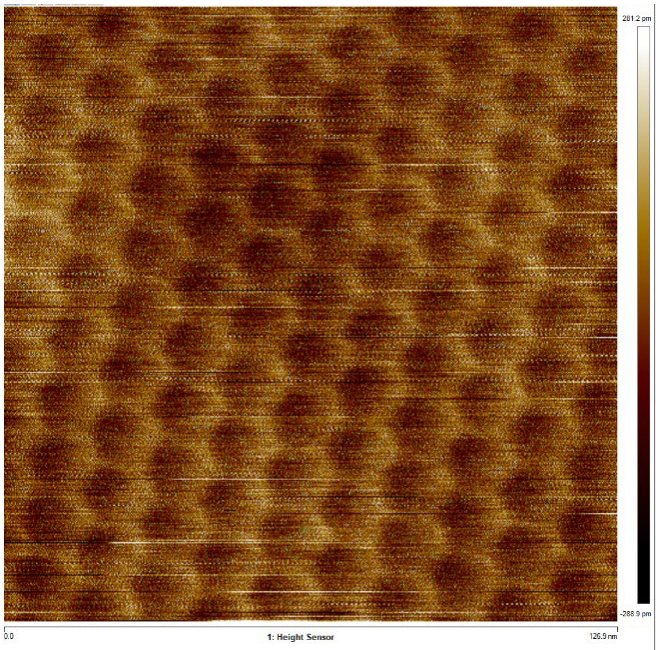

clean sample surface with moire superlattice formed between the Bernal bilayer graphene and underlying h-BN.

CITATIONS

- N/A

Advisor: Ali Yazdani (Physics)

Probing Correlated Superconductors and Their Phase Transitions on the Nanometer Scale

Researcher: **Cheng-Li Chiu** (Princeton Graduate)

Sponsorship: DOE

Our interest is to use scanning tunneling microscopy to study the electronic structure of gate tunable 2-dimensional devices including magic-angle twisted bilayer graphene[1], twisted double bilayer graphene[2], mono-layer graphene[3], and double-layer graphene. Our recent focus is on graphene in quantum Hall regime. By study the tunneling spectroscopy and imaging the local density of state, we were able to reveal the ground state of a highly interacting system. We are also developing a new sensing technique that can resolve the electron density of quantum Hall fluid with un-matched high energy and spatial resolution.

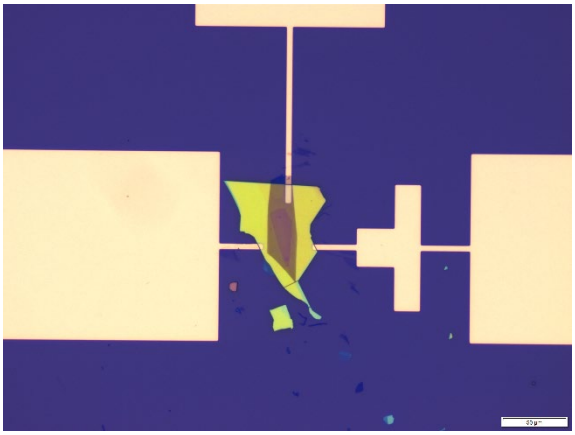

Figure 1: The image shows a sensing device. The gold contact from three side allows us to individually tunned the electro-chemical potential which control the electron density of our gate, sample, and sensing layer.

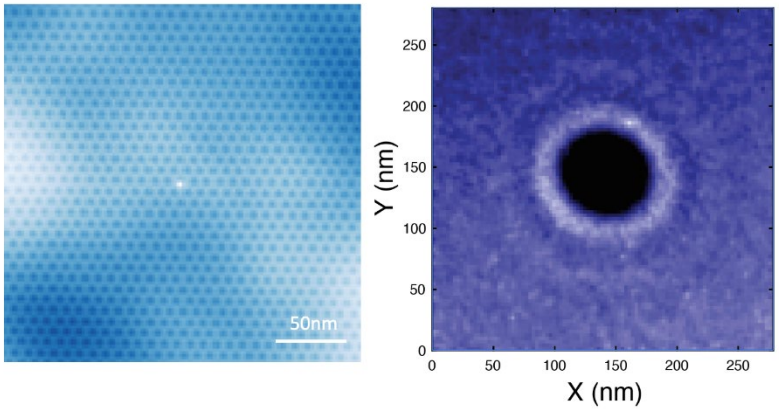

Figure 2: The image on the left shows a topography of a graphene. The periodic dark spot is from the hBN-graphene Moiré and the bright dot in the center is a defect. The image on the right shows a Friedel-oscillation-like fringes which is from the electrons screening a charge defect.

CITATIONS

- Xie, Y., Lian, B., Jäck, B. et al. Spectroscopic signatures of many-body correlations in magic-angle twisted bilayer graphene. Nature 572, 101–105 (2019).
- Liu, X., Chiu, CL., Lee, J.Y. et al. Spectroscopy of a tunable moiré system with a correlated and topological flat band. Nat Commun 12, 2732 (2021). https://doi.org/10.1038/s41467-021-23031-0
- Liu, X., Farahi, G., et al. Visualizing broken symmetry and topological defects in a quantum Hall ferromagnet. SCIENCE 2 Dec 2021 Vol 375, Issue 6578 pp. 321-326 DOI: 10.1126/science.abm3770

Advisor: Ali Yazdani (Physics)

Fractional Quantum Hall in Graphene

Researcher: **Yen Chen Tsui** (Princeton Graduate)

Sponsorship: Moore, ONR, DOE, and ARO-MURI

Fractional quantum Hall states (FQHs) emerge when a 2D electron system is subjected to a strong magnetic field. We performed millikelvin scanning tunneling microscopy (STM) study of the FQHs in Bernal-stacked bilayer graphene. Robust odd-denominator FQH sequences are observed, and their charge excitation gaps are characterized. Moreover, we also detected even-denominator FQHs in the lowest Landau levels, highlighting the extra orbital degeneracy for the many-body states. With the imaging power of STM, we can study the spatial variation of these FQH states, and the local excitations when these FQHs experience a defect potential. Our study helps with understanding the charge excitations of these FQHs and opens an opportunity to image anyons.

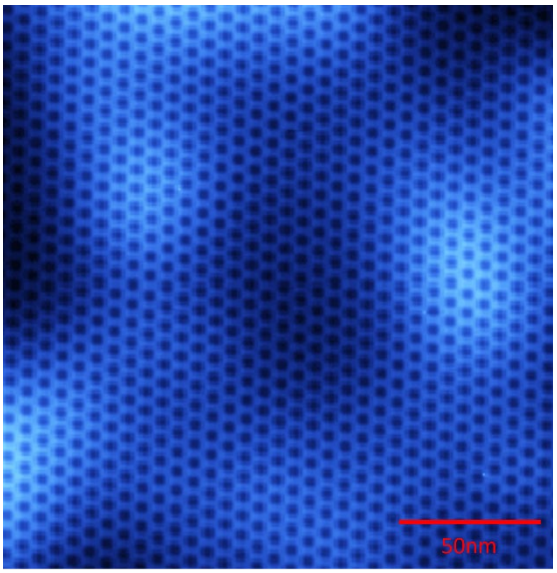

Figure 1: STM image on bilayer surface.

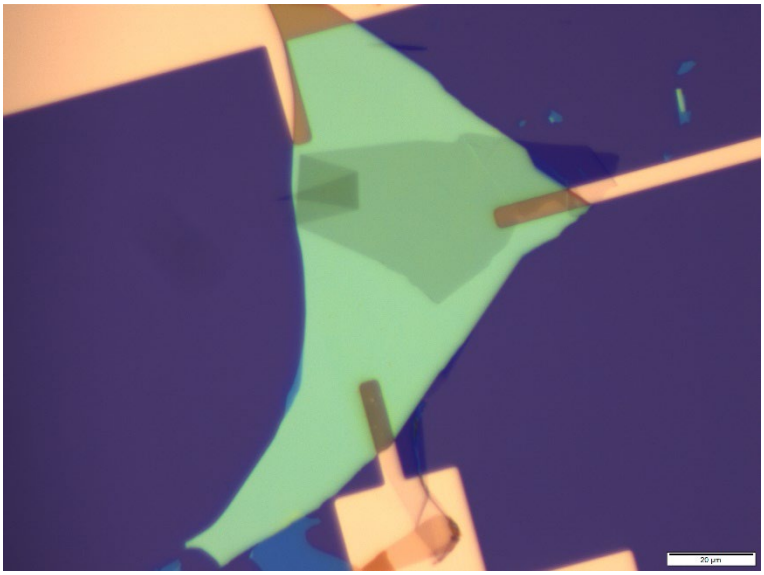

Figure 2: Device image.

CITATIONS

- N/A

External Academic MNFC Users

Advisor: Ryan Sochol (Mechanical Engineering, University of Maryland)

Leveraging Ex-Situ Direct Laser Writing for Biomedical Applications

Researcher: **Sunandita Sarker, Adira Colton, Olivia Young**

Sponsorship: N/A

Targeted microinjections of stem cells are being investigated to repair damaged tissue in the spinal cord, brain, and joints. The efficacy of the treatment is dependent on the microinjection technique as too many or too few stem cells can cause problems with the treatment. To address this, we are working to develop microneedle arrays to distribute the stem cells more evenly. We developed ex situ direct laser writing to achieve this. With this process we are able to print geometrically complex microfluidic structures directly atop tubing. We employed *ex-situ* direct laser writing to print microneedle arrays directly atop and fluidically sealed to 3D printed capillaries. We then tested the mechanofluidic integrity of the microneedle array-capillary interface by performing cyclic burst pressure tests. We found uncompromised fluidic sealing at 275 kPa. These results provide a foundation for new microinjections applications.

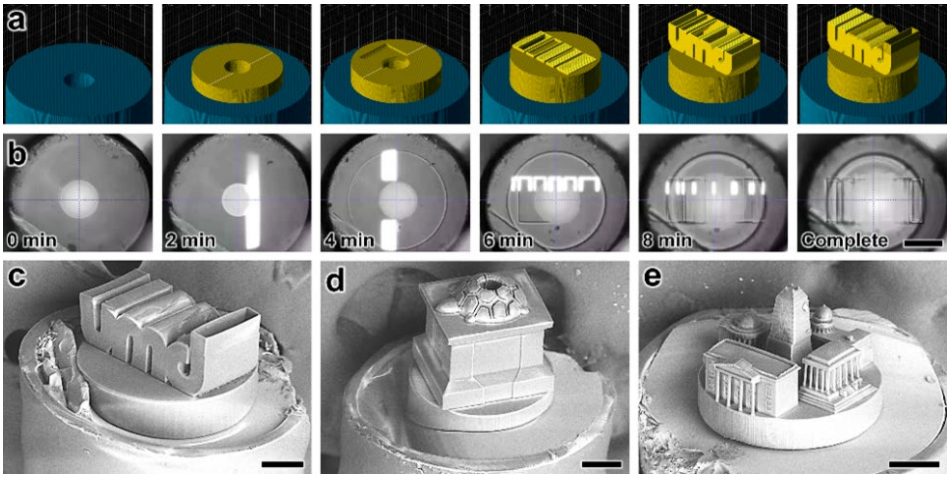

Figure 1: Fabrication results for esDLW-based printing of 3D microfluidic structures directly onto fused silica tubes.

(a) Computer-aided manufacturing (CAM) simulations and (b) corresponding micrographs of the esDLW printing process. Scale bar = 100 µm; Print time = 9 min. (c–e) SEM micrographs of the three demonstrative 3D microfluidic structures:

(c) "UMD" design, (d) Testudo statue design, and (e) landmarks of Washington, DC, design. Scale bars = 50 µm.

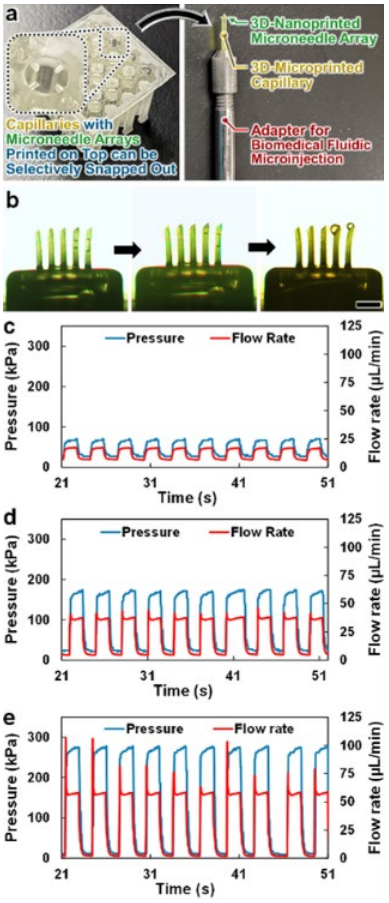

Figure 2: Experimental results for microfluidic characterizations. (a) Example of a microneedle array-capillary assembly individually released from the batch and then interfaced with an adapter for fluidic loading. (b) Sequential micrographs during fluidic infusion. Scale bar = 200 µm. (c–e) Results for cyclic burst-pressure testing with DI water during representative intervals for input pressure cycles targeting: (c) 75 kPa; (d) 175 kPa; and (e) 275 kPa.

CITATIONS

- Ruben Acevedo, Ziteng Wen, Ian B. Rosenthal‡, Emmett Z. Freeman‡, Michael Restaino, Noemi Gonzalez‡, and Ryan D. Sochol, "3D Nanoprinted External Microfluidic Structures via Ex Situ Direct Laser Writing," Proceedings of the 34th IEEE International Conference on Micro Electro Mechanical Systems (IEEE MEMS 2021).
- Sunandita Sarker, Adira Colton, Ziteng Wen, Xin Xu, Piotr Walczak, Miroslaw Janowski, Yajie Liang, and Ryan D. Sochol, "A Hybrid 3D Micro-Nanoprinting Approach for Biomedical Microinjection Needle Arrays," Proceedings of the 20th Solid-State Sensors, Actuators and Microsystems Workshop (Hilton Head 2022), Hilton Head Island, SC, USA.

Advisor: Anthony Sigillito (Electrical and Systems Engineering, University of Pennsylvania)

Silicon Quantum Dots

Researcher: **Noah Dylan Johnson, Seong Woo Oh**

Sponsorship: Penn Startup Fund

In the MNFC, the Sigillito group has primarily been using the metal deposition tools, laser writer (DWL-66+) and acid bay. We are trying to engineer silicon quantum dot devices on Si/SiGe heterostructures [1]. We have been doing the bulk of laser writing steps of our device fabrication in the MNFC. Since our device fabrication has multiple layers of laser writes and metal deposition, we care a lot about the overlay accuracy. The DWL-66+ at the MNFC allowed us to achieve a good enough overlay accuracy.

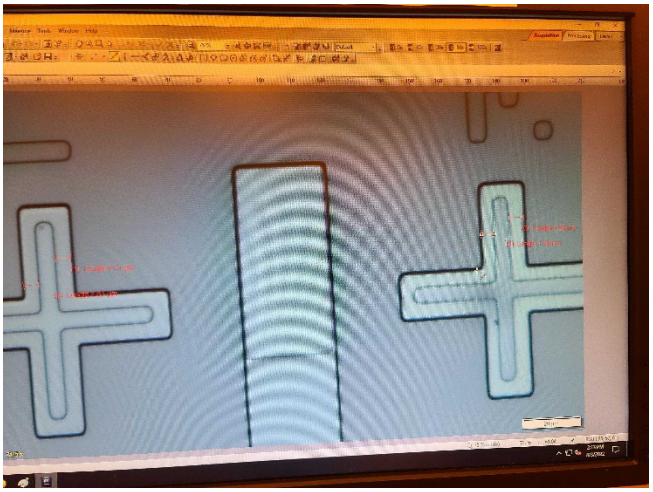

Figure 1 :Each layer of our device design file has its distinct alignment markers, allowing us to write subsequent layers with respect to previous layers.

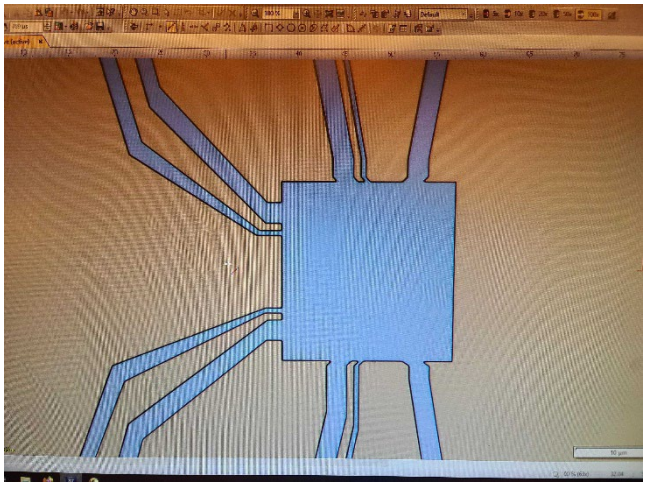

Figure 2:Ion implantation mask write done at the DWL-66+ Heidelberg at the MNFC.

CITATIONS

- [1] Sigillito et al., Phys. Rev. Appl. 11, 061006 (2019)

Industrial MNFC Users

Company: ChronosDx
Organic Transistor Development for Biosensing
Researcher: **James Tyrrell**

At ChronosDx, we are developing a novel bioassay platform that can measure the concentrations of wide range of proteins and DNAs at low concentrations. The primary application of this diagnostic platform is early cancer detection. The fundamental transducer of biomarker concentrations is an electrolyte-gated organic transistor. For applications in chemical sensing, the architecture of such organic transistors needs to be optimised. Using the MNFC facilities, we have developed a fabrication procedure for organic transistor fabrication and have produced such devices with a wide range of architectures. In doing so, we have found an initial optimised architecture for biosensing through electrical characterisation. The greater the signal amplification afforded by the organic transistors, the lower the concentration limit of the resulting biosensor. In early cancer stages, the small size of the tumor means that only very low concentrations of cancer-associated proteins and DNA molecules are circulating in the blood. Throughout this process, we have created organic transistors that have state-of-the-art performances and amplifications using only commercially available materials. This outcome allows us to progress onto the next stages of development of the biosensing platform

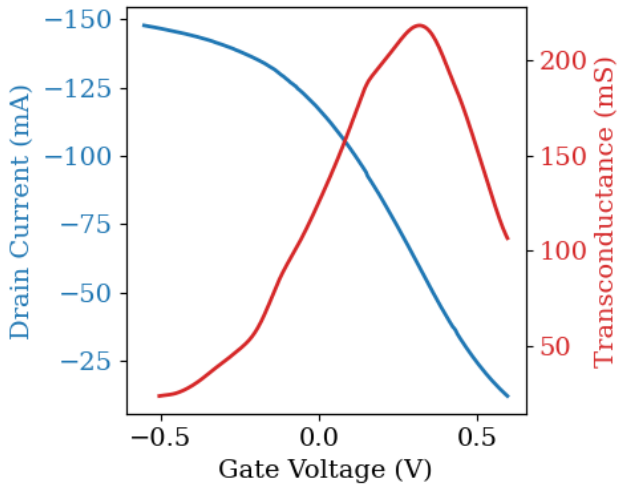

Figure 1: Organic Transistor transfer curve, providing a peak transconductance of 218 mS.

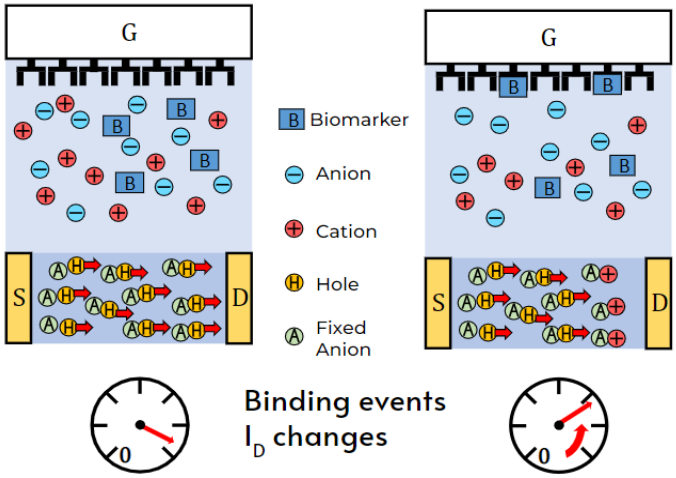

Figure 2: Operation mechanism of a biosensor that measures biomarker concentrations using an organic transistor architecture.

CITATIONS

- N/A

Company: Princeton Infrared Technologies
InGaAs Detector Arrays
Researcher: **Catherine Masie, Mike Lange**

Development of InGaAs imaging arrays and microlenses in InP substrate.

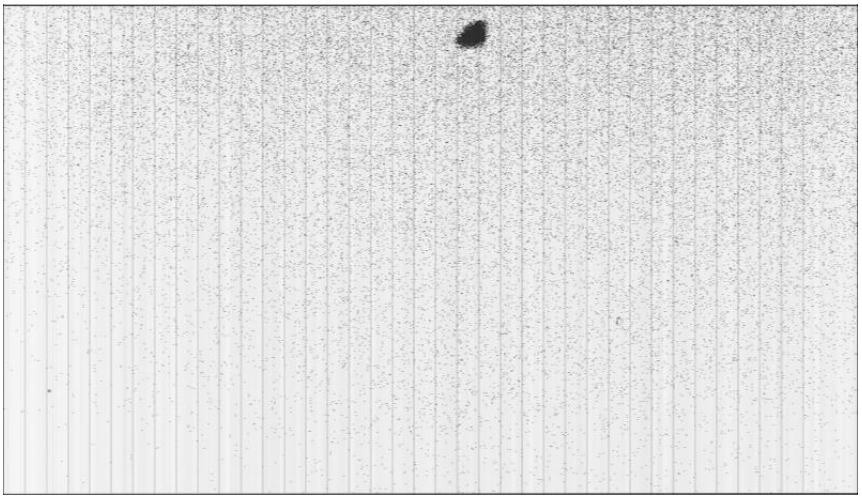

Figure 1: InGaAs detector array image.

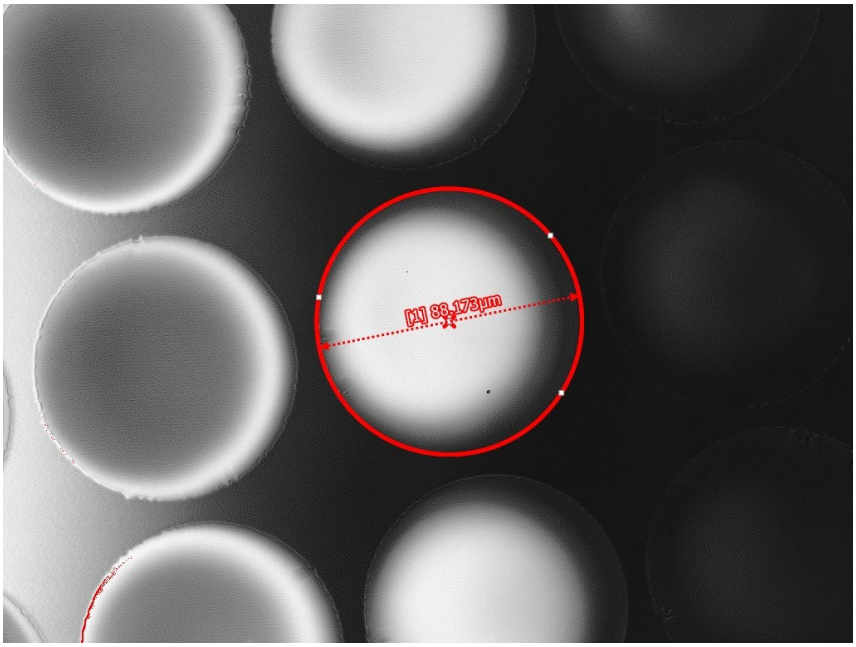

Figure 2: Microlens lens fabricated with ICP etching

CITATIONS

- N/A

Company: Tendo Technologies

Non-Metallic Elastic Velocity Sensor

Researcher: **Andojo Ongkodjojo Ong, Mark McMurray, Yuyang Fan, Marcus Hultmark**

Tendo Technologies, Inc. is the developer of a highly sensitive and accurate flow meter particularly suited for small volume fluids dispensing. Centered around the principle of elastic filament velocimetry (EFV), our flow meter is based on the non-metallic micro-ribbon structures, using polysilicon as the sensing material (as shown in Fig. 1). These sensors offer high sensitivity from the combination of higher Gage Factor (GF) and lower TCR (Temperature Coefficient of Resistance) compared with Platinum, which is the original material used for EFV sensors. These properties directly meet the needs of customers in several segments of industry from pharmaceutical dispensing, scientific R&D, and manufacturing

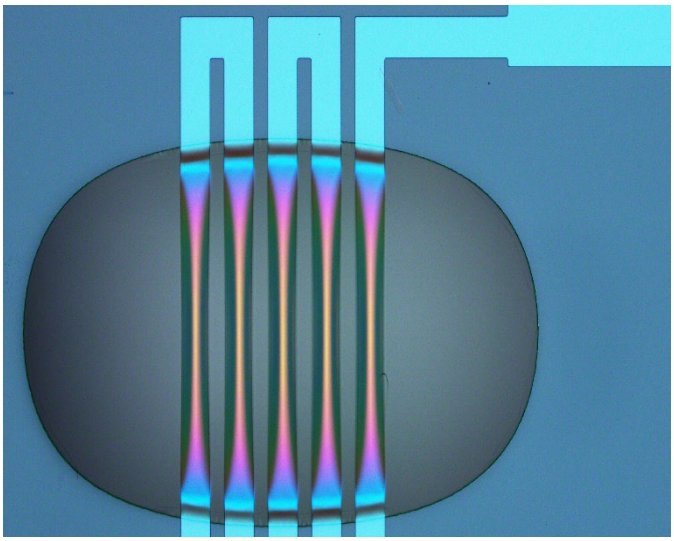

Figure 1: The polysilicon-based strain sensors with the five sensing elements suspended over the silicon substrate, having a beam length of ~ 430 µm, a beam width of 50 µm, and a thickness of ~ 100 nm.

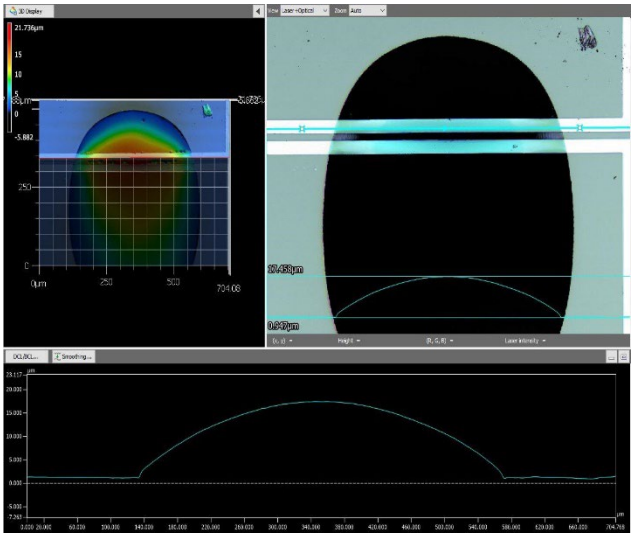

Figure 2: Confocal image of a polysilicon sensor subjected to 4.0psi air flow.

CITATIONS

- M. K. Fu, Y. Fan, C. P. Byers, T.-H. Chen, C. B. Arnold, and M. Hultmark, "Elastic Filament Velocimetry (EFV)", Measurement Science and Technology, 2017, Vol. 28, 025301 (12pp).

Company: Princeton Innotech Inc.
High Power Lasers
Researcher: **Michel Francois, James Wynn, Frederick Won**
Sponsorship: DOD SBIRs

Princeton Innotech is developing high power single surface emitting lasers using photonic crystal and grating based coupling approach between multiple surface emitting devices. The wafers are grown by external vendors by MOCVD growth technique and then fabricated in MNFC using optical lithography and EBL.

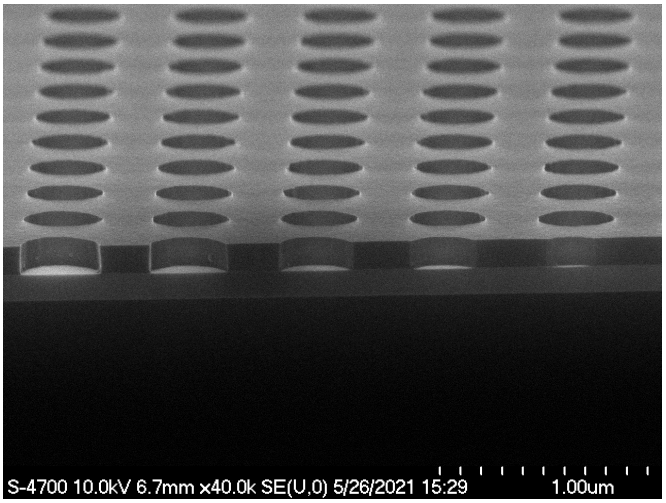

Figure 1: SEM picture of photonic crystal on surface emitting laser devices to render them single mode.

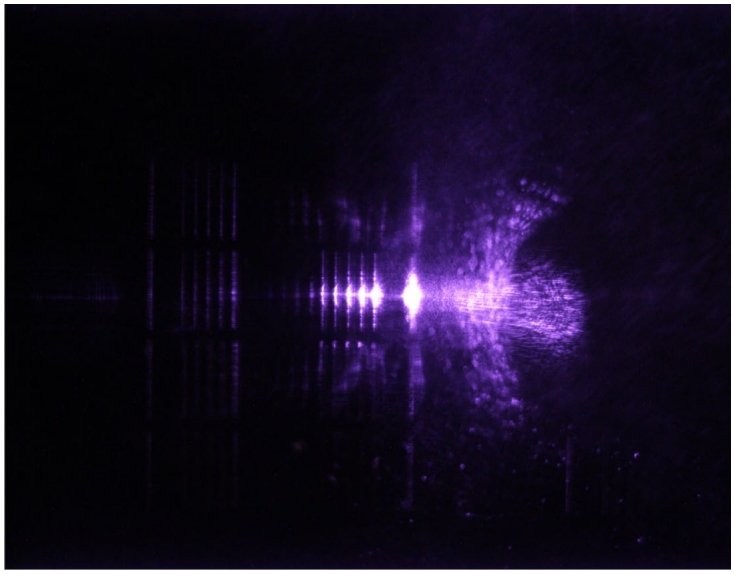

Figure 2: Mode transformation with gratings and waveguide for surface emitting laser.

CITATIONS

- N/A

MNFC

Versaline Deep Silicon Etch

Researcher: **Roman Akhmechet** (MNFC Senior Research Specialist)

The new Versaline DSE plasma etcher is supplementing our silicon dry etch capabilities. It has both deep/throughwafer etch recipe, as well as shallow precision etch recipe. In order to prepare the tool for MNFC Labmembers, several iterations of deep etch recipe have been run. The results can be seen in the images below. High aspect ratios have been demonstrated. Expected etch rate is 0.67 microns per cycle and depends greatly on total exposed area. Selectivity to photoresist is around 85:1.

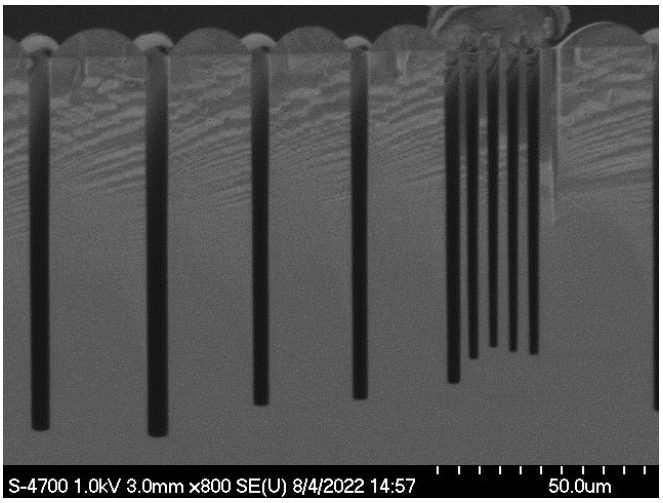

Figure 1: FastEtch recipe, 300 cycles.

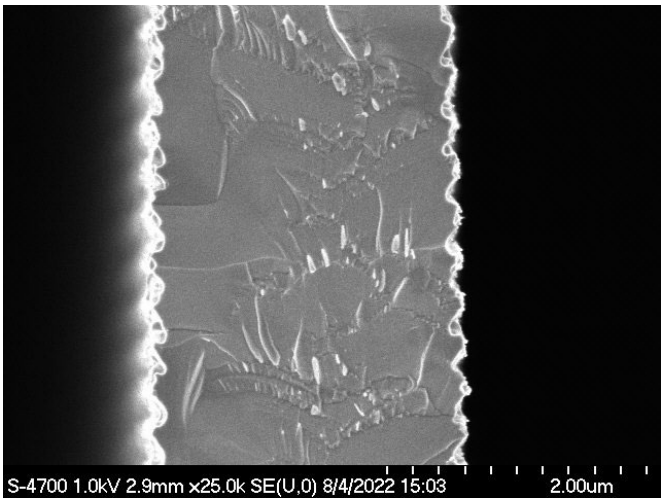

Figure 2: FastEtch recipe, close-up that shows scallops.

CITATIONS

- N/A

Nanoscribe PPGT2 3D Printer

Researcher: **Roman Akhmechet** (MNFC Senior Research Specialist)

The new Nanoscribe tool installed in the Soft Materials Bay is capable of printing 3-dimensional structures with voxel sizes as low as 200 nm in diameter. This tool utilizes two-photon polymerization with proprietary resins, and can target such applications as cell scaffolding and custom nano-needles. Some labmembers have demonstrate the ability to print directly on their other devices as opposed to a provided flat substrate.

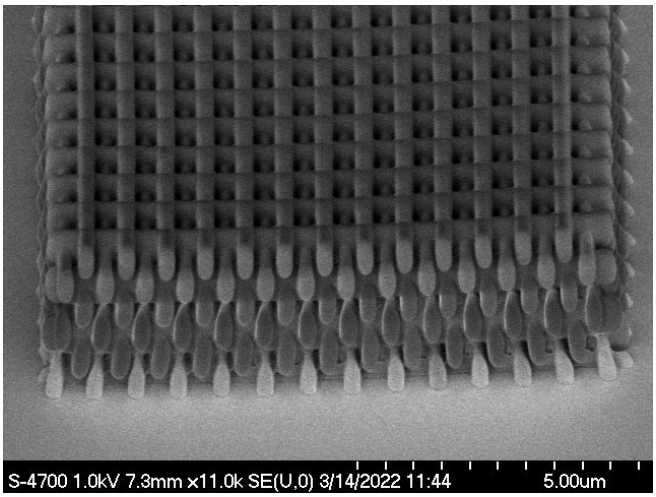

Figure 1: Initial characterization of Nanoscribe tool with 63x objective and IP-DIP2 resin, testing minimum resolution.

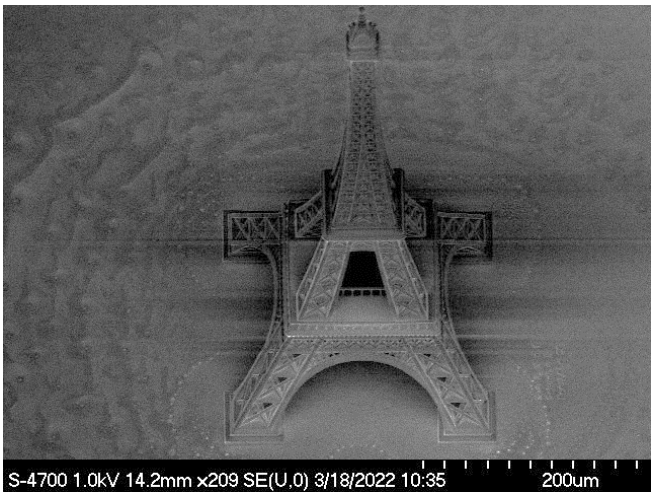

Figure 2: A tall feature printed using 63x objective and IP-DIP2 resin. The original STL model is freely available.

CITATIONS

- N/A

Other Research Performed in the MNFC

Advisor: Gregory D. Scholes (Chemistry)
Electron Transfer Through Entrained DNA Strands
Researcher: **Kyu Hyung Park** (Princeton Postdoc)
Sponsorship: Gordon and Betty Moore Foundation

Advisor: Glaucio H. Paulino (Civil and Environmental Engineering)
Multiscale Investigation of Origami Instability
Researcher: **Tuo Zhao** (Princeton Postdoc)
Sponsorship: NSF

Advisor: Nathalie P. de Leon (Electrical Engineering)
New Materials for Superconducting Qubits
Researcher: **Russell McLellan** (Princeton Graduate)
Sponsorship: NSF RAISE TAQS - University of Wisconsin

Advisor: Nathalie P. de Leon (Electrical Engineering)
Exploring New Materials to Construct Superconducting Qubits
Researcher: **Nana Shumiya** (Princeton Postdoc)
Sponsorship: AFOSR, NSF, TAQS, DARPA, DOE, PQI

Advisor: Nathalie P. de Leon (Electrical Engineering)
Superconducting Qubit Coherence
Researcher: **Ray Chang** (Princeton Graduate)
Sponsorship: NSF

Advisor: Andrew A. Houck (Electrical Engineering)
SFS Junctions and Quantum Phase Slip Junctions
Researcher: **Jeremiah Coleman** (Princeton Graduate)
Sponsorship: NQI

Advisor: Andrew A. Houck (Electrical Engineering)
Co-Design Center for Quantum Advantage: Optimizing Qubit and Resonator Coherence
Researcher: **Kevin Crowley** (Princeton Graduate)
Sponsorship: DOE

Advisor: Andrew A. Houck (Electrical Engineering)
Optimizing Qubit and Resonator Coherence
Researcher: **Matthew Bland** (Princeton Graduate)
Sponsorship: NSF, DOE

Advisor: Barry P. Rand (Electrical Engineering)
Top Emitting Perovskite LED
Researcher: **Jonathan Scott** (Princeton Graduate)
Sponsorship: AFOSR

Advisor: Kaushik Sengupta (Electrical Engineering)
Optical Biosensor
Researcher: **Chengjie Zhu** (Princeton Graduate)
Sponsorship: NSF

Advisor: Kaushik Sengupta (Electrical Engineering)
THz Coupled Oscillator Arrays
Researcher: **Hooman Saeidi** (Princeton Graduate)
Sponsorship: MURI

Advisor: Mansour Shayegan (Electrical Engineering)
Exotic Phases of Electrons in Interacting 2D Systems
Researcher: **Pranav Thekke Madathil** (Princeton Graduate)
Sponsorship: MOORE

Advisor: James C. Sturm (Electrical Engineering)
TFTs for Sensing Application in Large Area Electronic System
Researcher: **Mohammad Shafiqul Islam** (Princeton Graduate)
Sponsorship: Industrial

Advisor: James C. Sturm (Electrical Engineering)
Microfluidic
Researcher: **Weibin Liang** (Princeton Graduate)
Sponsorship: NIH/GPB STTR

Advisor: Jeffrey D. Thompson (Electrical Engineering)
New Materials for Quantum Systems
Researcher: **Christopher Phenicie** (Princeton Graduate)
Sponsorship: Eric and Wendy Schmidt Transformative Technology Fund

Advisor: Jeffrey D. Thompson (Electrical Engineering)
Topological Quantum Phases in 2D materials
Researcher: **Salim Ourari** (Princeton Graduate)
Sponsorship: AFOSR

Advisor: Jeffrey D. Thompson (Electrical Engineering)
Parallel Single-Shot Measurement and Coherent Control of Solid-State Spins Below the Diffraction Limit
Researcher: **Lukasz Dusanowski** (Princeton Postdoc), **Sharon Ruth Platt** (Princeton Graduate),
Sponsorship: DOE, DARPA, AFOSR, NSF

Advisor: Coleen T. Murphy (Molecular Biology)
C. Elegans in PDMS Chip
Researcher: **Salman Sohrabi** (Princeton Postdoc)
Sponsorship: NIH

Advisor: Barry P. Rand (Physics)
NbTiN Coplanar Waveguide Etching
Researcher: **James Loy** (Princeton Graduate)
Sponsorship: N/A

Advisor: M. Zahid Hasan (Physics)
Device Fabrication for Ultrafast Study
Researcher: **Maya Rubenstein** (Princeton Undergraduate)
Sponsorship: Moore

Advisor: M. Zahid Hasan (Physics)
Sample Device Preparation for Ultrafast Study
Researcher: **Yu-Xiao Jiang** (Princeton Graduate)
Sponsorship: DOE

Advisor: Nai Phuan Ong (Physics)
Conical Magnetic Josephson Junction
Researcher: **Bingzheng Han** (Princeton Graduate)
Sponsorship: N/A

Advisor: Suzanne T. Staggs (Physics)
Cosmology Detector Array
Researcher: **Claire Lessler** (Princeton Undergraduate)
Sponsorship: N/A

Advisor: Christopher G. Tully (Physics)
Graphene Single Electron Transistor for Neutrino Detector
Researcher: **Andi Tan** (Princeton Associate Research Scholar)
Sponsorship: Simons Foundation

Advisor: Ali Yazdani (Physics)
Imaging Anyons in Bernal Stack Graphene
Researcher: **Maksim Borovkov** (Princeton Graduate)
Sponsorship: ONR

Advisor: Ali Yazdani (Physics)
Research on 2D Materials (Physics)
Researcher: **Pearl Thijssen** (Princeton Graduate)
Sponsorship: NSF

Advisor: Marc Miskin (Electrical and Systems Engineering, University of Pennsylvania)
Thru Etching Microrobots
Researcher: **Maya Lassiter**
Sponsorship: N/A

Advisor: Charlie Johnson (Electrical and Systems Engineering, University of Pennsylvania)
Dicing Si Wafers
Researcher: **Christopher Kehayias**
Sponsorship: N/A

Advisor: Firooz Alatouni (Electrical and Systems Engineering, University of Pennsylvania)

Si Etch

Researcher: **Mohamad Idjadi, Jaeung Ko**

Sponsorship: N/A

Advisor: Michael Ohadi's (Mechanical Engineering, University of Maryland)

Fabrication of Manifold-Microchannels

Researcher: **Harsimranjit Singh**

Sponsorship: N/A

Advisor: Eric Lukosi (Nuclear Engineering, University of Tennessee)

Wire Bonding for Diamond Sensor

Researcher: **Corey Ahl**

Sponsorship: N/A

Company: SRI

SRI Device Fabrication

Researcher: **Lewis Haber**, **Xiaohui Wang**, **Wei Zhang**

Sponsorship: N/A

Company: Power Integrations, Inc

Power Transistors

Researcher: **Emilia Wrona, Michel Murphy, Simon Wang**

Sponsorship: N/A

Company: Sonder Research X

SU8 Process

Researcher: **David D. Hurley, Apeksha Rajamanthrilage, Shayna Beldner, Hwi Yong Lee**

Sponsorship: N/A

Company: ams-OSRAM

Researcher: **Jennifer Ren**

Wafer Dicing

Sponsorship: N/A

Company: SNOChip

Researcher: **Wei Ting Chen**

Nanostructures on Photonic Chips

Sponsorship: N/A

Company: EnaChip Inc

Researcher: **Anisha Mukherjee**

Wafer Level Magnetics

Sponsorship: N/A